Mps1 kinase signaling in mitosis

Nannette Jelluma

ISBN/EAN: 978-90-393-5340-0

© N. Jelluma, 2010

Printed by Gildeprint Drukkerijen B.V., Enschede, the Netherlands

Printing of this thesis was financially supported by CHROMAPHOR Analysen-Technik GmbH and Roche Diagnostics Nederland BV.

Cover photo: Giant Silkworm Moth (Rothschildia Orizaba), by Tobias Dansen.

Mps1 kinase signaling in mitosis

Signaaloverdracht door Mps1 kinase tijdens de celdeling

(met een samenvatting in het Nederlands)

Proefschrift

ter verkrijging van de graad van doctor aan de Universiteit Utrecht op gezag van de rector magnificus, prof.dr. J.C. Stoof, ingevolge het besluit van het college voor promoties in het openbaar te verdedigen op donderdag 10 juni 2010 des middags te 12.45 uur

door

Nannette Jelluma

geboren op 30 maart 1978 te Woerden

Promotor: Prof.dr. R.H. Medema
Co-promotor: Dr. G.J.P.L. Kops

Vincent: You know what they call a Quarter Pounder with Cheese in Paris?
Jules: They don't call it a Quarter Pounder with Cheese?
Vincent: No man, they got the metric system, they wouldn't know what the f**k a Quarter Pounder is.
Jules: What do they call it?
Vincent: They call it a **"**Royale with Cheese".
Jules: "Royale with Cheese".
Vincent: That's right.
Jules: What do they call a Big Mac?
Vincent: A Big Mac's a Big Mac, but they call it "Le Big Mac".
Jules: "Le Big Mac". What do they call a Whopper?
Vincent: I dunno, I didn't go in a Burger King.

PULP FICTION
-Quentin Tarantino-

(You won't know the facts until you've seen the fiction)

Contents

Chapter 1 **9**
General introduction

Chapter 2 **23**
Mps1 phosphorylates Borealin to control Aurora B activity
and chromosome alignment

Chapter 3 **51**
Small molecule kinase inhibitors provide insight into Mps1 cell cycle function

Chapter 4 **91**
Mps1 maintains mitotic checkpoint activity by preventing APC/C-mediated
disassembly of MCC

Chapter 5 **107**
Chromosomal instability by inefficient Mps1 auto-activation due to a
weakened mitotic checkpoint and lagging chromosomes

Chapter 6 **121**
Release of Mps1 from kinetochores by auto-regulation is crucial for timely
anaphase onset

Chapter 7 **135**
Summary & Discussion

References **143**

Samenvatting in het Nederlands **153**

Curriculum Vitae **156**

Publications **157**

Dankwoord **158**

Chapter 1

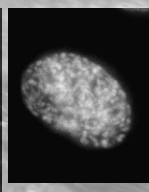

General introduction

Cell division

Cell cycle, growth and regeneration

For a multicellular organism to grow and to regenerate damaged tissue, it needs to continuously multiply and replace the cells it consists of. Cells can do so by going through the cell cycle, with the ultimate goal to divide into two daughter cells. The cell cycle consists of several phases; in G1-phase, the cell grows and increases biosynthesis to prepare for S-phase, in which duplication of all chromosomes takes place. After S-phase, the cell proceeds to G2-phase, in which the cell again grows and prepares for the last phase, M-phase or mitosis, which is the actual division phase of the cell cycle. G1-, S-, and G2-phase are collectively called interphase (Figure 1). The cell cycle is strictly regulated by oscillating activities of several Cyclin dependent kinases (Cdks). Entry in mitosis for example depends on activation of the Cyclin B1-Cdk1 complex, by increasing Cyclin B1 levels, and exit depends on Cyclin B1 degradation (reviewed in [1]).

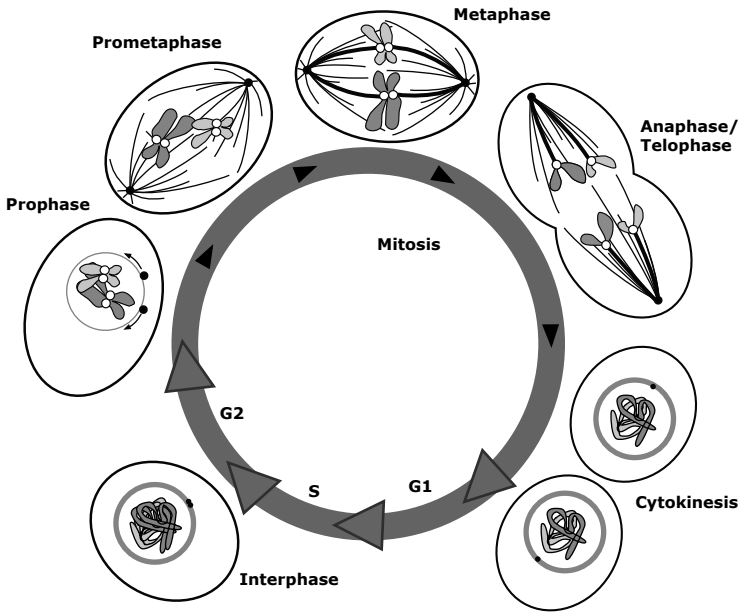

Figure 1.
Schematic representation of the different stages of the cell cycle, including the mitotic stages from prophase to cytokinesis.

For preservation of the genetic material in each cell in the organism (which in humans is 2x23 chromosomes), it is important that all chromosomes are duplicated before each division and equally divided over the two daughter cells in such a way that each daughter cell receives the same set of genetic material. Unequal division of chromosomes results in cells with abnormal chromosome numbers, also called aneuploidy (Figure 2) and may cause various problems in development of the organism. Although most irregularities in chromosome numbers per cell are not tolerated during development and cause embryonic lethality, some unequal chromosome numbers are tolerated early in development (for an overview of the effects of aneuploidy in development, see [2] and [3]). In humans, this can lead to, among other things, growth problems and mental retardation. For example, Down' s syndrome is caused by an extra copy of chromosome

21 (trisomie 21). Also, in most of human tumors, cells were found to contain abnormal amounts of chromosomes. This led to the hypothesis that unequal division of chromosomes might lead to acceleration of tumor growth, or might even initiate tumorigenesis (reviewed in [4] and discussed in more detail later in this introduction).

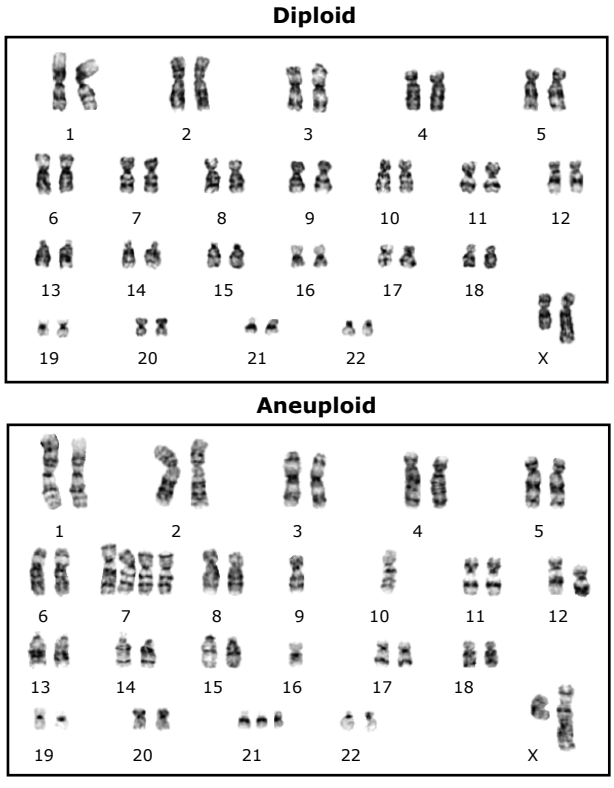

Figure 2.
Karyogram from hTERT-RPE (human immortalized retinal pigment epithelial) cells showing diploid (2x23) and aneuploid (non-diploid) chromosome content. Aneuploidy was induced by mitotic checkpoint dysfunction through Mps1 inhibition. Adapted from Chapter 3.

Mitosis

Errors of chromosome segregation during cell division can have dramatic consequences, and to understand how they occur, we need to understand the mechanism by which a cell divides its chromosomes over its two daughter cells during mitosis.

Mitosis consists of distinct phases (Figure 1 and reviewed in [5]). In the first phase, called prophase, chromosome pairs condense by reorganization of chromatin. This shortens chromosomes to allow cell division without cutting the chromosomes (reviewed in [6]). Each pair of duplicated chromosomes (sister chromatids) is held together by ring-like protein complexes called Cohesins (reviewed in [7]). These Cohesins mediate cohesion between sisters and are loaded onto duplicated chromosomes during S-phase[8]. Cohesins can be cleaved by a protease named Separase, which relieves sister cohesion resulting in sister chromatid splitting. During the early phases of mitosis, however, the activity of Separase is inhibited by Securin until the cell is ready to undergo chromosome segregation (reviewed in [9]).

The two sisters and a central constriction site can be distinguished cytologically (Figure 2). At the site of central constriction a specialized chromosomal structure called the centromere can be identified by the presence of the specific Histone variant CENP-A (reviewed in [10,11]). A large protein complex called the kinetochore is assembled on the centromere of each sister chromatid (reviewed in [12]). Since the kinetochores are the anchor sites for attachment of spindle microtubules, they play an essential role in correctly dividing the chromosomes over the two daughter cells, which will be discussed in more detail later in this introduction. In addition, two organelles called centrosomes that organize microtubules, mature and migrate to opposite sides of the cell nucleus (reviewed in [13]). In the next phase, prometaphase, the nuclear envelope (that surrounds and protects the DNA in interphase) breaks down (Nuclear Envelope Breakdown; NEB), and a bipolar mitotic spindle that will establish connections with the chromosomes is formed. Spindle formation involves microtubule nucleation from the two opposing centrosomes, as well as from all kinetochores, with the ultimate goal to incorporate all chromosomes into the mitotic spindle in a bioriented fashion (reviewed in [14,15]).

Upon biorientation, a pair of sister chromatids is moved to the middle of the spindle, called metaphase plate (reviewed in [16]). Alignment on the metaphase plate of the final pair defines the start of the next phase, metaphase, during which critical mitotic regulatory proteins such as Cyclin B1 and Securin are degraded. This triggers cells to enter the next phase of mitosis, anaphase, during which cleavage of Cohesins by Separase causes segregation of sister chromatids that are subsequently moved to the opposite sides of the cell by the action of the mitotic spindle (reviewed in [17]). As a result, of each chromosome pair, one sister goes to one side of the cell, and the other to the other side. Two identical sets of DNA thus end up in opposite sides of the cell. In telophase, a nuclear envelope reforms around each set and the DNA decondenses. In the final phase of mitosis, the cell is physically divided in two with each containing an identical set of chromosomes by a process called cytokinesis (reviewed in [18]).

Achieving biorientation of chromosomes in the mitotic spindle

All sister chromatid pairs have to attach and biorient in the mitotic spindle for correct segregation during anaphase. But how are the right connections of microtubules to the anchor points on the chromosomes, the kinetochores, achieved?

Kinetochore-microtubule interaction

Kinetochores are trilaminar protein structures, existing of the inner kinetochore (situated closest to the centromere), the outer kinetochore, and a central linker region (reviewed in [19]). Capture and stabilization of microtubules to kinetochores depends on multiple protein complexes situated at the outer kinetochore (reviewed in [20]). The core binding site is thought to be the KMN network (consisting of KNL1, Mis12, and the Ndc80-Hec1 complex)[21, 22]. Indeed, all components of this network are needed for structural integrity of the outer kinetochore and its microtubule binding ability[23,24]. Also, the Ska complex is essential for microtubule binding by the kinetochore and its localization depends on the KMN network[25-28]. Additional proteins such as the microtubule motor CENP-E have been described to play an essential role in kinetochore-microtubule binding[29]. CENP-E was also shown to be required together with its binding partner BubR1 for stabilization of kinetochore-microtubule interactions[30-32]. In yeast, the Dam-1/DASH complex has been implicated in kinetochore-microtubule interactions, but a human homologue of this complex has not been identified (reviewed in [33]).

Attachment-error correction by the Chromosomal Passenger Complex/Aurora B

Although direct biorientation is favored due to the geometric state of the spindle[34,35] three types of non-bipolar attachments occur during the biorientation process. These are: 1) Monotelic attachment: only one kinetochore is attached to one of the poles, 2) Merotelic attachment: one kinetochore is attached to both instead of to one of the poles, and 3) Syntelic attachment: both kinetochores are connected to the same pole (Figure 3). When anaphase is initiated in the presence of one of these types of attachments, pulling forces are not equal from both sides of the cell, resulting in unequal distribution over the daughter cells and thus aneuploidy (reviewed in [36,37]). Active destabilization of such erroneous attachments is needed to provide a new opportunity to attach in a bioriented fashion. Such an attachment-error-correction mechanism exists in the function of the Aurora B kinase[38,39]. Aurora B is a member of the Chromosomal Passenger Complex (CPC) together with Survivin, INCENP and Borealin (for a review about CPC see [40]). The CPC regulates several essential mitotic processes and shows a dynamic localization pattern during mitosis. The CPC localizes on chromosome arms in prophase, where it is involved in release of cohesion between arms without affecting centromeric cohesion. It then accumulates on chromatin regions in between the sister kinetochores, called inner centromeres, for the duration of prometaphase, where it regulates sister biorientation (see below). Finally, the CPC regulates cytokinesis through translocation to the cortex and midzone of the spindle, and subsequent concentration at the cleavage furrow and midbody (reviewed in [41]).

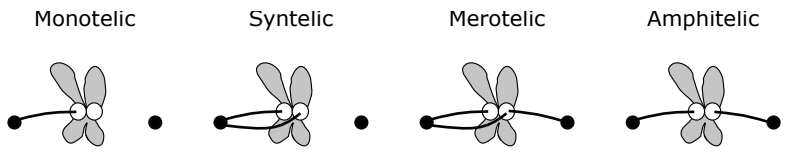

Figure 3.
Schematic representation of different types of kinetochore-microtubule attachments. All erroneous attachments have to be corrected by the attachment-error-correction mechanism in order to reach biorientation (amphitelic attachment).

Although these processes are conducted by the enzymatic activity of Aurora B, the other complex members also have distinct functions. Formation of the complex is essential for protein stability of its members[42,43]. Centromere localization of the complex depends on Survivin binding to INCENP and this was suggested to be mediated by Borealin[43,44]. Survivin and the amino-terminal helices of Borealin and INCENP together form a three-helical bundle that functions as the localization domain of the CPC, at least to the central spindle and midbody[45]. Phosphorylation of Survivin by Aurora B was also shown to be involved in localizing the CPC[46]. Aurora B is thought to auto-activate through auto-phosphorylating its activation loop by local clustering of the CPC[47]. Auto-activation is further enhanced by phosphorylation of INCENP on a TSS motif by Aurora B that induces an activating conformational change in Aurora B[48,49]. Aurora B also phosphorylates Borealin *in vitro*[50], but a biological function for this phosphorylation has not been described.

During prometaphase, the CPC selectively corrects erroneous attachments by destabilizing such attachments. Phosphorylation of the Ndc80-Hec1 complex by Aurora B *in vitro* weakens kinetochore-microtubule interactions[21,51]. More specifically, Aurora B phosphorylates the positively charged N-terminal microtubule-binding tail domain of Hec1 *in vitro*, and it was proposed that this prevents the tight binding of Hec1 and thus kinetochores to the negatively charged microtubules[52]. Another described mechanism by which Aurora B controls kinetochore-

microtubule attachments is by reducing the activity of the kinesin 13 microtubule depolymerase MCAK through phosphorylation[53,54]. Preventing or mimicking MCAK phosphorylation by Aurora B causes syntelic attachments[55] and MCAK is enriched at merotelic attachment sites in *Xenopus* S3 cells where it is phosphorylated by Aurora B[56]. Although some intriguing hypotheses have been put forward, it is unknown how inhibition of MCAK facilitates error-correction. Finally, in yeast, phosphorylation of Dam1 by Ipl1 (the budding yeast homologue of Aurora B) was proposed to be involved in the biorientation process[57,58].

In order to reach stable biorientation, Aurora B should leave attachments of bioriented sister chromatid pairs intact but destabilize erroneous attachments. Pulling forces from both poles on a bioriented pair results in mechanical tension and it was shown by D. Liu *et al.* that this tension results in spatial separation of Aurora B, located at the inner centromere, from its substrates on the outer kinetochores[59]. This reduces phosphorylation by Aurora B and increases stability of bioriented attachments, making it possible to achieve biorientation of all sister chromatid pairs (reviewed in [60]). Thus, Aurora B can selectively target kinetochore pairs that are not under full tension and destabilize erroneous attachments, until all chromosomes have stably bioriented.

Regulation of Anaphase Initiation

The error-correction mechanism under Aurora B control serves well to achieve biorientation. However, cells must in some way sense that biorientation is not achieved yet and hold anaphase initiation as long as needed. In order to understand this, it is essential to understand how anaphase is initiated in the first place.

The Anaphase Promoting Complex/Cyclosome (APC/C)

To initiate anaphase, Securin and Cyclin B need to be degraded. Securin protects Cohesin, a protein complex essential for sister chromatid cohesion, from the proteolytic cleavage activity of Separase. Securin degradation therefore leads to Cohesin cleavage, relieving the cohesion between sister chromatids (reviewed in [61]). Mitotic exit is initiated by degradation of Cyclin B. Cyclin B, as an activator of the mitotic kinase Cdk1, is required for mitotic entry by regulating numerous events, like nuclear envelope breakdown, chromosome condensation and spindle assembly. Degradation of Cyclin B inactivates Cdk1 and reverses all these events (reviewed in [62]).

The destruction of Securin and Cyclin B, as well as various other mitotic proteins, is mediated by the Anaphase Promoting Complex/Cyclosome (APC/C). APC/C is an E3 ubiquitin ligase that targets its substrates for degradation by the 26S proteasome. APC/C functions in mitosis in conjunction with the ubiquitin-conjugating enzymes (E2s) UbcH10 and Ube2S[63-67]. Substrates of APC/C require a specific motif that is recognized by the co-activators of APC/C, Cdc20 and Cdh1. The D-box motif (RxxL) can be recognized by both APC/C^{Cdc20} and APC/C^{Cdh1}, and the KEN-box motif (KEN) is more specifically required for recognition by APC/C^{Cdh1} after anaphase and in G1[68,69]. Right after NEB, APC/C^{Cdc20} is activated and ubiquitinates substrates like Cyclin A[70,71], needed for mitotic entry (reviewed in [72]), and Nek2A, implicated in centrosome separation[73]. To prevent chromosome missegregations, however, premature APC/C^{Cdc20} activity specifically towards Securin and Cyclin B is kept in check by the action of the mitotic checkpoint (discussed in detail in the next section) until full stable biorientation is reached.

Without APC/C activity, mitotic exit and therefore growth and regeneration are not possible. This is best illustrated by several studies done *in vivo*. APC/C mutations in flies caused late larval lethality and metaphase arrest in dividing cells[74]. In zebrafish and worms, APC/C mutations caused mitotic arrest followed by cell death[75,76]. In mice, loss of APC/C during embryogenesis

is lethal before embryonic day E6.5. Conditional inactivation of one of the subunits of APC/C, APC2, in quiescent hepatocytes resulted in re-entry into the cell cycle, followed by a metaphase arrest, causing liver failure[77]. Similarly, mice lacking Cdc20 function showed failed embryogenesis. Embryos arrested in metaphase at the two-cell stage with high levels of Cyclin B[78]. These studies all show that mitotic APC/C activation is absolutely essential for mitotic progression *in vivo* in a variety of organisms.

The Mitotic Checkpoint

Inhibition of APC/C^{Cdc20} specifically towards Securin and Cyclin B is achieved by a signaling cascade called the mitotic checkpoint that originates from unattached kinetochores (Figure 4). This signaling cascade is so robust that the signal of even one unattached kinetochore is sufficient to ensure that anaphase is not initiated before all chromosomes are attached[79]. Several proteins have been described in human cells to be essential for this checkpoint. These proteins (Mad1, Mad2, Bub3, and the kinases BubR1, Bub1, and Mps1) are considered to be the core checkpoint effectors, as depletion of these proteins leaves kinetochore structure intact, but abrogates the mitotic checkpoint. These checkpoint proteins all localize to unattached or non-bioriented kinetochores specifically, which is an essential feature of proteins involved in mitotic checkpoint signaling (Figure 4 and reviewed in [80]).

Although all the checkpoint proteins are essential for efficient checkpoint signaling, only a subset is involved in direct inhibition of APC/C^{Cdc20}. A mitotic checkpoint complex (MCC), initially reported to contain Mad2, BubR1 and Bub3[81-84], directly binds Cdc20 and inhibits the APC/C. These proteins were found to exchange rapidly on unattached kinetochores[85], supporting the idea that unattached kinetochores serve as a platform for a diffusible checkpoint signal in the form of an inhibitory complex (reviewed in [86]).

One of the members originally described as part of the MCC is the kinase BubR1. BubR1 can directly bind and inhibit Cdc20 *in vitro*[87-89] and was found in complex with inactive APC/C^{Cdc20} in cells that have engaged the mitotic checkpoint[82,90-92]. BubR1 is thought to act as a pseudo-substrate inhibitor of APC/C^{Cdc20} by competing with APC/C substrates through its KEN- and D-boxes[93,94].

Although BubR1 is a clear APC/C^{Cdc20} inhibitor *in vitro*, BubR1 acts synergistically with Mad2, and both are needed *in vivo* for efficient checkpoint function[87,95]. Mad2 undergoes a conformational change following dimerization with Mad1-bound Mad2 on unattached kinetochores. This change catalyzes Mad2-Cdc20 interaction that is essential for APC/C inhibition by MCC[96-99]. Since Mad1-bound Mad2 is identical to Cdc20-bound Mad2[100,101], it has been postulated that structural activation of Mad2 by dimerization can also occur on Cdc20-Mad2 complexes in the cytoplasm, potentially allowing fast amplification of the checkpoint signal[98]. Although never proven, such cytoplasmic amplification could account for the observation that only one unattached kinetochore is sufficient to halt anaphase (reviewed in [102]).

Despite the fact that Mad2 is needed for catalysis of MCC formation and checkpoint signaling, the initial observations that Mad2 is an actual component of MCC is now debated. Mad2 was proposed to facilitate checkpoint signaling by aiding formation of a BubR1-Bub3-Cdc20 complex, recently put forward as the actual APC/C inhibitory complex[103,104]. This relay model, however, does not yet account for the seemingly stoichiometric amounts of Mad2 found in APC/C-MCC affinity purification[82]. The question remains how MCC inhibits APC/C. Although mere Cdc20 sequestration was a favored model some years ago, recent structural analysis of APC/C-MCC complexes showed that binding of a BubR1-containing MCC complex causes a conformational change of APC/C^{Cdc20} that locks it in a closed, inactivated state[82]. This

suggests that MCC may have direct effects on the APC/C, but the exact mode of inhibition remains to be determined.

Although not implicated directly in APC/C^{Cdc20} inhibition, the other checkpoint proteins such as Mad1, Bub1, and Mps1 are required for checkpoint signaling (reviewed in [80]). As discussed above, Mad1 is essential for Mad2 recruitment to kinetochores and catalysis of MCC. Bub1 and Mps1 are protein kinases of which the activity is crucial for checkpoint signaling. Phosphorylation events are thus important in the checkpoint and could serve, for instance, to amplify the signal or allow rapid activation/inactivation of the signal. Bub1 was suggested to signal in the mitotic checkpoint by phosphorylating and thereby inhibiting Cdc20[105]. The kinase activity of Mps1 is required to recruit Mad1 and Mad2 to the kinetochores[106,107]. However, upstream regulation of Mps1 and the downstream signaling to Mps1 substrates in the checkpoint is unclear. The work presented in this thesis is focused on revealing this, and Mps1 is discussed in more detail later in this introduction.

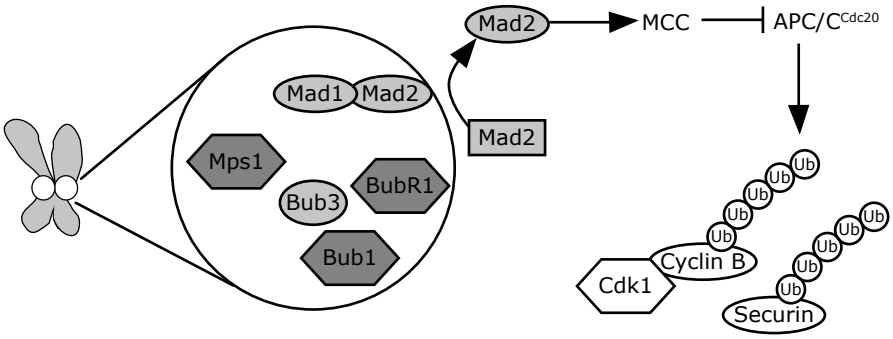

Figure 4.
Schematic representation of the mitotic checkpoint originating from an unattached kinetochore. MCC (Bub3, BubR1, (Mad2), see text for clarification) inhibits APC/C^{Cdc20} activity towards Securin and Cyclin B to prevent anaphase.

The above described checkpoint signaling is mediated through unattached kinetochores, but syntelically attached kinetochores are thought to indirectly activate the mitotic checkpoint as well. Aurora B destabilizes syntelic attachments through the attachment-error-correction mechanism, creating unattached kinetochores that can subsequently catalyze MCC production[108]. Although Aurora B is also involved in correction of merotelic attachments[109], this does not trigger the mitotic checkpoint as no transient unattached state occurs during the correction process. Merotelic attachments are therefore thought to be an important contributor to aneuploidy (reviewed in [36]).

Silencing the mitotic checkpoint

When all chromosomes are stably bioriented on the metaphase plate, the mitotic checkpoint must be silenced to allow for APC/C^{Cdc20} activation towards Securin and Cyclin B in order to initiate anaphase. Several mechanisms have been described to regulate this.

One of the simplest explanations lies in reduced concentration of checkpoint proteins on stably bioriented kinetochores[110], which would reduce checkpoint signaling and activate APC/C^{Cdc20}. This process is mediated by active, dynein-mediated transport of checkpoint proteins such as Mad2 and BubR1 along kinetochore bound microtubules towards centrosomes[111].

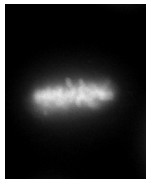

Besides reducing concentrations of checkpoint proteins on kinetochores, inhibition of some of these proteins can also result in checkpoint silencing. A described mechanism for checkpoint silencing as such is loss of BubR1 activation by the kinesin motor protein CENP-E upon microtubule binding[112,113]. CENP-E is an essential part of the mitotic checkpoint in *Xenopus* egg extracts[114] through direct activation of BubR1 in the absence of microtubules[112]. Microtubule capture by CENP-E relieves BubR1 activation and thereby inactivates the checkpoint [112,113].

Another checkpoint silencing mechanism is direct Mad2 inactivation through the action of p31^{comet} [115,116]. Purified p31^{comet} antagonizes the ability of Mad2 to inhibit APC/C^{Cdc20} *in vitro* and in *Xenopus* extracts, and depletion of p31^{comet} in cells led to a delay in mitotic exit[115,117]. Interestingly, although unrelated in primary sequence, p31^{comet} is a structural mimetic of Mad2 and prevents Mad2 activation by dimerizing with Mad1- or Cdc20-bound Mad2[115,116]. Mad2 inactivation by phosphorylation was also described as a possible contributing mechanism of checkpoint silencing. Although an upstream kinase is not known, Mad2 is heavily phosphorylated upon mitotic exit, and a phospho-mimetic mutant of Mad2 did not bind Mad1 or APC/C, and compromised the checkpoint[118].

Yet another way proposed to silence the checkpoint is mediated through a feedback loop by APC/C itself, by targeting the MCC. First, APC/C was shown to multi-ubiquitinate Cdc20[103,119], and S. Reddy *et al.* suggested that Cdc20 multi-ubiquitination destabilizes MCC, thereby enhancing APC/C^{Cdc20} activity to induce anaphase. They showed that this signaling depends on the E2 UbcH10. In addition, it was shown that silencing of the checkpoint in this way was counteracted by the de-ubiquitination enzyme USP44 *in vitro* and *in vivo*. Purified USP44 directly promotes de-ubiquitination of Cdc20, and USP44 depletion from cells increases Cdc20 ubiquitination and reduces Cdc20-Mad2 binding[120]. In disagreement with this proposed mechanism however, J. Nilsson *et al.* propose that Cdc20 ubiquitination achieves the opposite effect by aiding the checkpoint in keeping Cdc20-directed APC/C activity low[103]. Second, APC/C^{Cdc20}-mediated degradation of BubR1 was suggested to drive further APC/C^{Cdc20} activation and anaphase initiation. BubR1 was shown to be acetylated in prometaphase by the PCAF acetyl transferase. As BubR1 acetylation-site mutants were degraded by the APC/C, it was proposed that acetylation of BubR1 protects it from ubiquitination and is important for sustained checkpoint activity and that de-acetylation is needed for checkpoint silencing[121].

Although all described mechanisms may (in part) account for checkpoint silencing upon stable biorientation, the exact mechanism remains to be elucidated.

Mps1

Mps1 (Monopolar Spindle 1) was originally identified in the budding yeast *Saccharomyses cerevisae* (Mps1p) as a dual-specificity kinase important for spindle pole body (centrosome in vertebrates) duplication and cell cycle control[122,123], and found to be essential for checkpoint signaling[124,125]. Later, a functionally related protein was found in *Saccharomyses pombe* (Mph1 or Mps1p-like pombe homolog). Mph1 was reported not to be required for spindle pole duplication, but for checkpoint activation in response to spindle defects. Moreover, Mph1 was found to function upstream of Mad2, and overexpression of Mph1, like overexpression of Mad2, resulted in a metaphase arrest[126]. Several vertebrate homologs were identified shortly after *S. cerevisiae* Mps1p: hMps1 in humans (also called TTK or PYT)[127,128] and mMps1p (also called Esk) in mice[129]. hMps1 was found to be a dual-specificity kinase involved in cell cycle control and its activity and phosphorylation state increased upon mitotic checkpoint activation[127,128,130]. It nevertheless took several years and the identification of the *Xenopus* Mps1 homolog (xMps1) to ascribe a

role to Mps1 in the vertebrate mitotic checkpoint. Both human and *Xenopus* Mps1 localize to unattached kinetochores and act upstream of Mad1 and Mad2 kinetochore localization in a kinase-dependent manner[106,131]. Mps1 was further shown to associate with APC/C, suggesting a role for Mps1 more downstream in the checkpoint signaling cascade[106].

Comparable to the yeast Mps1p, mouse Mps1 was described to localize to centrosomes and to function in centrosome duplication[132]. For human Mps1, though, this role has always been debated. V. Stucke and co-workers showed that centrosome duplication is independent of hMps1[130], but H. Fisk and co-workers subsequently showed that hMps1 is required for centrosome duplication[133]. In support of this, Mps1 was shown to accelerate centrosome duplication by phosphorylation of Mortalin, a member of the Hsp70 chaperone protein family. Phosphorylated Mortalin in addition super-activates Mps1 on centrosomes[134].

The checkpoint function of Mps1 is evolutionary conserved and undebated. However, upstream regulation of Mps1 and downstream signaling in the checkpoint is largely unknown. Mps1 not only localizes to kinetochores, but also exchanges rapidly, like other checkpoint proteins such as BubR1 and Mad2[85]. It is unknown, however, how Mps1 is recruited to kinetochores or how its exchange is regulated. It was shown though that kinetochore localization of Mps1 depends on its non-catalytic N-terminal domain[106,135] and the presence of the Ndc80-Hec1 complex and the PRP4 kinase[135,136]. Furthermore, the C-terminal catalytic domain has affinity for microtubules, and microtubule binding may contribute to regulation of the kinase activity[135].

A few potential substrates of Mps1 in the mitotic checkpoint have been proposed. Mps1p can phosphorylate Ndc80/Hec1 *in vitro* and a phosphorylation-site mutant of Ndc80 compromised the mitotic checkpoint in yeast[137]. Nevertheless, although a phospho-mimetic Ndc80 mutant behaved normally with respect to microtubule binding and chromosome alignment, it could not restore checkpoint signaling in Mps1 deficient yeast cells[137]. Ndc80 is therefore unlikely to be the major effector of Mps1 in the mitotic checkpoint in yeast. In human cells, phosphorylation of the checkpoint protein BubR1 on four essential sites was found to partially depend on Mps1, but direct phosphorylation of BubR1 by Mps1 was not shown[138]. Another potential Mps1 substrate in the human checkpoint is BLM, a member of the RecQ helicases that are required for maintenance of genomic stability[139,140]. Mps1 directly phosphorylates BLM on multiple residues and cells expressing phospho-mutants of BLM displayed compromised ability to arrest in response to spindle poisons[141]. In yeast, direct phosphorylation of Mad1 by Mps1 was shown and implied to function in spindle checkpoint activation[125], but this has never been shown in other organisms.

Other downstream targets of Mps1 have been described, but are unlikely to mediate Mps1 function in mitotic checkpoint signaling. In a *Xenopus in vitro* system, phosphorylation by Mps1 was shown to relieve auto-inhibition of the kinesin motor protein CENP-E. As CENP-E is involved in chromosome congression, the authors suggested a role for Mps1 in control of chromosome congression through direct control of CENP-E[142]. In yeast, Mps1 was shown to phosphorylate Dam-1, thereby regulating efficient coupling of kinetochores to microtubules[143], however a human homologue of Dam1 has not been described. Another downstream target of Mps1 implicated Mps1 signaling in the DNA-damage response. The DNA damage checkpoint kinase CHK2, which stabilizes and activates its downstream target p53 by phosphorylation, was shown to be directly phosphorylated by Mps1 *in vitro*[144]. In human cells, depletion of Mps1 reduced CHK2 phosphorylation and impaired DNA-damaged induced growth arrest. In addition to this, Mps1 is negatively regulated by p53 upon DNA damage, and contributes to apoptosis of p53 mutant cells in response to DNA damage[145]. Possible cross-talk between the mitotic checkpoint and the DNA damage checkpoint is interesting, however a possible mechanism or function remains unclear.

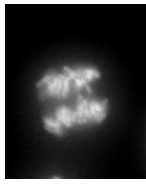

Implication of the Mitotic Checkpoint in Cancer

Tumorigenesis and the mitotic checkpoint

Loss of checkpoint function results in gross chromosome missegregations and eventually cell death[95,146]. However, it has been known for long that the majority of tumor cells are aneuploid[147] (reviewed in [148,149]), and increased rates of chromosome loss and gain (chromosomal instability or CIN) in cells derived from human tumors have been reported[150]. It has been suggested through several *in vivo* model systems that weakening of the mitotic checkpoint contributes to carcinogenesis, or may even induce spontaneous tumor formation (reviewed in [4]). Some examples of such systems are given below.

Homozygous deletion of Mad1 or Mad2 (-/-) in mice led to embryonic lethality, and early embryonic cells displayed gross chromosome missegregations and eventually cell death. Mice with heterozygous deletion of Mad1 or Mad2 (+/-) survived, but primary embryonic fibroblasts were more prone to become aneuploid compared to their wild-type counterparts[151,152]. Interestingly, $Mad2^{+/-}$ mice developed lung tumors at high rates at older age[153], and $Mad1^{+/-}$ mice displayed an increase of tumors in a large variety of tissues at older age[152]. Conversely, Mad2 levels are frequently increased in human tumors[154-156] and mice overexpressing Mad2 have high rates of aneuploidy and a wide range of neoplasias[157]. These studies imply a role for defects in mitotic checkpoint and aneuploidy in spontaneous tumorigenesis. On the other hand, heterozygous deletion of other checkpoint proteins (Bub1, Bub3 and BubR1) did not lead to spontaneous tumor formation, despite development of aneuploidy[158-161]. Nevertheless, treating $Bub3^{+/-}$ or $BubR1^{+/-}$ mice with carcinogens increased the level and speed of tumor formation[160,161]. Importantly, hypomorphic Bub1 mice that expressed less than 20% of Bub1 had significant increases in spontaneous formation of multiple tumors[159]. Furthermore, crossing Bub1 hypomorphs or $BubR1^{+/-}$ mice with $APC^{min/+}$ mice sensitized these mice to spontaneous formation of colonic tumors[162,163]. Bub1 hypomorphs also increased incidence of thymic lymphomas in p53 heterozygous mice[162]. These studies therefore imply that defects in the mitotic checkpoint and the resulting aneuploidy are not enough for spontaneous tumor formation, but can contribute to the efficiency of tumor formation when it is triggered by other events.

Surprisingly, Bub1 insufficiency had no impact on tumorigenis in $Rb^{+/-}$ mice and prevented neoplasia formation in the prostate of PTEN heterozygous mice[162]. Comparably, heterozygous deletion of CENP-E, which induces low rates of aneuploidy and slightly increases spontaneous tumor incidence, decreased tumor formation when tumors were induced with carcinogens or by homozygous deletion of the p19arf tumor suppressor[164].

These studies together show that the effect of aneuploidy on tumor formation is not straightforward. Effects seen in the different models seem to depend on tissue type, and additional functions of checkpoint proteins may account for the differences between models (reviewed in [165]). Also, the effects of the heterozygous deletions in these models are not inducible in an adult mouse. Instead they are present from early development, and these possible early effects cannot be excluded to play a role in later tumor formation. This makes it hard to compare with tumor formation in humans. Overall, answering the question whether aneuploidy can trigger tumor formations still remains largely unanswered.

The mitotic checkpoint as a therapeutic target

Since tumor cells cycle very rapidly, the mitotic checkpoint is an interesting target for cancer treatment. Most sporadic tumor cells are aneuploid and a significant fraction of those are likely to be chromosomally instable (CIN). This CIN phenotype may sensitize cells to cell death

by induction of extra chromosome missegregations through mitotic checkpoint inhibition[166], (reviewed in [4]). This could potentially result in selective killing of CIN tumors, while sparing healthy tissue. A possible downside to this approach is that partial inhibition could sensitize healthy tissue to tumorigenesis, or even induce tumor formation. Therefore, careful analyses have to be done in *in vivo* model systems to find out what the effect of checkpoint inhibition is on existing tumors and on the whole organism.

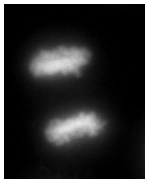

Scope of this thesis

As described earlier, many aspects of upstream regulation of Mps1 and downstream signaling in the checkpoint remain to be elucidated. The research described in this thesis focuses on Mps1 biology since Mps1 is an evolutionary conserved protein with a conserved essential function in the mitotic checkpoint. The fact that Mps1 is a protein kinase makes it a candidate contributor to amplification of the checkpoint signal and its activity could enable a faster switch from an active checkpoint to silencing of the checkpoint compared to for example protein degradation or translation events. With regards to cancer, Mps1 could be a good therapeutic target, especially because it is a kinase that can potentially be inhibited in the patient through administration of an inhibitory chemical compound.

In order to study Mps1 function in mitosis and the mitotic checkpoint, we designed an RNAi-based system in which endogenous Mps1 can be replaced by mutant alleles of Mps1. In addition, a potent Mps1 kinase inhibitor was developed and analyzed for specificity in collaboration with the Gray lab at Harvard Medical School, which opened new opportunities to study the effects of (short-term) Mps1 inhibition on mitosis and the mitotic checkpoint.

Outline of this thesis

In **Chapter 2**, we describe that Mps1 kinase activity is essential for mitotic checkpoint signaling and chromosomal stability. In this study, a previously unknown role for Mps1 activity in the attachment-error-correction mechanism was found. Mps1 phosphorylates Borealin, member of the CPC, thereby enhancing Aurora B activity. Through this pathway, Mps1 activity was found to be essential to achieve full biorientation of chromosomes. In **Chapter 3**, a novel selective Mps1 inhibitor (Mps1-IN-1) is presented. In **Chapter 4**, we investigated the mechanistic role of Mps1 in mitotic checkpoint signaling by examining the interplay between MCC, APC/C and Mps1. We found that Mps1 prevents APC/C mediated disassembly of MCC to maintain a mitotic arrest. In **Chapter 5**, identification of an auto-phosphorylation event on Mps1 that is required for full kinase activity and checkpoint signaling is described. Auto-phosphorylation on Threonine 676, which resides in the activation loop of the kinase domain, is required to prevent chromosome missegregations, but not cell death. A non-phosphorylatable mutant leads to chromosomal instability, showing that maximal Mps1 activity is needed for error-free chromosome segregation. In **Chapter 6**, we describe that Mps1 inhibition leads to a decrease in its turnover rate at unattached kinetochores and elevation of Mps1 protein levels on kinetochores. Preventing active Mps1 from turnover on kinetochores results in prolonged metaphase by chronic engagement of the mitotic checkpoint. Furthermore we show that Mps1 continuously directs its own release from kinetochores, and conclude that this allows satisfaction of the mitotic checkpoint and a fast metaphase-to-anaphase transition. In **Chapter 7**, our results described in this thesis are summarized and discussed in light of the present literature. Some future directions for research on Mps1 regulation and function are proposed.

Chapter 2

Mps1 phosphorylates Borealin to control Aurora B activity and chromosome alignment

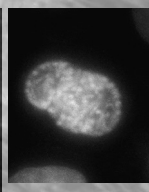

Nannette Jelluma[1,2], Arjan B. Brenkman[2], Niels J.F. van den Broek[2], Carin W.A. Cruijsen[1], Maria H.J. van Osch[2], Susanne M.A. Lens[1], René H. Medema[1], and Geert J.P.L. Kops[1,2]

[1]Department of Medical Oncology, Laboratory of Experimental Oncology, [2]Department of Physiological Chemistry and Cancer Genomics Centre UMC, Utrecht, Universiteitsweg 100, 3584 CG Utrecht, The Netherlands

Adapted from *Cell 132, 233-246, January 25 2008*

Abstract

Maintenance of chromosomal stability relies on coordination between various processes that are critical for proper chromosome segregation in mitosis. Here we show that monopolar spindle 1 (Mps1) kinase, which is essential for the mitotic checkpoint, also controls correction of improper chromosome attachments. We report that Borealin/DasraB, a member of the complex that regulates the Aurora B kinase, is directly phosphorylated by Mps1 on residues that are crucial for Aurora B activity and chromosome alignment. As a result, cells lacking Mps1 kinase activity fail to efficiently align chromosomes due to impaired Aurora B function at centromeres, leaving improper attachments uncorrected. Strikingly, Borealin/DasraB bearing phosphomimetic mutations restores Aurora B activity and alignment in Mps1-depleted cells. Mps1 thus coordinates attachment error correction and checkpoint signaling, two crucial responses to unproductive chromosome attachments.

Introduction

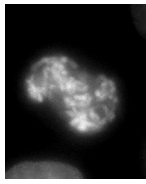

Equal segregation of chromosomes during cell division depends on a coordinated effort to attach and align all chromosomes before onset of anaphase. Proper execution of these processes is monitored by the mitotic checkpoint that halts cell-cycle progression until all paired sister chromatids are attached via their kinetochores to opposite poles (bioriented) and aligned on the metaphase plate. The mitotic checkpoint responds to lack of attachment of kinetochores to spindle microtubules or lack of tension between kinetochores of sister chromatids. Checkpoint signal transduction from the kinetochore depends on several kinases including Bub1, BubR1, and Mps1, and culminates in production of an inhibitor of the E3 ubiquitin ligase anaphase-promoting complex/cyclosome (APC/C), whose activity is required for anaphase onset[167]. The mitotic checkpoint is necessarily active when chromosomes establish bipolar attachments in order to align. Interestingly, some proteins essential for checkpoint signaling also contribute to attachment processes. For example, generation of stable attachments of kinetochores to spindle microtubules requires BubR1[30,168], while Bub1 is essential for centromeric cohesion in prometaphase[169,170] and establishment of end-on attachments[171,172]. Recently, TAO1/MARKK was found to be a novel kinase that is essential for both the mitotic checkpoint and chromosome alignment[173]. These kinases are therefore crucial activities in coordinating various mitotic processes, but direct substrates that exert control over these processes have yet to be identified for any of the kinases.

In early mitosis, as chromosomes attempt to biorient, various erroneous attachments are made that result in lack of tension between sister centromeres and that need to be corrected to allow proper chromosome alignment. This attachment error correction is controlled by the chromosomal passenger complex (CPC) of which the Aurora B kinase is the effector enzyme[38,39,168,174]. In vertebrates, the CPC facilitates error correction by Aurora B-dependent phosphorylation of the microtubule-binding Ndc80/Hec1 complex and the kinesin 13 microtubule depolymerase MCAK[21,53,55,175]. Aurora B activity is also required for the checkpoint response to lack of tension, likely through creating unattached kinetochores during the correction process[108], but direct, microtubule-independent involvement of Aurora B in checkpoint function has also been suggested[176,177]. At the metaphase-to-anaphase transition, Aurora B relocates from centromeres to the central spindle, where it conducts the final stages of cytokinesis. Besides Aurora B, the CPC includes INCENP, Survivin, and Borealin/DasraB (hereafter referred to as Borealin)[47,50,178-180]. Although specific functions in the spatiotemporal control of Aurora B activity have been suggested for each of these auxiliary proteins[181], a clear picture for how Aurora B is localized and activated at centromeres is lacking.

In *Saccharomyces cerevisiae*, Mps1 controls spindle-pole body duplication[122], spindle assembly[182], and the spindle-assembly checkpoint[124]. Mutant Mps1 alleles or chemical inhibition in yeast have implicated the enzymatic activity of Mps1 in its control over these processes[182-184]. In higher eukaryotes, the only undebated role for Mps1 during mitosis is in the mitotic checkpoint[106,130,131], which in *Xenopus* egg extracts depends on its kinase activity[131]. Mps1 has further been implicated in centrosome duplication, though this is controversial[130,133].

Using shRNA-based protein replacement, we set out to investigate the contribution of Mps1 kinase activity to mitotic progression in human cells. Here we show that Mps1 kinase activity is essential for chromosome alignment by enhancing Aurora B activity at the centromere, and we identify the Aurora B-regulatory protein Borealin/DasraB as an essential substrate that mediates this novel function of Mps1.

Results

Mps1 Kinase Activity Is Essential for Mitotic Checkpoint Signaling and Chromosomal Stability

To investigate what mitotic processes in human cells rely on Mps1 kinase activity, endogenous Mps1 was replaced with a kinase-deficient mutant of Mps1 (D664A)[130] in human cancer cell lines by simultaneous expression of plasmid-based Mps1 shRNA and RNAi-insensitive epitope-tagged Mps1 alleles (LAP-Mps1)[185] (Figures 1A, 1B, and S1A; see Experimental Procedures for details). Depletion of Mps1 prevented cells from accumulating in mitosis upon treatment with the spindle poison nocodazole, confirming a role for Mps1 in mitotic checkpoint activation (Figures 1C and 1D)[106,130,131]. Similar results were obtained with taxol (Figure S1B). As reported previously[106,107,133], the essential mitotic checkpoint proteins Mad1 and Mad2 but not CENP-E, BubR1 or Bub1 were absent from unattached kinetochores of cells lacking Mps1 (Table S1 and Figure S1C). Mitotic checkpoint signaling in response to nocodazole (Figures 1C and 1D) and taxol (Figure S1B), as well as Mad1 localization (Figures S1C and S1D) were restored by expression of wild-type but not kinase-dead Mps1 to similar levels. This proves that kinase activity of Mps1 is indispensable for the mitotic checkpoint in human cells. As expected from previous studies on mitotic checkpoint inhibition[95], Mps1 kinase activity was also essential for the maintenance of ploidy and survival of human cancer cells (Figures S1E and S1F).

To get insight into the roles of Mps1 kinase activity during unperturbed mitosis, chromosome segregation was analyzed by timelapse microscopy of chromosomes loaded with fluorescent histones (H2B-EYFP). Anaphase A movements were apparent in 69% of Mps1-depleted cells but the majority of those cells initiated anaphase with misaligned chromosomes (Figure 1E and Movie S1). In the remaining 31% of cells no metaphase plate was formed and no anaphase was noticeable before the onset of cytokinesis. Instead, cells displayed a "cut" phenotype: chromosomes remained condensed and hardly moved before the DNA pack was split in two by the incoming cleavage furrow during cytokinesis (Figures 1E, 1F, and Movie S2). Since Mps1 shRNA was transfected transiently, the difference in severity of the two observed phenotypes may be explained by differences in extent of knockdown of Mps1. Nevertheless, regardless of whether anaphase was observed or not, reducing Mps1 protein levels resulted in massive chromosome missegregation in 82% of all divisions analyzed (Figure 1E). This could be attributed specifically to inhibition of Mps1 kinase activity, as re-expression of shRNA-insensitive wild-type but not kinase-dead Mps1 restored proper chromosome segregation (Figures 1E and 1G).

Efficient Chromosome Alignment Requires Mps1

Initiation of chromosome segregation in the presence of misaligned chromosomes in cells lacking Mps1 kinase activity could simply have been due to premature APC/C activation, or may have been caused by problems in chromosome alignment. To discriminate between these possibilities, exit from mitosis was blocked by treatment with the proteasome inhibitor MG132, allowing cells more time to align their chromosomes. Strikingly, the majority of Mps1-depleted cells had misaligned chromosomes even after spending one hour in mitosis, while control cells had reached full alignment during this time (Figure 2A). These misalignments were independent of mitotic checkpoint inactivity, as cells depleted of Mad2 had no difficulty aligning all chromosomes (Figure 2B)[30]. Analysis of chromosome movements in real time further revealed that 85% of Mps1-depleted cells versus 10% of control cells showed misaligned chromosomes 30 min after entry into mitosis in the presence of MG132 (Figures 2C and 2D). After 2 hr, 52% of Mps1-depleted cells still contained one or more chromosomes that had not reached the metaphase plate compared to 3% of mock-shRNA cells. Replacement of endogenous Mps1 with a kinase-

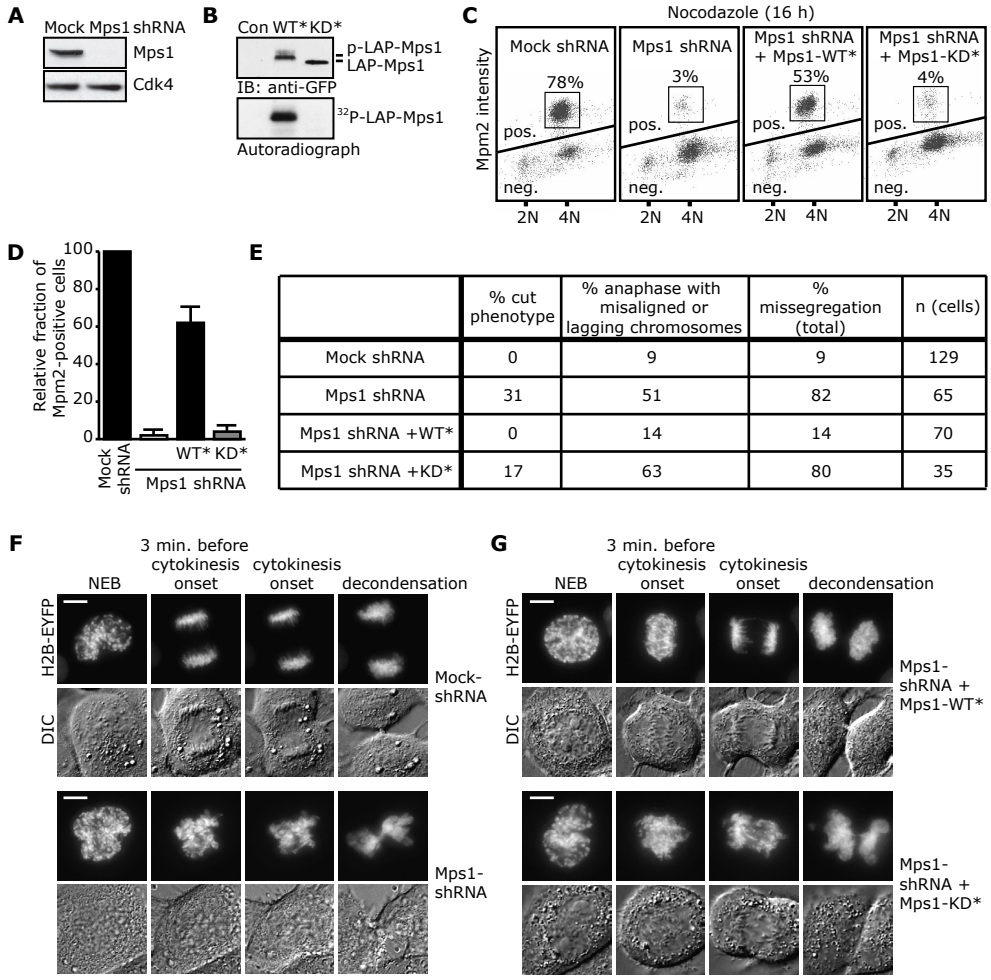

	% cut phenotype	% anaphase with misaligned or lagging chromosomes	% missegregation (total)	n (cells)
Mock shRNA	0	9	9	129
Mps1 shRNA	31	51	82	65
Mps1 shRNA +WT*	0	14	14	70
Mps1 shRNA +KD*	17	63	80	35

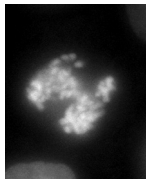

Figure 1. Mps1 Kinase Activity Is Essential for Mitotic Checkpoint Signaling and Chromosome Segregation

(A) Immunoblots of lysates of U2OS cells transfected with the indicated shRNA plasmids. (B) Kinase activity of anti-GFP immunoprecipitates of cells transfected with empty vector (Con) or RNAi-resistant (indicated by asterisks) LAP-tagged wild-type (WT*) or kinase-dead (KD*) Mps1. (C and D) Flow cytometric analysis of Mpm2 positivity within a population of cells transfected with mock or Mps1 shRNA plasmids along with the indicated RNAi-resistant Mps1 alleles and treated with nocodazole for 16 hr. Cells considered positive (pos.) or negative (neg.) for Mpm2 are indicated. Graph in (D) represents averages of five independent experiments (+/- SD). (E) Table summarizing data of timelapse analyses as performed under (F) and (G). "Percent anaphase with misaligned or lagging chromosomes" indicates all abnormal segregations in which anaphase chromosome movements were observed (excluding "cut" phenotypes). (F and G) Timelapse analysis of chromosome segregation (H2B-EYFP) and morphology (DIC) of cells transfected with H2B-EYFP along with the indicated shRNA plasmids (F) in combination with either empty vector or the various RNAi-resistant Mps1 alleles (G). Stills from the timelapse analyses that represent the indicated stages are presented. Scale bars are 5 μm.

dead mutant showed that chromosome alignment required Mps1 kinase activity (Figure 2E). In agreement with this, simultaneous treatment of prophase cells with MG132 and SP600125, a small molecule that inhibits Mps1 in mitotic human cells[186], caused severe misalignments that persisted until removal of the inhibitor 75 min after addition (Figure 2F and Movie S3). Together, these data show that Mps1 activity contributes to alignment of chromosomes on the metaphase plate in mitosis.

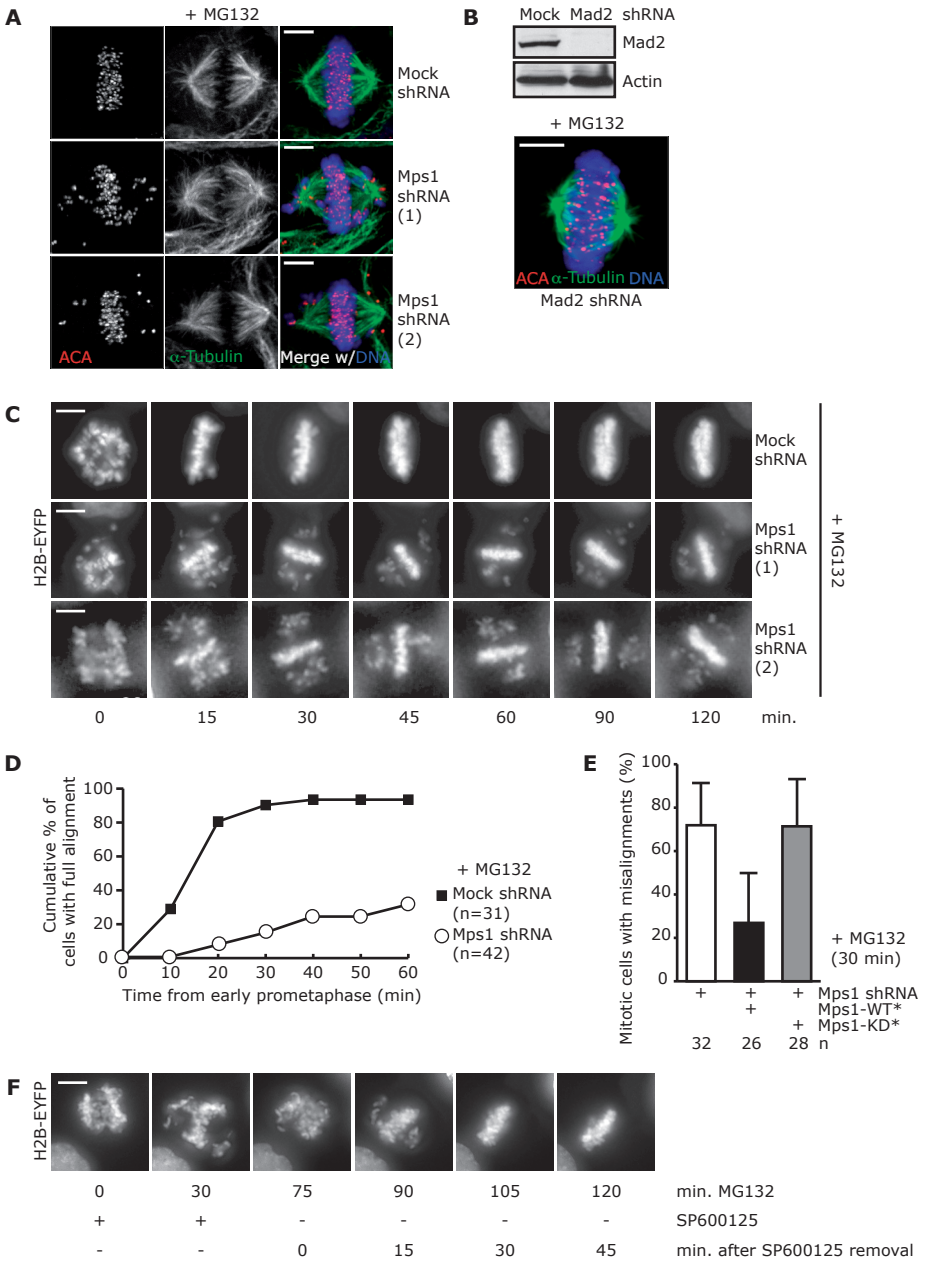

Interactions between Kinetochores and Spindle Microtubules Are Stable in Cells Lacking Mps1

We next examined what process required for chromosome alignment was defective in Mps1-depleted cells. The following observations suggested that misalignments were not caused by general defects in spindle assembly or stable microtubule capture by the kinetochore. First, interkinetochore distances of aligned chromosomes in Mps1-depleted cells were similar to those of control cells (Figure 3A), showing that sufficiently strong attachments were generated that could impose normal tension between sister centromeres. Second, no obvious differences in spindle morphology or density of cold-stable kinetochore microtubules were detected between mock- and Mps1-depleted cells (Figure 3B). As a control, Nuf2-depleted cells (Figure S6A) showed many misaligned chromosomes that lacked obvious interactions with spindle microtubules (Figure 3B). Third, alignment was maintained when SP600125 was added after chromosomes had reached full alignment (Figure 3C). These three measurements excluded fundamental defects in spindle assembly and stable microtubule capture by kinetochores in cells lacking Mps1. However, as they were primarily focused on the aligned chromosomes, we could not exclude the possibility that the misaligned chromosomes had experienced difficulties in microtubule capture. To examine this, kinetochores were analyzed for the presence of CLIP-170. This microtubule-binding protein localizes specifically to unattached kinetochores in a mitotic checkpoint-independent manner and leaves the kinetochore upon microtubule capture[187,188]. Kinetochores of both aligned and misaligned chromosomes in MG132-treated cells lacking Mps1 had no detectable CLIP-170, whereas the occasional misaligned chromosome in MG132-treated, mock-shRNA-transfected cells had recruited high levels of CLIP-170 on at least one of its kinetochores (Figures 3D and 3E). Because binding of CLIP-170 to unattached kinetochores did not depend on Mps1 in nocodazole- treated or early prometaphase cells (Figures 3F and 3G and Table S1), absence of CLIP-170 on kinetochores of the misaligned chromosomes in the MG132-treated, Mps1-depleted cells was indicative of attachment of those kinetochores to microtubules. Although ultrastructural analysis of kinetochore-microtubule interactions is needed to rigorously exclude possible defects in stability of these interactions, our indirect analyses indicate that such defects as a cause for misalignments in cells depleted of Mps1 is unlikely.

Mps1 Activity Is Required for Efficient Correction of Erroneous Attachments

In most Mps1-depleted cells, some misaligned chromosomes were adjacent to the spindle poles (Figures 2A and 3B). This phenotype is reminiscent of cells depleted of CENP-E activity, a plus-end-directed kinesin required for efficient chromosome congression (reviewed in [11]). Nevertheless, the many misaligned chromosomes in MG132-treated, Mps1-depleted cells as well as the occasional misalignment in mock shRNA cells recruited high levels of CENP-E (Figures 4A and 4B and Table S1). Similar results were obtained with nocodazole-treated cells or with cells

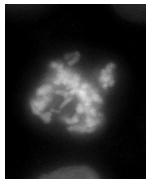

Figure 2. Lack of Mps1 Kinase Activity Causes Severe Chromosome Misalignments

(A and B) Chromosome alignment in HeLa cells transfected as in Figure 1F (A) or with Mad2 shRNA (B) and treated with MG132 for 1 hr. Cells were stained for α-Tubulin, centromeres (ACA), and DNA (DAPI). Eighty-four percent of cells analyzed as in (A) had misaligned chromosomes (average of four experiments). Scale bars are 5 μm. (C and D) Timelapse analysis of chromosome alignment in cells transfected with H2B-EYFP along with the indicated shRNA plasmids and treated with MG132 2-5 min prior to start of image acquisition. (E) Percentage (+/- SD) of cells containing misaligned chromosomes 30 min after onset of mitosis in the presence of MG132 of cells transfected as in Figure 1G and treated with MG132 for 30 min. (F) Timelapse analysis of HeLa cells stably expressing H2B-EYFP and treated simultaneously with MG132 and SP600125. In most instances (five of six), severe chromosome misalignment was observed for the duration of this treatment. Seventy-five minutes after the initial treatment, cells were washed, and image acquisition of the same cells in media containing only MG132 continued for 45 min. All cells had reached alignment by that time.

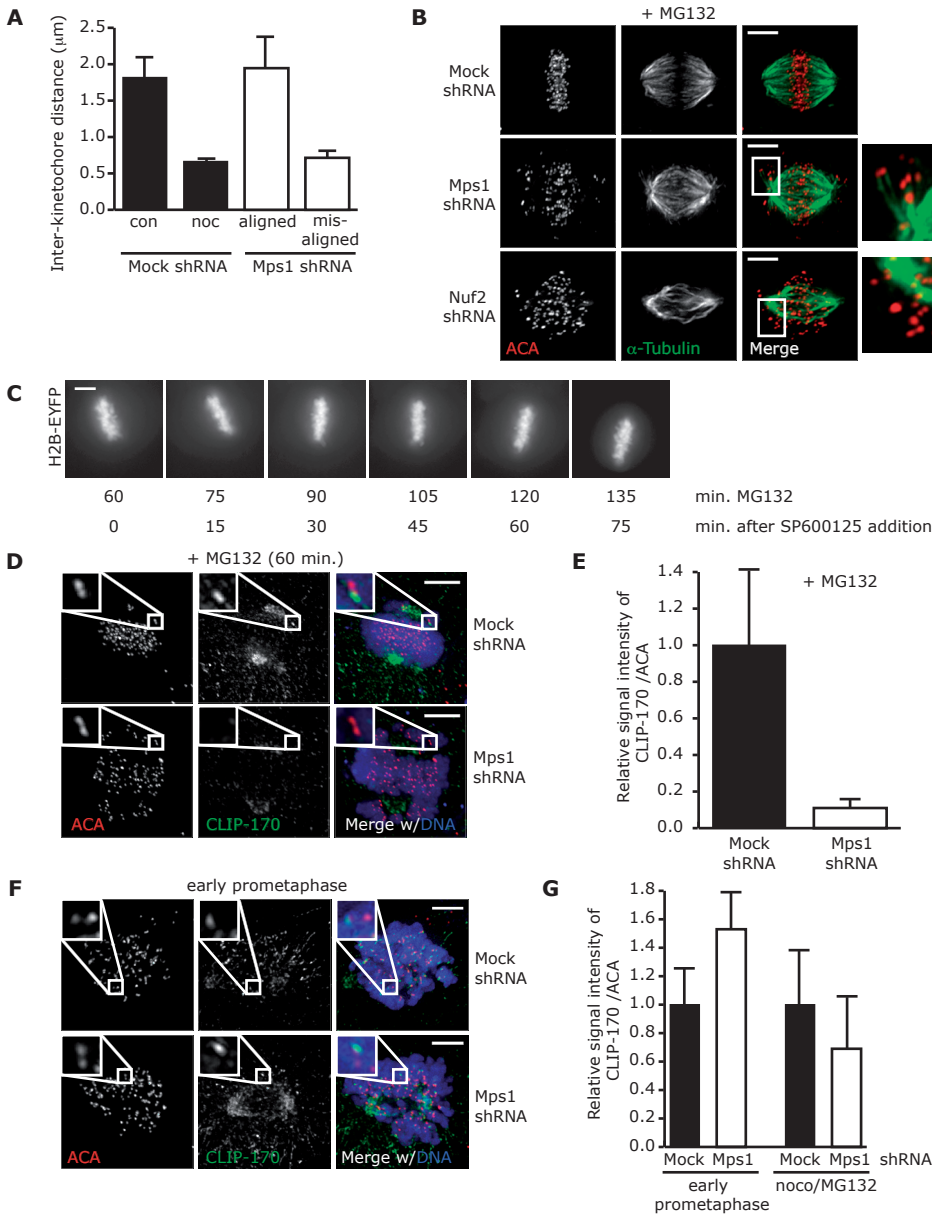

Figure 3. Mps1 Depletion Has No Severe Effect on Kinetochore-Spindle Microtubule Interactions

(A) Interkinetochore distances (+/- SEM) of cells transfected and treated as in Figure 2A or treated with nocodazole for 30 min (noc) and immunostained for centromeres (ACA). Distances were measured for at least five pairs per cell, ten cells per treatment, three independent experiments. (B) Calcium-resistant microtubules in cells transfected and treated as in (A) and immunostained for α-Tubulin and centromeres (ACA). Quantification of Tubulin levels revealed no difference between mock- and Mps1- depleted cells (not shown). (C) Timelapse analysis of HeLa cells stably expressing H2B-EYFP and treated with MG132. After 60 min, SP600125 was added and image acquisition continued. Thirty minutes after addition of SP600125, 86% (12 of 14) of cells had maintained alignment. (D–G) Immunolocalization of CLIP-170 and centromeres (ACA) in cells transfected as in Figure 2A and either left untreated (F and G), treated with MG132 (D and E) or nocodazole/MG132 (G) for 30 min. Details of graphs (+/- SEM) in (E) and (G) are displayed in Table S1. Scale bars are 5 μm.

treated with the Eg5 inhibitor S-trityl-L-cysteine (STLC)[189], which causes monopolar spindles with mono-oriented chromosomes but leaves microtubule dynamics unaffected (Figure 4B and Table S1).

We next investigated the ability of Mps1-depleted cells to correct faulty attachments, a process that is controlled by Aurora B kinase activity at centromeres[38,39,174]. To this end, Mps1-depleted cells were released from monastrol into MG132. Like STLC, monastrol causes monopolar spindles with large numbers of chromosomes that have syntelic or monotelic attachments[190]. Unlike STLC, monastrol is efficiently removed from cells, which allows the formation of a bipolar spindle in which full chromosome alignment requires correction of the improper attachments by Aurora B[38,191]. While complete alignment was achieved in control cells 90 min after release from monastrol, many misaligned chromosomes, a subset of which was clearly attached in a syntelic manner, were observed in almost all (97%) Mps1-depleted cells (Figure 4C). Similar results were obtained when SP600125 was used to inhibit Mps1 during release from monastrol (Figure S2A). Improper attachments lead to absence of tension between sister centromeres, causing Aurora B activity to destabilize kinetochore-spindle microtubule interactions, which results in unattached kinetochores[38,39,168,174]. To investigate if such destabilizations still took place in the absence of Mps1, CLIP-170 levels on kinetochores in cells treated with STLC were examined. Whereas 35% of kinetochores were unattached in mock-depleted cells, only 3% unattached kinetochores were detected in cells lacking Mps1 (Figures 4D and 4E). Together, these results support the hypothesis that attachment error correction by Aurora B is impaired when Mps1 is removed.

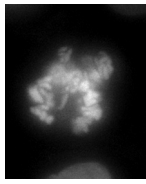

Mps1 Enhances Aurora B Activity at Centromeres

The contribution of Mps1 activity to attachment error correction was investigated by analyzing Aurora B localization and activity, which requires the auxiliary proteins INCENP, Survivin, and Borealin[40,41]. Interestingly, Aurora B was present at normal levels on inner centromeres of chromosomes in Mps1-depleted cells (Figures 5A and 5C and Table S2). In agreement with a role for Survivin in targeting Aurora B to the inner centromere[43], Survivin levels on inner centromeres and in Aurora B immunoprecipitates were unaffected by depletion of Mps1 (data not shown and see Figure 6H). As Survivin interacts with Aurora B indirectly by binding INCENP[43,179], this indicated that assembly of the CPC does not depend on Mps1 activity. In contrast, Aurora B kinase activity was diminished on centromeres of monastrol-treated, Mps1-depleted cells, as evidenced by low levels of phosphorylated CENP-A, an endogenous centromeric Aurora B substrate[192] (Figures 5B and 5C and Table S2) and low levels of phosphorylated Histone H3, another endogenous Aurora B substrate[41], in mitotic extracts (Figure 5D). Moreover, *in vitro* kinase activity of Aurora B immunoprecipitated from mitotically arrested cells was 3-fold lower in Mps1-depleted cells than in control cells (Figures 5E, 5F, S2B, and S2C). In agreement with this, Aurora B auto-phosphorylation on Thr232 was substantially diminished in Mps1-depleted cells (Figure S3 and Table S2). Aurora B activity has been proposed to control Mps1 localization in *Xenopus* egg extracts[193], which would be at odds with our observation that Mps1 activity controls Aurora B function. However, efficient inhibition of Aurora B activity by the inhibitory compound ZM447439[168] did not affect Mps1 localization to unattached kinetochores in HeLa cells (Figure 5G). Thus, our results support the hypothesis that Mps1 contributes to full Aurora B activity at inner centromeres of human cells without affecting its localization.

Direct Phosphorylation of the Aurora B Regulator Borealin by Mps1 Enhances Aurora B Activity and Is Essential for Chromosome Alignment

To examine if Mps1 could contribute to Aurora B function directly, various complex members

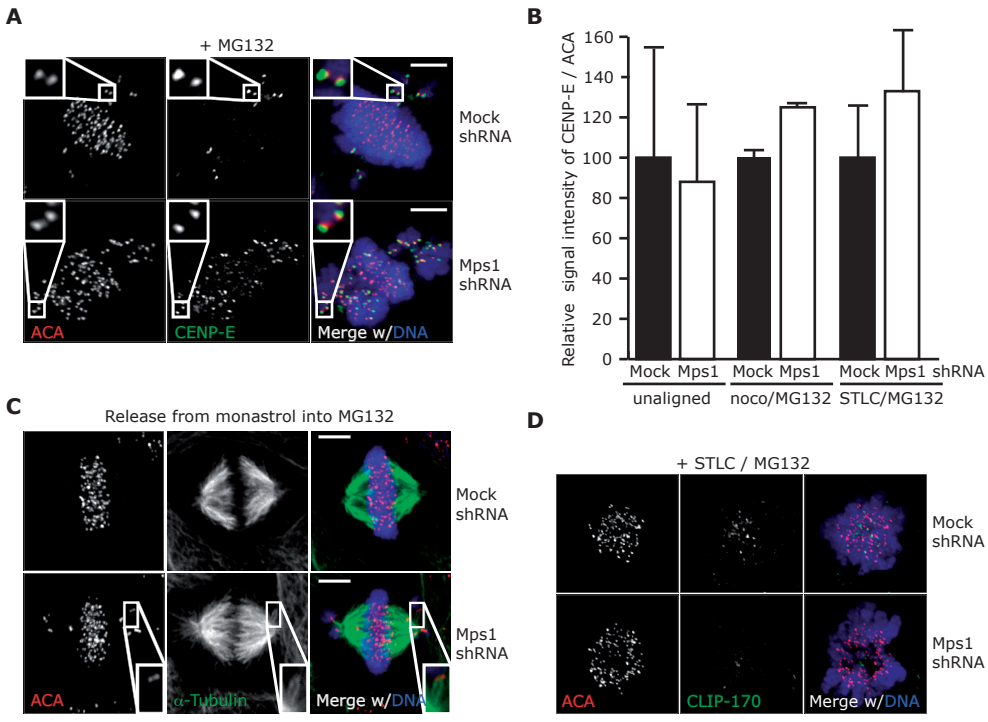

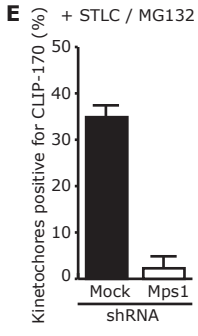

Figure 4. Mps1 Facilitates Attachment Error Correction
(A and B) Immunolocalization of CENP-E and centromeres (ACA) in cells transfected as in Figure 2A and treated with MG132 for 45 min (A) or with nocodazole/ MG132 or STLC/MG132 (B) for 60 min. Details of graph (+/- SEM) in (B) are displayed in Table S1. (C) Analysis of chromosome alignment in cells transfected with mock or Mps1 shRNA plasmids. Cells were treated with monastrol for 1 hr, after which MG132 was added for another hour to prevent Mps1-depleted cells from prematurely exiting mitosis. Cells were then released from monastrol into MG132 for 90 min. Enlarged region in Mps1 shRNA panel shows syntelic attachment of a pair of misaligned sister chromatids. Ninety-seven percent of Mps1-depleted cells showed misalignments in this assay (average of 40 cells from two experiments). (D and E) Immunolocalization of CLIP-170 and centromeres (ACA) in cells transfected as in Figure 2A and treated with STLC/MG132 for 60 min. CLIP-170-positive kinetochores in (E) were defined as having levels of more than 2X background (+/- SEM). Scale bars are 5 μm.

were tested as substrate for recombinant Mps1 in an *in vitro* kinase assay. Whereas Aurora B and Survivin were untouched by Mps1, Borealin was efficiently phosphorylated (Figure 6A). Analysis of the phosphorylated GST-Borealin protein by mass spectrometry identified four Mps1-dependent phosphorylation sites (Figures 6A and S4). GST-Borealin in which all four sites were mutated to alanine (4TA) was a poor substrate for Mps1, showing that the majority of Mps1-dependent phosphorylation sites had been identified (Figure 6B). To investigate the contribution of phosphorylation by Mps1 to Borealin function, shRNA-resistant VSV-tagged Borealin-4TA or Borealin-4TD (in which the phosphorylated threonines were substituted for phosphomimetic aspartate residues) were expressed in U2OS cells in the background of Borealin RNAi (Figures 6C and S5A) and fidelity of chromosome alignment was analyzed by treating cells with MG132 for 90 min. The severe defects in chromosome alignment upon Borealin depletion[47,50] were

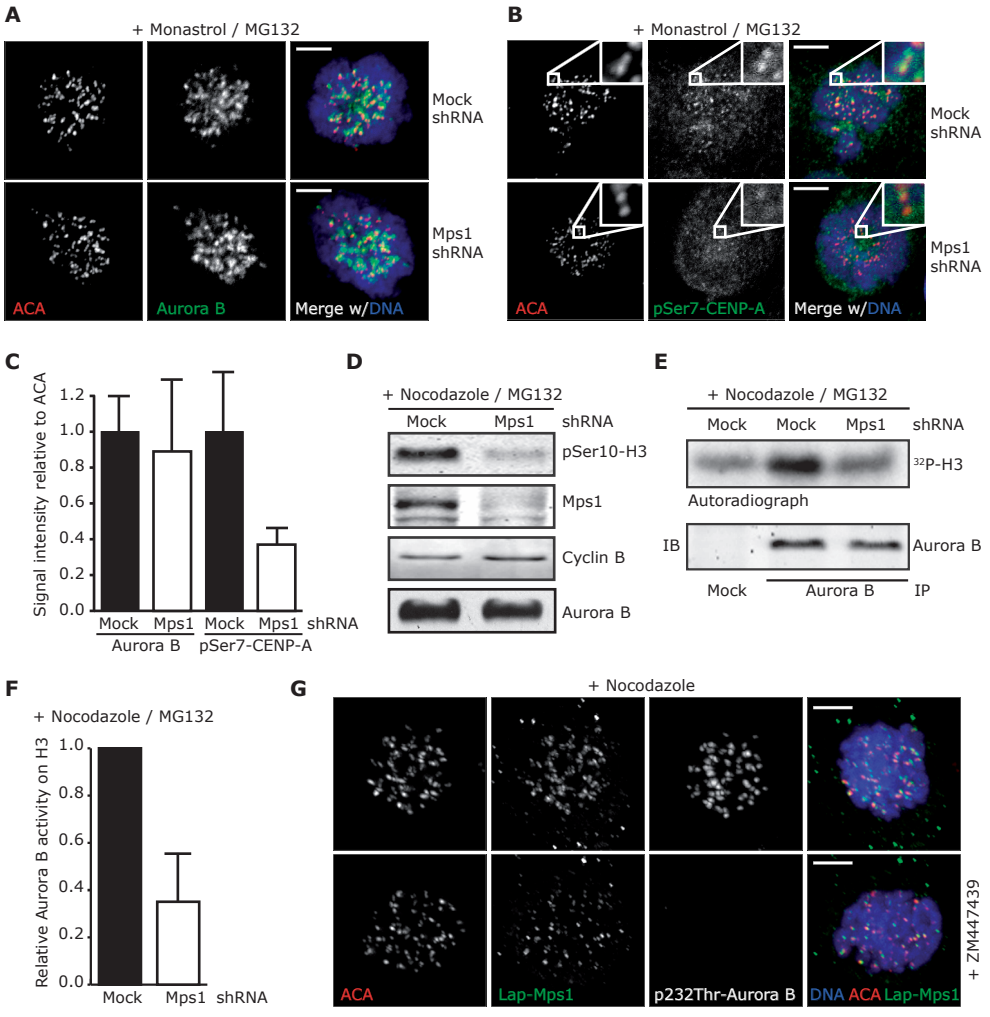

Figure 5. Full Aurora B Kinase Activity Requires Mps1
(A and B) Immunolocalization of Aurora B (A) or pSer7-CENP-A (B) and centromeres (ACA) in cells transfected with mock or Mps1 shRNA plasmids and treated with monastrol for 30 min. (C) Quantification of pSer7-CENP-A intensities as a ratio of the ACA signal at kinetochores of cells treated as in (B). Details of graph (+/- SEM) are displayed in Table S2. (D) Immunoblots of the indicated proteins in lysates of cells transfected with mock or Mps1 shRNA plasmids in combination with pBabe-puro, selected with puromycin and treated with nocodazole and MG132 for 2 hr. (E and F) *In vitro* kinase activity toward recombinant histone H3 by Aurora B immunoprecipitated from cells transfected and treated as in (D). Graph in (F) represents average of three independent experiments (+/- SD). (G) Immunolocalization of Mps1 (anti-GFP), pT232-Aurora B, and centromeres (ACA) of HeLa cells stably expressing LAP-Mps1 and treated with nocodazole +/- ZM447439 for 1 hr. Scale bars are 5 μm.

rescued by expression of both shRNA-resistant wild-type Borealin (Borealin-WT) or Borealin-4TD (Figure 6C). On the other hand, Borealin- 4TA, while correctly localized and expressed to similar levels as Borealin-WT (see Figures 6C, 6E, and S5B), was severely impaired in rescuing chromosome misalignments caused by Borealin depletion (Figure 6C). Therefore, residues of Borealin that are phosphorylated by Mps1 *in vitro* are critical for Aurora B function *in vivo*.

Like Borealin-WT, both Borealin-4TD and Borealin-4TA interacted with other members of the CPC (Figure 6D) and were able to direct Aurora B to inner centromeres in cells depleted of endogenous Borealin (Figure 6E). However, similar to what was observed in cells lacking Mps1, Borealin-depleted cells expressing Borealin-4TA displayed poor centromeric Aurora B activation (Figures 6F, 6G, and Table S2). Importantly, the low *in vitro* activity of CPCs immunoprecipitated from mitotic, Mps1-depleted cells (see Figure 5E) could be enhanced by preincubation with purified active Mps1 prior to the *in vitro* kinase reaction (Figure 6H). These data strongly suggest that Mps1 enhances Aurora B activity by directly phosphorylating Borealin.

Phosphomimetic Mutations in Borealin Restore Chromosome Alignment in Cells Lacking Mps1

To investigate the importance of Borealin phosphorylation to the control of chromosome alignment by Mps1, alignment was examined in Mps1-depleted cells expressing the Borealin-4TD mutant to mimic a state of constitutive phosphorylation by Mps1. Strikingly, Borealin-4TD, but not Borealin-WT, was very efficient in restoring chromosome alignment caused by Mps1 depletion (Figure 7A). The rescue by Borealin-4TD of misalignments in Mps1-depleted cells was nearly as effective as restoring Mps1 expression itself in these cells (Figure 7A). The requirement for Mps1 activity in the process of chromosome alignment could therefore, at least in large part, be bypassed by expression of constitutively phosphorylated Borealin. The rescue of misalignments by Borealin-4TD was specific for signaling by Mps1, as this mutant was unable to restore alignment in BubR1- or Plk1- depleted cells (Figure 7B)[30,168,194,195]. Importantly, Aurora B-dependent phosphorylation of CENP-A (Figures 7C and 7D and Table S2) as well as Aurora B auto-phosphorylation (Figures S3B and S3C and Table S2) were restored in Mps1- depleted cells expressing Borealin-4TD. Finally, to examine if Borealin is an effector in the control of Mps1 over the mitotic checkpoint, checkpoint response in Borealin-4TD-expressing, Mps1-depleted cells was determined by flow cytometry. Whereas Borealin-4TD was able to restore checkpoint signaling in taxol-treated cells depleted of endogenous Borealin, it was unable to do so in either nocodazole- or taxol-treated cells lacking Mps1 (Figure 7E), showing that it cannot bypass the requirement of Mps1 activity for mitotic checkpoint signaling. Together, these data identify Borealin as a major effector of the Mps1 kinase in the control of attachment-error correction and chromosome alignment.

Figure 6. Phosphorylation of Borealin by Mps1 Contributes to Activation of Aurora B

(A) GST-tagged proteins were incubated with kinase-deficient (KD) or active (WT) recombinant Mps1 and analyzed for phosphate incorporation (upper panel) and protein levels (lower panel). The phosphorylation sites identified on *in vitro* phosphorylated GST-Borealin by mass spectrometry are shown in the boxed alignment. (B) GST-Borealin-wild-type (WT) and -4TA were analyzed as in (A). Percentage of incorporated radiolabel relative to WT is indicated. (C) Chromosome alignment in U2OS cells transfected with mock or Borealin shRNA plasmids along with the indicated VSV-tagged Borealin mutants (separation lines in immunoblots in C and D indicate that irrelevant lanes on the gel were removed from the image) and treated with MG132 for 90 min. Graph indicates percentage of cells with proper chromosome alignment (averages of three experiments, at least 60 mitotic cells counted per experiment (+/- SD)) and representative images are shown. (D) Immunoblots of CPC members co-precipitating with the indicated LAP-Borealin mutants from U2OS cells treated with nocodazole for 16 hr. (E) Immunolocalization of Aurora B, Borealin (anti-VSV) and centromeres (ACA) in U2OS cells transfected with Borealin shRNA and the indicated VSV-tagged Borealin mutants and treated with nocodazole for 60 min. (F and G) Immunolocalization of pSer7-CENP-A and centromeres (ACA) in cells transfected with mock or Borealin shRNA plasmids along with the indicated VSV-tagged Borealin mutants and treated with monastrol and MG132 for 60 min. Details of graph (+/- SEM) in (G) are displayed in Table S2. (H) Kinase activity toward recombinant histone H3 (^{32}P-H3) by Aurora B immunoprecipitated from UTRM10 cells treated with or without doxycycline for 3 days (see Supplemental Experimental Procedures) and nocodazole/MG132 for an additional 3 hr. Precipitates were preincubated with His_6-Mps1-WT or -KD for 20 min after which Mps1 was removed by extensive washing. H3 and radiolabel were subsequently added. Scale bars are 5 μm.

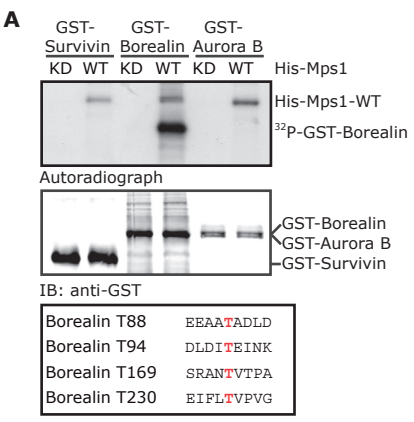
A
GST-Survivin
GST-Borealin
GST-Aurora B
KD WT KD WT KD WT
His-Mps1
His-Mps1-WT
32P-GST-Borealin
Autoradiograph
GST-Borealin
GST-Aurora B
GST-Survivin
IB: anti-GST
Borealin T88 EEAATADLD
Borealin T94 DLDITEINK
Borealin T169 SRANTVTPA
Borealin T230 EIFLTVPVG

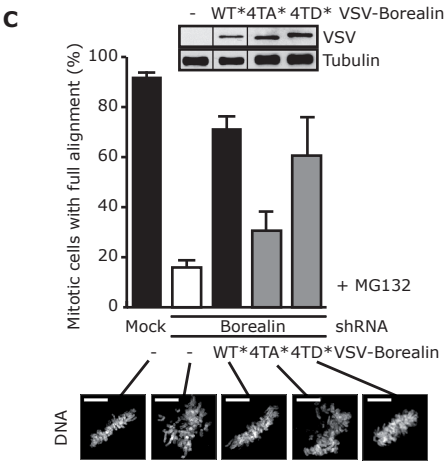
C
- WT*4TA* 4TD* VSV-Borealin
VSV
Tubulin
Mitotic cells with full alignment (%)
100
80
60
40
20
0
+ MG132
Mock
Borealin
shRNA
- - WT*4TA*4TD*VSV-Borealin
DNA

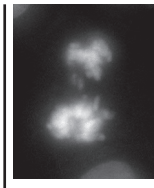

Chapter 2

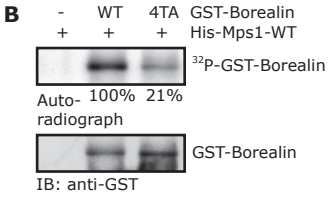
B
- WT 4TA GST-Borealin
+ + + His-Mps1-WT
32P-GST-Borealin
Auto-radiograph
100% 21%
GST-Borealin
IB: anti-GST

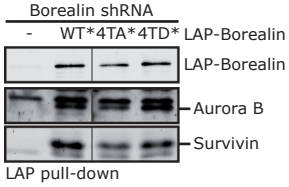
D
Borealin shRNA
- WT*4TA*4TD* LAP-Borealin
LAP-Borealin
Aurora B
Survivin
LAP pull-down

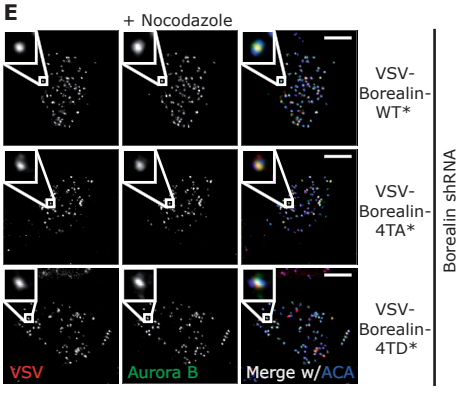
E
+ Nocodazole
VSV-Borealin-WT*
VSV-Borealin-4TA*
VSV-Borealin-4TD*
Borealin shRNA
VSV
Aurora B
Merge w/ACA

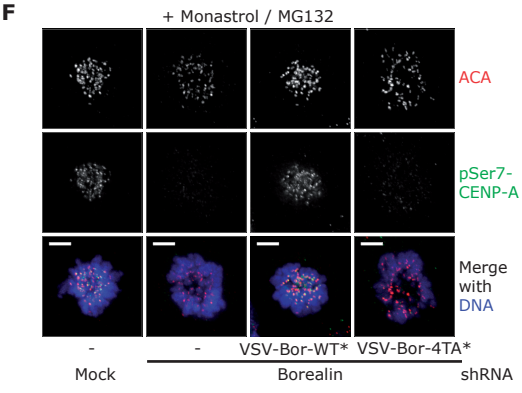
F
+ Monastrol / MG132
ACA
pSer7-CENP-A
Merge with DNA
- - VSV-Bor-WT* VSV-Bor-4TA*
Mock
Borealin
shRNA

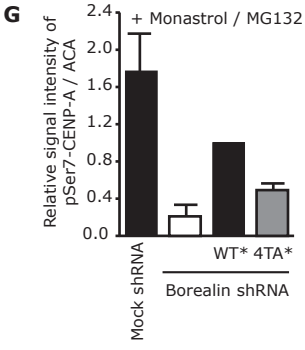
G
Relative signal intensity of pSer7-CENP-A / ACA
2.4
2.0
1.6
1.2
0.8
0.4
0.0
+ Monastrol / MG132
WT* 4TA*
Mock shRNA
Borealin shRNA

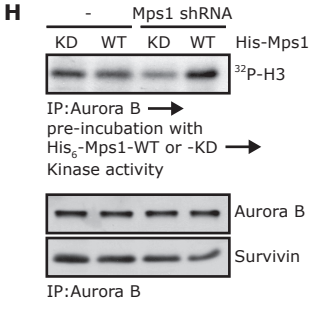
H
- Mps1 shRNA
KD WT KD WT His-Mps1
32P-H3
IP:Aurora B
pre-incubation with
His6-Mps1-WT or -KD
Kinase activity
Aurora B
Survivin
IP:Aurora B

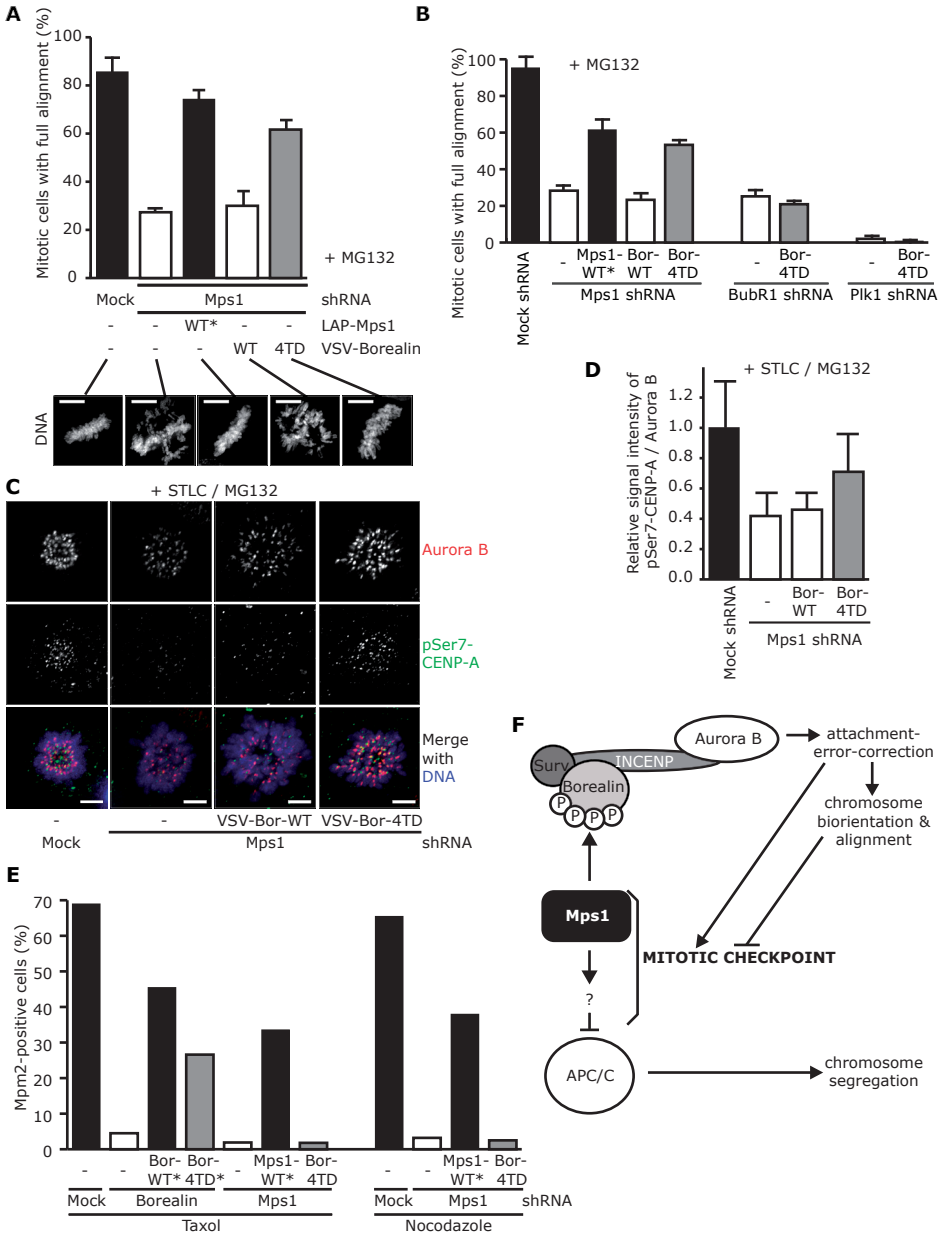

Figure 7. Phosphorylation of Borealin Is Essential in the Control of Chromosome Alignment by Mps1

(A and B) Chromosome alignment in cells transfected with the indicated shRNA plasmids along with LAP Mps1-WT or the indicated VSV-tagged Borealin mutants and treated with MG132 for 45 min. Graphs indicate percentage of cells with proper chromosome alignment (averages of three experiments, at least 60 mitotic cells counted per experiment (+/- SD)) and representative images are shown for experiment in (A). (C and D) Immunolocalization of pSer7-CENP-A and Aurora B in cells transfected with the indicated shRNA plasmids and VSV-Borealin-WT or -4TD and treated with STLC/MG132 for 60 min. Details of graph (+/- SEM) in (D) are displayed in Table S2. (E) Flow cytometric analysis of mpm2 positivity in a population of cells transfected with the indicated shRNA plasmids and either LAP-Mps1 WT* or VSV-tagged Borealin mutants and treated with nocodazole or taxol for 16 hr. (F) Model for the control of mitotic processes by Mps1 kinase activity. See text for clarification. Scale bars are 5 μm.

Discussion

A Conserved Role for Mps1 in Chromosome Alignment?

We have shown here that Mps1 kinase activity is indispensable for both the mitotic checkpoint and chromosome alignment in human cells (Figure 7F). A role for *Saccharomyces cerevisiae* Mps1 in spindle assembly was recently suggested and based on the observation that chemical inhibition of Mps1 resulted in improper spindle formation and chromosome positioning[182]. A mitotic checkpoint-independent role for Mps1 in regulating correct chromosome segregation thus appears to be conserved. Interestingly, Aurora B/Ipl1 mutant yeast strains have certain phenotypes in common with strains exposed to chemical inhibition of Mps1. These include elongated spindles at metaphase and chromosome missegregations at anaphase[182,196]. In *S. cerevisiae*, evidence of a link between Mps1 and Aurora B/Ipl1 activities has been reported. Cell-cycle arrest in response to Mps1 overexpression depends on Aurora B activity[197] and the yeast Mps1-inhibitor cincreasin at certain concentrations abrogates checkpoint signaling in response to lack of tension but not lack of attachment, very much like Aurora B/ Ipl1 mutants[183,197]. It is therefore possible that Mps1 also controls Aurora B activity in organisms other than mammals. Borealin orthologs have been identified in most model organisms (though not in yeast), some of which express two homologous Borealin-like proteins, related to the DasraA/B genes originally identified in *Xenopus laevis*[47,50]. In this respect, it is of interest to note that three of four residues (Thr169 is the exception) found phosphorylated by Mps1 are present in at least one of the Borealin-like proteins of most organisms.

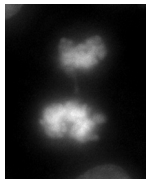

A Novel Function for Borealin in the Regulation of Aurora B

Our data suggest that Mps1 is an upstream activator of Aurora B kinase activity and that Borealin contributes to stimulation of the intrinsic kinase activity of Aurora B. Maximal activation of Aurora B at the centromere is regulated on many levels, including phosphorylation by Chk1[198] and local clustering that triggers a chromatin-dependent auto-activation loop[49,199]. Borealin has been proposed to facilitate this clustering as well as stabilize interactions between INCENP and Survivin[43,44]. We provide evidence that Borealin additionally contributes to Aurora B activation independent of its role in loading Aurora B onto centromeric chromatin, as Aurora B is properly localized yet not fully activated in Mps1-depleted cells.

Phosphorylation by Aurora B of the TSS motif in INCENP and auto-phosphorylation on T232 within its activation loop are essential for activating Aurora B[42,49,178,200]. Phosphorylation of Borealin by Mps1 does not contribute to Aurora B activity on such a fundamental level, as it enhances Aurora B activity by 2- to 4-fold, as judged by pSer7-CENP-A immunolocalization. Interestingly, whereas regulation of Aurora B activity by Mps1 is important for its function at the centromere, it does not seem to impact the function of Aurora B at the central spindle, as we have seen no defect in cytokinesis in Mps1-depleted cells (data not shown). Perhaps cytokinesis can proceed with low levels of Aurora B activity, while error-correction needs that activity to be enhanced by Mps1, or perhaps a different mechanism ensures enhanced Aurora B activity on the central spindle. On the other hand, phosphorylated Borealin, on top of its role in regulating Aurora B activity, may contribute to establishing interactions with proteins that are specifically required for Aurora B to correct faulty attachments but not for Aurora B to contribute to cytokinesis. Clarifying the role of Borealin and its modifications in activation of Aurora B at the centromere will require *in vitro* reconstitution of the full complex from purified components and biochemical analysis of *in vivo* complexes containing the various Borealin mutants.

Mps1 Kinase Activity Is Essential for the Mitotic Checkpoint

In agreement with a recent report in which a small molecule inhibitor was used[186], our data using a mutant allele show that Mps1 kinase activity is essential for the checkpoint in human cells and, as a consequence, for survival of those cells. Studies using immunodepletion from *Xenopus* extracts have previously shown that Mps1 is required for proper recruitment of Bub1, BubR1, and CENP-E to unattached kinetochores[131,193,201]. In addition, Aurora B was shown to control the localization of Mps1 to kinetochores in this experimental system[193]. In contrast, we and others have shown in human cells that depletion of Mps1 to levels sufficient to completely inhibit mitotic checkpoint signaling and induce severe misalignments leaves Bub1, BubR1, and CENP-E at kinetochores (this study and [106,107,133,202]). Likewise, inhibition of Aurora B activity by RNAi[135] or ZM447439 (this study) does not prevent Mps1 from binding kinetochores in human cells. What underlies the difference between these two systems with regards to interdependencies of kinetochore localization? The frog kinetochore in extracts may behave like an all-or-none system more so than the human kinetochore. It is newly assembled upon addition of the sperm DNA to the extract and may therefore be less mature than that of human mitotic cells. Perhaps the slight reduction in, for instance, Bub1 and BubR1 localization to kinetochores in human cells to cells depleted (see Table S1) can be more readily detected in the less rigidly structured kinetochores that must assemble and disassembly rapidly in the very short embryonic cell cycles.

Coordination between Chromosome Alignment and the Mitotic Checkpoint

Like Mps1, the other three kinases that have roles in the mitotic checkpoint, BubR1, Bub1, and TAO1, also contribute to chromosome alignment[30,168,172,173]. BubR1 is required for establishment of stable attachments of chromosomes to spindle microtubules[30] and Bub1 is required for formation of proper end-on attachments[172]. The mechanisms by which they exert these functions are unclear, but interestingly, BubR1 was proposed to inhibit Aurora B activity to allow stable attachments to be formed[30]. The data presented here add a new layer to the control of coordination between processes required for chromosome alignment and the mitotic checkpoint. A general principle is thus emerging in which kinases that set up the requirements for faithful chromosome segregation also signal to the cell-cycle machinery to halt until those requirements are met. These kinases are therefore crucial in the maintenance of chromosomal stability, and molecular insights into their activities will likely be valuable in our understanding of the origins of chromosomal instability in development and cancer.

Experimental Procedures

Plasmids and shRNA-Based Protein Replacement

Construction of the various plasmids and mutants were carried out as described in Supplemental Data. Cells were cotransfected with a marker plasmid along with pSuper-Mps1 or pSuper-mock and shRNA-insensitive pCDNA3- LAP-Mps1-WT or -KD (D664A) in a 1:7:3 ratio. This ratio was based on the optimal functional rescue by wild-type, as determined by titration of the wild-type allele in relation to the shRNA. Borealin protein replacements were done similarly. Marker plasmids were pSpectrin-GFP for flow cytometry, pEYFP-H2B, or pH2B-dsRed for imaging and pBabe-Puro for colony outgrowth.

Tissue Culture, Transfections, and Treatments

U2OS and HeLa cells were grown in DMEM with 8% FBS, supplemented with pen/strep. Transfections were done using the calcium phosphate method (U2OS) or Effectene (QIAGEN)

(UTRM10, HeLa). Thymidine (2.5 mM), nocodazole (200 ng·ml^{-1}), taxol (1 μM), MG132 (10 μM), monastrol (200 μM), STLC (10 μM), and puromycin (1 μg·ml^{-1}) were all from Sigma. SP600125 (10 μM) was from BioMol. ZM447439 (2 μM) was from Tocris Bioscience.

Flow Cytometry, Colony Outgrowth, and Immunoblotting
Cells were released from a 24 hr thymidine-induced block into nocodazole or taxol for 16 hr and analyzed as described[167]. Flow cytometric analysis of transfected cells was based on Spectrin-GFP expression. Colony outgrowth analyses were done as described[203]. As control, a fraction of cells was lysed 48 hr posttransfection and analyzed by immunoblotting for expression of exogenous Mps1. Immunoblotting was done using standard protocols, and the antibodies used are described in Supplemental Data.

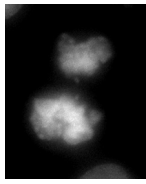

Immunoprecipitations and In Vitro Kinase Assays
Conditions for immunoprecipitations of Aurora B using anti-Aurora B antibodies (Abcam) and for pull-downs of LAP-Borealin using S-protein-Agarose (Novagen) were copied from[50], with minor modifications as described in Supplemental Data.

Immunofluorescence Microscopy and Live Cell Imaging
Immunofluorescence microscopy was carried out as described in Supplemental Data. For live cell imaging, cells were plated in 2-well chambered glass-bottom slides (LabTek), transfected and imaged in a heated chamber (37°C and 5% CO2) using a 40X/1.3NA oil objective on a Zeiss Axiovert 200M microscope equipped with a 0.55NA condensor and controlled by a lambda-DG4 (Roper Scientific) and MetaMorph software. Twelve bits DIC (25 msec exposure) and yellow fluorescent (75 msec exposure) images were acquired every 3 min using a Photometrics CoolSnap HQ CCD camera (Roper Scientific). Images were processed using MetaMorph software. Images of H2B-EYFP are maximum intensity projections of all Z planes.

Acknowledgments

The authors thank A. Musacchio, S. Taylor, D. Cleveland, N. Galjart, W. Earnshaw, I. Cheeseman, and M. Timmers for reagents, K. Mulder for technical advice, F. Zwartkruis for critically reading the manuscript, and G. Vader for LAP-Borealin, helpful discussions and critically reading the manuscript. This work was supported by grants awarded to G.J.P.L.K. (UU-2006-3664 and VIDI-91776336), R.H.M. (ZonMW 91846616), and S.M.A.L. (VIDI-91766332). A.B.B. was supported by grants from the EU (LSHC-CT-2004-503438).

Supplemental Data

Supplemental Figures

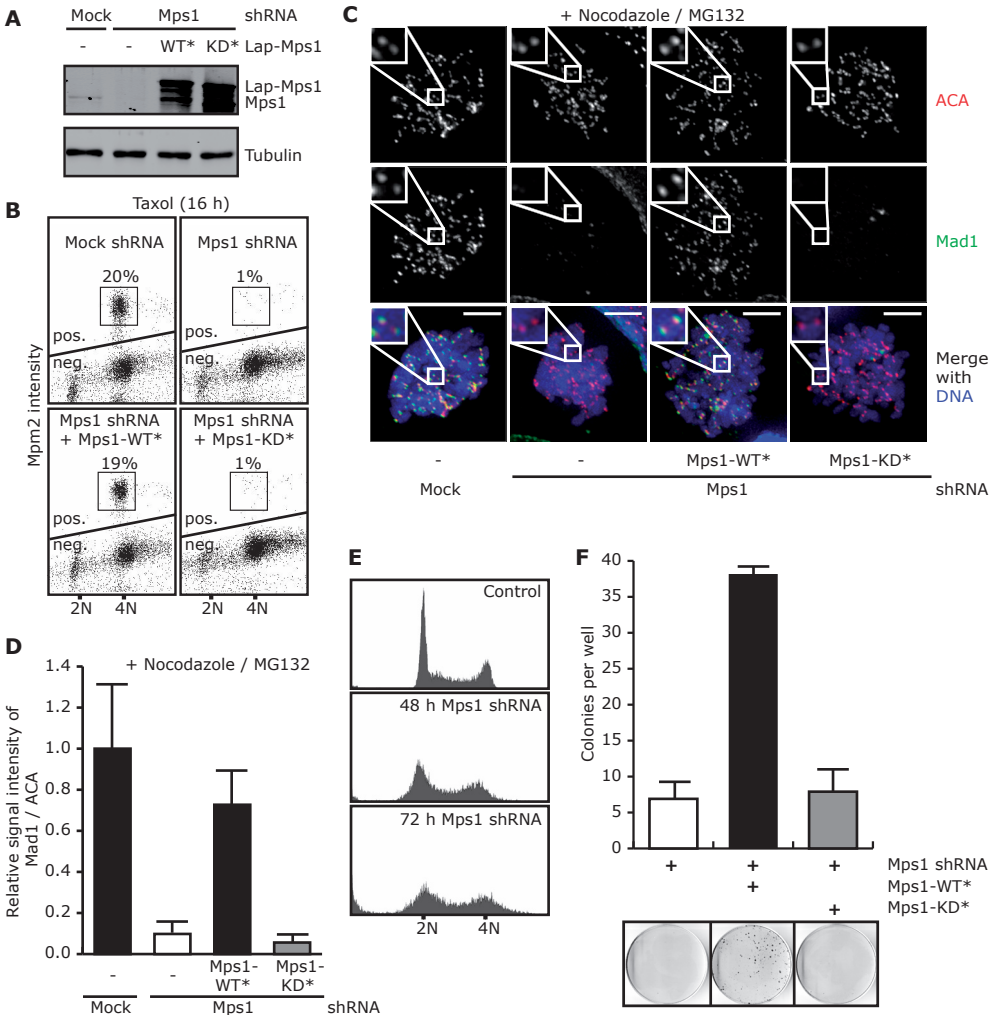

Figure S1. Mps1 kinase activity is essential for recruitment of Mad1 to kinetochore and for survival.
(A) Immunoblot of lysates of U2OS cells transfected with the indicated shRNA plasmids and LAP-Mps1 mutants. (B) Flow cytometric analysis of Mpm2-positivity in a population of cells transfected as in Figure 1C and treated with taxol for 16 hours. Analysis was done as in 1C. (C, D) Immunolocalization of Mad1 and centromeres (ACA) in cells transfected with the indicated shRNA plasmids and RNAi-resistant Mps1 alleles and treated with nocodazole for 30 minutes. Details of graph (+/- SEM) in 1D are displayed in Table S1. (E) Flow cytometric analysis of DNA content (PI) of U2OS cells transfected with the indicated shRNA plasmids along with pBabe-puro and selected with puromycin. (F) Colony outgrowth of cells transfected and selected as in S1E but grown for 9 days. Graph represents averages of three independent experiments (+/- SD). Scale bars are 5 μm.

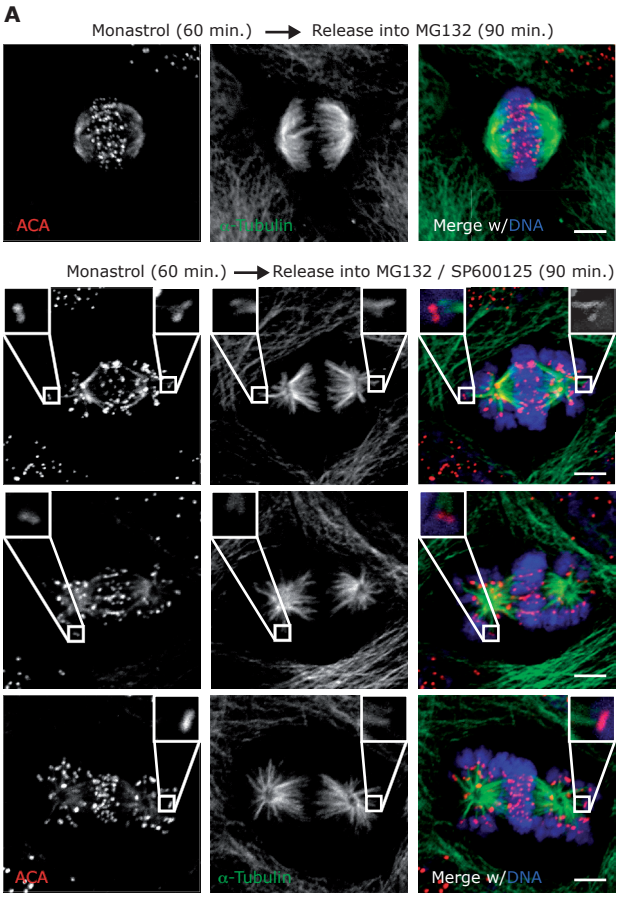

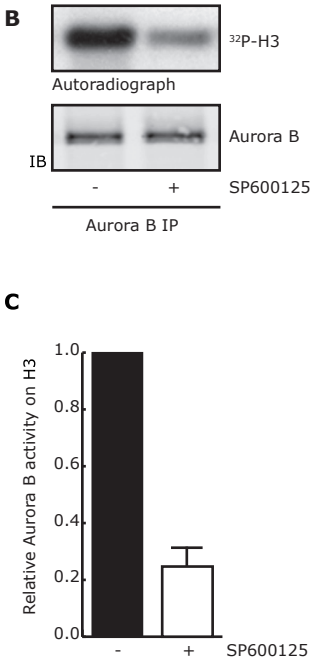

Figure S2. Syntelic attachments are left uncorrected in cells treated with SP600125.
(A) Immunolocalization of α-Tubulin and centromeres (ACA) in cells treated with monastrol for 60 minutes and released into MG132 with or without SP600125 for 90 minutes. Three examples of SP600125-treated cells are shown. Enlarged regions show syntelic attachments. (B, C) Kinase activity towards recombinant histone H3 of Aurora B immunoprecipitated from cells treated with nocodazole for 16 hours, followed by addition of MG132 +/- SP600126 for an additional hour. Graph in (C) represents average of three independent experiments (+/- SD). Scale bars are 5 μm.

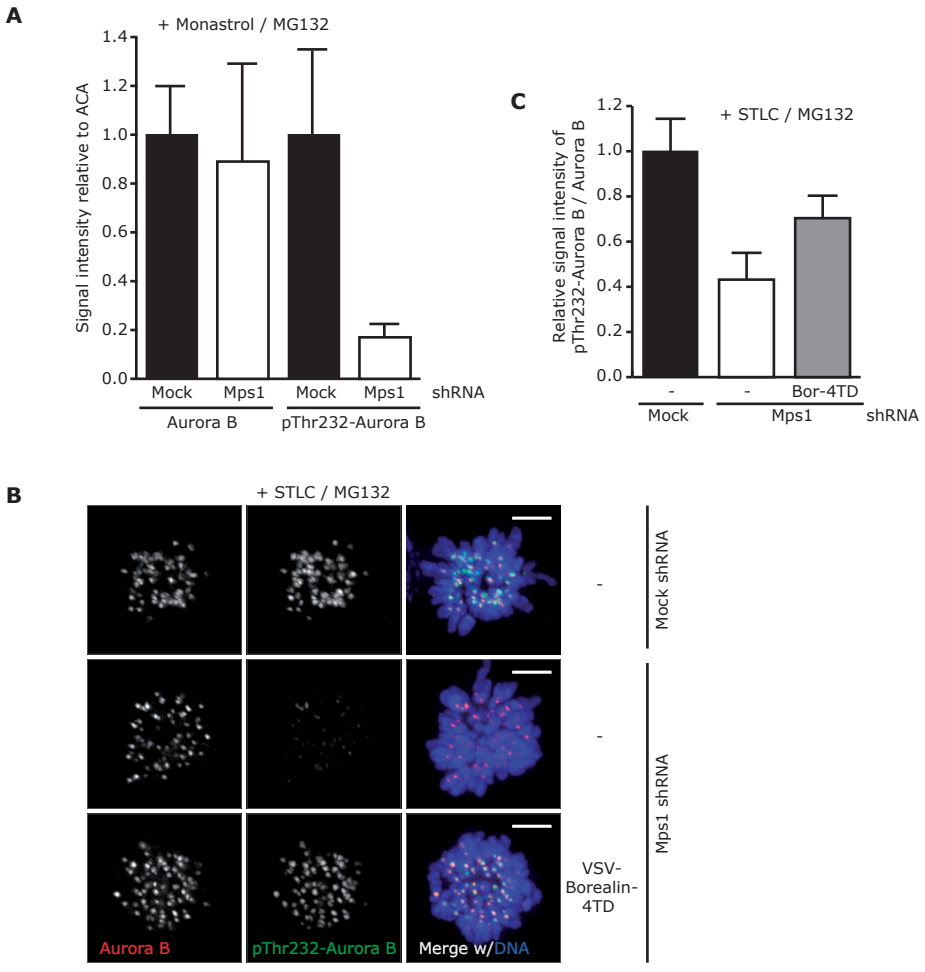

Figure S3. High intrinsic kinase activity of Aurora B requires Mps1.
(A) Quantification of Aurora B and pThr232-Aurora B kinetochore intensities as a ratio of the ACA signal of cells transfected and treated as in 5A. Details of graph (+/- SEM) are displayed in Table S2. (B, C) Immunolocalization of pT232-Aurora B and Aurora B in cells transfected with the indicated shRNA plasmids and VSV-Borealin-4TD and treated with STLC/MG132 for 60 minutes. Details of graph (+/- SEM) in S3C are displayed in Table S2. Scale bars are 5 μm.

A

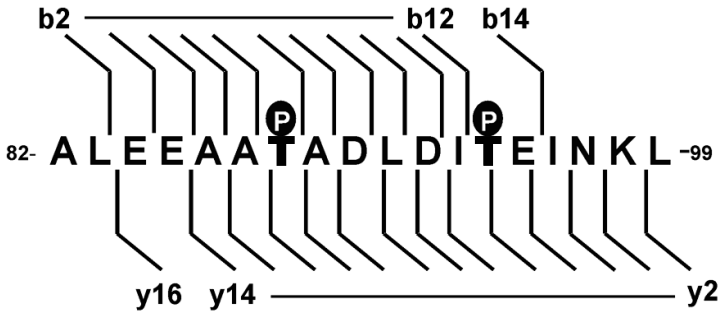

B

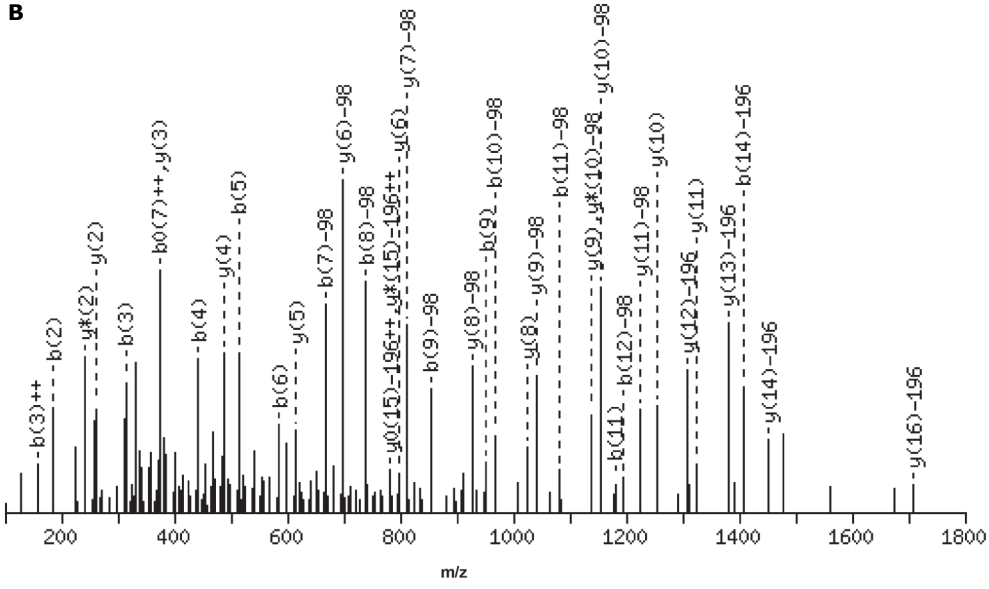

C

Amino Acid Position	Peptide Sequence	Phosphorylated Residue	Mascot Score	Peptide Charge State
82-99	ALEEAA**T**ADLDI**T**EINKL	Thr88, Thr94	118	2+
87-99	A**T**ADLDI**T**EINKL	Thr88, Thr94	69	2+
90-99	DLDI**T**EINKL	Thr94	50	2+
91-99	LDI**T**EINKL	Thr94	57	2+
167-176	AN**T**VTPAVGR	Thr169	52	2+
226-240	EIFL**T**VPVGGGESLR	Thr230	34	2+
222-237	ADSKEIFL**T**VPVGGGE	Thr230	50	2+

Figure S4. Identification of phosphorylated Borealin peptides by mass spectrometry.
Sequence (A) and MS/MS spectrum (B) of the Thr88, Thr94 doublephosphorylated peptide of Borealin (aa 82-99) as identified by MASCOT software (See Experimental Procedures). Identified b and y ions are indicated as well as their neutral losses. The locations of the phosphorylations are indicated by a circled P and the Thr residues are indicated in bold. (C). Table summerizing MS data of all phosphorylated peptides identified on Borealin *in vitro* phosphorylated by Mps1.

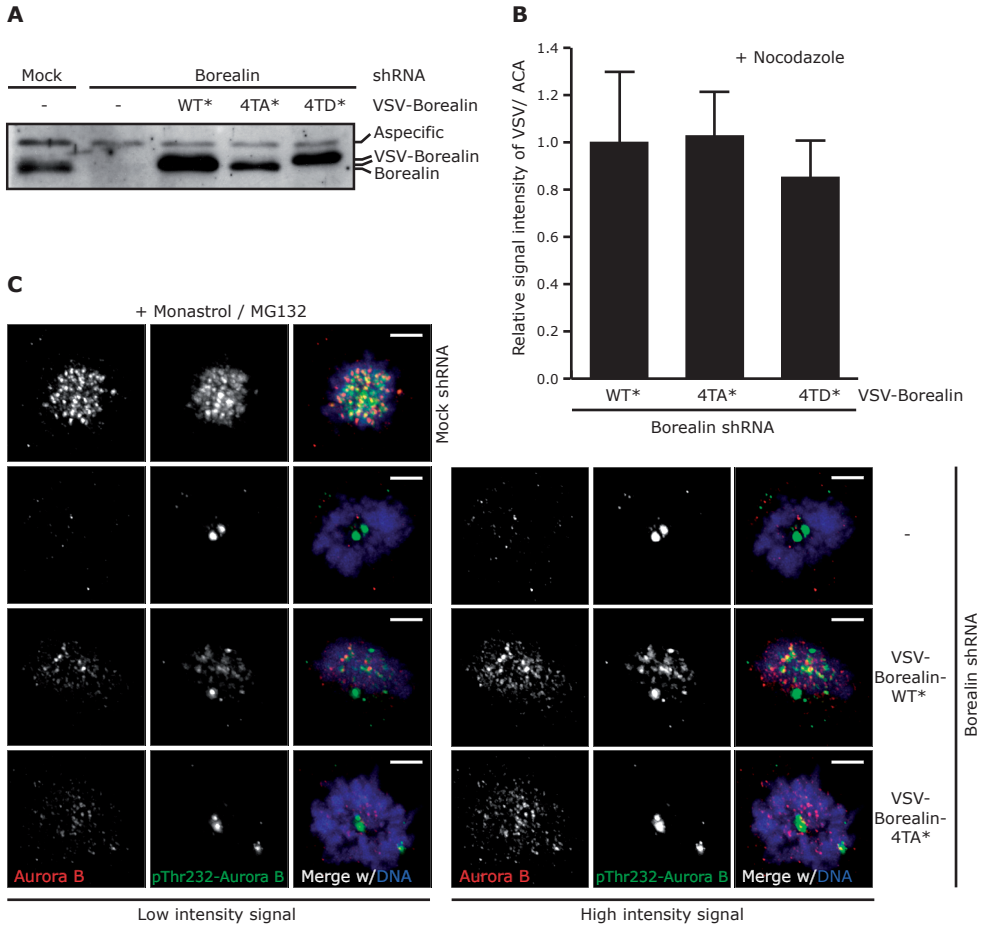

Figure S5. Low intrinsic kinase activity of Aurora B in cells expressing Borealin-4TA.
(A) Immunoblot of lysates of mitotic U2OS cells transfected with the indicated shRNA plasmids and VSV-Borealin mutants. (B) Quantification of the levels of the indicated VSV-Borealin mutants on centromeres of cells treated with nocodazole for 60 minutes. (C) Immunolocalization of pThr232-Aurora B and Aurora B in cells transfected with mock or Borealin shRNA plasmids along with the indicated VSV-tagged Borealin mutants and treated with monastrol for 30 minutes. The two high-intensity signals that remain after Borealin shRNA are likely centrosomes. Specificity of pT232 signals was verified by treatment with ZM447439 (data not shown). Scale bars are 5 μm.

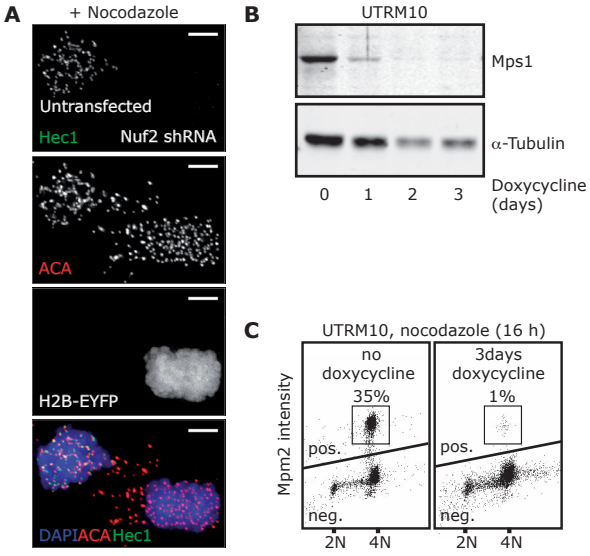

Figure S6. Efficiency of Nuf2 depletion and inducible depletion of Mps1 in U2OS cells.
(A) Immunolocalization of Hec1 and centromeres (ACA) in cells either untransfected (no H2B-EYFP signal, left) or transfected with Nuf2 shRNA plasmid (H2B-EYFP-positive, right) and treated with nocodazole for 30 minutes. (B) Immunoblots of lysates from UTRM10 cells (clonal U2OS cells that stably carry the Tet repressor and pSuperior-retro-puro-Mps1 for inducible expression of shRNAs targeting Mps1) treated with doxycycline for 1, 2 or 3 days, or left untreated (0). (C) Flow cytometric analysis of Mpm2-positivity of UTRM10 cells left untreated or treated with doxycycline for 3 days and treated with nocodazole for 16 hours. Scale bar is 5 μm.

Supplemental Movies

Three supplemental movies can be found online at http://www.cell.com/cgi/content/full/132/2/233/DC1/.

Movie S1. Mps1-depleted cells show massive chromosome missegregations
U2OS cells were transiently transfected with H2B-EYFP and Mps1 shRNA. Cells were filmed from prophase with time-intervals of 3 minutes per frame. Left, H2B-EYFP; right, DIC.

Movie S2. Mps1-depleted cells display a "cut" phenotype
U2OS cells were transfected and imaged as in Movie S1.

Movie S3. Alignment Defects Are Reversible by Removal of an Mps1 Inhibitor
HeLa cells stably expressing H2B-EYFP were treated with MG132 and SP600125 and filmed for 1 hr and 12 min. Then the cells were washed in media containing only MG132, and filming continued at 1:18. Note the fast realignment of misaligned chromosomes once SP600125 had been removed.

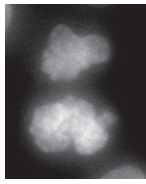

Signal	**Mad1**		**Mad2**		**BubR1**	**BubR1**	**BubR1**
Control	ACA	% of cells showing the phenotype (high or low Mad1)	ACA	% of cells showing the phenotype (high or low Mad2)	ACA	ACA	ACA
Treatment	Noco + MG132		Noco + MG132		Noco + MG132	STLC + MG132	asynch
Duration	60 min		60 min		60 min	60 min	
mock shRNA	100 +/- 33 (74)*	100% high (75 of 75)	100 +/- 12 (76)	100% high (66 of 66)	100 +/- 39 (90)	100 +/- 27 (120)	100 +/- 26 (58)
Mps1 shRNA	10 +/- 9 (80)	93% low (72 of 77)	0 +/- 7 (53)	89% low (67 of 75)	71 +/- 24 (123)	72 +/- 14 (151)	51 +/- 12 (85)
Mps1 shRNA + LAP-Mps1-WT*	73 +/- 22 (51)	91% high (67 of 74)					
Mps1 shRNA + LAP-Mps1-KD*	6 +/- 5 (53)	94% low (52 of 55)					

Signal	**Bub1**	**Bub1**	**Bub1**	**CENP-E**	**CENP-E**	**CENP-E ****
Control	ACA	ACA	ACA	ACA	ACA	
Treatment	Noco + MG132	STLC + MG132	asynch	Noco + MG132	STLC + MG132	
Duration	60 min	60 min		60 min	60 min	
mock shRNA	100 +/- 19 (89)	100 +/- 35 (63)	100 +/- 24 (78)	100 +/- 4 (66)	100 +/- 30 (126)	100 +/- 52 (23)
Mps1 shRNA	75 +/- 12 (92)	53 +/- 30 (77)	41 +/- 9 (95)	125 +/- 1 (135)	133 +/- 32 (61)	88 +/- 35 (57)

Signal	**CLIP-170**	**CLIP-170**	**CLIP-170 ****	
Control	ACA	ACA	ACA	% of cells showing the phenotype (high or low CLIP-170)
Treatment	Noco + MG132	asynch	MG132	
Duration	60 min		45 min	
mock shRNA	100 +/- 32 (111)	100 +/- 24 (84)	100 +/- 42 (19)	100% high (9 of 9)
Mps1 shRNA	69 +/- 35 (93)	153 +/- 26 (77)	11 +/- 6 (47)	98% low (37 of 39)

Table S1. Quantification of Signal Intensities of Antibodies to the Indicated Proteins on Kinetochores
Signal intensities are calculated as ratio to the control signal. This ratio was set to 100% in mock shRNA samples, and +/- SEM is indicated. ∗ number of kinetochores analyzed is in brackets. ∗∗ only kinetochores of misaligned chromosomes were analyzed.

Signal	**Aurora B**	**pSer7-CENP-A**		**pSer7-CENP-A**	
Control	ACA	Aurora B	% of cells showing the phenotype (high or low pCENP-A)	ACA	% of cells showing the phenotype (high or low pCENP-A)
Treatment	monastrol + MG132	STLC + MG132		monastrol + MG132	
Duration	60 min	60 min		60 min	
mock shRNA	100 +/- 21 (168)*	100 +/- 32 (123)	100% high (44 of 44)	100 +/- 17 (204)	100% high (49 of 49)
Mps1 shRNA	89 +/- 23 (178)	41 +/- 16 (89)	82% low (37 of 45)	37 +/- 8 (256)	65% low (37 of 57)
Mps1 shRNA + VSV-Borealin-WT		46 +/- 11 (78)	81 % low (22 of 27)		
Mps1 shRNA + VSV-Borealin-4TD		71 +/- 22 (104)	78% high (29 of 37)		

Signal	**pThr232-Aurora B**		**pThr232-Aurora B**	
Control	Aurora B	% of cells showing the phenotype (high or low pT232-Aurora B)	ACA	% of cells displaying the phenotype (high or low pT232-Aurora B)
Treatment	STLC + MG132		monastrol + MG132	
Duration	60 min		60 min	
mock shRNA	100 +/- 13 (154)	100% high (39 of 39)	100 +/- 17 (79)	100% high (71 of 71)
Mps1 shRNA	43 +/- 10 (131)	83% low (24 of 29)	35 +/- 6 (88)	75% low (41 of 55)
Mps1 shRNA + VSV-Borealin-4TD	71 +/- 9 (101)	76% high (25 of 33)		

Signal	**pSer7-CENP-A**	
Control	ACA	% of cells displaying the phenotype (high or low pCENP-A)
Treatment	STLC + MG132	
Duration	60 min	
mock shRNA	100 +/- 25 (68)	100% (60 of 60)
Borealin shRNA	12 +/- 9 (98)	84% (56 of 67)
Borealin shRNA + VSV-Borealin-WT*	57 +/- 16 (77)	79% (48 of 61)
Borealin shRNA + VSV-Borealin-4TA*	27 +/- 7 (61)	64% (45 of 70)

Table S2. Quantification of Signal Intensities of Antibodies to the Indicated Proteins on Kinetochores
Signal intensities are calculated as ratio to the control signal, and +/- SEM is indicated. This ratio was set to 100% in mock shRNA samples. ∗ number of kinetochores analyzed is in brackets.

Supplemental Experimental Procedures

Plasmids

The pSuper-based shRNA plasmids used in this study: Mock (AGATTCTAGCTAACTGTTC), Mps1 (GACAGATGATTCAGTTGTA), Nuf2 (GCATGCCGTGAAACGTATA), Borealin[43], BubR1[95] and Plk1[195]. Mps1 cDNA was ligated in-frame to the 3' end of cDNA encoding the LAP tag (a gift from I. Cheeseman) and subcloned to pCDNA3. Kinase-dead (D664A) and shRNA-insensitive Mps1 (modified codons 288 and 289) were obtained by site-directed mutagenesis. pCR3-VSV-Borealin has been described[43] and Borealin mutants were obtained by site-directed mutagenesis. pEYFP-LAP-Borealin was created by ligating digested PCR fragments of the various Borealin mutants to pEYFP-LAP.

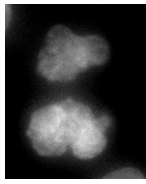

Tissue culture

UTRM10 cells were created by infection of U2OS cells stably expressing Tet repressor (a gift from M. Timmers) with retrovirus carrying pSuperior-retro-puro-Mps1 (see Figure S6 for characterization of cell line), and grown on media with Tet System-approved FBS (Clontech).

Antibodies

The following antibodies were used for immunblots, immunoprecipitations or immunofluorescence: Mps1 (Upstate Biotechnology), Cdk4 (Santa Cruz), α-Tubulin (Sigma), GFP (custom rabbit polyclonal), pSer10-Histone H3 (Upstate Biotechnology), Borealin (a gift from W. Earnshaw), Cyclin B1 (GNS1, Santa Cruz), GST (Santa Cruz), VSV (Sigma), Mad1 (a gift from A. Musacchio), BubR1 (a gift from S. Taylor), CENP-E (a gift from D. Cleveland) and CLIP-170 (a gift from N. Galjart), Bub1 (Abgent), Mad2 (Covance), ACA (Cotrex Biochem), pSer7-CENP-A (Upstate), pT232-Aurora-B (Rockland), Aurora-B (for immunoblot: BD Biosciences, for immunoprecipitations: Abcam). Secondary antibodies for immunofluorescence (Alexa-488, -568 and -647) were from Molecular Probes.

Tandem Mass Spectrometry

In-gel proteolytic digestion of bands stained by simplyblue (Biorad) was performed essentially as described[204] using trypsin, chymotrypsin and elastase (Roche), alone or in combinations. Samples were subjected to nanoflow liquid (LC) chromatography (Agilent 1100 series) and coupled to a QTOF Micro tandem mass spectrometer (Micromass Waters, UK). A survey scan was performed from 400-1200 amu·s^{-1} and precursor ions were sequenced in MS/MS mode at a threshold of 150 counts. Data were processed and subjected to database searches with a 0.25 Da mass tolerance for both precursor ion and fragment ion. The identified phosphorylated peptides were confirmed by manual interpretation of the spectra. Total coverage of Borealin with the combined digestions was 71%.

Immunoprecipitations and in vitro kinase assays.

Conditions for immunoprecipitations of Aurora B using anti-Aurora B antibodies (Abcam) and for pull-downs of LAP-Borealin using S-protein-Agarose (Novagen) were copied from [50], with minor modification. Precipitates were washed twice with lysis buffer, twice with kinase buffer (50 mM Tris pH 7.5, 10 mM $MgCl_2$, 0.5 mM DTT, 1 mM Na_3VO_4, 1 mM β-glycerophosphate), and incubated for 30 minutes at 30°C with 3 µg Histone H3 (Roche) in the presence of 20 µM ATP and 5 µCi ^{32}P-γATP (^{32}P-H3) or 40 µM ATP only (pSer10-H3). His_6-tagged Mps1 was purified from High5 cells infected with baculovirus carrying the pFastBacHT-Mps1 construct.

GST-tagged Borealin, Borealin mutants, Survivin and Aurora B were purified from BL21 bacteria after induction with 1 mM IPTG for 2 hours. 0.5 µg GST-fusion protein was incubated with His_6-Mps1 in the presence of 50 mM Tris, pH7.5, 10 mM $MgCl_2$, 20 µM ATP and 5 µCi ^{32}P-γATP for 30 minutes at 30°C.

Immunofluorescence microscopy.
Cells, plated on 12 mm coverslips, were pre-extracted with 0.2% TritonX-100 in 100 mM PIPES pH6.8, 1mM $MgCl_2$ and 5mM EGTA for 1 minute before fixation with ice-cold methanol or 4% PFA in PBS with 2% sucrose. Coverslips were blocked with 3% BSA in PBS for 1 hour, incubated with primary antibody for 16 hours at 4°C (the antibodies used are described in Supplement), washed with PBS/0.1% Triton X-100 and incubated with secondary antibodies for an additional 1 hour at room temperature. Coverslips were washed and submerged in PBS containing DAPI, washed again and mounted using ProLong Antifade (Molecular Probes). Calcium-treatments were done by adding 0.1 mM $CaCl_2$ to the pre-extraction. All images except those displayed in Figures 2A, 2B, 4C, 5A, 5B, and S2A were acquired on a DeltaVision RT system (Applied Precision) with a 60X/1.42NA PlanApoN objective (Olympus) using SoftWorx software. Images are maximum projections of a deconvolved stack and adjusted (identically within experiments) for sharpness and levels with Adobe Photoshop CS. For quantification, all images of similarly stained experiments and acquired with identical microscope and illumination-settings were analyzed using SoftWorx. Average pixel intensities of regions encompassing centromeres were determined in the various channels and ratios were calculated by correcting the intensities for those of various background regions. Images of Figures 2A, 2B, 4C, 5A, 5B, and S2A were acquired on a Zeiss 510 Meta confocal laser scanning microscope with a 63X/1.4NA Plan-ApoChromat objective using the Zeiss LSM software with 8X zoom. For quantification of these experiments, maximum intensity projections were imported into MetaMorph software (Universal Imaging) and further analyzed as described above.

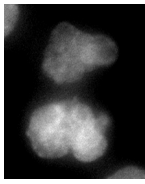

Chapter 2

Chapter 3

Small molecule kinase inhibitors provide insight into Mps1 cell cycle function

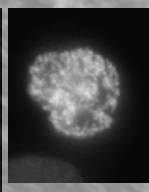

Nicholas Kwiatkowski[1,4], Nannette Jelluma[6], Panagis Filippakopoulos[5], Meera Soundararajan[5], Michael S. Manak[3], Mijung Kwon[2], Hwan Geun Choi[1,4], Taebo Sim[1,4], Quinn L. Deveraux[7], Sabine Rottmann[7], David Pellman[2], Jagesh V. Shah[3], Geert J.P.L. Kops[6], Stefan Knapp[5], Nathanael S. Gray[1,4]

[1]Department of Cancer Biology and [2]Department of Pediatric Oncology Dana Farber Cancer Institute, [3]Renal Division, Brigham and Women's Hospital, Harvard Institutes of Medicine, [4]Department of Biological Chemistry and Molecular Pharmacology, Harvard Medical School, Boston, Massachusetts 02115 USA, [5]Structural Genomics Consortium and the Department of Clinical Pharmacology, University of Oxford, Old Road Campus, Roosevelt Drive, Oxford, OX3 7DQ, UK, [6]Department of Physiological Chemistry and Cancer Genomics Centre, UMC Utrecht, Universiteitsweg 100, 3584 CG, Utrecht, The Netherlands, and [7]Genomics Institute of the Novartis Research Foundation, 10675 John Jay Hopkins Dr., San Diego, California 92121, USA.

Adapted from *Nature Chemical Biology 6(5):359-68, May 2010*

Abstract

Mps1, a dual-specificity kinase, is required for the proper functioning of the spindle assembly checkpoint and the maintenance of chromosomal stability. As Mps1 function has been implicated in numerous phases of the cell cycle, it is expected the development of a potent, selective small molecule inhibitor of Mps1 would greatly facilitate dissection of Mps1-related biology. We describe the cellular effects and Mps1 co-crystal structures of novel, selective small molecule inhibitors of Mps1. Consistent with RNAi studies, chemical inhibition of Mps1 leads to defects in Mad1 and Mad2 establishment at unattached kinetochores, decreased Aurora B kinase activity, premature mitotic exit, and gross aneuploidy, without any evidence of centrosome duplication defects. However, in U2OS cells possessing extra centrosomes, an abnormality found in some cancers, Mps1 inhibition increases the frequency of multipolar mitoses. Lastly, Mps1 inhibitor treatment resulted in a decrease in cancer cell viability.

Introduction

The successful segregation of chromosomes in mitosis requires the timely coordination of cell cycle events to ensure the bipolar attachment of sister chromatids via their kinetochores to the mitotic spindle prior to the initiation of anaphase. Deregulation of this process or uncoupling of its component parts can lead to aneuploidy and chromosomal instability (CIN), recognized hallmarks of cancer. Mps1, a dual-specificity kinase[123], was first identified in *Saccharomyces cerevisiae* (Mps1p) where it was shown to function in multiple pathways critical to the maintenance of genomic integrity, including spindle pole body (SPB) duplication[122,184], mitotic spindle assembly[182], and the spindle assembly checkpoint (mitotic checkpoint)[122]. The spindle assembly checkpoint (SAC), a conserved pathway in eukaryotes, is responsible for monitoring mitotic spindle attachment at kinetochores. In response to a lack of microtubule occupancy at kinetochores or a lack of tension between sister kinetochores the checkpoint prevents the early onset of anaphase until all chromosomes make stable bipolar attachments to the mitotic spindle (reviewed in [205]). Evidence from functional and localization experiments in mammalian cells have demonstrated that Mps1 is required for the maintenance of the mammalian SAC[106,107,131,193]. In contrast to its unequivocal role in the mammalian SAC, its purported role in centrosome (mammalian equivalent of SPB) duplication in S-phase and subsequent bipolar spindle assembly is a topic of considerable debate[130,133,135,206]. Nevertheless, the necessity of Mps1 kinase activity for the fidelity of the cell cycle and genomic stability is well established.

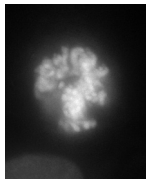

Investigating how Mps1 kinase activity and its dynamic localization during the cell cycle participate in the coordination of multiple cell cycle processes requires the ability to rapidly inhibit Mps1 kinase activity at specific phases of the cell cycle; a level of temporal control that cannot be attained using RNAi or other common genetic methods. Small molecules that are cell permeable and can inhibit Mps1 kinase activity with rapid and reversible kinetics may provide a powerful tool to probe cell cycle-related Mps1 functions. ATP-competitive inhibitors of mitotic kinases Aurora A/B, cyclin-dependent kinase 1 (Cdk1), and Polo-like kinase 1 (Plk1) have proven invaluable to elucidate the temporal function and potential therapeutic relevance of these proteins due to their ability to inhibit kinase activity in a dose-dependent and rapid fashion (reviewed in [207]).

In contrast to partial inactivation of Mps1 kinase activity, complete depletion of Mps1 or replacement of wild-type Mps1 activity with a kinase-dead Mps1 D664A allele results in cell death[208-211 (Chapter 2 & 5 of this thesis)]. Similar findings with checkpoint components Mad2[95,146,153,212] and BubR1[160,203] support the view that complete spindle checkpoint abrogation is lethal to cells, while decreased checkpoint stability results in non-lethal chromosomal instability (reviewed in [213]). Targeted chemical inhibition of Mps1 may therefore prove to be an efficient means of pharmacologically evaluating the consequences of inactivating the checkpoint as 1) epistasis experiments suggest Mps1 functions near the apex of the SAC signaling cascade[106,107,214], 2) Mps1 kinase activity is essential to checkpoint function[85], and 3) kinases make excellent targets for inhibitor development. A selective Mps1 kinase inhibitor will also address the question of whether targeted ablation of the mitotic checkpoint in rapidly proliferating tumor cells is a potential therapeutic approach.

Previously, three Mps1 inhibitors have been reported in the literature while other potential inhibitors have been discovered by high-throughput *in vitro* screens but lack characterization of cellular activity[215,216]. The first, cincreasin, was shown to be effective at inhibiting Mps1 kinase activity in *S. cerevisiae* but was reported to be ineffective in mammalian cells[183]. The second inhibitor, 1NM-PP1, was designed to inhibit Mps1 kinase function in yeast but only in the

context of a sensitizing mutation in Mps1[182]. The third, a dual JNK, Mps1 inhibitor SP600125 was reported but it exhibited very poor selectivity (Supplementary Figure S1A, Supplementary Table S1), which would likely limit its utility as a selective probe of Mps1 function[186].

Here we describe the discovery and characterization of two new classes of potent and selective ATP-competitive Mps1 kinase inhibitors and their co-crystal structures with Mps1 kinase domain. Mps1-IN-1 (**1**) and Mps1-IN-2 (**2**) (Mps1 Inhibitor 1 and 2) inhibit Mps1 with moderate potency, exhibiting half-maximal inhibitory concentrations (IC_{50}) of 367 nM and 145 nM respectively. Consistent with RNAi studies, chemical inhibition of Mps1 leads to defects in Mad1 and Mad2 establishment at unattached kinetochores, premature mitotic exit and reduced Aurora B kinase activity leading to the manifestation of gross aneuploidy. We found no evidence of centrosome duplication defects upon inhibition of Mps1 kinase activity. However, in U2OS cells possessing extra centrosomes Mps1 inhibition results in a catastrophic mitosis causing massive chromosome missegregation. Finally, we demonstrate that SAC silencing by Mps1 inhibition results in aneuploidy and decreases the viability of both cancer and 'normal' cells.

Results

Identification of Lead Compounds for Mps1 inhibition

In an effort to discover novel classes of selective small molecule inhibitors of Mps1 and other kinases we screened a diverse library of heterocyclic ATP-site directed kinase scaffolds using an *in vitro* ATP-site competition binding assay[215,217]. Approximately 400 compounds were profiled at a concentration of 10 μM against a panel of 352 diverse kinases. By screening this 'library' of inhibitors versus this large panel of kinases we were able to generate a selectivity-annotated library (SAL), which allowed us to rapidly identify compounds capable of selectively inhibiting Mps1 as well as other kinases of interest. Several different scaffolds including 2,6-disubstituted purines, 2,4-disubstituted pyrrolopyridines, and dihydropyrimidodiazepinones emerged as potential Mps1 inhibitor scaffolds. We focused our attention primarily on the latter two scaffolds as they demonstrated the highest degree of selectivity among available lead scaffolds. The 2,6-disubstituted purine series, though potent for its Mps1 target proved to be a more promiscuous scaffold class. Several iterative rounds of synthesis and biochemical and cellular kinase profiling resulted in the discovery of the two inhibitor series, which we named Mps1-IN-1 and Mps1-IN-2 (Mps1 Inhibitor 1 and 2) (Figure 1A, synthetic chemistry routes available in Supplementary Figure S2).

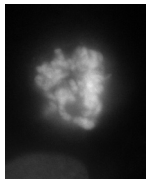

Mps1-IN-1 and 2 inhibited Mps1 kinase activity with half-maximal inhibitory concentrations (IC_{50}) of 367 nM and 145 nM respectively when screened at 1 μM ATP (apparent Km for ATP < 1 μM) (Figure 1B). Both compounds demonstrated greater than 1000-fold selectivity relative to the 352 member kinase panel with the major exceptions of Alk and Ltk for Mps1-IN-1 and Gak and Plk1 for Mps1-IN-2 (Supplementary Figure S1B, Supplementary Tables S1 and S2). The Alk activity of Mps-IN-1 is not unexpected as this series of pyrrolopyridines is structurally similar to TAE684, a known potent Alk inhibitor[218]. Given the restricted tissue expression of both Alk[219] and Ltk[219] these off-target interactions would not be expected to significantly interfere with the use of Mps1-IN-1 in cell types typically used to study the spindle checkpoint. Mps1-IN-2 was overall more selective than Mps1-IN-1, but possesses significant activity against Plk1, which is consistent with this compound being a ring-expanded version of a highly potent Plk1 (and Plk2, Plk3) inhibitor: BI-2536[220]. Although the Plk1 activity of Mps1-IN-2 limits its use as a selective Mps1 inhibitor, the compound does provide a unique tool to investigate the combined inhibition of Plk1 and Mps1. In addition because these two compounds do not share any common off-targets with the exception of Mps1, the phenotypes they have in common are likely to result from Mps1 inhibition. The majority of cellular experiments in this study were performed with Mps1-IN-1.

Crystal structure of Mps1 Kinase Domain

Mps1 shares only weak sequence homology (~20% in kinase domain) with kinases of known structure. To this end we determined the crystal structure of the catalytic domain (F515-Q794) of Mps1 at 2.3 Å resolution (Supplementary Table S3). The structure of Mps1 revealed the characteristic bilobal domain architecture and secondary structure elements of protein kinases (Supplementary Figure S3A). Following deposition of the coordinates into the protein database (http://www.rcsb.org/pdb/home/home.do) two more apo-structures were published[216,221]. Our structural model superimposed with an r.m.s.d of 0.78 Å and 0.5 Å with these models that have been refined at 2.7 Å and 3.17 Å, respectively.

Mps1 adopts an inactive conformation as indicated by incorrect positioning of the regulatory helix αC, the lack of a salt bridge between the conserved αC glutamate (E571) and the active

site lysine (K553), and an unstructured activation loop (M671-V684). In the lower kinase lobe the loop region between residues S699-K708 was also disordered. Interestingly, a polyethylene glycol molecule present in the crystallization solution was visible in the electron density as a ring around the catalytic lysine (K553).

The observed inactive conformation is surprising considering that nine phosphorylation sites were detected by ESI-MS after expression of Mps1 in bacteria. However, none of these sites were visible in the electron density in the apo-crystal structure suggesting that the location of the auto-phosphorylation sites is confined to the unstructured regions of the protein. Homogeneously de-phosphorylated protein was obtained by co-expressing λ-phosphatase. However, no crystals were obtained using the unphosphorylated protein.

Binding modes of Mps1-IN-1 and methoxy-Mps1-IN-2

Mps1-IN-1 was co-crystallized and structural models were refined at 2.74 Å resolution (Supplementary Table S3). As expected, the inhibitor bound to the ATP binding pocket of Mps1 forming a hydrogen bond with the hinge backbone (E603). The structure of the complex superimposed well with the apo-structure and main structural differences of the protein backbone were confined to the phosphate-binding loop (P-loop) region (Supplementary Figure S3B). The inhibitor was well defined by electron density (Figure 1D). The binding mode was stabilized by a number of hydrophobic interactions involving the gatekeeper residue M602 as well as I663, L654 and the P-loop residues V539 and I531 (Figure 1C, Supplementary Figure S3B). Both Mps1-IN-1 and the polyethylene glycol molecule occupied the ATP binding sites simultaneously.

We co-crystallized a close analog of Mps1-IN-2, methoxy-Mps1-IN-2 (**3**), which contains a methoxy instead of an ethoxy substituent at the ortho-position of the C2-aniline. Though a strong selectivity determinant, the ethoxy group of Mps1-IN-2 would not be expected to alter the overall binding mode of the molecule from that of what is seen for methoxy-Mps1-IN-2. Methoxy-Mps1-IN-2 forms a hydrogen bond with the hinge residue G605 and forms a tight contact with the same hydrophobic residues as Mps1-IN-1 (Figure 1C, Supplementary Figure S3B). The polyethylene glycol molecule was however not present in the methoxy-Mps1-IN-2 complex structure. The most significant structural change relative to the Mps1-IN-1 complex was that the activation segment became ordered revealing three phosphorylated amino acid residues (T675, T676 and S677) and formed an antiparallel β-sheet interaction with the P-loop (Figure 1C). The high charge density of the three consecutive phosphorylated residues is compensated by 2 Mg^{2+} ions that are coordinated by the phosphate oxygens. However, this conformation of the activation segment may be a consequence of crystal contacts. Auto-phosphorylation on T676 has been shown to activate Mps1[210,222] (Chapter 5 of this thesis) but the functional role of the other two phosphorylation sites is unknown.

Mps1-IN-1 and Mps1-IN-2 abrogate SAC function

We first investigated whether chemical inhibition of Mps1 would elicit similar phenotypes to that of Mps1 RNAi-mediated knockdown, including silencing of the SAC in mammalian cells[130]. Silencing of the SAC, a surrogate readout of Mps1 activity, can be assessed by monitoring events that signal that the cell has progressed through mitosis such as disappearance of phosphorylated histone H3 pSer10 (pHistone H3) or degradation of Cyclin B. As assessed by flow cytometry, administration of Mps1-IN-1 to U2OS cells arrested in mitosis using nocodazole, resulted in a dose-dependent accumulation of 4c pHistone H3 negative cells (Supplementary Figure S4A). Likewise, levels of Cyclin B protein, which accumulate in G2 and are sustained during an activated spindle checkpoint[130], dropped with increasing concentration of Mps1-IN-1 or -2, but

could be reversed by addition of the proteasome inhibitor, MG132 (Figure 2A). Downregulation of these mitotic markers indicate that both compounds cause a dose-dependent escape from a checkpoint-mediated mitotic arrest. Mitotic escape induced by Mps1-IN-1 was rapid with DNA de-condensation and nuclear envelope reassembly apparent in as early as 20 minutes with the majority of cells escaping within 1 hour, as compared to DMSO-treated control cells that

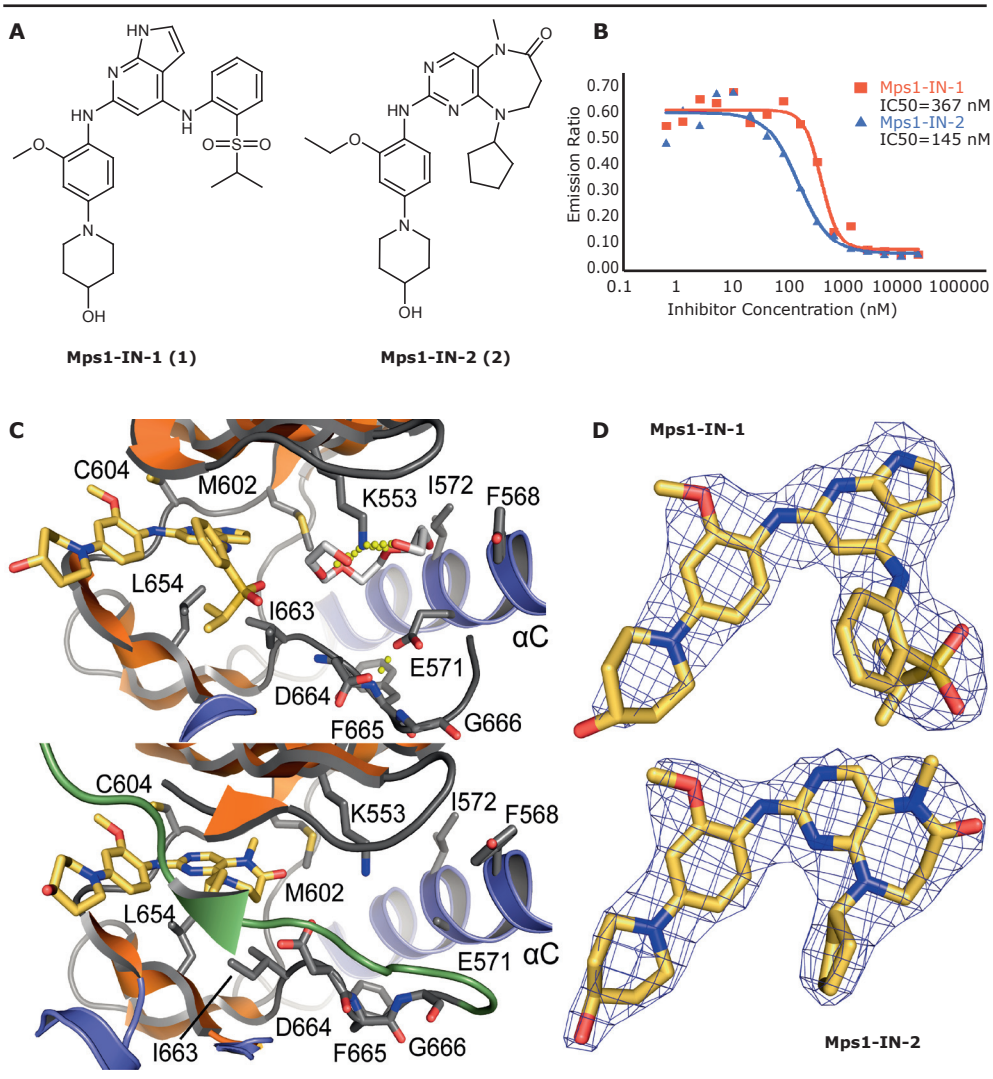

Figure 1. Mps1-IN-1 and Mps1-IN-2 inhibit Mps1 kinase activity and bind Mps1 in the ATP-binding site

(A) The chemical structures of two ATP-competitive Mps1 kinase inhibitors, Mps1-IN-1 and Mps1-IN-2, are derived from two scaffold series: pyrrolopyridine and pyrimidodiazepinone respectively. (B) *In vitro* kinase assays using the Lanthascreen technology were performed to assess the *in vitro* activity of compounds 1 and 2. 5 $\mu g \cdot ml^{-1}$ Mps1 (~ 40 nM) kinase was used in each reaction with 1 μM ATP (Km,app < 1 μM) and 200 nM AF-647 E4Y substrate. (C) Active site of Mps1 in complex with Mps1-IN-1 (upper panel) and the methoxy derivative of Mps1-IN-2 (methoxy-Mps1-IN-2 - lower panel). The most important residues interacting with the inhibitor are shown in stick representation and are labeled. The polyethylene glycol molecule coordinating the conserved active site lysine (K553) in the Mps1-IN-1 complex is also shown. Carbon atoms of Mps1-IN-1 and Mps1-IN-2 are shown in yellow to discriminate from Mps1 kinase residue side chains. (D) 2FoFc electron density map contoured at 2σ around the inhibitor molecules.

exhibited sustained arrest (Figure 2B and 2C). Similar results were obtained when the SAC was activated using other spindle perturbing agents such as the Tubulin stabilizer taxol and the kinesin-5 inhibitor *S*-trityl cysteine (Supplementary Figure S4B). These results suggest that Mps1 activity is required to maintain mitotic arrest under conditions affecting both attachment and tension.

To probe the effects of Mps1-IN-1 on an unperturbed mitosis, U2OS cells expressing fluorescently-tagged histone H2B (H2B-GFP) cells were treated with the inhibitor and the time spent in mitosis, from nuclear envelope breakdown (NEBD) to anaphase initiation, was assessed**.** Mps1-IN-1 administration resulted in a dose-dependent decrease in the time spent in mitosis with nearly 100% U2OS cells initiating anaphase within 20 minutes (10 μM Mps1-IN-1) as compared to roughly 10% in DMSO-treated cells (Figure 2D, Supplementary Figure S5A and Movies S1 and S2). Acceleration of mitosis kinetics in Mps1-IN-1-treated cells had direct consequences on genomic stability with cells exhibiting significant signs of chromosome misalignment and chromosome missegregation (Supplementary Figures S5A-C) manifesting aneuploidy (Figure 2E, left two panels and Supplementary Figures S5D, S5E), phenomena previously reported for RNAi-mediated knockdown of Mps1 and other checkpoint components[95,186,210-212] (Chapter 2 & 5 of this thesis).

Mutation of the kinase active site gatekeeper residue from Methionine (M) to Glutamine (Q) in Mps1 (M602Q) was previously shown reduce the potency of inhibition by the ATP-competitive small molecule inhibitor, SP600125 without significantly disrupting Mps1 kinase activity or proper kinetochore localization[186]. To investigate whether the M602Q mutation would also confer resistance to the new inhibitors, a radioenzymatic immunoprecipitation kinase assay was performed using WT or M602Q LAP-Mps1. The M602Q Mps1 mutant was 5- and 19-fold less sensitive to Mps1-IN-1 and Mps1-IN-2 respectively (Supplementary Figures S6A, S6B).

To investigate the effect of this mutation on intracellular inhibitor activity, endogenous Mps1 was replaced with the putative inhibitor resistant allele of Mps1 (M602Q). This was achieved by simultaneous expression of a plasmid-based Mps1 shRNA and an RNAi-insensitive LAP-tagged Mps1 M602Q allele to generate a stable U2OS cell line expressing LAP-Mps1 M602Q (UTRM10 Mps1 M602Q) (Figure 2F)[210, 211] (Chapter 2 & 5 of this thesis). Expression of LAP-Mps1 M602Q restored pHistone H3 positivity to wild-type levels in the presence of Mps1-IN-1 and Mps1-IN-2 up to concentrations of 1 and 10 μM respectively (Figure 2G). In contrast, treatment with VX-680[223], a potent pan-Aurora kinase inhibitor that causes a similar mitotic arrest override, was still capable of executing an efficient mitotic escape. Additionally, expression of LAP-Mps1

Figure 2. Mps1-IN-1 and Mps1-IN-2 induce bypass of a checkpoint-mediated mitotic arrest
(A) Immunoblot of Cyclin B from U2OS cells treated with Mps1 inhibitors. U2OS cells were arrested in mitosis by combination treatment of thymidine and nocodazole prior to treatment with nocodazole or co-administration with Mps1 inhibitor +/- MG132 for 4 hrs. (B) HeLa S3 cells expressing histone H2B-GFP were treated with nocodazole +/- Mps1-IN-1. Cells were followed by live imaging to determine exit from mitosis via nuclear envelope reassembly. 150 cells of each cell population were counted. (C) Selected frames from a timelapse series of cells after treatment as in (B). Time is given in minutes:seconds. (D) Cumulative percentage of cells initiating anaphase. U2OS H2B-GFP cells were treated with DMSO or Mps1-IN-1 and imaged using fluorescence timelapse microscopy. Time refers to the duration between nuclear envelope breakdown (NEBD) and anaphase initiation. 100 cells of each cell population were analyzed. (E) FACS analysis of UTRM10 cells expressing LAP-Mps1 WT or M602Q treated with Mps1-IN-1 or DMSO for 48 hrs. (F) Immunoblot showing induction of the RNAi-resistant LAP-tagged proteins. Clones were harvested and the relative levels of LAP-Mps1 in mitosis were compared to the UTRM10 parental cell line[210,211] (Chapter 2; Chapter 5). (G) Immunoblot of pHistone H3 in UTRM10 cells expressing LAP-Mps1 WT or M602Q after treatment with Mps1 inhibitors. UTRM10 cell lines arrested in mitosis by combination treatment of thymidine and taxol were treated with taxol +/- inhibitor. All graphics were obtained from three independent experiments. Scale bars in C are 10 μm.

M602Q reduced the aneuploidy and chromosome missegregation phenotypes caused by Mps1-IN-1 (Supplementary Figure S7, Figure 2E, compare left and right panels). Finally, Mps1 has been reported to reside in a hyper-phosphorylated and activated form during checkpoint activation due in large part to auto-phosphorylation[210] (Chapter 5 of this thesis). Addition of Mps1-IN-1 to UTRM10 LAP-Mps1 WT cells causes a dose-dependent reduction in hyper-phosphorylated

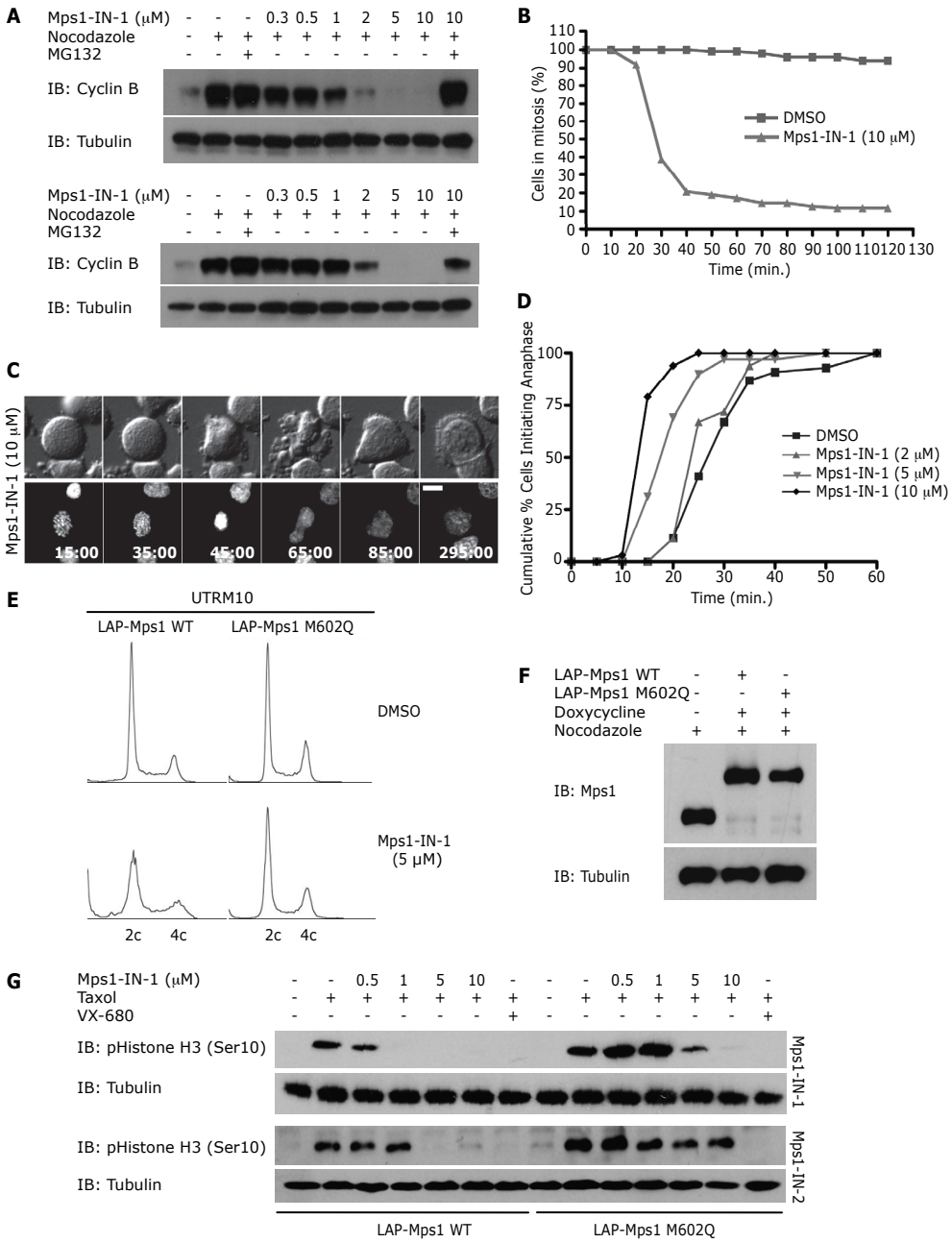

Mps1 as demonstrated by a decrease in phosphorylation-induced mobility shift (Supplementary Figure S6C, compare lanes 2 -5). In contrast, UTRM10 LAP-Mps1 M602Q cells maintained high levels of hyper-phosphorylated Mps1 in the presence of Mps1-IN-1 (Supplementary Figure S6C, compare lanes 7-10). Together these findings support the assertion that Mps1-IN-1 and -2 override the checkpoint through direct inhibition of Mps1.

Mps1-IN-1 disrupts recruitment of Mad2 to kinetochores

The effect of chemical inhibition of Mps1 kinase activity on the localization of Mad2, an essential component of the mitotic checkpoint, was examined next. Previous reports examining the kinetochore localization of checkpoint components, particularly Mad1 and Mad2, after RNAi-mediated knockdown of Mps1 have yielded conflicting results[106,186,208]. In this study, the use of timelapse fluorescence microscopy allowed us to determine the effect of inhibition of Mps1 kinase activity on the establishment of Mad2 at unattached kinetochores in the presence or absence of nocodazole.

To this end, a PtK2 cell line stably expressing hsMad2-EYFP (Supplementary Method) was used to determine whether Mps1 kinase activity is required for the checkpoint activation and initial establishment of Mad2 at unattached kinetochores. Mps1-IN-1-treated hsMad2-EYFP PtK2 cells were followed as they entered mitosis and the levels of Mad2 at kinetochores were quantified. As compared to DMSO-treated control cells, Mps1-IN-1-treated cells exhibited an 80% decrease in kinetochore-bound Mad2 (Figures 3A and 3B, Supplementary Movies S3 and S4). As a result, Mps1-IN-1-treated cells spent roughly 40% less time in mitosis as compared to DMSO-treated cells (Figure 3C). Similar results were obtained when cells entered mitosis in the presence of both Mps1-IN-1 and nocodazole to stimulate checkpoint response. Mps1-IN-1 and nocodazole co-treated cells displayed a 70% reduction in the amount of kinetochore-bound Mad2 as compared to nocodazole-treated cells (Figures 3A and 3B, Supplementary Movies S5 and S6). Mps1-IN-1-treated cells were unable to establish a proficient checkpoint in the presence of nocodazole and exited mitosis prematurely (Figure 3C). The disappearance of hsMad2 (and hsMad1) from kinetochores following Mps1-IN-1 treatment was corroborated in HeLa cells using indirect immunofluorescence (Supplementary Figure S8). These results clearly demonstrate that Mps1 kinase activity is required for the recruitment of Mad2 to kinetochores and SAC activation.

Figure 3. Mps1-IN-1 treatment causes disruption in recruitment of Mad2 to kinetochores
(A) Establishment of Mad2 at the kinetochores is dependent on Mps1 kinase activity when cells enter mitosis. PtK2 cells stably expressing HsMad2-EYFP were treated with either Mps1-IN-1 (10 μM) (N=29) or Mps1-IN-1 (10 μM) and nocodazole (N=25) and then imaged entering mitosis. Corresponding controls were PtK2 cells stably expressing HsMad2-EYFP treated with DMSO (N=26) or treated with nocodazole only (N=20) and then imaged entering mitosis. Normalized average kinetochore density representing Mad2-EYFP at kinetochores was measured and background corrected for each experimental case and control. Error bars represent the 95% confidence interval of each data set (* p-value = $5.63 \cdot 10^{-09}$, ** p-value = $7.39 \cdot 10^{-07}$ Student's t test). (B) Representative images of PtK2 cells stably expressing HsMad2-EYFP that were treated as in (A). The top panel are images of HsMad2-EYFP fluorescence and the bottom panel are corresponding phase images. Scale bar is equal to 10 μm. (C) Inhibition of Mps1 kinase activity affects mitotic timing. Randomly cycling PtK2 cells stably expressing HsMad2-EYFP were treated with either Mps1-IN-1 (10 μM) (N=29) alone or with Mps1-IN-1 (10 μM) and nocodazole (N=25) and then imaged entering mitosis from nuclear envelope breakdown (NEB) through to nuclear envelope reassembly (NER). Untreated PtK2 cells (N=26) or those treated with nocodazole only (N=20) were also imaged. Average time spent in mitosis (from NEB to NER) is shown. Error bars represent the 95% confidence interval of each data set (* p< $2.23 \cdot 10^{-08}$, ** p<$3.08 \cdot 10^{-08}$, Student's t test).

Mps1-IN-1 affects the kinase activity of Aurora B

Previous evidence has suggested that an epistatic signaling relationship exists between Mps1 and Aurora B, whereby Mps1 modulates the cellular kinase activity of Aurora B[211] (Chapter 2). This finding suggested a plausible mechanism whereby an activated checkpoint could serve to initiate or modulate the tension-sensing process of attachment error correction with the Mps1-Aurora B interaction acting as a bridge between the two processes.

We sought to use Mps1-IN-1 as a means to test this epistatic relationship. Both HeLa and U2OS cells were released from a thymidine block and prior to mitotic entry were treated with

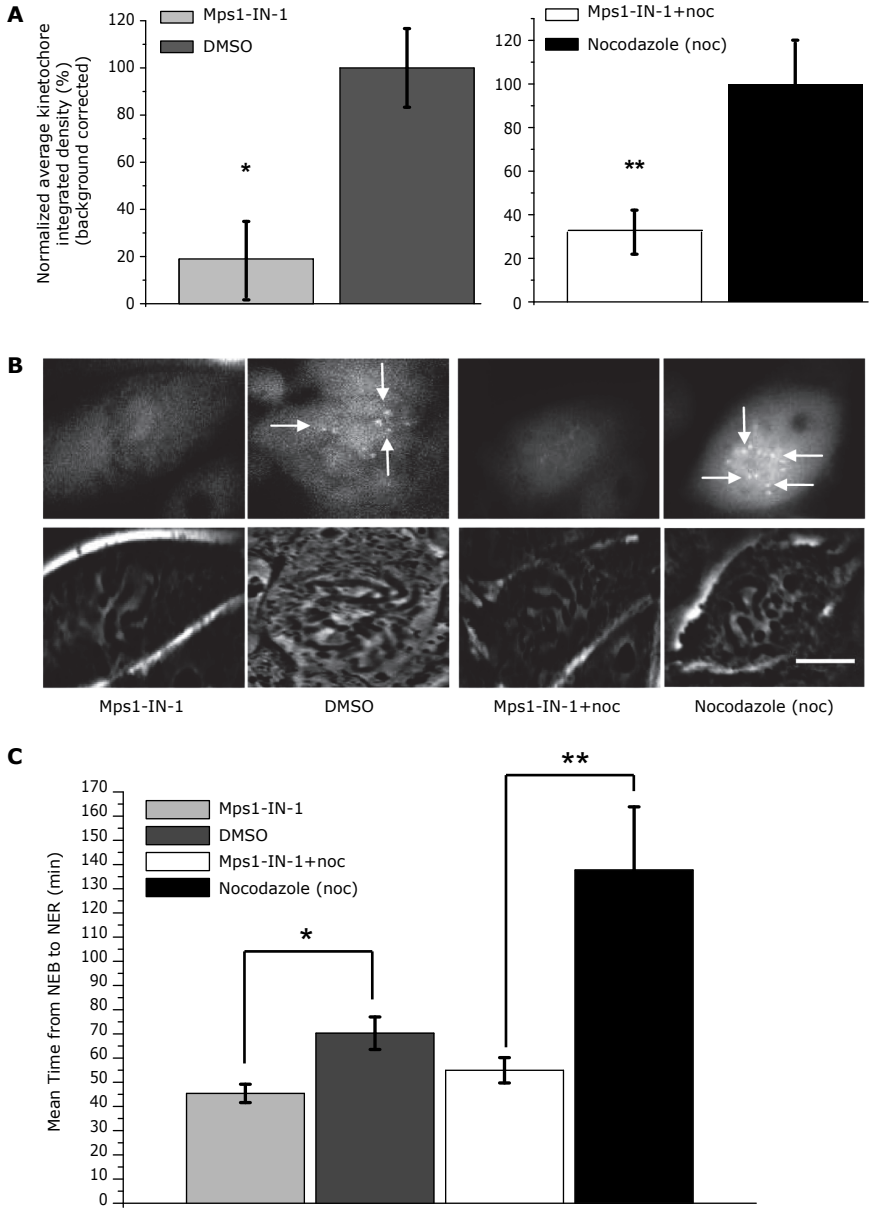

Mps1-IN-1 or DMSO vehicle for 1 hr. Cells were subsequently treated with taxol and MG132 (Figure 4A) and mitotic cells were collected by shake-off. The sustained Cyclin B levels corroborated that the collected cells were mitotic, yet a reduction in pHistone H3 (Ser10) signal (a direct Aurora B substrate) upon Mps1-IN-1 treatment was apparent in both cell lines (Figure 4B). Additionally, Mps1-IN-1 treatment caused a dose-dependent reduction in the phosphorylation status of Aurora B at threonine-232 (Thr232), an activation loop phosphorylation of the kinase that is responsible for increased kinase activity[200], further suggesting that inhibition of Mps1 reduces Aurora B kinase activity (Figure 4C, lanes 2-4). The reciprocal experiment showed that treatment with VX-680 inhibited the activation and phosphorylation of Aurora B (Thr232), but did not adversely affect the hyperphosphorylation status of Mps1, as evidenced by the maintained phosphorylation-induced mobility shift in the Mps1 protein band (Figure 4C). Direct inhibition of Aurora B by Mps1-IN-1 is unlikely as *in vitro* assays indicate that Mps1-IN-1 does not exhibit activity against Aurora B (Figure 4D, Supplementary Table S1). These results support the hypothesis that Mps1 kinase activity regulates Aurora B intracellular kinase activity.

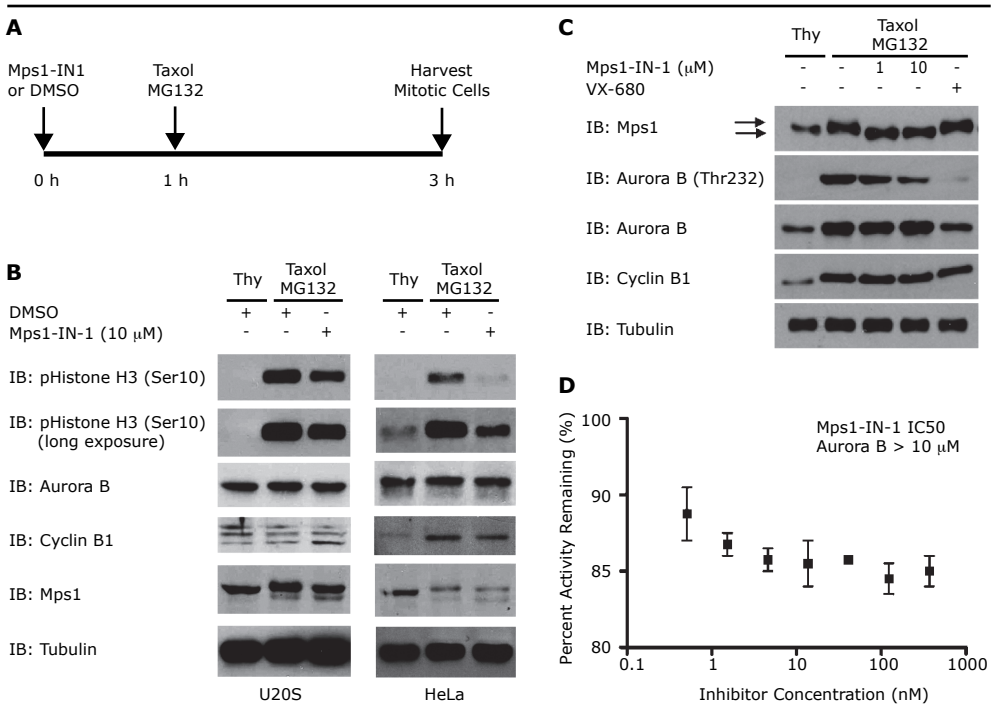

Figure 4. Mps1-IN-1 treatment decreases intracellular Aurora B kinase activity
(A) Schematic of the treatment regimen used to assess the effect of Mps1-IN-1 treatment on intracellular Aurora B kinase activity during taxol treatment in HeLa and U2OS cells. (B) Mps1-IN-1 treatment decreases the phosphorylation of pHistone H3 (Ser10), a direct substrate of Aurora B. Immunoblot of HeLa and U2OS cells treated as described in (A). An antibody to pHistone H3 (Ser10) was used to assess the kinase activity of Aurora B, while the mobility shift in Mps1 was used to assess the relative amount of Mps1 auto-phosphorylation. Cyclin B levels served as a mitotic marker. (C) Mps1-IN-1 treatment decreases the phosphorylation of Aurora B in its activation loop (Thr232). U2OS cells were treated as described in (A). An antibody to pAurora B (Thr232) was used to assess the phosphorylation of Aurora B, while the mobility shift in Mps1 was used to assess the relative amount of Mps1 auto-phosphorylation. Cyclin B levels served as a mitotic marker. Arrows indicate phosphorylation-induced shift of Mps1 total protein band. (D) *In vitro* kinase assay using the Lanthascreen technology was performed to assess the *in vitro* activity of Mps1-IN-1 on Aurora B. Aurora B kinase (5 nM) was used in each reaction with ATP at the apparent Km (63.7 nM) and the substrate, 30 nM Kinase Tracer 236.

Mps1-IN-1 does not affect centrosome duplication

The founding member of the Mps1 kinase family (Mps1p of *S. cerevisiae*) has been implicated in the duplication of the yeast spindle pole body (SPB) due to the phenotypic manifestation of monopolar spindles after Mps1p inactivation[122,184]. Additional evidence with murine Mps1 (mMps1) suggested mMps1 to be required for centrosome duplication supporting the notion that this function was evolutionary conserved in mammalian cells[132]. However, conflicting reports in human cells have raised questions as to whether human Mps1 (hMps1) is required for centrosome (re)duplication[130,133,135,206].

To determine if Mps1 kinase activity is indeed necessary for centrosome duplication we treated synchronized cells with 10 μM Mps1-IN-1 (Figure 5A), a concentration known to inhibit all checkpoint-associated Mps1 kinase activity (Figure 2A and Supplementary Figure S4A), for two cell cycles. Mitotic cells were then scored for the number of centrioles they contained. Untreated mitotic cells have 2 centrioles per centrosome (4 per cell), whereas mitotic cells exhibiting centrosome duplication defects would have fewer. Analysis of cells after one cell cycle ensures that all mitotic cells scored had passed through only one S-phase in the presence of Mps1-IN-1; a level of time resolution that can only be attained with small molecule intervention. Analysis of cells after two cell cycles allows one to visualize the appearance of monopolar spindles that would arise by dilution of centrioles by passage through successive rounds of cell division without concomitant centriole duplication. Using this scheme we found no significant difference between vehicle- and compound-treated cell populations after 1 or 2 cell doublings as the mean percentage of mitotic cells containing less than 4 centrioles (centrin dots) remained unchanged within one standard deviation (Figures 5B and 5C).

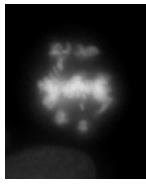

Hydroxyurea treatment of U2OS has been shown to result in overduplication of centrioles. To determine whether Mps1-IN-1 treatment disrupts centriole overduplication during a prolonged S-phase arrest, UTRM10 cells were co-treated with hydroxyurea and Mps1-IN-1 (10 or 25 μM) or DMSO vehicle for 48 hours. Similar to the results obtained with cycling cells, no effect of Mps1 inhibition on centriole overduplication was seen with the fraction of each cell population remaining statistically unchanged (Figure 5F). In accordance with compound treatment, shRNA-mediated ablation of Mps1 in UTRM10 cells displayed no significant difference in centrosome duplication from DMSO control despite the lack of detectable Mps1 protein (Figures 5D, 5E). Therefore, we conclude that in the presence of Mps1-IN-1 or shRNA-mediated knockdown of Mps1 we find no evidence for Mps1-dependent effects on centrosome duplication.

Mps1-IN-1 increases multipolar cell divisions in extra centrosomal cells

Centrosome amplification is a common feature of many cancer cells. Recently, several groups have reported that cells with extra centrosomes activate the spindle assembly checkpoint[224-226]. SAC-dependent delay of anaphase onset is an important mechanism to protect against the harmful consequences of extra centrosomes by providing time for cancer cells to cluster extra centrosomes, enabling bipolar spindle assembly and normal cell division[224,226]. A natural hypothesis is whether Mps1-IN-1-induced checkpoint abrogation would be preferentially cytotoxic to cancer cells with extra centrosomes.

To determine if Mps1-dependent SAC activation promotes bipolar divisions in mammalian cells harboring extra centrosomes we characterized mitosis in U2OS cells where centrosome number can be controlled by the inducible expression of Plk4. Plk4 kinase is the 'master regulator' of centriole duplication and its overexpression induces centrosome amplification[227]. As expected, doxycycline treatment of cells rapidly induced extra centrosomes, generating populations of cells where ~80% contain extra centrosomes (Figure 6A). Despite the presence of extra centrosomes,

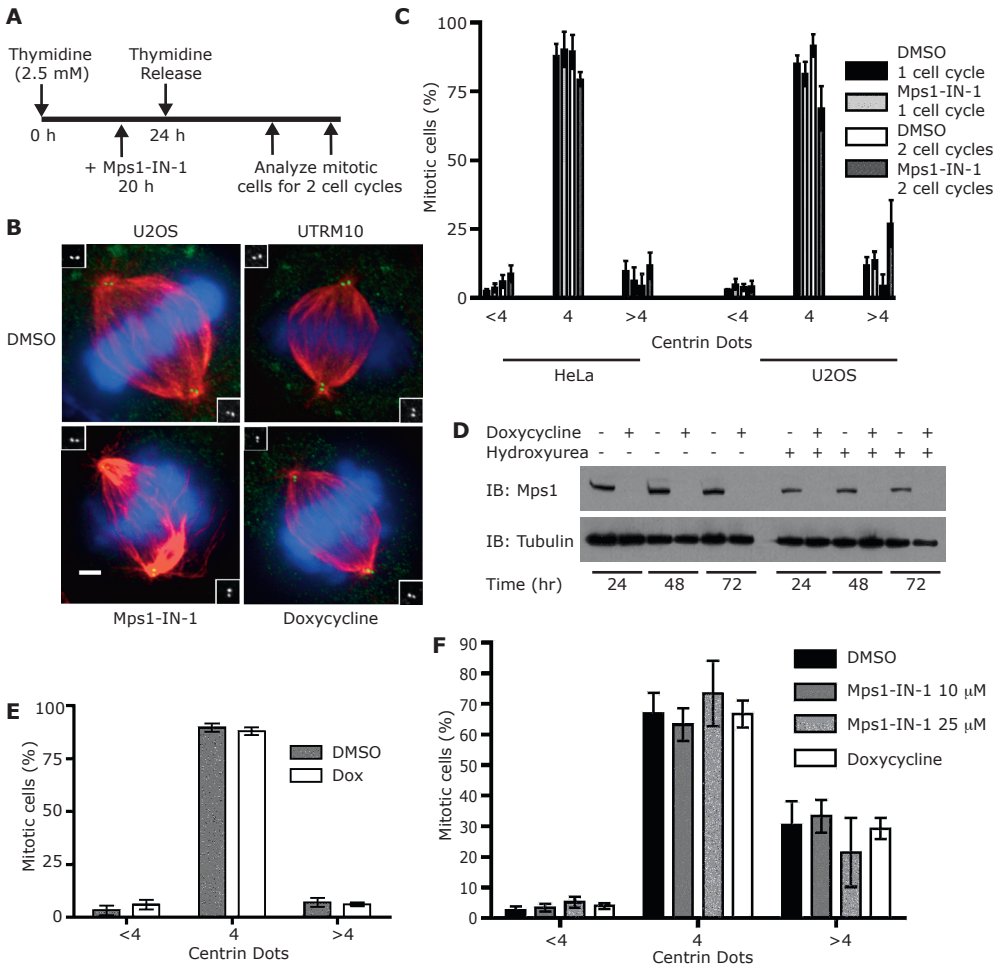

Figure 5. Mps1-IN-1 compound treatment does not affect centrosome duplication
(A) Schematic of the treatment regimen used to assess the effect of Mps1-IN-1 treatment on centrosome duplication in HeLa and U2OS cells. (B) Immunofluorescence images of U2OS cells treated with Mps1-IN-1 or doxycycline to induce Mps1 shRNA expression. Centrin, α-Tubulin and DNA are shown in green, red and blue, respectively. Insets show high magnification images of centrin staining. (C) Mps1-IN-1 treatment does not affect centrosome number in cycling HeLa S3 or U2OS cells. The centriole number of mitotic spindles from synchronized cycling cells treated with Mps1-IN-1 or DMSO was quantitated using centrin staining. Cells counted (1 and 2 cell cycles): HeLa DMSO - 288 and 260 cells, HeLa Mps1-IN-1 - 296 and 260 cells, U2OS DMSO - 300 and 234 cells, U2OS Mps1-IN-1 - 300 and 135 cells. (D) Immunoblot showing shRNA-mediated depletion of endogenous Mps1 in UTRM10 cells by doxycycline treatment. (E) Depletion of Mps1 does not affect centrosome number in UTRM10 cells. The centriole number of mitotic spindles from cycling cells treated with doxycycline for 72 hrs. was scored as in (C). 304 DMSO-treated mitotic cells and 267 doxycycline-treated mitotic cells were scored. (F) UTRM10 cells co-treated with hydroxyurea and either Mps1-IN-1, doxycycline, or DMSO vehicle for 48 hours were scored using centrin staining. Cells counted: DMSO - 443, Mps1-IN-1 10 μM/25 μM - 433/433, doxycycline - 485. All graphics represent mean +/- SD and were obtained from three independent experiments. Scale bar in B is 10 μm.

the majority of extracentrosomal cells (~80%) successfully divide in a bipolar manner because of efficient clustering of the extra centrosomes (Figure 6B) and multipolar metaphase figures are resolved into bipolar spindles prior to anaphase onset (Figure 6C). To directly determine if SAC inhibition by Mps1-IN-1 induces multipolar anaphases in extracentrosomal cells, U2OS cells expressing H2B-GFP were synchronized with a double thymidine block, released for 6-7 hrs and treated with Mps1-IN-1, with or without Plk4 overexpression. Note that this protocol excludes the possible consequences of inhibiting Mps1 on centriole duplication, a controversial point in mammalian cells[130,133]. Timelapse imaging to monitor time from NEBD to anaphase onset revealed that the induction of extra centrosomes (+Dox) led to a ~ 2 fold delay in anaphase onset (Figures 6D and 6E, Supplementary Movie S7). In these cells, Mps1-IN-1 treatment abolished the anaphase delay (Figures 6D and 6E, Supplementary Movie S8). Moreover, Mps1-IN-1 treatment resulted in marked increase in multipolar anaphases (Figure 6F, Supplementary Movie S8). Approximately 60% of Mps1-IN-1-treated cells enter anaphase prematurely and undergo fragmentary divisions into multiple daughter cells. By contrast, without Mps1-IN-1 treatment cells spent more time in metaphase, eventually achieving bipolar metaphase plates, and dividing normally into two daughters (Figure 6F). Thus, Mps1-IN-1 blocks the SAC dependent delay in anaphase onset that occurs in cancer cells with extra centrosomes. Surprisingly, despite the increased frequency of fragmentary cell divisions, no detectable additional cytotoxicity as assessed by MTS assay of Mps1-IN-1 was attained as compared to the parental U2OS cell lines (Supplementary Figure S9A).

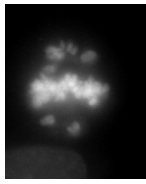

Mps1-IN-1 treatment decreases cell viability

Recent experimental evidence has given rise to the idea that complete spindle checkpoint inactivation is lethal to cells, while partial inactivation is associated with non-lethal chromosomal instability[95,146,153,210 (Chapter 5 of this thesis)] (reviewed in [213]). Cells in which endogenous Mps1 was removed and reconstituted with LAP-Mps1 T676A, a de-activating mutation in the activation loop of Mps1, suffered no detectable decrease in cell viability despite exhibiting a weakened checkpoint and errors in chromosome segregation[210 (Chapter 5 of this thesis)]. In contrast, cells depleted of endogenous Mps1 and reconstituted with LAP-Mps1 KD exhibited no cell growth. These genetic results suggest that complete and selective inhibition of Mps1 kinase activity represents another way to inhibit cell growth but it remains unclear whether selective cytotoxicity can be achieved towards cancer cells.

First, to examine the effect of chemical inhibition of Mps1 on cell proliferation, HCT116 colorectal cells, demonstrated to have a competent spindle checkpoint[228], were treated with Mps1-IN-1 at various concentrations and analyzed for cell number over a 4-day period. After 96 hour treatment with 5-10 μM Mps1-IN-1, the proliferative capacity of HCT116 cells was reduced to 33% that of DMSO control (Figure 7A), during which time this cell population exhibited gross signs of aneuploidy and accumulation of cells with <2c DNA content (Figure 7B). The cytotoxic concentrations of 5-10 μM Mps1-IN-1 are consistent with concentrations previously shown to inhibit all Mps1-dependent SAC activity. In congruence with proliferation results, concentrations of 5-10 μM Mps1-IN-1 caused severe loss of cell viability and clonal survival in a colony outgrowth assay (Figures 7C, 7D). Similar concentrations of Mps1-IN-1 were found to have anti-proliferative effects when tested against a small panel of tumor cell lines and non-cancerous 'normal' cell lines[229,230] (Supplementary Figures S9B and S10A). Consistent with previous reports[210 (Chapter 5 of this thesis)], shRNA- (Supplementary Figure S10B and S10C) and siRNA- (Supplementary Figure S11) mediated silencing of endogenous Mps1 also resulted in decreased cell viability[210 (Chapter 5 of this thesis)].

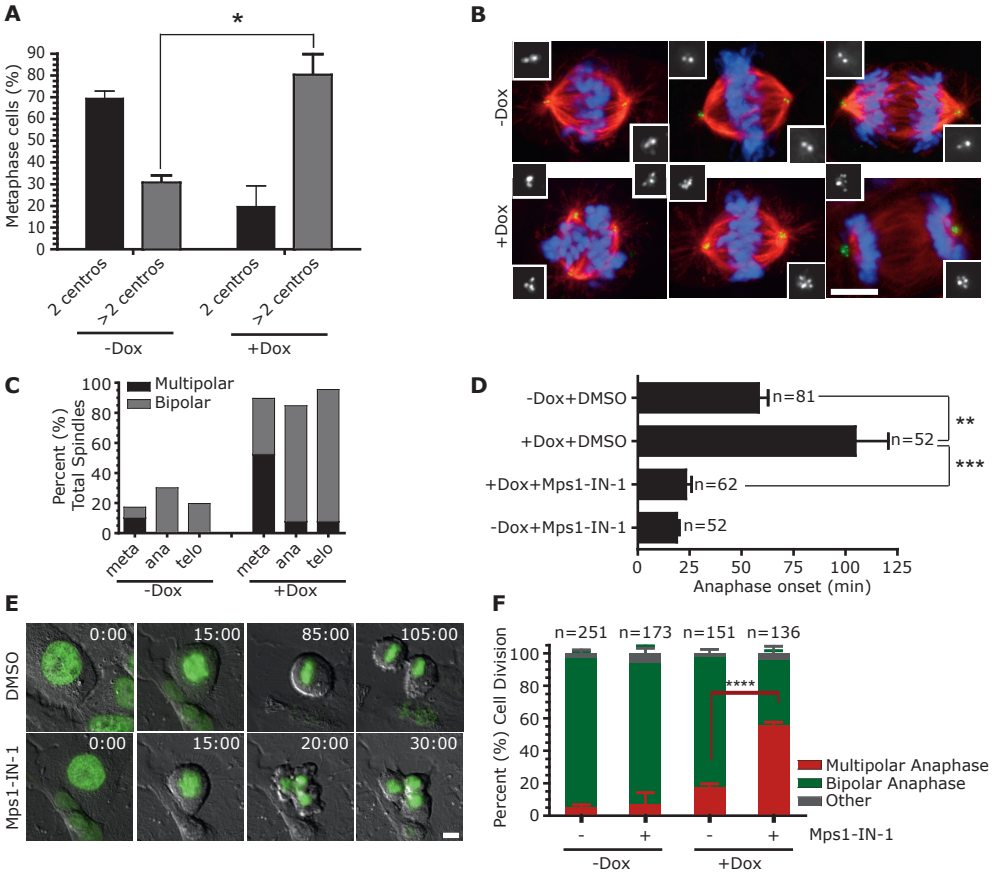

Figure 6. Mps1-IN-1 drives cancer cells with extra centrosomes into a catastrophic anaphase. (A) Doxycycline (Dox) inducible Plk4 overexpression induces extra centrosomes in U2OS cells. Metaphase spindles with 2 or more centrosomes (centros.) were quantified after treatment with doxycycline or DMSO by centrin staining. ~300 spindles were scored. (B) Cells cluster extra centrosomes, passing through a multipolar intermediate before undergoing bipolar divisions. Immunofluorescence images of cells from (A). Centrin, α-Tubulin and DNA are shown in green, red and blue, respectively. Insets show high magnification images of centrin staining. (C) Resolution of metaphase multipolar spindles into bipolar spindles in anaphase in cells with extra centrosomes. Quantitation of bipolar or multipolar spindles during metaphase, anaphase and telophases in cells with extra centrosomes. ~300 spindles were scored. (D) Extra centrosomes lead to delays in anaphase onset in an Mps1 (SAC)-dependent manner. (E) In extra centrosomal cells, the abrogation of SAC by Mps1-IN-1 treatment induces multipolar anaphases/telophases (bottom panels), whereas SAC-dependent delay enables bipolar division in the absence of Mps1-IN-1 (upper panels). Timelapse still images taken from movies of U2OS H2B-GFP after Plk4 overexpression. Time is shown in minutes after NEBD. Cells were synchronized with double thymidine blocks and released for 6 hrs. prior to Mps1-IN-1 treatment. (F) Quantitation of bipolar or multipolar anaphases/telophases in (E). All graphics represent mean +/- SD (*p-value = $7.11 \cdot 10^{-05}$, **p-value = 0.0011, *** p-value = $2.46 \cdot 10^{-07}$, **** p-value = 0.0024, Student's t test, 3 independent experiments). Scale bars in B, E are equal to 10 μm.

Interestingly, loss of viability induced by compound treatment (or Mps1 siRNA) was associated with induction of apoptosis as exemplified by PARP cleavage beginning after 48 hours (Figure 7E, Supplementary Figures S11A and S12A). This cleavage was shown to be specific to caspase activation as the co-administration of Z-VAD-FMK, a pan-caspase inhibitor, prevented PARP cleavage (Supplementary Figure S12A) but was unable to rescue the anti-proliferative defects

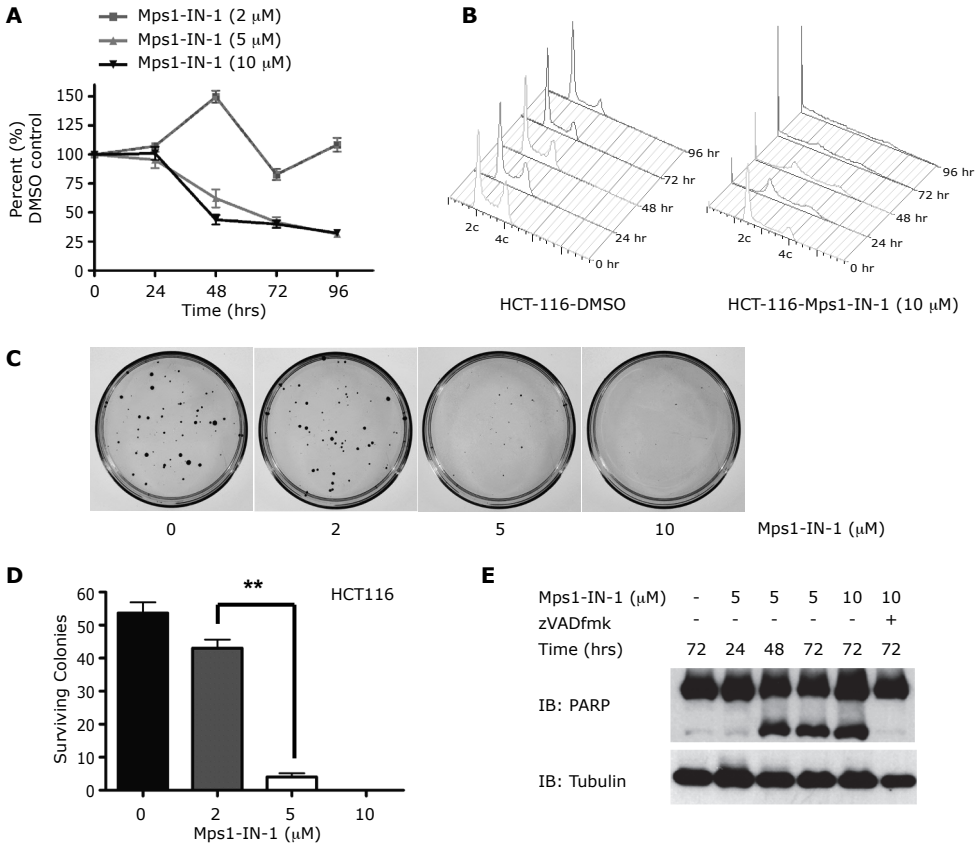

Figure 7. Mps1 is required for cell viability
(A) HCT116 cells were treated with Mps1-IN-1 (2, 5, 10 μM) for 24, 48, 72, and 96 hours. Effects on cell proliferation were quantified by measuring fluorescence of Syto60 nucleic acid stain emitted at 695 nm (excitation 635 nm). Values were normalized to DMSO control for each time point. All graphics represent mean +/- SD and were obtained from 4 independent experiments. (B) FACS profile of HCT116 cells treated with DMSO vehicle or Mps1-IN-1 (10 μM) for the indicated time points. (C) Colony outgrowth assay of HCT116 cells treated with DMSO vehicle or Mps1-IN-1 (2, 5, 10 μM). Cells were plated at a density of 200 cells/60-mm dish and harvested for crystal violet staining after 10 days. (D) Quantitation of colony outgrowth assays for HCT116 cells treated with DMSO vehicle or Mps1-IN-1 (2, 5, 10 μM). All graphics represent mean +/- SD and were obtained from 3 independent experiments (**p-value = $3.22 \cdot 10^{-05}$, Student's t test). (E) Immunoblot of PARP cleavage of HCT116 cells treated with Mps1-IN-1 at the indicated concentrations. Cell lysates were harvested after 24, 48, and 72 hours for immunoblot detections.

elicited by Mps1-IN-1, suggesting a possible caspase-independent cell death also becoming activated (Supplementary Figure S12B). However, treatment of non-cancerous 'normal' cell lines, hTERT-RPE1 and MCF10A cells, with high doses of Mps1-IN-1 (25 μM) (also Mps1 siRNA in hTERT-RPE1) caused moderate aneuploidy and associated decrease in colony survival (Supplementary Figures S10A and S11), however with little-to-no apoptosis-associated PARP cleavage (Supplementary Figure S12C). Further research using primary cultures or through *in vivo* investigations will be required to establish whether a 'therapeutic window' with respect to induction of apoptosis or other forms of cell death exists between normal and cancerous cell lines upon inhibition of Mps1 kinase activity.

Discussion

Previous reports have highlighted the utility of inhibiting Mps1 by chemical inhibition. However, these reports used either non-selective inhibitors or inhibitors that were specific to a particular chemical genetics background[182,183,186]. Here, we described the discovery of a selective Mps1 inhibitor Mps1-IN-1 and a dual Mps1/Plk1 inhibitor Mps1-IN-2 by screening a kinase directed library against a large panel of 352 diverse kinases. The basis for recognition of these new compounds by the ATP-site of Mps1 was demonstrated by co-crystallography with the kinase domain. We demonstrated that these inhibitors recapitulated many of the hallmarks of Mps1 inhibition and SAC abrogation that have been previously demonstrated using RNAi approaches. The cellular specificity for Mps1 inhibition was demonstrated by introduction of an inhibitor-resistant allele of Mps1 (M602Q).

Using the combined approach of a selective Mps1 inhibitor, Mps1-IN-1, to afford rapid inhibition of Mps1 kinase activity and timelapse microscopy we reported the first direct experimental evidence that shows that Mps1 is required for the checkpoint activation and establishment of Mad2 at kinetochores as cells enter mitosis. Cells that entered mitosis in the presence of Mps1-IN-1 exhibited severe defects in the establishment of kinetochore-bound Mad2, leading to a premature mitotic exit. Overall our results suggest that Mps1 kinase activity is essential for the establishment of and sustained activity of the spindle checkpoint.

Additionally, we used Mps1-IN-1 treatment to test the hypothesis that Mps1 lies upstream of Aurora B in checkpoint signaling. Inhibition of Mps1 kinase activity led to a decrease in phosphorylation of a direct Aurora B substrate (Histone H3) and of Thr232 in the activation loop of Aurora B. Inhibition of Aurora B by VX-680, a potent pan-Aurora inhibitor, had no reciprocal effect on Mps1 activation. These results support the notion that Mps1 activity is necessary for full enzymatic activity of Aurora B and thus serves to regulate attachment error correction, a tension-sensing process.

At concentrations of Mps1-IN-1 known to inhibit Mps1 mitotic kinase activity or using shRNA-mediated depletion of Mps1, we find no quantitative effect on centrosome number in HeLa or U2OS cells, consistent with some findings[130,135] but not with others that have suggested that minimal Mps1 kinase activity is required to fulfill its centrosome-associated function[132,133,206].

We demonstrated that Mps1 inhibition results in aneuploidy and a gradual loss of cell viability over several cell doublings as exemplified by decreased proliferative capacity, decreased clonal survival, an increase in the number of cells with sub-2c DNA content and induction of apoptosis. These results as well those conducted using shRNA/siRNA-mediated ablation of Mps1 suggest that massive chromosome loss could serve as a mechanism by which Mps1 inhibition (and checkpoint inactivation) ultimately leads to loss of cell viability. In extra centrosome containing cells, Mps1-IN-1 treatment resulted in catastrophic multipolar anaphase. Interestingly, though these cells were particularly sensitive to Mps1 inhibition, as exemplified by a 4-fold decrease in the time spent in mitosis, the proliferative capacity of these cells was not significantly affected as compared to the parental U2OS cell line (2-fold decrease in time spent in mitosis). This suggests that the effects on mitosis kinetics may not be the sole determining factor affecting cell proliferation and viability. Alternatively, the fold increase in aneuploidy upon compound treatment may represent a saturation point with respect to the induction cell death, beyond which the cell-type, genetic background, and specific chromosomes lost/gained becomes the over-riding factor influencing cell death. A detailed study of chromosome missegregation in the presence of compound in different cell types may shed light as to whether the overall rate of

chromosome missegregation and/or the frequency of specific chromosomal loss correlate with decreased proliferative capacity and viability. Interestingly, recent data suggest that sensitizing tumor cells to checkpoint inhibition by administration of sub-lethal doses of taxol may provide an avenue to augmenting chromosome loss and induction of cell death[166].

Finally, high dosage compound treatment in the 'normal' cell lines, hTERT RPE1 and MCF10A, did elicit an anti-proliferative effect though not associated with PARP cleavage. Given our current data it remains unclear whether this differential apoptotic induction in 'normal' vs. tumor cell lines can form the basis of a therapeutic window for which inhibitors of Mps1 (and more generally against the SAC) can be used as potential anti-cancer agents. Recent evidence showed that administration of sub-lethal doses of taxol (a checkpoint activator) combined with checkpoint inhibition produced differential cell death responses in cancer versus normal cell lines[166]. However, more extensive profiling of Mps1-IN-1 and analogs with improved potency for inhibition of Mps1 against a larger panel of 'normal' and tumorigenic cell lines and in tumor models will be required to determine if a therapeutic advantage against tumor cells can be obtained.

Methods

Chemistry

Compounds from both scaffold classes were synthesized using existing procedures (WO 03/020722, WO2005080393, WO2009032694). See online Supplementary Methods[239] for synthetic schemes and procedures.

Plasmids, Transfections and Treatments

The pSuper-based shRNA plasmid used in this study: Mps1 (GACAGATGATTCAGTTGTA) was constructed as described previously[211]. LAP WT *MPS1* cDNA subcloned into pCDNA3 was constructed as described previously[211]. shRNA-insensitive Mps1 (modified codons 288 and 289) was obtained by site-directed mutagenesis[211]. LAP-Mps1 M602Q (shRNA insensitive) was obtained by site directed mutagenesis of codon 602. The PtK2 (Male *Potorous tridactylus* kidney epithelial cells) cell lines stably expressing *Homo sapiens* (hs) *MAD2* were generated via retroviral plasmids[231]. siRNA transient transfections were performed using Dharmacon siGENOME TTK (*MPS1*) siRNAs (cat#s D-004105-01 and D-004105-03) and control siRNA-A (Santa Cruz Biotechnology, cat# sc-37007) with Lipofectamine RNAiMax (Invitrogen) following the manufacturer's protocol for reverse transfections. Thymidine (2.5 mM), nocodazole (200 $ng \cdot ml^{-1}$), taxol (1 μM), MG132 (10 μM), *S*-trityl cysteine (10 μM), hydroxyurea (4 mM) and doxycycline (2 $\mu g \cdot ml^{-1}$) were all from Sigma. Puromycin (2 $\mu g \cdot ml^{-1}$) was from Invivogen and Z-VAD-FMK (50 μM) was from BD Biosciences. VX-680 (2 μM) was custom synthesized using published synthetic methods. SP600125 (10 μM) was from Calbiochem.

Cell Culture

HeLa S3, U2OS, and A549 cells were grown in Dulbecco's Modified Eagle's Medium (DMEM, Sigma), and all HCT116 cells were grown in McCoy's 5A (Invitrogen), and hTERT-RPE1 cells were grown in DMEM and Ham's F-12, 50/50 Mix (Cellgro-Fisher) supplemented with sodium bicarbonate (Invitrogen) and hygromycin B (Invitrogen) to final concentrations of 0.348% and 10 $\mu g \cdot ml^{-1}$ respectively. UTRM10 cells were generated and grown as previously described[210,211]. MCF10A cells were cultured as described previously[230]. All PtK2 (Male *Potorous tridactylus* kidney epithelial) cells were cultured in Advanced MEM media (Invitrogen), 2% FBS, pen/

strep, and 2mM GlutaMAX™ (Invitrogen). Doxycycline-inducible *PLK4*-overexpressing U2OS cells were a gift from Dr. Nigg[227]. H2B-GFP expressing cells were a gift from Dr. King. The HCT116 $p53^{+/+}$, $p53^{-/-}$, $BAX^{+/+}$, and $BAX^{-/-}$ cell lines were a gift from Dr. Vogelstein. All cell lines were supplemented with 10% FBS (Sigma) and 100 $U \cdot ml^{-1}$ penicillin, 100 $\mu g \cdot ml^{-1}$ streptomycin (Invitrogen) and cultured at 37°C in a humidified chamber in the presence of 5% CO_2, unless otherwise noted.

Kinase Screening

The screening method is described in Supplementary Table S4[239]. The data presented in Figure 1 and Supplementary Figure S1 were generated at Ambit Biosciences, using binding assays as previously described[215,217]. Kinome trees shown in Figure 1C were generated using the KinomeScan TreeSpot kinome data visualization tool.

Immunoprecipitations and in vitro kinase assays

Conditions for immunoprecipitations of LAP-Mps1 using S-protein agarose (Novagen) have been described previously[210,211], with minor modifications in Supplementary Research Data.

Flow Cytometry and Immunoblotting

Cells were released from a 24 hr thymidine-induced block into nocodazole or taxol for 2 hr prior to co-treatment with microtubule poison and test compound for 4 hours and analyzed using immunoblotting and flow cytometry. For immunoblotting standard protocols were followed. Flow cytometric analysis of cells was performed as described in Supplementary Material using an anti-phospho-Histone H3 (Ser10) antibody (Upstate).

Immunofluorescence and Timelapse Microscopy

Immunofluorescence microscopy was carried out as described in Supplementary Material. For timelapse microscopy, cells were plated in 35 mm glass bottom microwell (14 mm, No 1.5 coverglass) dishes (MatTek Corporation), transfected and/or treated with chemical reagents and imaged in a heated chamber (37°C and 5% CO_2). Timelapse images from mitotic timing experiments were captured using a Nikon TE2000E Automated Inverted Microscope (Nikon USA) using a 20X/0.75 NA Plan Apochromat objective lens. Twelve bit phase (25 msec exposure) and green fluorescent (50 msec exposure) images were acquired every 2 minutes using a Hamamatsu Orca AG Cooled CCD Camera and stored on a computer using Metamorph software. Timelapse images from mitotic escape and chromosome missegregation experiments were captured using a Nikon TE2000U Inverted Microscope (Nikon USA) using a 60X/1.4 NA oil objective lens. Twelve bit DIC (200 msec exposure) and green fluorescent (180 msec exposure) images were acquired every 5 minutes (5 z-planes) using a Hamamatsu Orca ER Cooled-CCD camera and analyzed in Metamorph. Images of UTRM10 cells transfected with H2B-EYFP were captured on an Olympus IX-81 Microscope (Olympus) using a 20X/0.5 NA UPLFLN objective lens. Twelve bits yellow fluorescent (20 msec exposure) images were acquired every 3 minutes (5 z-planes) using a Hamamatsu ORCA-ER Cooled-CCD camera and processed using Cell-M software. All images collected to look at chromosome missegregation were (H2B-EYFP or H2B-GFP) are maximum intensity projections of all z-planes. For timelapse imaging of doxycycline-inducible PLK4 overexpressing U2OS cells, cells were synchronized with thymine for 18 hrs and released to doxycycline for 10 hrs followed by 2nd thymidine treatment for additional 18 hrs. Cells were then released to medium for 6hrs prior to 5 μM of Mps1-IN-1 treatment.

Mad2 Kinetochore Establishment Assay
PtK2 cells were treated with Mps1-IN-1 (10 μM) or DMSO vehicle for 1 hour before co-administration with either DMSO vehicle or nocodazole. Timelapse microscopy was used to follow cells as they entered mitosis, as judged by nuclear envelope breakdown (NEBD) and kinetochore-localized HsMad2-EYFP fluorescence was quantified and background corrected as described in Supplementary Material.

*Centrosome Duplication Experiments***.**
HeLa S3, U2OS, and UTRM10 cells were plated on 12 mm coverslips. Cells were treated with Mps1-IN-1 with or without hydroxyurea as described and analyzed for centrosome duplication with a centrin antibody (see Supplementary Material). Similarly, UTRM10 cells stably expressing a doxycycline-inducible Mps1 shRNA construct were treated with doxycycline, immunoblotted to assess extent of Mps1 depletion and analyzed for centrosome duplication.

Proliferation, Colony Outgrowth, and Karyotyping Assays
Proliferation and colony formation assays were performed as previously described[95,209]. For karyotyping, asynchronous cells were treated with Mps1-IN-1 (10 μM) for 24 hours, the medium was removed and replaced with medium containing 100 ng·ml^{-1} colcemid (Irvine Scientific) for 2 hours to arrest cells in metaphase prior to harvesting. Processing of cells was carried out as described in Supplementary Material.

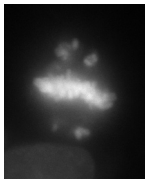

Acknowledgments

The authors thank Drs. R. King, B. Vogelstein, and E. Nigg for reagents and Drs. R. King, T. Mitchison, A. Abrieu, U. Eggert, C. Walsh, F. Sigoillot, and E. Chung for helpful discussions. The authors also thank Ambit Biosciences and Invitrogen Corporation for technical support in initial compound screening and enzymatic activity assays respectively as well as the Nikon Imaging Facility (HMS) and the Dana Farber Flow Cytometry Lab (DFCI) for technical help and instrument use. The Structural Genomics Consortium is a registered charity (number 1097737) that receives funds from the Canadian Institutes for Health Research, the Canadian Foundation for Innovation, Genome Canada through the Ontario Genomics Institute, GlaxoSmithKline, Karolinska Institutet, the Knut and Alice Wallenberg Foundation, the Ontario Innovation Trust, the Ontario Ministry for Research and Innovation, Merck & Co., Inc., the Novartis Research Foundation, the Swedish Agency for Innovation Systems, the Swedish Foundation for Strategic Research and the Wellcome Trust.

Supplementary Information

Supplementary Figures

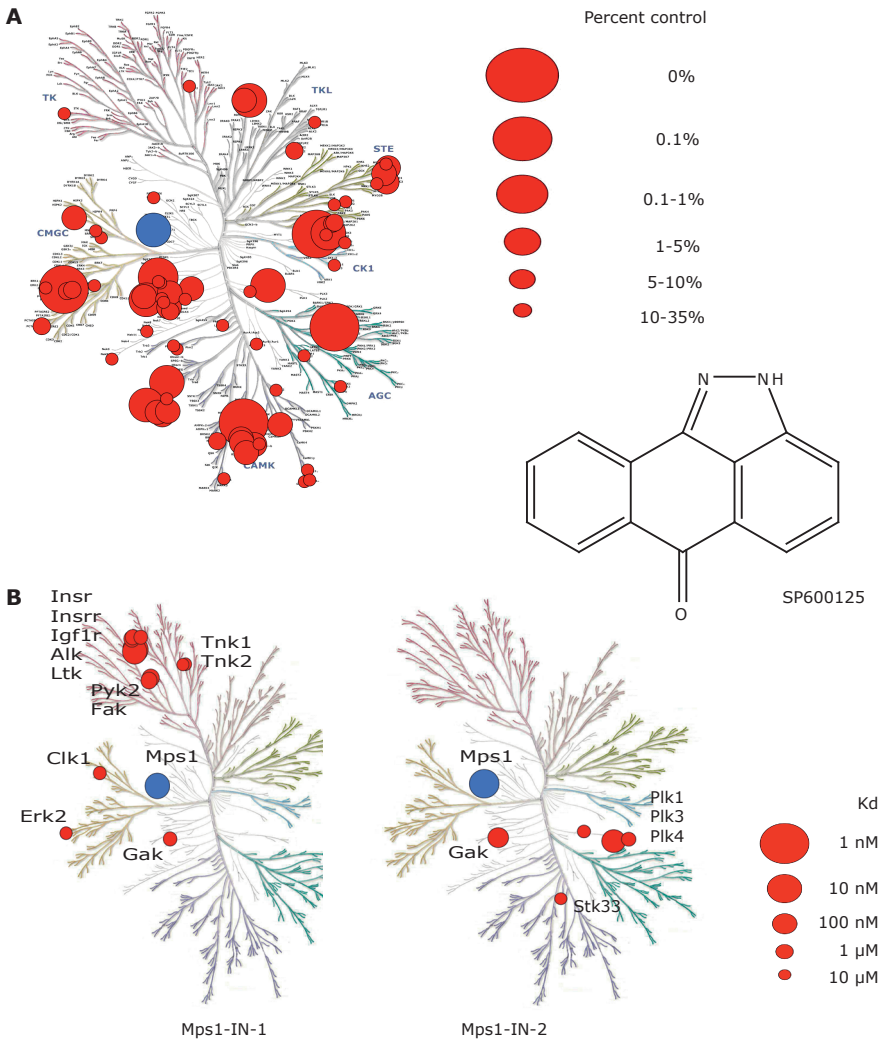

Figure S1. Kinome Interaction Maps of SP600125, Mps1-IN-1 and Mps1-IN-2
(A) Kinome interaction map of SP600125 constructed using raw data from Ambit binding assay shown in Supplementary Table S1 using the program TREEspot™ (KinomeScan, Ambit). The sizes of the circles indicate the relative binding score for that kinase (see legend). The blue sphere indicates Mps1 (TTK). (B) Kinome interaction map of Mps1-IN-1 and Mps1-IN-2 constructed using K_d data from Ambit binding assay shown in Supplementary Table S2 using the program TREEspot™ (KinomeScan, Ambit). The sizes of the circles indicate the relative K_d value for that kinase (see legend). The blue sphere indicates Mps1 (TTK).

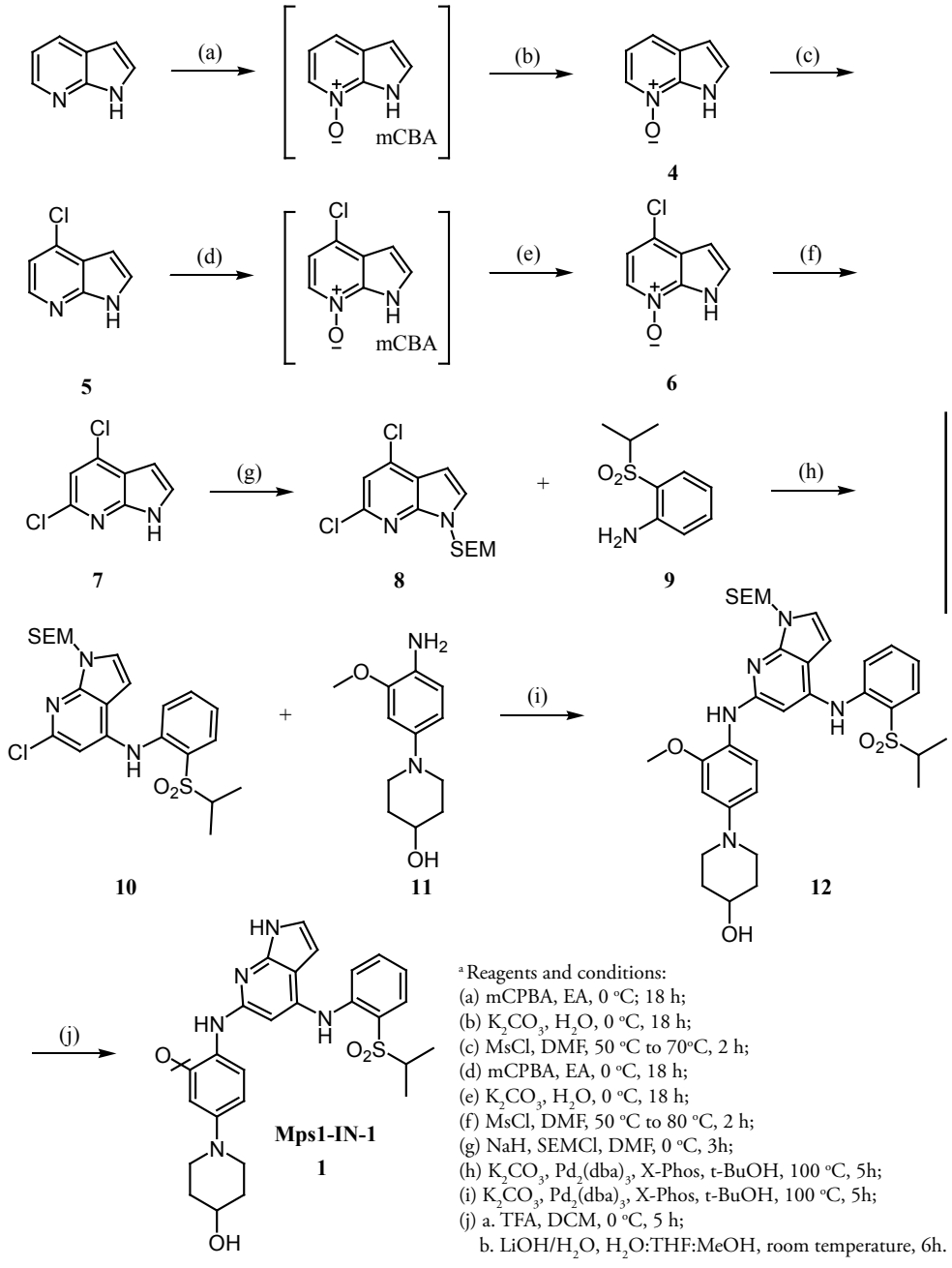

Figure S2A. Synthetic Route to Mps1-IN-1[a]

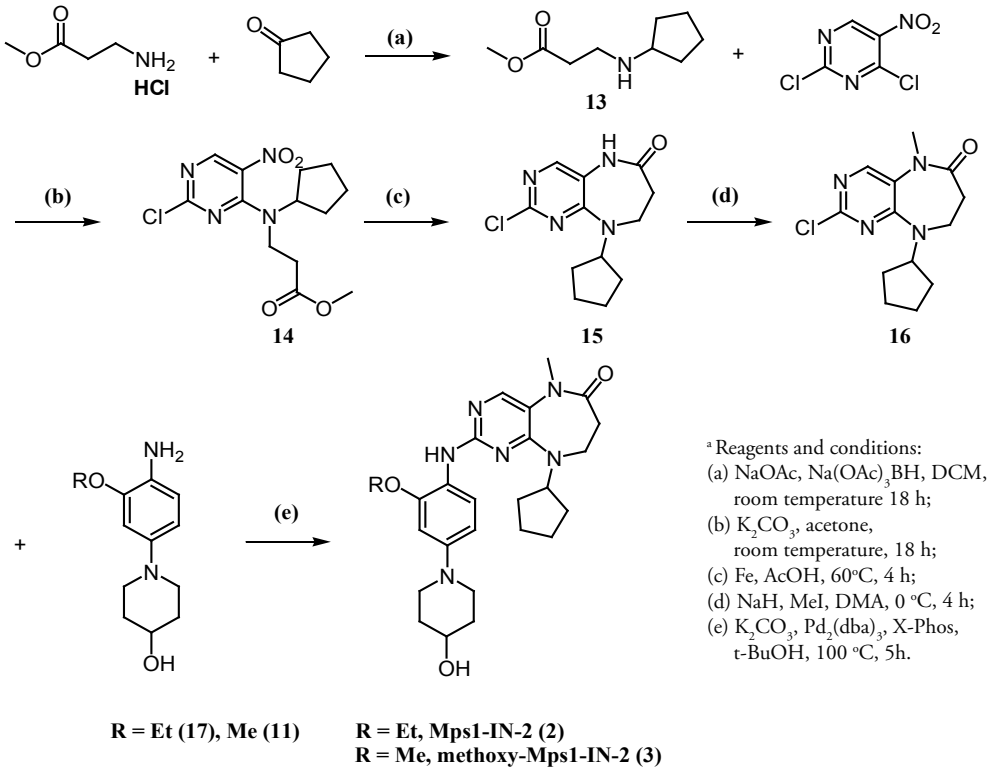

Figure S2B. Synthetic Routes to Mps1-IN-2 and methoxy-Mps1-IN-2[a]

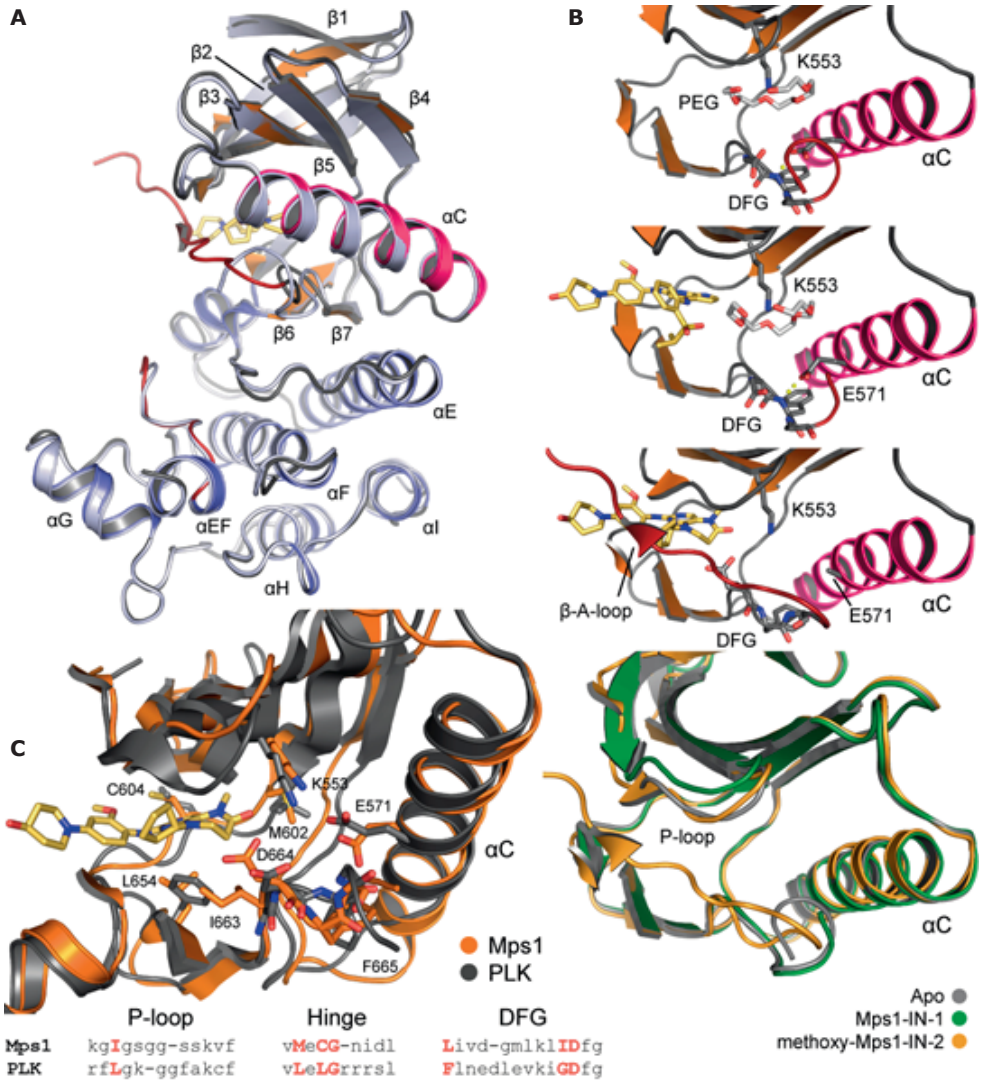

Figure S3. Mps1 kinase domain crystal structures: apo-structure and co-crystal structures with Mps1-IN-1 and methoxy-Mps1-IN-2.
(A) Superimposition of the apo-structure of Mps1 and the methoxy-Mps1-IN-2 complex. The apo structure is colored in light blue and the Mps1-IN-2 complex is colored by structural elements (β-sheets are colored in orange, helices in blue, the activation segment in red, and αC in pink). Interestingly, in the complex of methoxy-Mps1-IN-2, the tri-phosphorylated activation segment is partially ordered and interacts with the P-loop. Carbon atoms of Mps1-IN-1 and methoxy-Mps1-IN-2 are shown in yellow to discriminate from Mps1 kinase residue side chains. (B) Detailed view of the Mps1 active site. Shown is the apo-structure in complex with a polyethylene glycol molecule (top panel), in complex with Mps1-IN-1 (top middle panel), in complex with methoxy-Mps1-IN-2 (bottom middle panel), and a superimposition of the apo-structure with the methoxy-Mps1-IN-2 complex (bottom panel). Carbon atoms of Mps1-IN-1 and methoxy-Mps1-IN-2 are shown in yellow to discriminate from Mps1 kinase residue side chains. (C) Superimposition of Plk1 (shown in gray) with Mps1 (orange). The structures were superimposed using corresponding Cα position of the lower kinase lobes. Most important active site residues forming contact with the inhibitor are shown in stick representation. Carbon atoms of residue side chains in Mps1 are colored in orange and in Plk1 in gray, respectively. A structure based sequence alignment highlighting the main residue differences for the three active site motives are shown in the lower panel. Differences are highlighted in red. Carbon atoms of Mps1-IN-1 and methoxy-Mps1-IN-2 are shown in yellow to discriminate from kinase residue side chains.

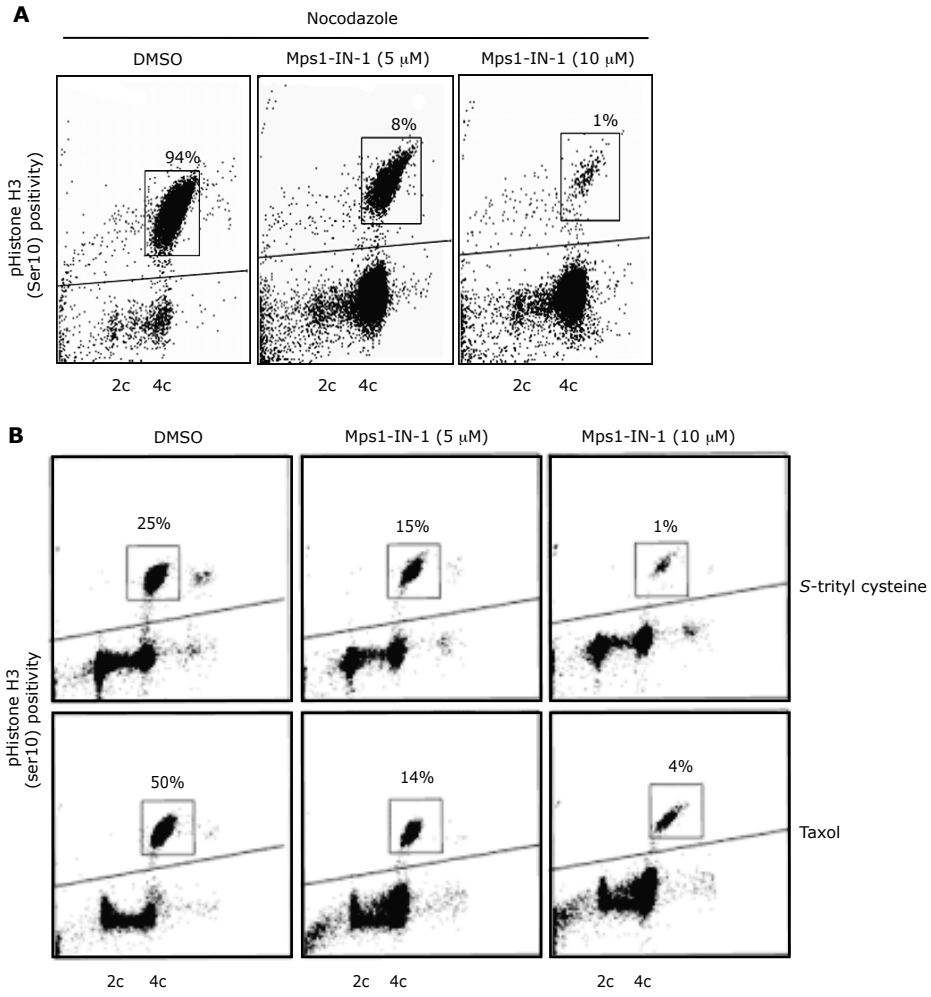

Figure S4. Mps1-IN-1 induces bypass of nocodazole, *S*-trityl cysteine- and taxol-induced mitotic arrest

(A) pHistone H3 positivity (y-axis) versus propidium iodide staining (x-axis) of U2OS cells treated with nocodazole or nocodazole/Mps1-IN-1. Mitotic cells were obtained by shake-off and re-seeded with medium containing nocodazole or nocodazole/Mps1-IN-1. Figures in the upper box represent the percentage of pHistone H3-positive 4c population. (B) pHistone H3 positivity (y-axis) versus propidium iodide staining (x-axis) of HeLa cells treated with either taxol or *S*-trityl cysteine alone or in combination with Mps1-IN-1. Mitotic cells were obtained by incubation with taxol or *S*-trityl cysteine for 16 hrs. prior to treatment with medium containing taxol or s-trityl cysteine alone or in combination with Mps1-IN-1. Figures in the upper panel represent the percentage of pHistone H3-positive 4c population remaining after each indicated treatment.

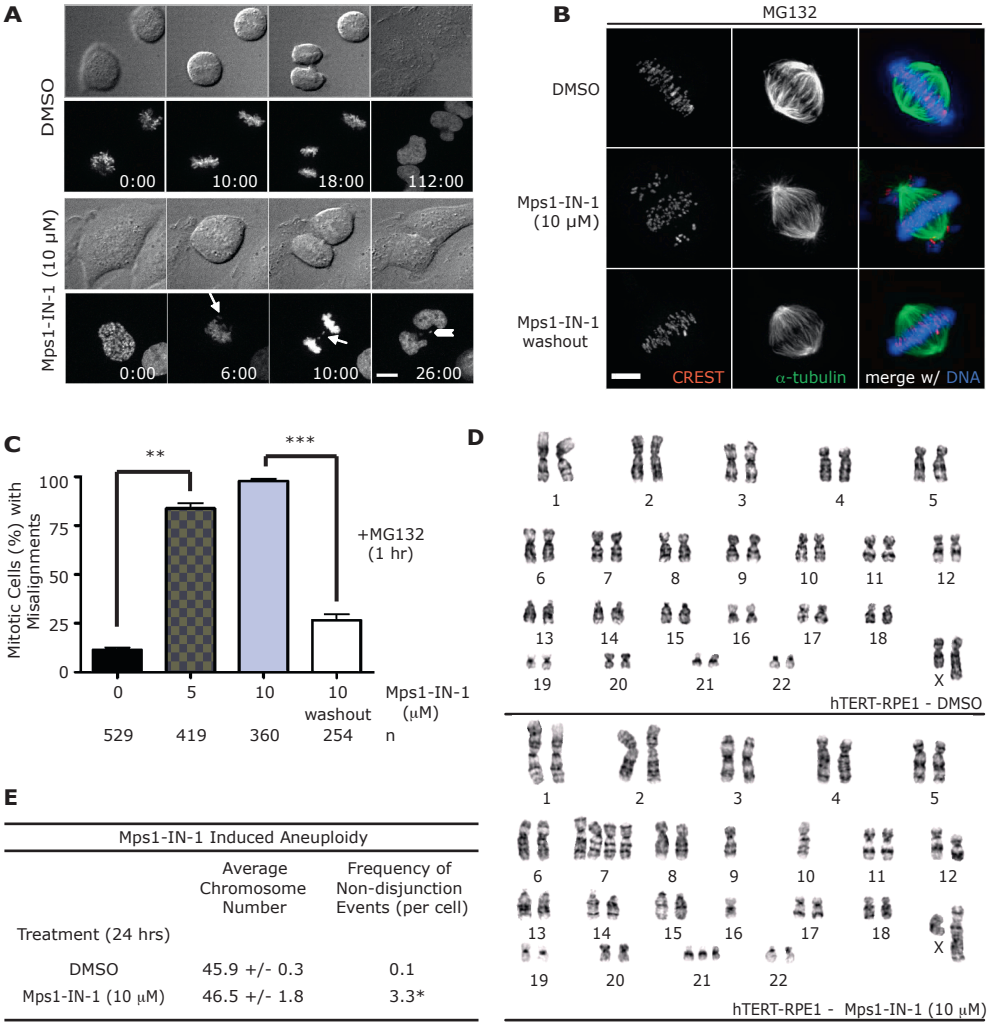

E

Mps1-IN-1 Induced Aneuploidy		
Treatment (24 hrs)	Average Chromosome Number	Frequency of Non-disjunction Events (per cell)
DMSO	45.9 +/- 0.3	0.1
Mps1-IN-1 (10 μM)	46.5 +/- 1.8	3.3*

Figure S5. Mps1-IN-1 induces chromosome misalignment and chromosome missegregation
(A) Selected frames from a timelapse series of U2OS histone H2B-GFP after treatment with DMSO vehicle or Mps1-IN-1 (10 μM). Arrows indicate missegregated chromosomes. Arrowheads indicate satellite nuclei resulting after DNA de-condensation and nuclear envelope reformation. Scale bar is equal to 10 μm. Time is given in minutes.seconds and t=0 is set to NEBD. (B, C) U2OS cells were treated with Mps1-IN-1 (5 μM, 10 μM) for 4 hrs, then co-treated with MG132 for 60 minutes or for 30 minutes then replaced with medium containing only MG132 for an additional 30 minutes. Cells treated only with MG132 for 60 minutes serves as a control. Cells were fixed and stained with anti-Tubulin-FITC antibody, DAPI to visualize chromosomes, and anti-CREST antibody to visualize kinetochores. Cells were quantified by number of cells exhibiting misaligned chromosomes. **p-value = $7.82 \cdot 10^{-08}$, ***p-value = $4.20 \cdot 10^{-06}$, Student's t test. (D) Karyotypes of hTERT-RPE1 cells treated either with DMSO vehicle control (top panel) or Mps1-IN-1 (10 μM) for 24 hrs (bottom panel). (E) Average chromosome number and frequency of non-disjunction in the cell populations from (D). Average chromosome number represents mean +/- SD (n = 25 cells). *p-value = $2.22 \cdot 10^{-10}$. All graphics represent mean +/- SD. n refers to total number of cells analyzed from each population (from 3 independent experiments). Scale bar is equal to 5 μm.

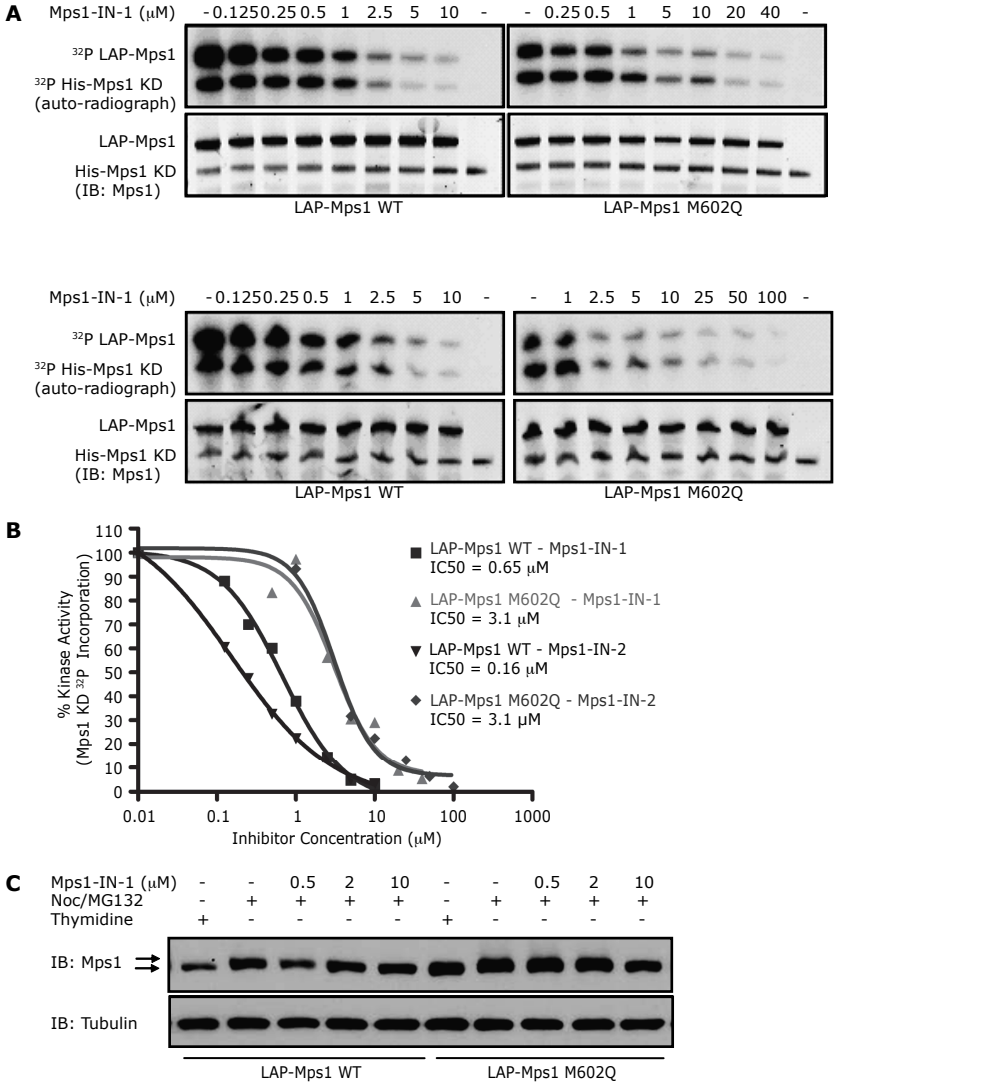

Figure S6. Compound treatment inhibits kinase activity and auto-phosphorylation in vitro and in cells but can be reversed by LAP-Mps1 M602Q expression

(A) Kinase assays using LAP-Mps1 WT and M602Q kinases were performed as described in Methods and Materials section using His_6-tagged Mps1 KD as a substrate. ^{32}P signals were normalized to protein loading levels. (B) IC_{50} curves for Mps1-IN-1 and Mps1-IN-2 generated from an *in vitro* kinase assay using immunoprecipitated LAP-Mps1 WT or LAP-Mps1 M602Q. His_6-tagged Mps1 KD served as substrate and the ATP concentration was 10 μM. Data points were generated by dividing the absolute ^{32}P signals for the substrate by the amount of LAP-Mps1 kinase protein (to normalize for protein levels). Data from each condition was normalized independently to its own DMSO-treated reaction (100%) for visual clarity in the presentation of the graphic. In the presence of LAP-Mps1 WT, Mps1-IN-1 and 2 exhibited IC_{50}s of 0.65 and 0.16 μM respectively. In the presence of LAP-Mps1 M602Q both Mps1-IN-1 and Mps1-IN-2 possess IC_{50}s of 3.1 μM, representing 5-fold and 19-fold decreases in compound activity, respectively. (C) Immunoblot of Mps1 in U2OS cells stably expressing either LAP-Mps1 WT or LAP-Mps1 M602Q after Mps1-IN-1 treatment. Mitotic cells were obtained by combined thymidine arrest and nocodazole treatment followed by mitotic shake-off, which were then re-seeded with medium containing nocodazole/MG132 or nocodazole/Mps1-IN-1/MG132. After 90 minutes treatment cells were harvested and lysates were probed for Mps1. Thymidine serves as a negative control whereby in G1/S state Mps1 resides in a hypo-phosphorylated state. Arrows indicate phosphorylation-induced mobility shift of Mps1 total protein band.

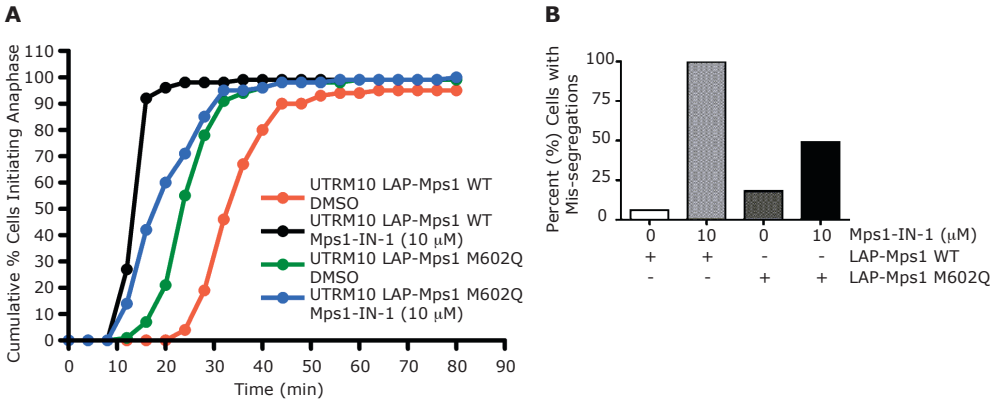

Figure S7. Expression of LAP-Mps1 M602Q in UTRM10 cells reduces chromosome missegregation induced by Mps1-IN-1

(A) Anaphase initiation results from timelapse microscopy performed on UTRM10 cells stably expressing LAP-Mps1 WT or LAP-Mps1 M602Q in the presence or absence of Mps1-IN-1 (10 μM). UTRM10 cells were transiently transfected with H2B-EYFP and analyzed by timelapse microscopy as indicated in Methods. Time to anaphase initiation is described as time from nuclear envelope breakdown (NEBD) to beginning of anaphase. (B) UTRM10 cells expressing LAP-Mps1 WT or LAP-Mps1 M602Q were transiently transfected with an H2B-EYFP construct and were treated with DMSO or Mps1-IN-1 (10 μM). Cells expressing H2B-EYFP were analyzed by timelapse fluorescence microscopy to assess chromosome missegregation. Cells exhibiting unaligned chromosomes at the time of anaphase initiation were categorized as having missegregated chromosomes.

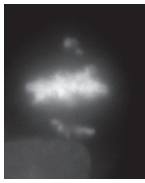

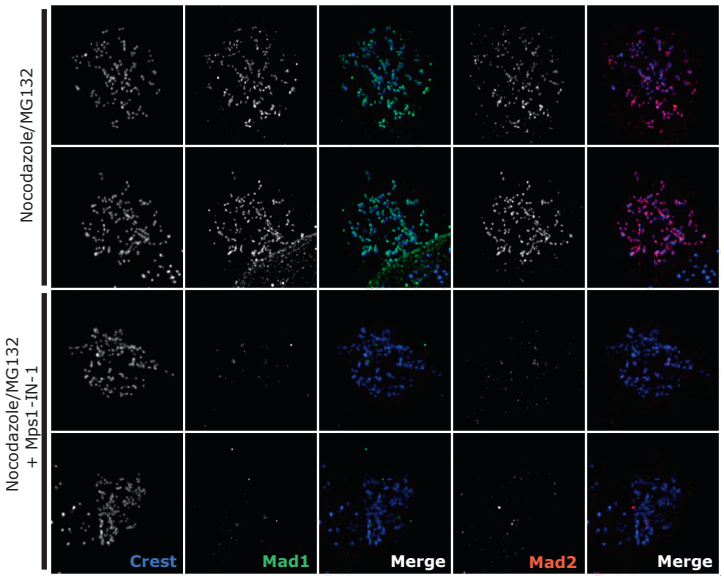

Figure S8. Mps1-IN-1 treatment disrupts kinetochore localization of hsMad1 and hsMad2

HeLa cells were treated with Mps1-IN-1 (10 μM) or DMSO vehicle for 1 hr. The cells were then co-treated with nocodazole and MG132 (with Mps1-IN-1 or DMSO) for 30 minutes. Mitotic cells were analyzed for the kinetochore localization of hsMad1 (green) and hsMad2 (red) by co-localization with CREST kinetochore marker (blue). The middle column of panels depict merged images of CREST and hsMad1 (blue and green) and the last column of panels depict merged images of CREST and hsMad2 (blue and red).

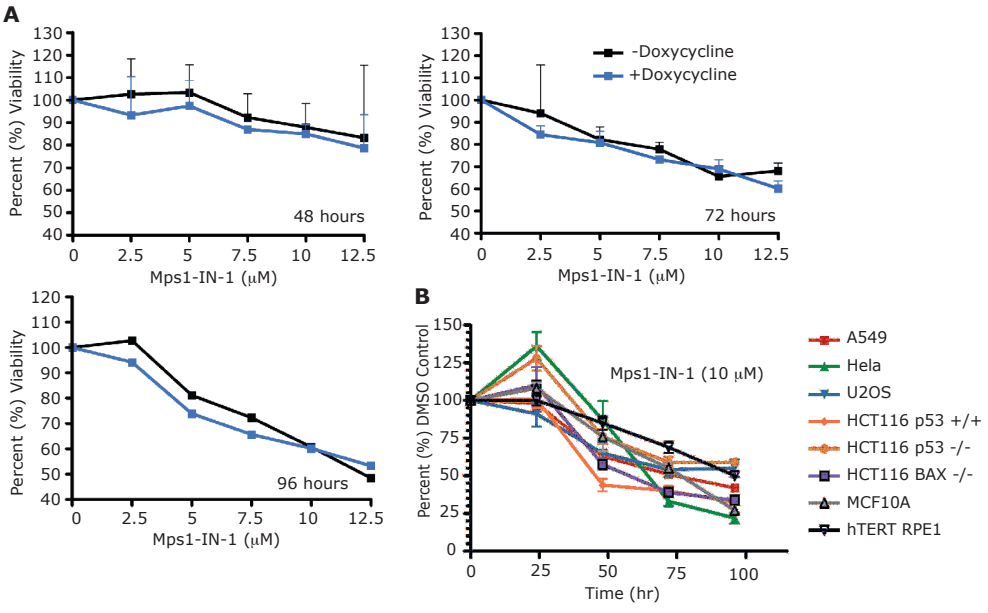

Figure S9. Loss of Mps1 kinase activity decreases proliferative capability of cells
(A) Effects of Mps1-IN-1 treatment on proliferation of U2OS cells with and without Plk4 overexpression (plus doxycycline). Cells were treated with Mps1-IN-1 at the indicated concentrations for 48, 72, and 96 hours and proliferation was followed by MTS assay (see Supplementary Materials). All graphics represent mean +/- SD (except 96 hrs) and were obtained from 2 independent experiments. (B) Tumor and normal cells were treated with Mps1-IN-1 (10 μM) for 24, 48, 72, and 96 hours. Effects on cell proliferation were quantified by measuring fluorescence of Syto60 nucleic acid stain emitted at 695 nm (excitation 635 nm). All graphics represent mean +/- SD and were obtained from 4 independent experiments.

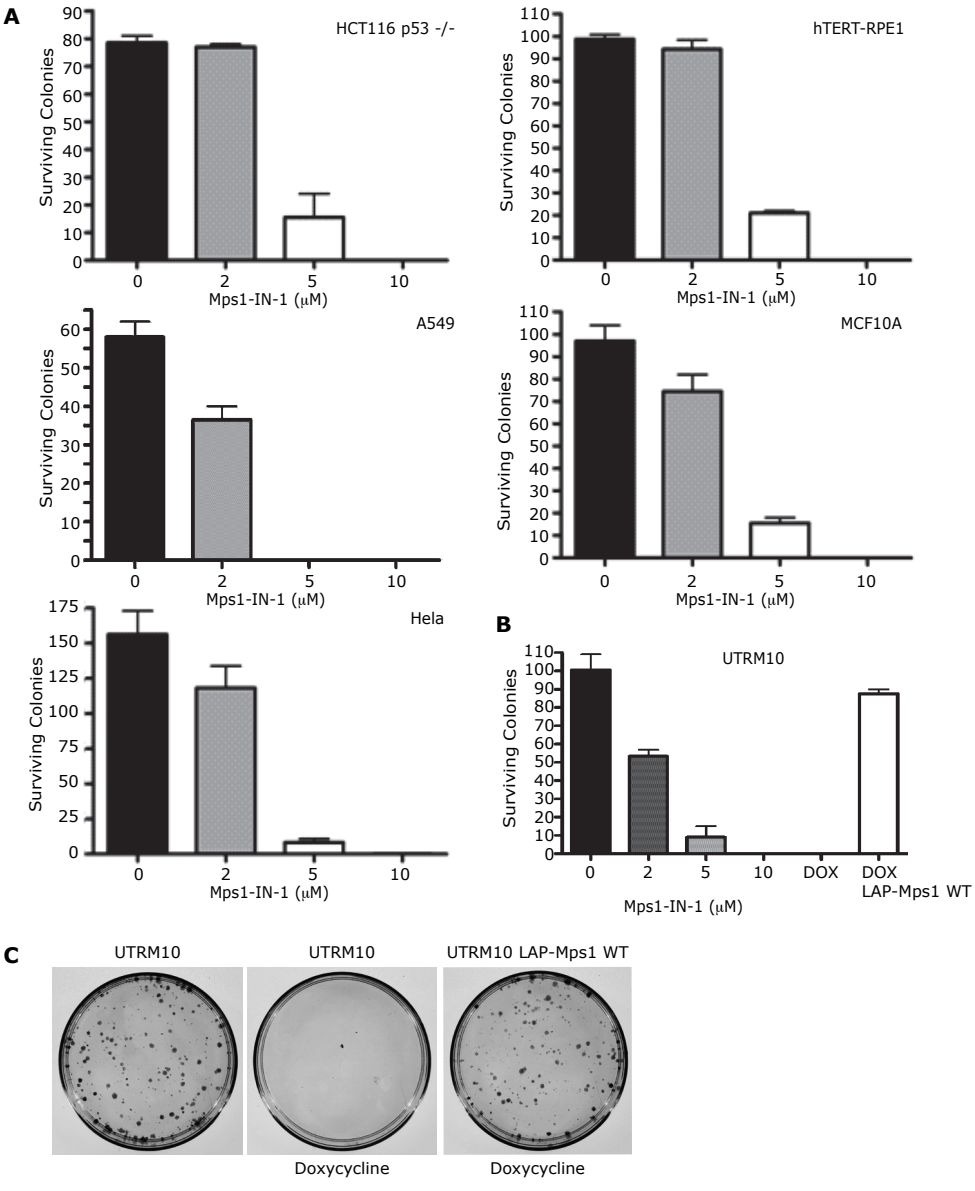

Figure S10. Mps1-IN-1 causes Loss of Cell Viability in Tumor and Non-cancerous Cell Types
(A) Representative colony outgrowth assay results for tumor cells: HCT116 p53$^{-/-}$, A549, and HeLa, as well as for non-cancerous cells: MCF10A and hTERT-RPE1 cells. Cells were plated at a density of 200 cells/60-mm dish, treated the indicated concentrations of Mps1-IN-1 and harvested for crystal violet staining after 10 days. All graphics represent mean +/- SD and were obtained from 3 independent experiments. (B) Quantitation of colony outgrowth assays for UTRM10 cells. UTRM10 cells were treated either with DMSO vehicle, doxycycline to induce Mps1 shRNA expression, or doxycycline with simultaneous expression of shRNA resistant LAP-Mps1 WT. All graphics represent mean +/- SD and were obtained from 3 independent experiments. (C) Colony outgrowth assay for UTRM10 cells. UTRM10 cells were treated either with DMSO vehicle, doxycycline to induce Mps1 shRNA expression, or doxycycline with simultaneous expression of shRNA resistant LAP-Mps1 WT.

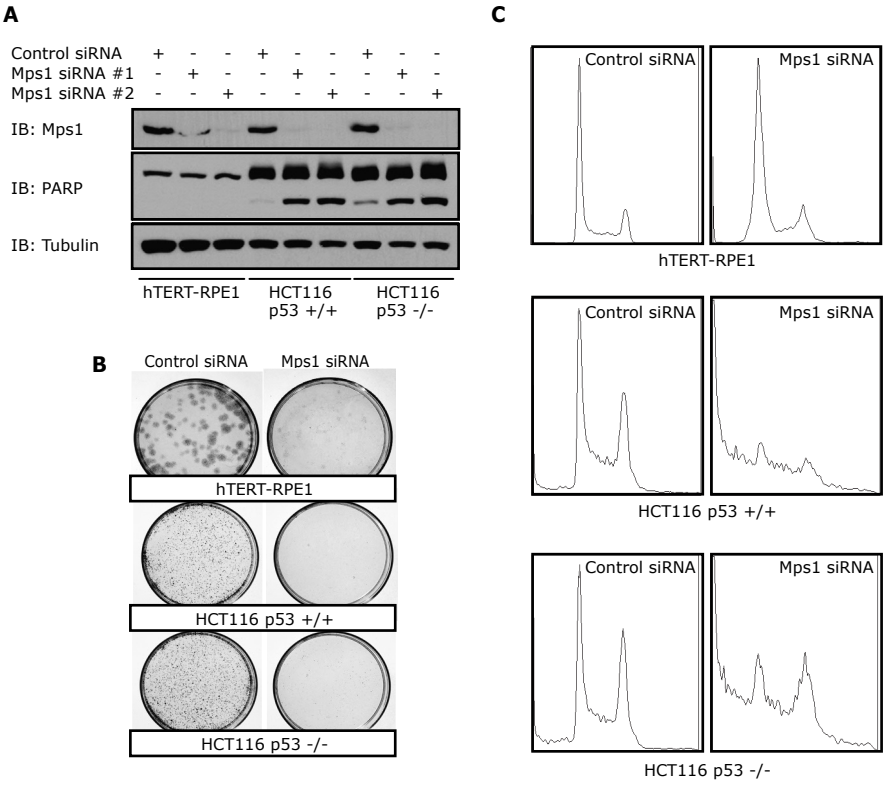

Figure S11. siRNA knockdown of Mps1 induces cell death and apoptosis-associated PARP cleavage in cancer cells but not does not induce apoptosis in normal cells
(A) hTERT-RPE1, HCT116 p53 +/+, and HCT116 p53 -/- cells were transfected with control siRNA or two Mps1 siRNAs. 72 hrs post transfection lysates were harvested to detect the levels of Mps1 and PARP cleavage. (B) Colony outgrowth assay for HCT116 p53 +/+, HCT116 p53 -/-, and hTERT-RPE1 cells treated with either control siRNA or Mps1 siRNA. Colony outgrowth as a result of 9 day-growth period. (C) FACS profiles of cells in (A) after siRNA-mediated knockdown of Mps1 levels.

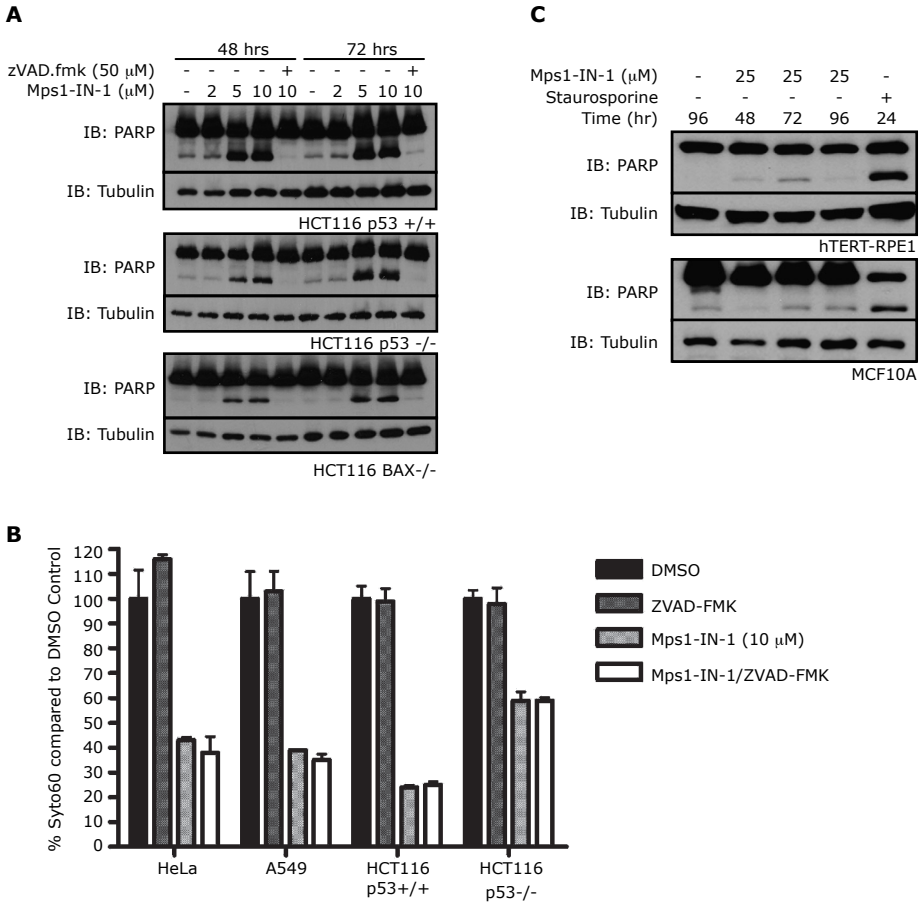

Figure S12. Mps1-IN-1 induces apoptosis-associated PARP cleavage in cancer cell lines but not normal cell lines

(A) Immunoblot of PARP cleavage of HCT116, HCT116 p53 -/-, and HCT116 Bax -/- cells treated with Mps1-IN-1 at the indicated concentrations. Cell lysates were harvested after 48 and 72 hrs for immunoblot detections. (B) Proliferation assays of HeLa, A549, HCT116 p53 +/+, and HCT116 p53 -/- cells. Cells were treated either with DMSO vehicle, ZVAD-FMK pan-caspase inhibitor, Mps1-IN-1 (10 μM), or Mps1-IN-1 and ZVAD-FMK. After 96 hrs the effects on cell proliferation were quantified by measuring fluorescence of Syto60 nucleic acid stain emitted at 695 nm (excitation 635 nm). All graphics represent mean +/- SD and were obtained from 3 independent experiments. (C) Immunoblot of PARP cleavage of hTERT-RPE1 and MCF10A cells treated with Mps1-IN-1 at the indicated concentrations. Cell lysates were harvested after 24, 48, 72, and 96 hours for immunoblot detections. Staurosporine serves as a positive control treatment for induction of PARP cleavage in these cell lines.

Supplementary Movies and Tables

Eight supplementary movies and four supplementary tables can be found with online; http://www.nature.com/nchembio/journal/v6/n5/abs/nchembio.345.html#supplementary-information[239].

Movie S1
This representative timelapse movie, related to Figure 2D and Supplementary Figure S5A, shows U2OS H2B-GFP cells treated with DMSO vehicle. Mitotic progression and DNA segregation were followed by Histone H2B movement in fluorescent channel (serves as control for Movie S2). Based on time from nuclear envelope breakdown (NEBD, t=0 min.) to anaphase initiation these cells spent 14 and 20 minutes in mitosis (90% cells completed mitosis in 40 minutes). Frame rate equals five frames per second. Time is given in minutes.seconds.

Movie S2
This representative timelapse movie, related to Figure 2D and Supplementary Figure S5A, shows a U2OS H2B-GFP cell treated with Mps1-IN-1 (10 μM). Mitotic progression and DNA segregation were followed by Histone H2B movement in fluorescent channel. Based on time from nuclear envelope breakdown (NEBD, t=0 min.) to anaphase initiation this cell spent 8 minutes in mitosis (90% cells completed mitosis in 18 minutes). Frame rate equals five frames per second. Time is given in minutes.seconds.

Movie S3
This representative timelapse movie, related to Figures 3A and 3B, shows a PtK2 cell stably expressing HsMad2-EYFP treated with vehicle control (serves as control for Movie S4). Clear fluorescent signal was detectable above background at the kinetochores as the cell entered mitosis. Scale bar is equal to 10 micron. Frame rate equals seven frames per second. Time is given in minutes.seconds.

Movie S4
This representative timelapse movie, related to Figures 3A and 3B, shows a PtK2 cell stably expressing HsMad2-EYFP treated with Mps1-IN-1 (10 μM). No fluorescent signal was detectable above background at the kinetochores as the cell entered mitosis. Scale bar is equal to 10 micron. Frame rate equals seven frames per second. Time is given in minutes.seconds.

Movie S5
This representative timelapse movie, related to Figures 3A and 3B, shows a PtK2 cell stably expressing HsMad2-EYFP treated with nocodazole (serves as control for Movie S6). Clear fluorescent signal was detectable above background at the kinetochores as the cell entered mitosis. Scale bar is equal to 10 micron. Frame rate equals seven frames per second. Time is given in minutes.seconds.

Movie S6
This representative timelapse movie, related to Figures 3A and 3B, shows a PtK2 cell stably expressing HsMad2-EYFP treated with Mps1-IN-1 (10 μM) and nocodazole. Relative to untreated cells and nocodazole control limited fluorescent signal was detectable above background at the kinetochores as the cell entered mitosis. Scale bar is equal to 10 micron. Frame rate equals seven frames per second. Time is given in minutes.seconds.

Movie S7
This representative timelapse movie, related to Figures 6E and 6F, shows an U2OS H2B-GFP cell treated with DMSO vehicle after induced PLK4 overexpression (serves as a control for Movie S8). Mitotic progression and DNA segregation were followed by Histone H2B movement in fluorescent channel. Based on time from nuclear envelope breakdown (NEBD, t=20 min.) to anaphase initiation this cell spent 100 minutes in mitosis. Frame rate equals five frames per second. Time is given in minutes.seconds.

Movie S8
This representative timelapse movie, related to Figures 6E and 6F, shows an U2OS H2B-GFP cells treated with Mps1-IN-1 (10 μM) after induced PLK4 overexpression. Mitotic progression and DNA segregation were followed by Histone H2B movement in fluorescent channel. Based on time from nuclear envelope breakdown (NEBD, t=30 min.) to anaphase initiation this cell spent 20 minutes in mitosis. Frame rate equals five frames per second. Time is given in minutes.seconds.

Table S1. Raw data from Ambit kinase binding assay
This table contains the raw data from the Ambit kinase binding assays for Mps1-IN-1, Mps1-IN-2, and SP600125 (all at 10 μM). Scores from this primary screen are from a single run and are reported as "percent of DMSO control." Scores are related to the probability of a hit, but are not strictly affinity. In a 10 μM screen: >10% of DMSO control can be interpreted as the probability of being a false positive

is <20% and reflects a K_d likely > 1 μM, 1-10% the likelihood of a false positive is <10%, and <1% the probability of a false positive is <5% with a K_d likely <1 μM, and a score of '0' indicates a strong hit. K_d values are obtained by performing replicate assays at different concentrations of the test compound. Mps1 is listed here as TTK.

Table S2. K_d values of kinases exhibiting detectable binding affinities (using Ambit binding assay) for Mps1-IN-1 and Mps1-IN-2.
(--- indicates K_ds were not obtained for that compound/kinase combination because Ambit raw score was too high).

Table S3. Data collection and refinement statistics for Mps1 kinase domain apo structure and co-crystal structures with Mps1-IN-1 and methoxy-Mps1-IN-2.

Table S4. Small molecule screening data.
This table contains details of the small molecule kinase screen which was used to investigate potential Mps1 inhibitors. Data from this primary screen relevant to Mps1-binding compounds, including Mps1-IN-1 and Mps1-IN-2, can be found in Supplementary Table S1.

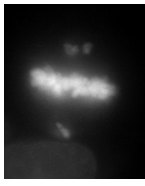

Supplementary Methods

Reagents and Antibodies

Mps1-IN-1 and Mps1-IN-2 were used at concentrations indicated in figures/figure captions and were synthesized according to synthetic schemes in Figure S2. The following antibodies were used for immunoblots or immunofluorescence: Anti-Mps1, NT (Millipore), Anti-Phospho-Histone H3 (ser10) (Upstate Biotechnology), Cyclin B1 Ab-2 (Thermo Scientific), Anti-Aurora B (Invitrogen), Anti-phospho-Aurora A (Thr288)/Aurora B (Thr232)/Aurora C (Thr198) (Cell Signaling), Anti-α-Tubulin DM1A (Sigma), PARP (Cell Signaling), anti-CREST (Immunovision), and Centrin2 (Santa Cruz Biotechnology. Secondary antibodies for immunofluorescence (Alexa Fluor-488 and -594) were from Molecular Probes. For DNA staining Hoechst 33342 (Invitrogen) was used.

Protein Expression and Purification

The kinase domain of human TTK (residues S519 –E808) was sub-cloned by ligation independent cloning into a pET derived pLIC vector with a TEV-cleavable (*) N-terminal 6xHis tag (MHHHHHHSSGVDLGTENLYFQ*SM). The expression vector was transformed into an E. coli BL21 (DE3) phage resistant Rosetta strain. Cells were grown at 37°C in Luria-Bertani (LB) medium containing 50 $\mu g \cdot ml^{-1}$ kanamycin and 35 $\mu g \cdot ml^{-1}$ chloramphenicol until an OD_{600} of 0.6-0.8. The temperature was adjusted to 20°C and expression was induced using 1 mM IPTG for 4 hours. The cells were lysed using an EmulsiFlex high-pressure homogenizer and purified using a two-column procedure, involving step elution (30, 50, 100, 200 300 mM imidazole) of the recombinant protein from a nickel-Sepharose affinity resin and a subsequent S75 Superdex gel filtration column. Protein of approximately 95% purity as judged by SDS-PAGE was used for crystallization. Protein identity was confirmed using liquid chromatography electrospray ionization mass spectroscopy. The calculated mass of the His tagged protein was 36064 Dalton. The ESI-MS spectra showed multiple peaks with 80 Dalton mass differences, typical for the presence of phosphorylation sites. The maximal detected mass was 36785 Dalton suggesting the presence of up to 9 phosphorylation sites. The identity of the protein was also reconfirmed by DNA sequencing of both DNA strands of the expression construct.

Crystallization

All crystallizations were carried out using the sitting drop vapor diffusion method at 4 °C. The apo enzyme (I) was grown by mixing 150 nL of the protein (11 $mg \cdot ml^{-1}$) with an equal volume of reservoir solution containing 55% w/v PEG300, 0.25 M NaCl and 1 M Na/K phosphate pH 6.4. The complex with Mps1-IN-1 (II) was grown into 300 nL drops composed of equal volumes of native protein (11 $mg \cdot ml^{-1}$) and 1 mM of the ligand mixed with a reservoir solution containing 40 % PEG300, 0.25 M NaCl and 0.1 M Na/K phosphate pH 5.6. The complex with methoxy-Mps1-IN-2 (III), was grown by mixing 75 nL of native protein (11 $mg \cdot ml^{-1}$) and 1 mM of the ligand with 150 nL of reservoir solution containing 25 % PEG3350, 0.2 M $MgCl_2$ and 0.1 M Bis-Tris pH 5.5. Crystals grew to diffracting quality within 2-3 weeks in all cases.

Data Collection and Structure solution

Crystals were cryo-protected using the well solution supplemented with additional ethylene glycol and were flash frozen in liquid nitrogen. Data were either collected at the Swiss Light Source on beamline X10SA using a MAR225 detector at 0.97912 Å (I) and 097642 Å (II) or at Diamond on beamline I02 using an ADSC QUANTUM315 detector at 0.9782 Å (III).

Indexing and integration was carried out using MOSFLM[232] and scaling was performed with SCALA[233]. Initial phases for the apo enzyme (I), were calculated by molecular replacement with PHASER[234] using an ensemble comprising of the core C-lobe of several known kinases (PDB IDs 2QKR, 2H9V, 2F2U and 2EUE). Several rounds of manual building in COOT[235] and refinement in REFMAC5[236] allowed ARP/wARP[237] to build most of the model into the density and the building was completed manually with COOT. The final model of (I) was used to obtain phases for the complexes with Mps1-IN-1 and methoxy-Mps1-IN-2. In all cases thermal motions were analyzed using TLSMD[238] and hydrogen atoms were included in late refinement cycles. Data collection and refinement statistics can be found in Supplemental Table S2[239]. The models and structure factors have been deposited with PDB accession codes: 3CEK (I), 3GFW (II), 3H9F (III).

Lanthascreen In vitro Kinase Assays

Activity assays were conducted using LanthaScreen Eu time-resolved FRET (TR-FRET) technology from Invitrogen. Briefly, 5 μL of 400 nM Alexa Fluor 647-labeled poly glu,tyr substrate and 10 $\mu g \cdot ml^{-1}$ TTK were added to 2.5 μL of inhibitor in 4% DMSO at 4-fold the final concentration to be tested. To this was added 2.5 μL of 4 μM ATP to initiate the reaction. Corning 3676 assay plates were used, and assay buffer consisted of 50 mM HEPES pH 7.5, 0.01% BRIJ-35, 10 mM $MgCl_2$, and 1 mM EGTA. After a 1 hour reaction, 5 μL of 6 nM Eu-PY20 antibody (Invitrogen) that had been dissolved in 20 mM Tris, pH 7.5 and 0.01% NP-40 containing 30 mM EDTA was added, and after a 30 minute incubation FRET was measured between the Eu-labeled antibody and the Alexa Fluor labeled, phosphorylated product of the kinase reaction. Assay plates were read using a BMG PheraStar using standard Eu-based TR-FRET settings with excitation at 340 nm and emission monitored at 615 nm (donor) and 665 nm (acceptor). Emission intensities were measured over a 200 μS window following a 100 μs post-excitation delay. The LanthaScreen® Eu kinase binding assay (Invitrogen, Madison WI) was used to assess compound binding to TTK by monitoring displacement of a fluorescently labeled, ATP site-directed kinase inhibitor (Kinase Tracer 236) from the kinase active site. Each 15 μL assay contained 5 nM TTK, variable amounts of test compound, 30 nM Kinase Tracer 236, 2 nM Eu-anti-GST Antibody, and 1% DMSO (residual from compound dilution) in Kinase Buffer A (50 mM HEPES pH 7.5, 10 mM $MgCl_2$, 1 mM EGTA, 0.01% Brij-35). Binding assays were initiated by addition of 5 μL of test compound (from 2-fold dilution series) to 5 μL of a kinase/antibody mixture, followed by addition of 5 μL of antibody. Assay plates were read using a BMG PheraStar using standard Eu-based TR-FRET settings with excitation at 340 nm and emission monitored at 615 nm (donor) and 665 nm (acceptor). Emission intensities were measured over a 200 μs window following a 100 μs post-excitation delay.

Immunoprecipitations and in vitro kinase assays

U2OS cells were transfected with LAP-Mps1 WT or M602Q pCDNA 3.1 constructs or empty vector (4 μg/10-cm dish) using the calcium phosphate method. Twenty-four hours post-transfection cells were treated with thymidine for 24 hrs. Cells were released into nocodazole for 16 hrs and mitotic cells were collected by shake-off. Cells were lysed using the following lysis buffer: 50 mM Tris pH 8.0, 1% NP40, 150 mM NaCl, protease and phosphatase inhibitors for 10 minutes at 4°C. Immunoprecipitation was performed using S-protein agarose (Novagen) for 2 hours at 4°C. Precipitates were washed twice with lysis buffer and twice more with kinase buffer (50 mM Tris pH 7.4, 10 mM $MgCl_2$, 0.5 mM DTT, protease and phosphatase inhibitors), and incubated for 30 minutes at 30°C with 0.3 μg recombinant His_6-tagged Mps1-KD in the

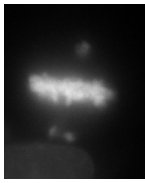

presence of 40 μg ATP, 5 μCi ^{32}P-γATP, and inhibitors. ^{32}P signal intensities were measured with a Storm phospho-imager. Western blots were incubated with anti-Mps1 and LAP-Mps1 signal intensities were measured with Odyssey.

Immunofluorescence
U2OS and HeLa cells used in immunofluorescence experiments were plated on poly-D-Lysine-coated 12-mm coverslips. In experiments examining chromosome missegregation (by kinetochore localization (CREST) and DNA structure) samples were pre-extracted with 0.2% Triton X-100 in 100 mM PIPES pH 6.8, 1 mM $MgCl_2$, and 5 mM EGTA for 1 minute before fixation with 4% Shandar Zinc Formal-Fixx™ (Thermo electron corporation) at room temperature for 20 minutes. For visualization of centrioles, cells were fixed with cold methanol at -20°C for 10 minutes and then permeabilized with 0.2% TritonX-100 in PBS (PBST). All coverslips were then blocked with 3% BSA in 0.1% PBST for 1 hour, incubated with primary antibodies for 1 hour at room temperature, washed with 0.1% PBST, and incubated with secondary antibody for an additional 1 hour at room temperature. Coverslips were then washed and stained with PBS containing Hoechst 33342, washed, and mounted using ProLong Antifade (Molecular Probes). Images for kinetochore staining were acquired on a DeltaVision RT system (Applied Precision) with a 60X/1.42NA PlanApoN objective (Olympus) using SoftWorx software. Images are maximum projections of a deconvolved stack and adjusted (identically within experiments) for sharpness and levels with Adobe Photoshop CS. Images for centriole staining were analyzed on an Axiovert 200M inverted microscope (Zeiss). Images were acquired with a CCD camera (CoolSnap, Photometrics) and Slidebook software (Intelligent Imaging Inovations).

Fluorescence-Activated Cell Sorting Analysis (FACS)
Cells were treated with compound for various periods of time. Cells were trypsinized, washed once in phosphate-buffered saline (PBS), and fixed overnight at –20°C with 80% ethanol in PBS. Cells were washed three times with PBS. Finally, cells were resuspended in PBS containing 0.1% Triton X-100, 25 $\mu g \cdot ml^{-1}$ propidium iodide (Molecular Probes), and 0.2 $mg \cdot ml^{-1}$ RNase A (Sigma) and incubated for 45 minutes at 37°C. For detection of Phospho-Histone H3 (ser10) by FACS cells were fixed as described above. After fixation, cells were resuspended in 1 mL of 0.25% Triton X-100 in PBS and incubated on ice for 15 minutes. After centrifugation, the cell pellet was suspended in 100 μL of PBS containing 1% bovine serum albumin (BSA) and 0.75 μg of Anti-Phospho-Histone H3 (ser10) (Millipore) and incubated at room temperature for 3 hours. The cells were then washed with PBS containing 1% BSA and incubated with FITC-conjugated goat anti-mouse immunoglobulin G antibody (Molecular Probes) diluted at a ratio of 1:30 in PBS containing 1% PBS. After 45 minutes at room temperature in the dark, the cells were stained with propidium iodide and RNaseA as described above. Cell cycle distribution was determined on a BD FACScan (BD Biosciences) and analyzed on FlowJo (Treestar).

Mitotic Escape Assay
HeLa (or U2OS cells) were plated at roughly 40% cell density. The following day the cells were treated with medium containing thymidine for 24 hours. After thymidine block, the cells were washed with PBS and replaced with fresh medium for 8 hours. After which time medium containing nocodazole was added for 2 hours. The medium was removed carefully and replaced with medium supplemented with nocodazole and test compound at the desired concentration (with the final concentration of DMSO below 0.2%). After 4 hours, the cells were harvested and the mitotic index was determined by immunoblot or FACS analysis.

Mad2 Kinetochore Establishment Assay

PtK2 cells were treated with Mps1-IN-1 (10 μM) or DMSO vehicle for 1 hour before co-administration with either DMSO vehicle or nocodazole. Timelapse microscopy was used to follow cells as they entered mitosis, as judged by nuclear envelope breakdown (NEBD). Timelapse PtK2 images were captured using a Nikon Eclipse Ti inverted microscope (Nikon USA) with a 60X/1.4 NA Plan Apochromat objective lens. Cells were maintained at 37°C using an InVivo Scientific microscope incubator (World Precision Instruments Inc.). Twelve bit phase (10 ms exposure, 2x2 binning) and yellow fluorescent (500 ms exposure, 2x2 binning) images were acquired either every 2 minutes for a total of 120 to 180 minutes or every 3 minutes for a total of 24 hours using a Photometerics Coolsnap HQ camera (Roper Scientific) and stored on a computer using Nikon Elements software (Nikon USA). Kinetochore HsMad2-EYFP fluorescence was quantified and background corrected as previously described[231].

Karyotyping

An asynchronous cell population of hTERT-RPE1 cells was treated with either DMSO vehicle or Mps1-IN-1 (10 μM) for 24 hours, the medium was removed and replaced with medium containing 100 ng·ml^{-1} colcemid (Irvine Scientific) for 2 hours to arrest cells in metaphase. Cells were trypsinized and collected by centrifugation. Cells were incubated in 0.075 M KCl for 20 minutes at room temperature. Fixative solution (3:1 Methanol: Acetic Acid) was added and incubated for 1 minute at room temperature. Cells were centrifuged for 10 minutes, supernatant removed and resuspended gently in fixative solution and incubated for 1 minute prior to re-centrifugation (repeat two more times). Cell pellets were stored at 4°C prior to Giemsa stain metaphase spread karyotyping.

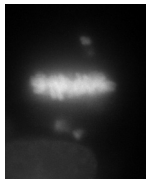

Proliferation Assay of PLK4-overexpressing U2OS cells

U2OS cells expressing doxycycline-inducible *PLK4* were plated in 96 well plates. A double thymidine block was performed using the following treatment regimen: thymidine for 18-20 hrs., release for 10 hrs. with doxycycline induction of *PLK4* during this time, then a second thymidine block, followed by release. Six hours after the 2nd thymidine release, Mps1-IN-1 (or DMSO vehicle) was added and the proliferation of the cell populations was monitored with Cell Titer GLO assay following the manufacturer's (Promega) instructions.

Data Presentation and Statistics

All the results presented in graphics are reported as the mean +/- SD unless otherwise noted. All statistical analyses herein represent comparison of continuous variables performed using an unpaired (two-tailed) t test. All graphics and statistics were generated using GraphPad Prism or Microsoft Excel.

Chapter 4

Mps1 maintains mitotic checkpoint activity by preventing APC/C-mediated disassembly of MCC

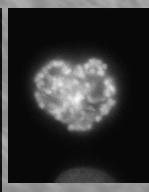

Nannette Jelluma, Adrian T. Saurin, Geert J.P.L. Kops

Department of Physiological Chemistry and Cancer Genomics Centre, UMC Utrecht, Universiteitsweg 100, 3584 CG, Utrecht, The Netherlands

Abstract

The mitotic checkpoint prevents premature chromosome segregation by producing a soluble inhibitor of the E3 ubiquitin ligase anaphase promoting complex/cyclosome (APC/C). The APC/C in turn ubiquitinates components of this inhibitor, known as the mitotic checkpoint complex (MCC). Although the consequence of this is debated, it may cause feedback activation of APC/C and rapid anaphase onset upon satisfaction of the mitotic checkpoint. Here we show that feedback inhibition of MCC function by the APC/C exists in cells and that this is prevented in prometaphase by the mitotic checkpoint kinase Mps1. Cells with reduced APC/C activity had a stable pool of MCC despite full attachment and biorientation of all chromosomes. This pool was completely removed by additional inhibition of Mps1 activity, resulting in anaphase onset and mitotic exit. Like Mad2 depletion, Mps1 inhibition in cells with normal APC/C activity accelerated mitosis. This acceleration was reverted to normal by additional depletion of APC/C activity in Mps1-inhibited but not Mad2-depleted cells. We propose that Mps1 promotes mitotic checkpoint activity by protecting MCC from APC/C-mediated disassembly.

Introduction

Anaphase is initiated by the anaphase promoting complex/cyclosome (APC/C), an E3 ubiquitin ligase that targets various substrates for degradation by the proteasome. For metaphase-to-anaphase transition, APC/C-mediated polyubiquitination and subsequent destruction of Cyclin B and Securin is essential (reviewed in [240]). APC/C activity is tightly regulated throughout the cell cycle and involves the cell-cycle phase-specific co-activators Cdc20 and Cdh1 as well as inhibitors such as Emi1 and the mitotic checkpoint complex (MCC) (reviewed in [240-244]). APC/C activity in interphase is regulated by a balance between Cdh1 and Emi1, whereby Emi1 prevents DNA re-replication and promotes mitotic entry[245]. In mitosis, Cdc20-mediated APC/C activity towards metaphase substrates such as Securin and Cyclin B is prevented by the action of the mitotic checkpoint until all chromosomes have stably attached to spindle microtubules. This regulation by the mitotic checkpoint prevents premature anaphase initiation and chromosome missegregations (reviewed in [205]).

Whenever unattached kinetochores are present, the mitotic checkpoint promotes the formation of the MCC that directly binds to and inhibits the APC/C. A critical component of the MCC is BubR1, which acts as a pseudo-substrate inhibitor of APC/C^{Cdc20} [93,94]. BubR1 can directly bind Cdc20 *in vitro*[87-89] and is found in complex with inactive APC/C in cells that have engaged the mitotic checkpoint[82,90-92]. The mitotic checkpoint protein Mad2 catalyzes MCC formation by interacting with Cdc20 after undergoing a conformational change following dimerization with Mad1-bound Mad2 on unattached kinetochores[96-99]. Mad2 may be part of the MCC[81-84] but was recently proposed to facilitate checkpoint signaling by aiding formation of a BubR1-Bub3-Cdc20 complex rather than partaking in APC/C inhibition directly[103,104]. Nevertheless, Mad2 can be co-precipitated with APC/C^{Cdc20}-MCC complexes[81,82,246-248], can inhibit Cdc20-mediated APC/C activity *in vitro*[247], albeit less efficient than BubR1[89], and promotes BubR1's ability to inhibit Cdc20-mediated APC/C activity *in vitro*[87,104].

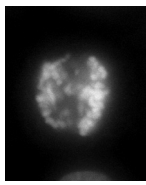

When all chromosomes have stably attached to the mitotic spindle, APC/C^{Cdc20} is rapidly activated towards Cyclin B and Securin to induce anaphase. Recent evidence indicates the existence of APC/C-mediated MCC destabilization and/or degradation feedback mechanisms that explain this rapid APC/C^{Cdc20} activation. APC/C was shown to ubiquitinate Cdc20[103,119], but the proposed effect on Cdc20 function is debated. Possibly, Cdc20 ubiquitination, aided by the E2 UbcH10 and counteracted by USP44, destabilizes MCC and effectively shuts off checkpoint signaling[119,120]. In agreement with other data[249], however, J. Nillson *et al.* propose that Cdc20 ubiquitination achieves the opposite effect by aiding the checkpoint in keeping Cdc20-dependent APC/C activity low. In addition to Cdc20, BubR1 was recently shown to be targeted by APC/C for degradation, promoting further APC/C^{Cdc20} activation and anaphase initiation[121].

Careful phenotype analysis of RNAi-mediated knockdown of mitotic checkpoint proteins showed that MCC components can be distinguished from the other mitotic checkpoint proteins. While, by definition, knockdown of all factors abrogates mitotic delay introduced by spindle poisons, only depletion of proposed Cdc20-binding MCC members (Mad2 and BubR1) causes a marked reduction in mitotic timing in an unperturbed mitosis[250]. Depletion of non-MCC components, for example Mad1 or Bub1, abrogates the mitotic checkpoint, but leaves mitotic timing intact[250]. It was proposed that timing functions are maintained by a pool of cytoplasmic Mad2 and BubR1, acting independently of kinetochores, during normal cell cycle progression[250]. This MCC pool could prevent APC/C activity towards Securin and Cyclin B long enough for most cells to achieve stable biorientation of all chromosomes, thus leaving the duration of mitosis unaffected. In this model, additional catalysis of MCC formation is essential to further delay

mitosis when unattached kinetochores persist, for instance when cells are treated with spindle poisons.

Mitotic checkpoint function upon addition of spindle poisons also depends on the kinase activity of Mps1, which localizes to unattached kinetochores. Mps1 kinase activity additionally regulates attachment-error-correction, and absence of Mps1 activity results in gross chromosome missegregations in an unperturbed mitosis in vertebrate cells[106,130,211 (Chapter 2 of this thesis)]. Although Mps1 activity was shown to be essential for Mad1 and Mad2 localization to unattached kinetochores[106,107,211 (Chapter 2 of this thesis)], it is unknown if this is the primary function for Mps1 in the control of mitotic checkpoint activity. Here we examined the interplay between mitotic timing, MCC, APC/C and Mps1 and find that Mps1 prevents APC/C mediated disassembly of MCC to maintain a mitotic arrest.

Results

Based on the effect of protein depletion on the duration of mitosis, the mitotic checkpoint proteins can be divided into 2 groups: Those that are essential for checkpoint activity (e.g. Mad1, Bub3, Bub1), and those that are additionally essential for maintaining a normal mitotic timing (Mad2 and BubR1)[250]. To examine if Mps1 can be classified into either of these groups, time from nuclear envelope breakdown to start of membrane furrowing (NEB-to-furrowing) of cells depleted of Mps1 by RNAi was determined by live cell microscopy, and time at which half the population had undergone furrowing (half-time) was scored. Knock-down of Mps1 in U2OS cells caused reduced NEB-to-furrowing half-time, from 27 to 18 minutes (Figure 1A). This could be reverted to normal by ectopic expression of LAP-tagged wild-type Mps1 (LAP-Mps1-WT), but not of a kinase-dead mutant (D664A, LAP-Mps1-KD[211] (Chapter 2 of this thesis)) (Figure 1A), indicating that the kinase activity of Mps1 is essential for normal mitotic timing. These data confirm our previous results using a specific chemical inhibitor of Mps1, Mps1-IN-1[239] (Chapter 3 of this thesis). NEB-to-furrowing half-time of cells lacking Mps1 kinase activity was comparable to timing of cells depleted of BubR1 (27 to 17 minutes, Figure 1A), justifying phenotypic classification of Mps1 to the group of MCC proteins. In agreement with this, inhibition of Mps1 activity by Mps1-IN-1 or SP600125[186] strongly reduced binding of Mad2 to BubR1 in mitotic HeLa cells (Figures 1B, 1C). In contrast to BubR1 or Mad2, however, Mps1 was never reported to be a component of the MCC, and we also have not detected Mps1 in large-scale MCC precipitations[251]. Together, these data indicate that Mps1 is required to maintain a level of MCC that is sufficient to inhibit APC/C activity in the initial phases of mitosis.

To test whether shortened NEB-to-furrowing time in Mps1-inhibited cells was due to premature APC/C activation, mitotic progression was monitored in cells depleted of APC/C activity through siRNA-mediated knock-down of either the essential APC/C cullin subunit APC2 or of its E2 UbcH10[63,64,252,253]. APC2 or UbcH10 depletion delayed mitosis for several hours (Figures 2A-E). As expected, this delay occurred in metaphase (Figures 2C, 2D, 3C, 4A), and prometaphase duration (time to full alignment) was unaffected by APC/C depletion (Figures 2C, 2D, 4A). Strikingly, however, codepletion of APC/C and Mad2 or Mps1 abrogated this metaphase delay (Figures 2B, 2E). A similar reversion was seen when APC/C-depleted cells were treated with Mps1-IN-1 (Figures 2A, 2C), showing that inefficient RNAi as a result of combining siRNAs was an unlikely cause of the phenotypic reversal. These data further showed that the level of APC/C inhibition achieved in these studies, although delaying cells in metaphase for hours, was insufficient to completely prevent Cyclin B/Securin degradation and mitotic exit. Indeed, this is similar for Cyclin A (an APC/C substrate of which degradation is not inhibited by the mitotic checkpoint[70,71]), since degradation is slowed but not prevented by APC2 depletion (Figure 2F). These data reveal two important observations. Firstly, that siRNA-mediated knockdown of APC/C components causes a prolonged metaphase delay that is entirely dependent on components of the mitotic checkpoint (Mad2 and Mps1). Secondly, that these components can be separated by their ability to restore normal (Mps1) or fast (Mad2) mitotic timing in APC/C depleted cells (Figures 2A-C, 2E). Therefore, unlike Mad2 depletion, the accelerated mitosis seen following Mps1 depletion/inhibition is dependent upon APC/C activity.

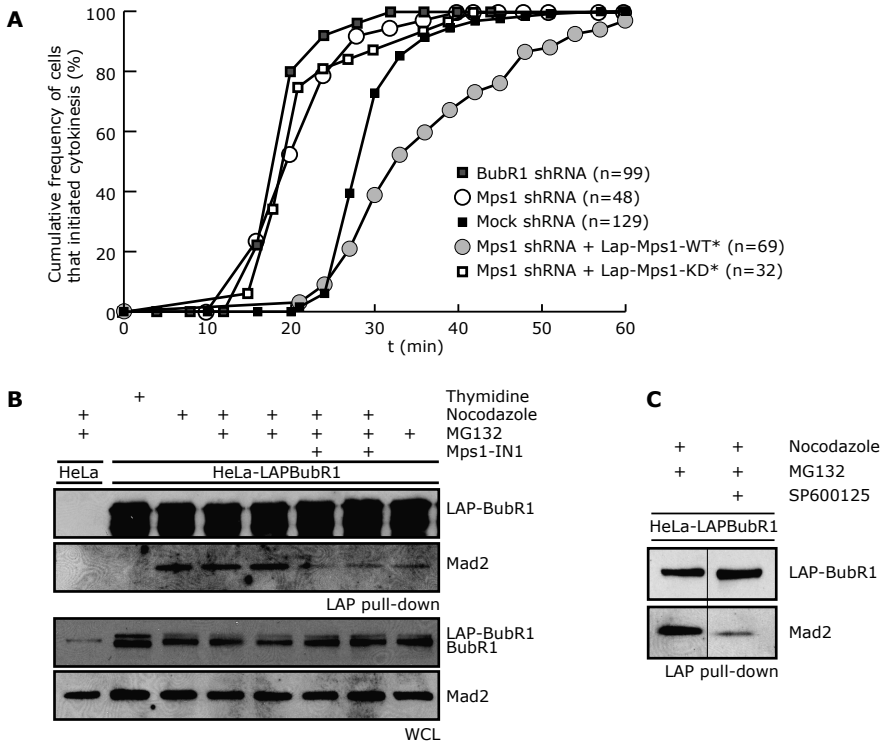

Figure1. Mps1 activity is essential for mitotic checkpoint, normal mitotic timing and levels of BubR1-Mad2 complexes.
(A) Graph showing cumulative frequency of U2OS cells transfected with the indicated plasmids that initiated cytokinesis versus time (t). Nuclear envelope breakdown (NEB) was set to t=0. Asterisks indicate RNAi resistance. (B, C) Immunoblots showing co-precipitation of Mad2 with LAP-BubR1 (LAP pull-down) (B, C) and total protein levels (WCL) (B) from lysates of mitotic HeLa cells stably expressing LAP-BubR1, transfected with siRNA and treated as indicated.

A mitotic checkpoint-dependent delay in mitosis could indicate the presence of kinetochores that are unattached or are in states of low tension. A number of observations showed that no unattached or low-tension kinetochores persisted in APC/C-depleted cells and no detectable MCC catalysis occurred. First, BubR1 and Mad2 levels on kinetochores in these metaphases were as low as in control metaphase cells (Figure 3A). Second, live cell imaging of mitosis in APC/C-depleted cells showed that LAP-BubR1 left kinetochores readily when a metaphase plate was formed (Figure 3B). As BubR1 leaves kinetochores only upon establishment of tension across bioriented sister kinetochores[254,255], this showed that all chromosomes in APC/C-depleted cells had properly bioriented. Third, APC/C RNAi cells were delayed in metaphase (Figure 2C) and no missegregations were observed in cells that subsequently underwent anaphase after long and varying metaphase delays (Figures 2C, 3C).

Mps1 is required for efficient Mad2 recruitment to unattached kinetochores and thus likely promotes catalysis of MCC formation by such kinetochores[106,107,208,211] (Chapter 2 of this thesis). To

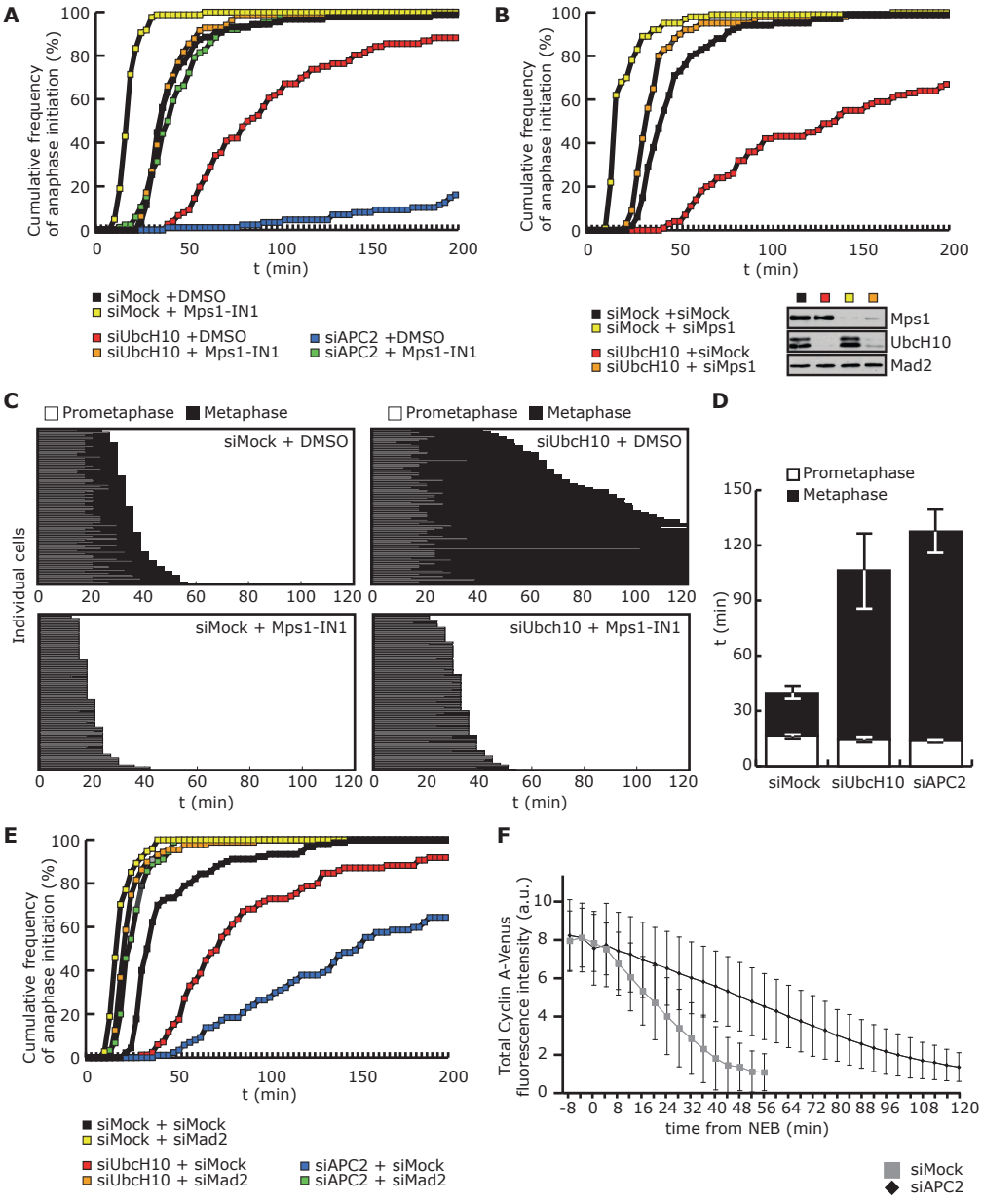

Figure 2. Metaphase delay upon APC/C knock-down depends on Mps1 activity and mitotic checkpoint signaling.
(A, B, E) Graphs showing cumulative frequency of HeLa cells that initiated anaphase versus time (t). Nuclear envelope breakdown (NEB) was set to t=0. Cells were transfected with the indicated siRNAs (A, B, E), and treated with DMSO or with Mps1 inhibitor (Mps1-IN-1) before start of timelapse (A, E). For each condition n=80 cells. Protein levels after siRNA treatment are shown in case of double siRNA treatment (B). (C) Bar graphs showing time spent in prophase and metaphase of HeLa cells treated as indicated. Each horizontal bar represents a single cell. (D) Bar graph showing average time that HeLa cells treated with the indicated siRNAs spent in prometaphase and in metaphase. Error bars represent standard error of the mean within two individual experiments in which minimums of 20 cells per condition were analyzed. (F) Graph showing mean Cyclin A-Venus degradation over time in cells treated with the indicated siRNAs.

examine whether the ability of Mps1 to delay mitosis of APC/C-depleted cells depended on its role in kinetochore-driven MCC formation, cells depleted of APC/C activity were monitored by live cell microscopy and allowed to establish full biorientation, satisfy the mitotic checkpoint and proceed to metaphase before Mps1 inhibitor was added. Strikingly, all metaphase-arrested APC2 or UbcH10 RNAi cells rapidly exited mitosis upon addition of Mps1-IN-1, irrespective of time spent in metaphase (Figure 4A). Thus, even long after full biorientation (Figure 3), Mps1 activity

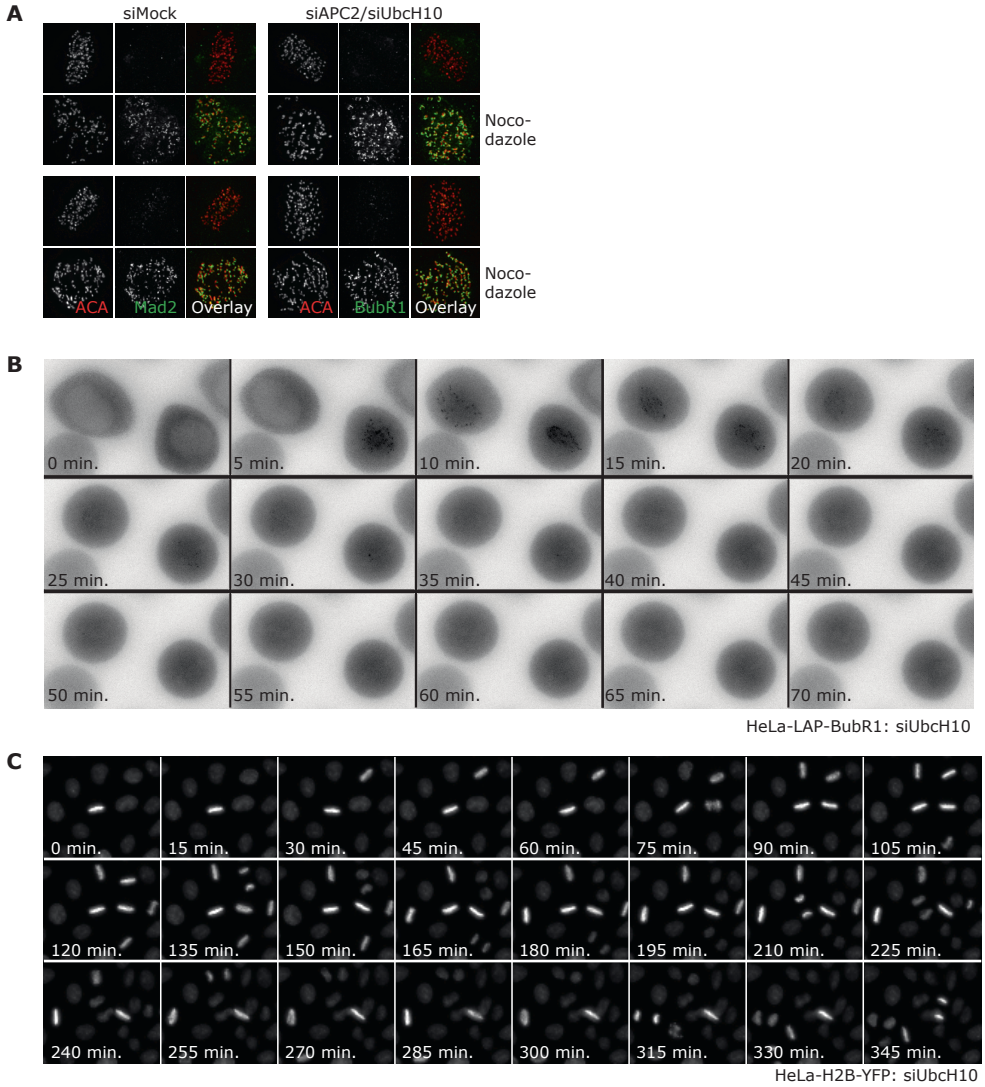

Figure 3. Checkpoint-dependent metaphase delay upon APC/C knock-down occurs in the absence of unattached kinetochores.
(A) Mad2 and BubR1 localization on kinetochores (as determined by co-localization with kinetochore marker ACA) in HeLa cells treated with siRNA as indicated. Shown are metaphase cells and prometaphase cells (Nocodazole). (B) Timelapse images of HeLa cells stably expressing LAP-BubR1 transfected with siUbcH10. Black signal represents EYFP signal of LAP-BubR1. (C) Timelapse images of HeLa cells transfected with siUbcH10. DNA is visualized by stable expression of H2B-EYFP.

continued to prevent anaphase onset in APC/C-depleted cells. These data have two important implications. First, Mps1 has a role in the checkpoint other than kinetochore-derived MCC formation. This could be uncovered only after reduction of APC/C activity. Second, sufficient Mps1 activity remains in metaphase to restrain low levels of APC/C activity.

Given that APC/C depletion caused a checkpoint-dependent metaphase delay and Mps1 maintained mitotic duration in an APC/C-dependent fashion, we next set out to examine the hypothesis that Mps1 activity prevents APC/C-mediated disassembly of MCC. To examine this, presence of MCC was determined under various conditions using immunoprecipitation from cell lysates. Importantly, Mad2 and Cdc20 co-precipitated with LAP-tagged BubR1 in HeLa cells depleted of APC2 and UbcH10 (Figure 4B, third lane). Since the immunoprecipitations were done from the mitotic fractions of APC/C-depleted cells, we conclude that a stable pool of MCC existed in APC/C-depleted, metaphase-arrested cells. We next wished to examine the effect of Mps1 inhibition on MCC stability in APC/C-depleted metaphase cells. To delay mitotic exit after Mps1 inhibition long enough to allow collection of mitotic cells for biochemical analysis, APC2 and UbcH10 were co-depleted to achieve more stringent APC/C inhibition than single depletions. Combined RNAi of these two proteins delayed exit after Mps1 inhibition for at least 30 minutes in 90% of cells (Figure 4A). Judged by hyperphosphorylation, Mps1 was found to be active in the metaphases before inhibition, and addition of Mps1-IN-1 for 15 minutes caused complete hypophosphorylation, indicative of significant inhibition (Figure 4C, third lane). These metaphase cells were then analyzed for MCC content. Whereas uninhibited APC2/UbcH10-depleted metaphase cells contained a significant amount of Mad2-bound BubR1, this interaction was completely lost after 15 minutes of Mps1 inhibition (Figure 4D, third lane).

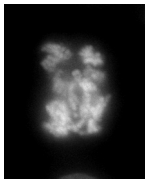

Addition of nocodazole to APC2/UbcH10-depleted cells raised the amount of MCC to significantly higher levels than those in nocodazole-treated control siRNA cells (Figure 4D, fourth lane), further showing that APC/C activity counteracts MCC build-up. Inhibiting Mps1 under these conditions did not remove MCC altogether within the duration of inhibition but nevertheless strongly reduced its levels (Figure 4D, fifth lane). Live monitoring of chromosome de-condensation after addition of Mps1 inhibitor showed that the elevated levels of MCC in UbcH10-depleted cells treated with nocodazole could restrain mitotic exit 4-5-fold longer than those in untreated UbcH10-depleted cells (Figure 4E). Mitotic exit was delayed to an average of 1.5 hours, which was about twice the time it took for nocodazole-treated control cells to exit mitosis after Mps1 inhibition (Figure 4E). Together, these data support the hypothesis that the time to mitotic exit is a function of APC/C-mediated disassembly of MCC, counteracted by Mps1 activity.

Discussion

We have shown here that APC/C-depleted cells contain an MCC pool that is protected from APC/C-mediated disassembly by Mps1 activity. We conclude that Mps1 is involved in a feedback mechanism between MCC and APC/C that allows a rapid switch from APC/C inhibition to APC/C activation towards metaphase substrates such as Cyclin B and Securin.

Knockdown of Mps1 resulted in acceleration of mitosis, comparable to knockdown of Mad2 or BubR1 (Figure 1A and [250]). It was proposed by P. Meraldi *et al.* that a cytosolic pool of MCC restrains anaphase early in prometaphase before further MCC formation can be catalyzed by unattached kinetochores[250]. This model explains why knock-down of non-MCC components of the mitotic checkpoint does not result in acceleration. As opposed to RNAi of Mad2 or BubR1, which removes all MCC from cells, removal of, for instance, Mad1 is unlikely to affect the

kinetochore-independent pool of MCC since Mad1 serves to promote MCC catalysis. Mps1 activity is needed for Mad1 and Mad2 enrichment on unattached kinetochores and therefore thought to be required for MCC catalysis. Nevertheless, its depletion or inhibition accelerated mitosis, which is suggestive of a role in maintaining MCC function independent of kinetochores.

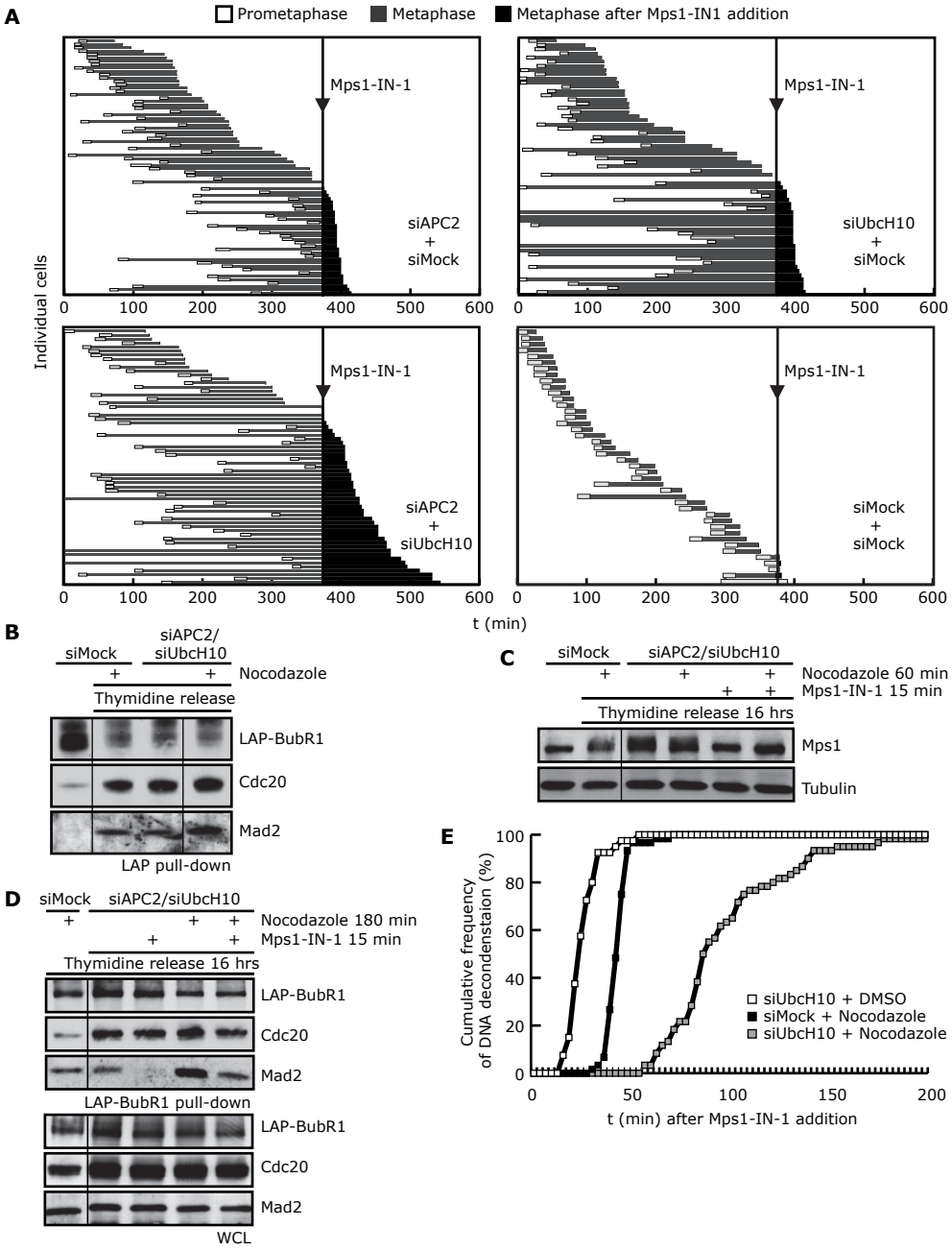

Unlike Mad2 and BubR1[82], Mps1 has never been reported to be part of MCC. Our observations on the relation between MCC, Mps1 and APC/C, however, provide an explanation for the Mps1-depletion phenotype. APC/C inhibition by UbcH10 or APC2 RNAi reverted the accelerated timing of Mps1-IN-1- or Mps1 siRNA-treated cells (Figures 2A-C), but not of Mad2 siRNA-treated cells (Figure 2E). This difference can be explained if depletion of Mad2 directly leads to absence of MCC altogether while loss of Mps1 activity affects stability of MCC. Without significant catalysis, MCC can be formed at a basal rate that is expected, however, to be insufficient for sustained checkpoint activity[256] and cannot prevent accelerated mitosis in Mps1-inhibited cells. We propose a model in which the accumulation of MCC that is formed at this basal rate is counteracted by continuous disassembly by the APC/C (Figure 5). Mps1, in turn, prevents APC/C from doing so, thus maintaining a certain amount of MCC. In such a model, stabilization of MCC by lowering APC/C-mediated MCC disassembly is expected to delay mitotic exit to some extent, even in the face of Mps1 inhibition (Figure 5). The data presented in this chapter are fully consistent with this.

The mechanism by which APC/C affects MCC stability is unclear. APC/C can ubiquitinate Cdc20 and BubR1 *in vitro*, and this was proposed to cause MCC destabilization and/or degradation[103,119,249]. Our data offer no further insight into this matter. Although we see a clear increase in the amount of Cdc20 in APC/C-depleted metaphase cells (Figure 4D and [103]), we see no evidence for degradation of MCC components after Mps1 inhibition (Figure 4D). It cannot, however, be excluded that MCC degradation does occur but is not reflected in the total cellular protein levels of the MCC components. Our data and those of others are consistent with a model in which APC/C is allowed to target various substrates in prometaphase, including Cyclin A and possibly Cdc20, but is prevented by Mps1 from targeting MCC for disassembly. Upon stable biorientation of all chromosomes, however, the brake imposed by Mps1 is removed, APC/C disassembles MCC and induces rapid feedback activation that ultimately results in anaphase initiation.

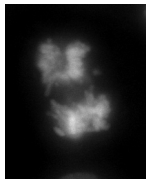

Although it is clear that Mps1 activity protects MCC stability, it is unclear at what level this occurs. We have not been able to show that Mps1 modifies any of the MCC components directly by phosphorylation (not shown). However, Mps1 can *in vitro* phosphorylate two proteins that could impact MCC stability (Supplemental Figures S1A and S1C). The first is the deubiquitinating enzyme USP44 that was proposed to counteract the action of APC/C-UbcH10 in targeting MCC for destabilization[120] and is therefore expected to protect the MCC. Furthermore, USP44 is needed for normal mitotic timing and mitotic checkpoint activity[120]. We verified that knock-down of USP44 caused acceleration of mitosis (Supplemental Figure

Figure 4. Continuous Mps1 activity prevents MCC destabilization and anaphase initiation in APC/C knock-down cells.
(A) Bar graphs showing time spent in prophase and metaphase of HeLa cells treated as indicated. Mps1 was inhibited as indicated after start of timelapse imaging by adding Mps1-IN-1. Each horizontal bar represents a single cell. (B) Immunoblot showing co-precipitation of Mad2 and Cdc20 with LAP-BubR1 (LAP pull-down) from lysates of mitotic HeLa cells transfected with siRNA and treated as indicated. (C) Immunoblot showing Mps1 protein mobility shift from lysates of mitotic HeLa cells transfected with siRNA and treated as indicated (lane 2-6) or from lysate of asynchronous HeLa cells (lane 1). (D) Immunoblots showing co-precipitation of Mad2 and Cdc20 with LAP-BubR1 (LAP pull-down) and total protein levels (WCL) from lysates of mitotic HeLa cells, stably expressing LAP-BubR1, transfected with siRNA and treated as indicated. (E) Graphs showing cumulative frequency of HeLa cells stably expressing H2B-EYFP that initiated DNA de-condensation versus time (t), after addtition of Mps1-IN-1 at t=0. Cells were transfected with the indicated siRNAs, and treated with DMSO or nocodazole. Only cells that were mitotic at t=0 were analyzed, for each condition n=60 cells.

S1B). The second is UbcH10, the APC/C-associated E2 ubiquitin-conjugating enzyme. UbcH10 promotes the ability of APC/C to counter mitotic checkpoint activity[119]. Possibly, phosphorylation of USP44 activates it towards MCC de-ubiquitination while phosphorylation of UbcH10 inhibits its activity towards MCC ubiquitination. USP44 and UbcH10 are therefore interesting candidates for further research on the role of Mps1 activity in stabilizing MCC. Interestingly, the possibility exists that Mps1 itself is a target of APC/C. Knock-down of APC/C activity resulted in sustained Mps1 activity. Further studies are needed to pinpoint the exact actions of Mps1 and APC/C in this APC/C-MCC feedback mechanism.

In summary, we found that the role of Mps1 activity in the mitotic checkpoint lies not only in facilitating catalysis of MCC formation by recruiting Mad2 to unattached kinetochores. Mps1 is also involved in stabilization of already formed MCC by preventing APC/C-mediated disassembly of MCC. These functions of Mps1 together result in maximal MCC levels to ensure strong inhibition of APC/C activation towards Cyclin B and Securin.

Figure 5. Model of involvement of Mps1 in a feedback loop between MCC and APC/C
(A-D) Colors indicate active (green) or inactive (red) states of APC/C and Mps1, font size indicates quantities of proteins/complexes, and fat lines indicate dominant regulations, along the axis of the duration of mitosis (time (t) in minutes). (A) Control situation showing the switch in metaphase from high MCC levels inhibiting APC/C to APC/C activation and MCC inhibition. (B) Knock-down of Mps1 results in lack of negative control of APC/C until metaphase, resulting in premature anaphase. (C) APC/C knock-down results in metaphase arrest by reduced levels of total APC/C activity. Due to its low total activity, APC/C is not able to sufficiently target Cyclin B for degradation, nor to positively regulate itself by targeting MCC, since MCC is protected by Mps1 activity. (D) Double knock-down of Mps1 and APC/C causes low APC/C activity, which can however not be negatively regulated by Mps1 (by protection of MCC, direct or indirect). APC/C can therefore positively regulate itself by MCC destabilization and finally gain enough activity to target Cyclin B for degradation.

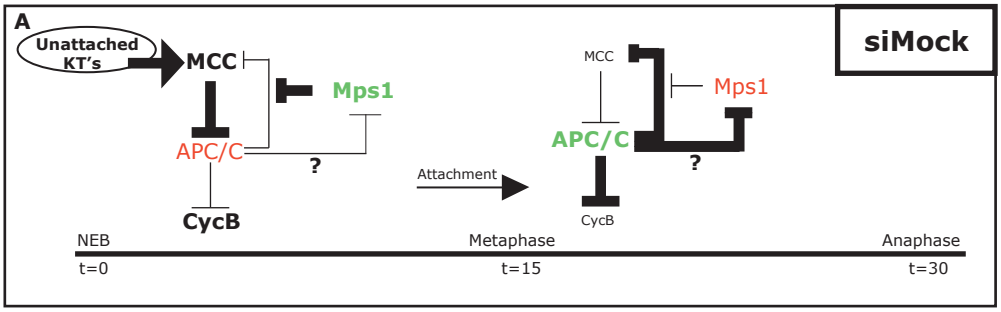
A
siMock
Unattached KT's
MCC
Mps1
APC/C
?
CycB
Attachment
MCC
Mps1
APC/C
?
CycB
NEB
Metaphase
Anaphase
t=0
t=15
t=30

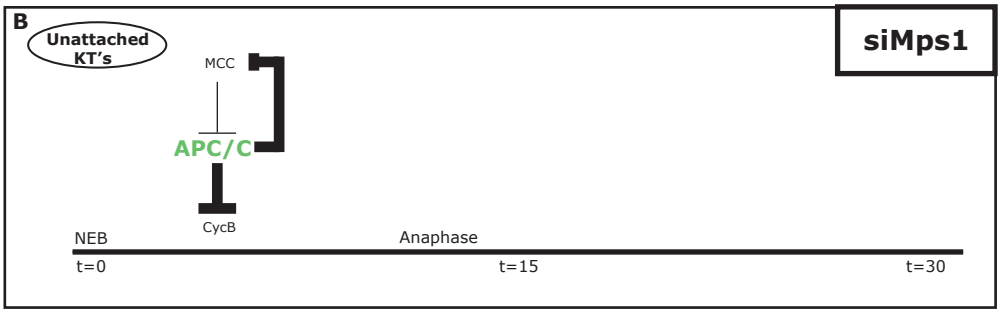
B
siMps1
Unattached KT's
MCC
APC/C
CycB
NEB
Anaphase
t=0
t=15
t=30

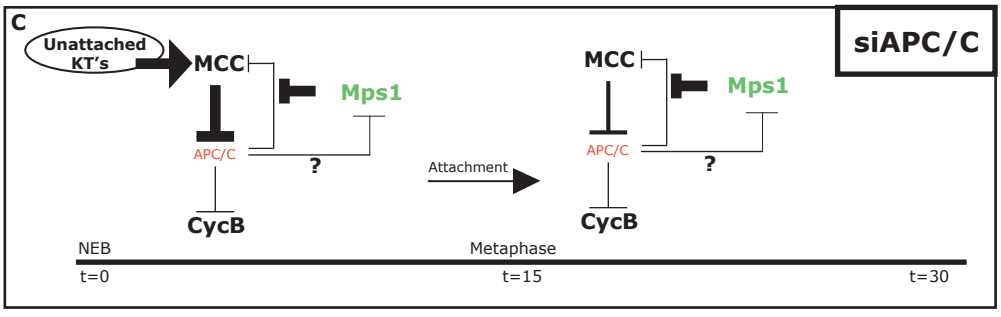
C
siAPC/C
Unattached KT's
MCC
Mps1
APC/C
?
CycB
Attachment
MCC
Mps1
APC/C
?
CycB
NEB
Metaphase
t=0
t=15
t=30

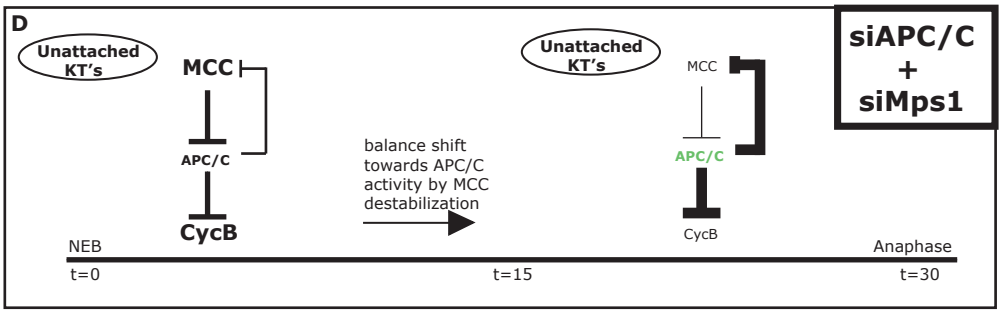
D
siAPC/C
+
siMps1
Unattached KT's
MCC
APC/C
CycB
balance shift
towards APC/C
activity by MCC
destabilization
Unattached KT's
MCC
APC/C
CycB
NEB
Anaphase
t=0
t=15
t=30

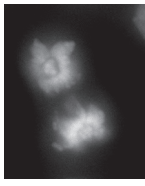

Materials and Methods

Cell culture, plasmids and transfections

U2OS, HeLa and stable H2B-EYFP or LAP-BubR1 expressing cells were grown in DMEM with 8% FBS, supplemented with pen/strep. pSuper-Mock, pSuper-Mps1, pcDNA-LAP-Borealin, pcDNA- LAP-Mps1 and pSuper-BubR1 have been described[95,211]. LAP-USP44 plasmid was created by inserting USP44 cDNA in-frame at the 3' end of cDNA encoding the LAP tag (a gift of I. Cheeseman). Endogenous Mps1 replacement assays in U2OS cells were done as in [211], by Calcium Phosphate transfection. A tetracycline-inducible U2OS/TR cell line expressing Cyclin A-Venus was made by stable integration of pcDNA4-Cyclin A-Venus into a U2OS clone stably expressing the tetracycline repressor protein (pcDNA6/TR).

siRNA transfections were done with HiPerfect (Qiagen), according to the manufacturer's instructions (reverse transfection protocol). All siRNA oligos (Dharmacon) were transfected at an end concentration of 20 nM. Target sequences were: Mock: AGAUUCUAGCUAACUGUUC, Mps1: GACAGAUGAUUCAGUUGUA[211]; UbcH10: GUAUAGGACUCUUUAUCUU; APC2 (Dharmacon J-003200-13); Mad2: UACGGACUCACCUUGCUUG[95]; USP44: GAAUUGGAGUAUCAAGUUA[120].

Timelapse live cell imaging

Live cell imaging was done on an Olympus IX-81 microscope, controlled by Cell-M software (Olympus), in a heated chamber (37°C and 5% CO2) using a 20X/0.5NA UPLFLN or a 60X/1.42 PlanApo objective. Images were acquired with a Hamamatsu ORCA-ER camera. Images were processed for analysis to maximum intensity projections of all Z-planes and using Cell-M software. In APC/C depletion experiments, stable H2B-EYFP expressing HeLa cells were transfected and blocked in S-phase with thymidine (2.5 mM, Sigma) for 24 hours. Cells were imaged after release from thymidine by acquiring EYFP signal fluorescent images every 3 minutes.

Immunoprecipitation and immunoblotting

Stable LAP-BubR1 expressing HeLa cells were harvested by mitotic shake-off after indicated treatment with Nocodazole (200 $ng \cdot ml^{-1}$, Sigma), MG132 (10μM, Sigma), SP600125 (10 μM, BioMol), and/or Mps1-IN-1 (10 μM, a kind gift of N.S. Gray[239]) and lysed in 150 mM NaCl, 50 mM Hepes pH7.5, 5 mM EDTA and 0.1% NP40. LAP-BubR1 was precipitated from the lysates with S-protein agarose (Novagen). Precipitates were analyzed with standard immunoblotting procedures. Antibodies used for immunoblotting were anti-Mps1-NT (Upstate Biotechnology), anti-α-Tubulin (Sigma), Anti-BubR1 (Bethyl), anti-Mad2 (Bethyl and custom rabbit serum), anti-UbcH10 (Boston Biochem), anti-Cdc20 (Santa Cruz (mouse)), and anti-GFP (custom rabbit serum).

Immunofluorescence

For immunofluorescence analysis, cells were treated 45 minutes before fixation with or without Nocodazole (200 $ng \cdot ml^{-1}$, Sigma). Fixation and immunostaining were done as described in [211]. Antibodies used were anti-Mad2 (custom rabbit serum) and anti-BubR1 (Bethyl). Images were acquired on a DeltaVision RT system (Applied Precision) with a 100X/1.40NA UPlanSApo objective (Olympus) using SoftWorx software. Images are maximum projections of a deconvolved stack and adjusted (identically within experiments) with SoftWorx and Adobe Photoshop CS3.

Kinase assays

In vitro recombinant kinase assay:

Recombinant active Mps1^{211} was incubated together with His$_6$-UbcH10 (Boston Biochem) in kinase buffer (50 mM Tris pH 7.4, 10 mM $MgCl_2$, 0.5 mM DTT, 40 μM ATP) at 30°C for 30 minutes.

IP kinase assay:

U2OS cells transfected with the various LAP-tagged protein constructs were harvested and lysed in 150 mM NaCl, 50 mM Hepes pH7.5, 5 mM EDTA and 0.1% NP40. LAP-tagged proteins were precipitated from the lysates with S-protein agarose (Novagen) and incubated together with recombinant active Mps1^{211} in kinase buffer (50 mM Tris pH 7.4, 10 mM $MgCl_2$, 0.5 mM DTT, 40 μM ATP) at 30°C for 30 minutes.

Supplementary Information

Supplementary Figure

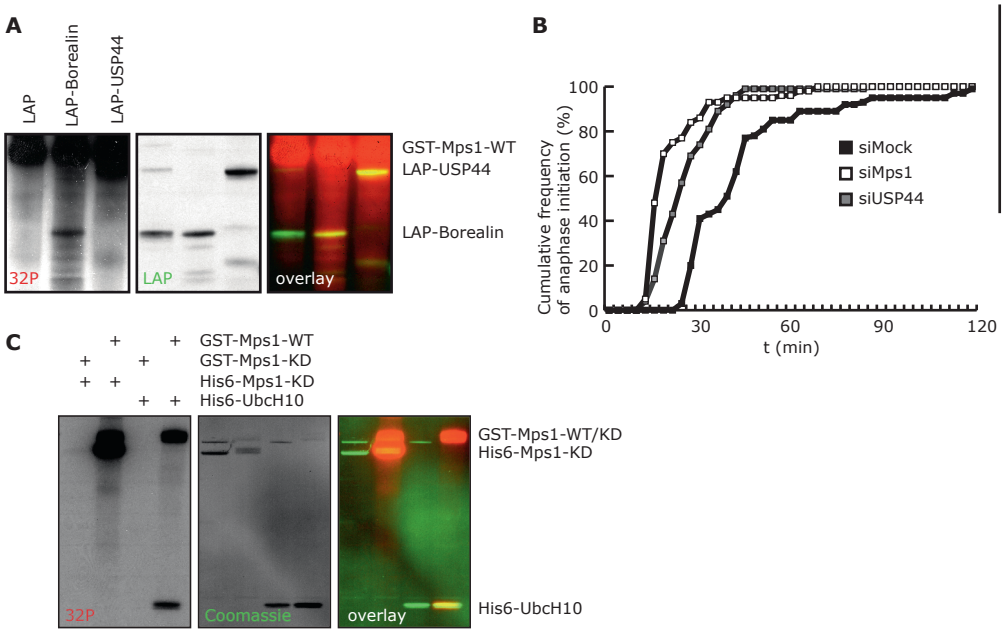

Figure S1. UbcH10 and USP44 are possible targets for Mps1 to prevent APC/C-mediated MCC disassembly

(A) *In vitro* kinase activity of recombinant Mps1 towards precipitated (LAP-tag pull-down) LAP-USP44 (third lane). LAP-tag alone serves as a negative control and LAP-Borealin as a positive control[211] (Chapter 2 of this thesis). (B) Mitotic timing of HeLa cells transfected with siRNA as indicated. Graph shows cumulative frequency of cells that initiated anaphase versus time (t). For each condition n=80 cells. (C) *In vitro* kinase activity of recombinant wild-type (WT) and kinase-dead (KD) Mps1 towards recombinant UbcH10.

Chapter 5

Chromosomal instability by inefficient Mps1 auto-activation due to a weakened mitotic checkpoint and lagging chromosomes

Nannette Jelluma[1,2], Arjan B. Brenkman[1], Ian McLeod[3], John R. Yates III[3], Don W. Cleveland[4], René H. Medema[2], Geert J. P. L. Kops[1,2]

[1]Department of Physiological Chemistry and Cancer Genomics Centre, UMC Utrecht, Utrecht, The Netherlands, [2]Department of Medical Oncology, Laboratory of Experimental Oncology, UMC Utrecht, Utrecht, The Netherlands, [3]Department of Cell Biology, The Scripps Research Institute, La Jolla, California, United States of America, [4]Ludwig Institute for Cancer Research and Department of Cellular and Molecular Medicine, University of California San Diego, La Jolla, California, United States of America

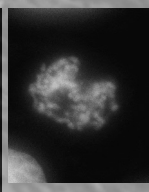

Adapted from *PLoS ONE, volume 3, issue 6, e2415*

Abstract

Chromosomal instability (CIN), a feature widely shared by cells from solid tumors, is caused by occasional chromosome missegregations during cell division. Two of the causes of CIN are weakened mitotic checkpoint signaling and persistent merotelic attachments that result in lagging chromosomes during anaphase. Here we identify an auto-phosphorylation event on Mps1 that is required to prevent these two causes of CIN. Mps1 is phosphorylated in mitotic cells on at least 7 residues, 4 of which by auto-phosphorylation. One of these, T676, resides in the activation loop of the kinase domain and a mutant that cannot be phosphorylated on T676 is less active than wild-type Mps1 but is not kinase-dead. Strikingly, cells in which endogenous Mps1 was replaced with this mutant are viable but missegregate chromosomes frequently. Anaphase is initiated in the presence of misaligned and lagging chromosomes, indicative of a weakened checkpoint and persistent merotelic attachments, respectively. We propose that full activity of Mps1 is essential for maintaining chromosomal stability by allowing resolution of merotelic attachments and to ensure that single kinetochores achieve the strength of checkpoint signaling sufficient to prevent premature anaphase onset and chromosomal instability. To our knowledge, phosphorylation of T676 on Mps1 is the first post-translational modification in human cells of which the absence causes checkpoint weakening and CIN without affecting cell viability.

Introduction

Aneuploidy is a trait widely observed in tumor cells from all types[257]. Aneuploidy in these cells is the result of occasional chromosome missegregations, a phenotype referred to as chromosomal instability or CIN. Various defects in the processes that control chromosome segregation and subsequent cell division can cause CIN[4] and these include but are not limited to tetraploidization, defective mitotic checkpoint function and unresolved merotelic chromosome attachments[258-260].

The mitotic checkpoint prevents chromosomal instability by delaying anaphase onset until all chromosomes are correctly attached to the mitotic spindle. To ensure faithful chromosome segregation, the mitotic checkpoint has to be sufficiently strong to delay anaphase when as little as one chromosome is not correctly attached to the spindle. Weakening of the mitotic checkpoint promotes aneuploidy and it has been proposed that this can contribute to tumorigenesis[4,260]. Recent examination of a number of studies that have investigated mitotic checkpoint responses in a wide variety of tumor cells indicated that about two thirds of those tumors have a reduced capacity to maintain a mitotic arrest when challenged with spindle poisons[260]. Despite many investigations, molecular explanations for such checkpoint weakening have yet to be found. Genes encoding checkpoint components are very infrequently mutated (reviewed in [4, 260]) and, although reported in some instances, altered expression of checkpoint proteins or mRNA does not appear to correlate well with the status of CIN (e.g. [156,261,262]). It is therefore likely that checkpoint activity is affected by other means, one of which may be a change in the level of functionally relevant post-translational modifications or by misregulated enzymatic activities that are crucial for checkpoint signaling. Finding the relevant modifications that contribute to checkpoint signal strength and investigating their status in chromosomally instable tumor cells might give important information on how checkpoint signaling may have become compromised in those tumors.

Faithful chromosome segregations requires all chromosomes to be bi-oriented, with each sister kinetochore attached to one pole. Most erroneous attachments are sensed, directly or indirectly, by the mitotic checkpoint as they involve lack-of-attachment or lack-of-tension, and are corrected by the chromosomal passenger complex of which Aurora B is the effector kinase[40]. Merotelic attachments, however, escape detection by the mitotic checkpoint. A chromosome is attached in a merotelic fashion when it is bioriented while one of its kinetochores has attachments to both poles. This chromosome is therefore attached as well as under tension. Merotely has been suggested as a frequent cause of CIN in tumor cells[258,263]. Interestingly, slight inhibition of Aurora B caused frequent persistent merotelic attachments that resulted in lagging chromosomes in anaphase and aneuploidy of the resulting daughter cells[56,109]. Reduced Aurora B activity may therefore be an important cause of chromosome missegregations and CIN in tumor cells.

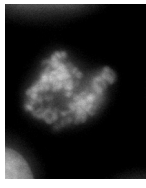

Monopolar spindle 1 (Mps1) is a kinase that is essential for the mitotic checkpoint as well as for efficient Aurora B activation to allow attachment-error correction[130,131,205,211 (Chapter 2 of this thesis)]. Despite its central role in ensuring faithful chromosome segregation, little is known about how Mps1 is activated in mitosis or how Mps1 activity correlates with chromosomal stability.

Results

Mps1 is hyperphosphorylated during mitosis, coinciding with a peak in its enzymatic activity[130]. To get insight into the mechanisms of activation of Mps1, mitotic Mps1 was analyzed for the presence of phosphorylated residues. To this end, a HeLa cell line stably expressing low levels of LAP-tagged (Localization and Affinity Purification[185]) Mps1 was used (Figures 1A, 1B). LAP-Mps1 was isolated from mitotic cells by tandem affinity purification and analyzed for phospho-peptides using mass spectrometry. A total of 8 phosphorylated residues were found (Figure 1C). In agreement with a recent study[264], one of the identified phospho-residues, T676, is located in the activation (T)-loop of the kinase domain (Figure 1D). Another potential T-loop phosphorylation on T686 was identified, but confidence of assignment to this site was quite low (see more on this below). Similar identification of phosphorylation sites on *in vitro* auto-phosphorylated recombinant GST-Mps1 purified from insect cells (see Figure S1A) revealed that three additional residues were *in vitro* phosphorylated, and that five of the residues found phosphorylated *in vivo*, including T686, were the result of auto-phosphorylation (Figure 1C). In agreement with this, T676 and T686 were recently found phosphorylated on bacterially expressed recombinant Mps1[222].

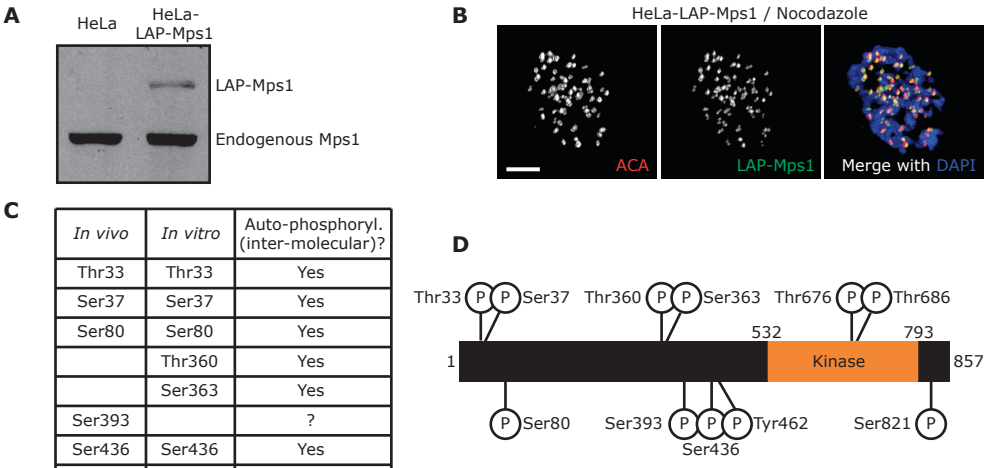

In vivo	*In vitro*	Auto-phosphoryl. (inter-molecular)?
Thr33	Thr33	Yes
Ser37	Ser37	Yes
Ser80	Ser80	Yes
	Thr360	Yes
	Ser363	Yes
Ser393		?
Ser436	Ser436	Yes
Tyr462		?
Thr676		?
Thr686	Thr686	Yes
	Ser821	Yes

Figure 1. Mps1 is phoshorylated during mitosis on at least 7 residues.
(A, B) A monoclononal HeLa cell line stably expressing LAP-tagged Mps1 (HeLa-LAP-Mps1) was analyzed for expression level of LAP-Mps1 relative to endogenous Mps1 as shown by immunoblot (anti-Mps1) (A) and localization of LAP-Mps1 (anti-GFP) together with centromeres (ACA) and DNA (DAPI) (B). Scale bar is 5 μm. (C) List of phosphorylation sites identified by mass spectrometry on LAP-Mps1 isolated from mitotic HeLa-LAP-Mps1 cells (left column, *in vivo*) or on recombinant Mps1 isolated from insect cells (middle column, *in vitro*). Phosphorylation sites on recombinant Mps1 were designated 'auto-phosphorylations' when sites were not found on similarly expressed and isolated recombinant kinase-dead Mps1. (D) Schematic overview of phosphorylated residues on Mps1.

Many protein kinases are activated by phosphorylation on T-loop residues[265]. Since both T676 and T686 were reported recently to contribute to kinase activity[264,222], we created Threonine-to-Alanine mutants of these two sites (T676A and T686A) to study their contribution to mitotic checkpoint signaling, attachment-error-correction and chromosome segregation. To this end, endogenous Mps1 was depleted from U2OS cells using shRNA and replaced with either LAP-tagged wild-type (WT) Mps1 or the T676A or T686A mutants (for details on this assay, see [211] (Chapter 2 of this thesis)). A kinase-dead (KD) mutant (D664A) was used as negative control. Expression levels of the different mutants are shown in Figure 2A. As expected, depletion of Mps1 prevented cells from accumulating in mitosis upon nocodazole treatment, indicative of a dysfunctional mitotic checkpoint, and caused defects in chromosome alignment. The T686A mutant, like the D664A mutant, was unable to restore either checkpoint signaling (Figures 2B, 2C) or chromosome alignment (Figure 2D). The position of this Threonine in the kinase domain is very well conserved amongst kinases. It is thought to play a structural role in organizing the catalytic region[266], but in certain kinases, phosphorylation of this site was shown to be necessary for full kinase activity[267]. To discriminate between whether T686A was non-functional due to compromised structural integrity of the kinase domain or due to lack of phosphorylation, a mutant bearing a phospho-mimetic mutation on this site (Aspartic Acid or Glutamic Acid) was tested. Neither Mps1-T686D nor -T686E could restore spindle checkpoint function (Figure S1B). Even though it is formally possible that the D/E substitutions do not mimic phosphorylation on this site, these data are more consistent with a structural role for T686. In support of this, we have been unable to detect T686 phosphorylation in tissue culture cells using a phospho-specific antibody, even though this antibody was able to recognize *in vitro* auto-phosphorylated Mps1 (data not shown).

In contrast to T686A, the T676A mutant restored proper chromosome alignment (Figure 2D) to the same extent as wild-type. This indicated that attachment-error-correction by Aurora B was not affected, in contrast to cells devoid of Mps1 activity[211] (Chapter 2 of this thesis), see discussion for more details). The T676A mutant also rescued mitotic checkpoint signaling in cells treated with nocodazole (Figures 2B, 2C) to the same extent as wild-type Mps1. Nocodazole treatment presumably causes maximal mitotic checkpoint signaling due to the fact that all kinetochores are unattached. Therefore, defects that do not cause complete inactivation of the checkpoint may not be identified in assays in which nocodazole is used, such as the experiment in Figure 2B. Since the mitotic checkpoint evolved to prevent the missegregation of one or a few chromosomes and therefore requires maximal activity per kinetochore, the contribution of phosphorylation on T676 was studied in more detail by following unperturbed mitotic progression of Mps1-depleted U2OS cells expressing LAP-Mps1-T676A using fluorescence timelapse microscopy. DNA was visualized by co-transfecting H2B-EYFP. 48% (312 out of 656) of cells expressing T676A exited mitosis with one or more lagging and/or misaligned chromosomes, compared to 18% of controls cells (Figures 2E, 2F, Movie S1, S2). Of cells that missegregated chromosomes, 58% entered anaphase with both misaligned and lagging chromosomes, while 23% and 19% displayed either misaligned or lagging chromosomes, respectively (Figure 2G). This strongly suggested that cells expressing Mps1-T676A have a diminished capacity to i) delay anaphase onset when few chromosomes are unaligned and ii) resolve misattachments that are not sensed by the mitotic checkpoint. This, in turn, promotes chromosomal instability.

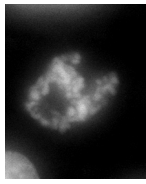

The relationship between chromosome missegregations and Mps1 kinase activity was investigated by examining the kinase activities of the T-loop mutants compared to wild-type and kinase-dead Mps1. Since Mps1 very efficiently phosphorylates another molecule of Mps1 (Figure S1A), kinase

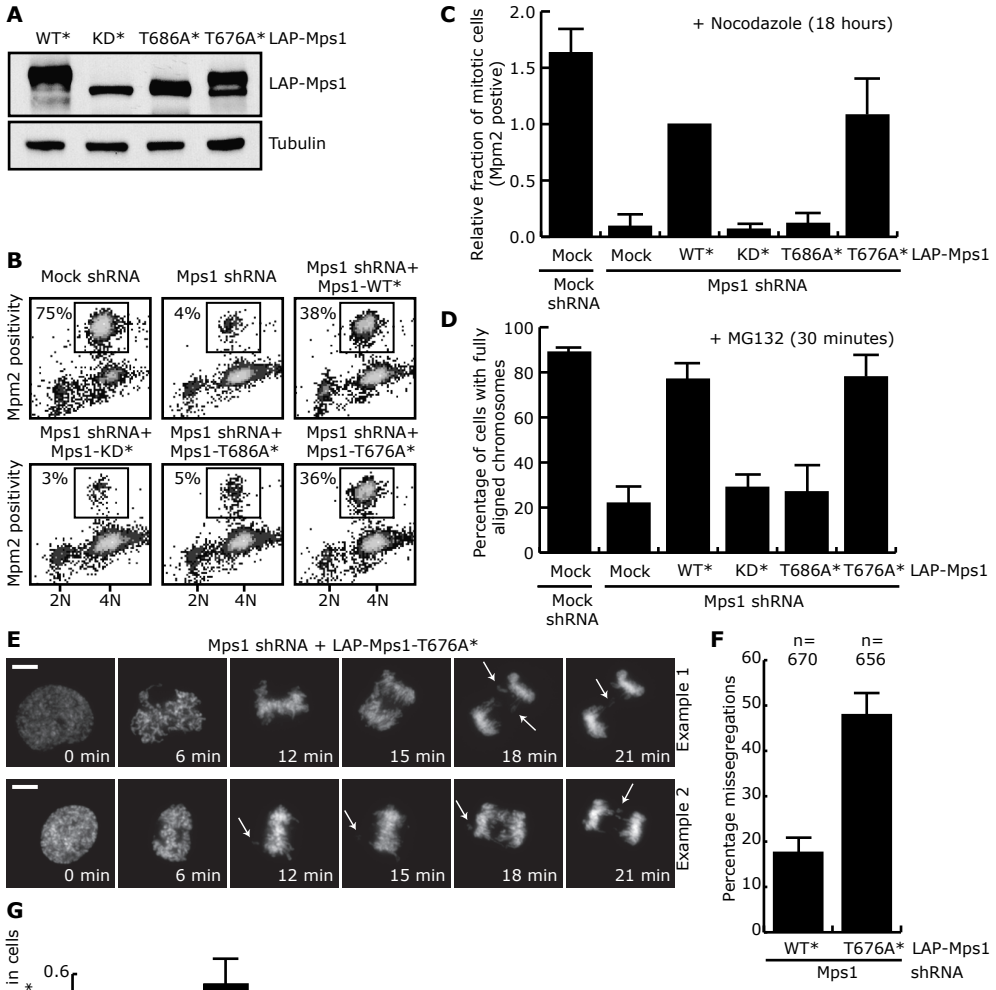

Figure 2. T676 phosphorylation is required for correct chromosome segregation and full checkpoint signaling.

(A) Expression levels, as shown by immunoblot (anti-Mps1), in asynchronously growing cells of LAP-Mps1 mutants (asterisk (*) indicates mutations that confer resistance to Mps1 shRNA) transiently transfected into U2OS cells. (B) Flow cytometric analysis of the fraction of mitotic cells transfected with Mock or Mps1 shRNA together with the indicated plasmids (asterisk (*) indicates mutations that confer resistance to Mps1 shRNA), and treated with nocodazole for 18 hrs. (C) Quantification of (B), average of three experiments (+/- SD). (D) U2OS cells transfected as in 2B were treated for 30 minutes with MG132. Fixed cells were stained with DAPI and the percentage of cells with all chromosomes aligned to the metaphase plate was determined (n = 30 cells). Graph represents the average of three experiments (+/- SD). (E) Mitotic progression of U2OS cells transfected as in 2B along with H2B-EYFP Mps1 was followed by live cell imaging. Stills from two representative cells showing anaphase with misaligned/lagging chromosomes (arrows) are shown (see Movie S1 and Movie S2). Scale bar is 5 μm. (F) Quantification of (E), average of three experiments (+/- SD), n = total amount of cells. (G) Graph showing the fraction of total missegregations as displayed in 2F with misaligned chromosomes, lagging chromosomes, or both in cells expressing Mps1-T676A.

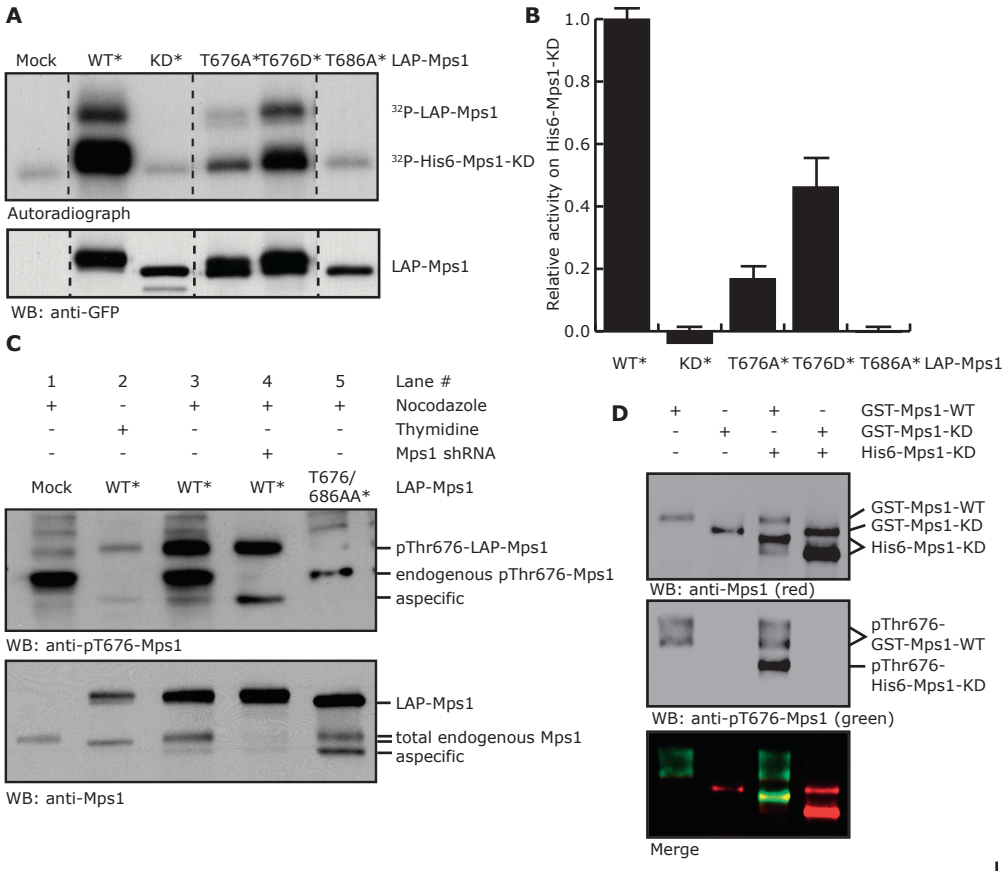

Figure 3. Lack of T676 auto-phosphorylation reduces Mps1 kinase activity.
(A) Kinase activity of LAP-Mps1 mutants (asterisk (*) indicates mutations that confer resistance to Mps1 shRNA) extracted from mitotic U2OS cells was examined by *in vitro* kinase activity towards recombinant kinase-dead His-Mps1 (D664A). (B) Quantification of (A). Relative values to LAP-Mps1-WT were calculated after subtraction of the background signal derived from 'mock' immunoprecipitations (first lane in Figure 3A). Average of three experiments (+/- SD). (C) Western blot showing phosphorylation specifically on T676 in lysates from U2OS cells transfected with the indicated constructs (asterisk (*) indicates mutations that confer resistance to Mps1 shRNA). (D) Western blot showing *in vitro* intermolecular auto-phosphorylation on T676. Combinations (as indicated) of recombinant wild-type GST-Mps1(-WT), kinase-dead GST- and His-Mps1(-KD) were subjected to *in vitro* kinase reactions, after which proteins were analyzed for reactivity to pT676 antibody (green) and Mps1 antibody (red) by immunoblot.

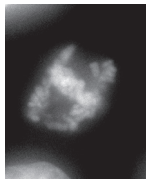

activities of LAP-Mps1 proteins immunoprecipitated from mitotic U2OS cells were examined by using purified recombinant kinase-dead Mps1 as substrate. The substrate (His_6-Mps1-KD (D664A)) can subsequently be separated from the kinase (LAP-Mps1) by virtue of its faster mobility on gel. The T686A mutant showed background levels of kinase activity (Figures 3A, 3B), confirming that this mutant is kinase-dead[222]. In agreement with the inability of T686D or T686E to restore spindle checkpoint function, these mutants were also devoid of kinase activity (data not shown). T676A however, showed reduced kinase activity, to about 20% compared to the activity of wild-type Mps1 (Figures 3A, 3B). Phospho-mimetic mutations (Aspartic Acid, Figure 3B; or Glutamic Acid, not shown) could restore activity to about 50% compared to wild-type. Thus although activity could not be fully restored by mimicking phosphorylation

on T676, these results indicate that phosphorylation on this site plays an important role in ensuring full Mps1 activation during mitosis. To investigate whether this holds true in cells, we examined whether phosphorylation of T676 is induced specifically during mitosis by probing cell lysates with an antibody recognizing phosphorylated T676 (anti-pT676-Mps1). Lysates of cells expressing wild-type LAP-Mps1 or a LAP-Mps1-T676/686AA double point mutant, as well as lysates of cells depleted of endogenous Mps1 by RNAi were used as control for antibody specificity. Endogenous Mps1 was not phosphorylated on T676 in U2OS cells treated with thymidine to block cells in Sphase, but was highly phosphorylated on T676 in mitosis (Figure 3C). Note that the exogenous LAP-Mps1-wild-type was partially phosphorylated on T676 and supershifted in S-phase (see lane 2, Figure 3C), indicating that exogenous Mps1 can be activated during S-phase. Since activity of LAP-Mps1-WT immunoprecipitated from asynchronous cells is equal to that immunoprecipitated from mitotic cells (not shown), activation of exogenous Mps1 in non-mitotic cells is probably due to overexpression of the protein that can cause spontaneous auto-activation in the absence of kinetochores[264]. Probing recombinant kinase-dead Mps1 that was *in vitro* phosphorylated by wild-type Mps1 with the pT676-Mps1 antibody revealed that even though T676 was not identified as an auto-phosphorylation site by MS analysis (Figure 1C), T676 is auto-phosphorylated in an intermolecular manner (Figure 3D).

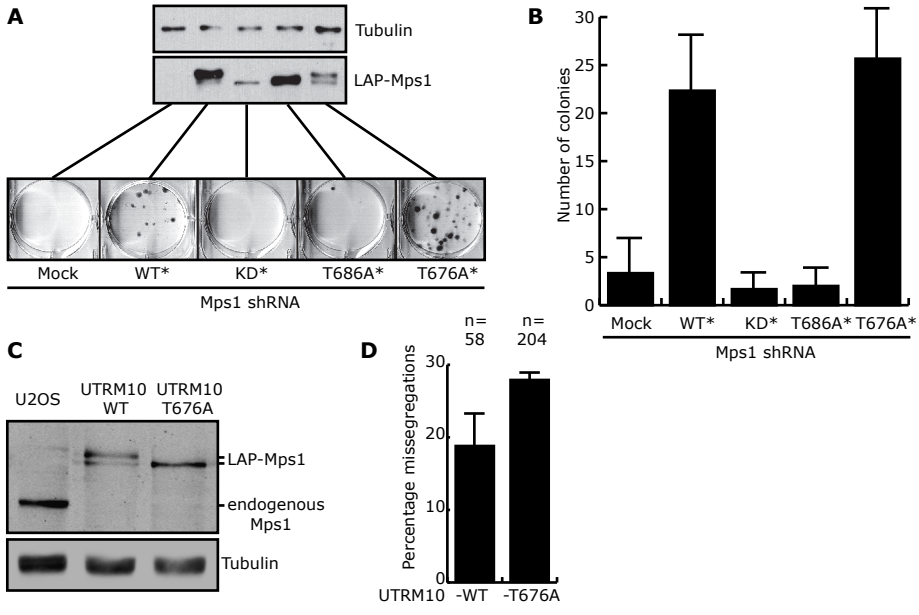

Figure 4. T676 phosphorylation is required for maintaining chromosomal stability but not cell viability.
(A) U2OS cells were transfected as in 2B along with pBabe-puro, grown under puromycin selection for two weeks after which surviving colonies were stained. Immunoblot (anti-Mps1) shows expression levels in lysates taken 3 days after transfection of the different LAP-Mps1 mutants. (B) Quantification of the number of colonies counted in 4A, average of three experiments (+/- SD). (C) Immunoblot (anti-Mps1) showing expression levels of endogenous Mps1 and LAP-Mps1 in lysates of U2OS cells, and UTRM10 cells continuously expressing Mps1 shRNA through doxycycline treatment[211] (Chapter 2 of this thesis) that stably express wildtype LAP-Mps1 (UTRM10-WT) or LAP-Mps1-T676A (UTRM10-T676A). (D) Graph shows average percentages of UTRM10-T676A and UTRM10-WT cells that missegregate chromosomes as observed with live cell imaging (as in 2E), (+/- SD), n = total amount of cells.

Mps1 activity is indispensable for cell viability, but viability is maintained in CIN tumor cells that have a weakened mitotic checkpoint[260]. Since cells in which endogenous Mps1 was replaced with LAP-Mps1-T676A showed a reduction in Mps1 kinase activity and a weakened checkpoint, these cells were tested for viability in a clonogenic assay. For this, U2OS cells were transfected with Mps1 shRNA and the indicated LAP-Mps1 mutants, along with pBabe-puro. The cells were then grown on puromycin for two weeks, to allow analysis of viability of transfected cells only. As expected[211] (Chapter 2 of this thesis), LAP-Mps1-KD or -T686A expressing cells could not grow out to form colonies and thus proved to be unviable in the long term. Surprisingly, LAP-Mps1-T676A-expressing cells were able to grow out roughly the same amount of colonies as cells expressing wild-type LAP-Mps1 (Figures 4A, 4B). This indicated that replacing endogenous Mps1 with an Mps1-T676A mutant did not significantly reduce cell viability. To more rigorously address the behavior of cells expressing LAP-Mps1- T676A, a cell line was created that is devoid of Mps1 but stably expresses LAP-Mps1-T676A at levels similar to the endogenous protein prior to its removal by RNAi (UTRM10-T676A) (Figure 4C). These cells have been maintained in culture in our lab for months without obvious proliferation defects. Importantly, when imaged live, UTRM10-T676A cells displayed an increased tendency for chromosome missegregations compared to a similar cell line expressing wild-type LAP-Mps1 to endogenous levels (UTRM10-WT) (Figures 4C, 4D). Thus, complete depletion of Mps1 kinase activity results in cell death but residual kinase activity of about 20 percent keeps cells viable yet induces chromosomal instability.

Discussion

We show here that auto-activation of Mps1 by T676 auto-phosphorylation is essential for full kinase activity and maintenance of chromosomal stability, but not for cell viability. In two recent studies, T676 of human Mps1 was identified as an important phosho-site for the regulation of Mps1 activity[222,264]. All three studies agree that Mps1 lacking this phosphorylation has strongly reduced but still clearly detectable kinase activity. J. Kang *et al.* report that mitotic arrest in response to nocodazole of cells expressing T676A was reduced 2-fold[264], whereas we found no such decrease. This may be due to cell type-dependent differences in sensitivity of the checkpoint to the level of Mps1 inhibition. A more intriguing explanation, however, is the possibility that the measure that the authors of that study used to mark mitotic cells, phosphorylation of histone H3, is inadequate when analyzing effects of Mps1 inhibition on checkpoint signaling, as we have recently shown that this phosphorylation is dependent on Mps1 kinase activity in mitotic cells[211] (Chapter 2 of this thesis).

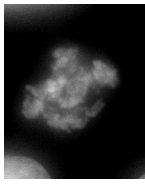

J. Kang *et al.* found 10 phosphorylation sites on Mps1 isolated from mitotic cells[264]. Our combined data from *in vivo* and *in vitro* phosphorylated Mps1 confirms five of those sites, and these include T360, S363, S436, T676 and S821. It is unclear why there is discrepancy between the remaining five sites found in the study by J. Kang *et al.* and the five additional sites from our *in vivo* analysis. As absence of phosphorylation of a peptide in mass spectrometric analyses is a poor indicator of lack of phosphorylation of that sequence in cells, it is quite possible that Mps1 is phosphorylated on all reported sites, totaling therefore 15 phosphorylated residues. Analysis of Mps1 using phospho-specific antibodies or other means, combined with thorough functional analysis of single point mutants is needed to pinpoint functionally relevant phosphorylations on Mps1 and distinguish actual *in vivo* sites from mass spec artifacts.

Cells in which endogenous Mps1 was replaced with T676A display increased frequency of chromosome missegregations as evidenced by an increase in anaphases in the presence of

misaligned and/or lagging chromosomes. It is unclear what causes chromosomes to lag at anaphase in these cells. Possibly, these chromosomes are unattached but fail to activate the mitotic checkpoint due to diminished Mps1 activity. More likely, the laggers point to an inability to correct merotelic attachments. Such correction is performed by Aurora B activity, that itself is regulated by Mps1[211] (Chapter 2 of this thesis). Therefore, lagging chromosomes in T676A cells may be due to diminished Aurora B activity, resulting in persistent merotely. We have not, however, observed a detectable reduction in Aurora B activity, as T676A cells treated with MG132 properly aligned all chromosomes, suggestive of functional attachment-error correction, and since levels of Ser7 phosphorylation of the Aurora B substrate CENP-A were indistinguishable from control (data not shown). Consistent with this, treatment of cells with low concentrations of a specific Aurora B kinase inhibitor did not cause observable inhibition of Aurora B at the level of substrate phosphorylation, chromosome alignment or cytokinesis yet resulted in persistent merotely in a significant fraction of cells[109]. Therefore, it is likely that a small, virtually undetectable, local reduction in Aurora B activity in cells expressing Mps1-T676A underlies the occasional lack of correction of a merotelic attachment in these cells.

Cells expressing Mps1-T676A arrested potently when treated with nocodazole but initiated anaphase in the presence of misaligned chromosomes. Thus, although T676 phosphorylation is not essential when the combined signals from all kinetochores is strong, it is needed for amplified checkpoint signaling from one or a few misaligned chromosomes. This supports the hypothesis that weakening of the mitotic checkpoint can cause non-lethal chromosomal instability. The contribution of such checkpoint weakening to CIN in tumor cells was recently questioned by a study in which filming of chromosome segregation in CIN tumor cells did not reveal checkpoint defects but suggested merotely as the most common way to aneuploidy in these cells[263]. Clearly in the three cell lines examined in that study, checkpoint signaling strength was sufficient to delay anaphase onset until all chromosomes had bioriented. In various other tumor cells, however, checkpoint strength was found to be diminished[260], and recent evidence from mouse models indicate that in cases where such weakening occurs, it can contribute to carcinogenesis[159,164,268] and references in [4]). The extent of the contribution of checkpoint weakening to tumor formation is thus controversial and conclusions will await examination of chromosome segregation in large panels of cells from patient tumors. Alternatively, establishment of good biomarkers for detection of weak checkpoint signaling, such as antibodies to post-translational modifications that determine strong vs weak signaling, may facilitate this.

Despite original claims that mutations in components of the checkpoint machinery could underlie CIN[228], subsequent extensive mutational analysis of cells from many types of tumors has not confirmed this as a means to decrease the efficiency of checkpoint signaling (reviewed in [4]). Similarly, misexpression of checkpoint components has been observed[4] but it is unclear if this is the origin of CIN in those cells and there is no apparent consensus about whether up- or downregulation correlates with aneuploid status of the cells examined (e.g. [156,261,262]). For instance, disruption of the Rb tumor suppressor pathway causes CIN by upregulating Mad2 whereas inactivation of the REST tumor suppressor causes CIN by decreasing expression of Mad2[269,270]. Similarly, mice either overexpressing Mad2 or underexpressing Mad2 develop cancer, albeit that affected organs, tumor types and latency periods differ[153,157]. It is thus possible that checkpoint weakening in tumor samples at the molecular level is caused by altered activity of checkpoint components or by altered posttranslational modifications that contribute to efficiency of the mitotic arrest.

The data presented here place Mps1 as a central activity to prevent chromosomal instability. Reduced Mps1 kinase activity allows weakened mitotic checkpoint signaling as well as lagging

chromosomes at anaphase, two major defects suggested to contribute to CIN in tumor cells[260,263]. Phosphorylation of T676 in Mps1 provides the first specific post-translational modification in human cells as a cause for this. Many more such modifications may exist and it will be interesting to examine if any are affected in CIN tumor cells.

Materials and Methods

Cells

U2OS cells were grown in DMEM with 8% FBS, supplemented with pen/strep. UTRM10 cells[211] were grown similarly with the exception that tet-approved FBS was used. UTRM10-T676A and -WT cells were created by transfecting UTRM10 cells (Effectene, Qiagen) with LAP-Mps1-T676A or -WT and selecting for survivors by continuous culture in 1 $\mu g \cdot ml^{-1}$ doxycycline (Sigma). Clones were subsequently chosen based on expression of the LAPtagged Mps1 protein and absence of endogenous Mps1. Thymidine (2.5 mM), nocodazole (200 $ng \cdot ml^{-1}$) and puromycin (1 $\mu g \cdot ml^{-1}$) were all from Sigma.

Plasmids, cloning and transfections

pSuper-mock, pSuper-Mps1, pcDNA3-LAP-Mps1-WT and -D664A have been described[211]. Point mutations were generated by site-directed mutagenesis. All sequences were verified by automated sequencing. Mps1 was depleted from U2OS cells using shRNA and replaced by RNAi-resistant LAP-Mps1-wildtype, -kinase-dead (D664A), -T676A, or -T686A, by transfection with calcium phosphate (for details on this protein replacement assay see [211]).

Antibodies

pT676-Mps1 antibodies were raised in rabbits using the peptide CMQPDTpTSVVKDS coupled to KLH as antigen (Eurogentec). Phospho-specific polyclonal antibody used in this study was affinity purified using the described peptide after removal of non-phosphospecific antibodies with an unphosphorylated version of the peptide. Anti-Mps1-NT was from Upstate Biotechnology, ACA was from Cotrex Biochem and α-Tubulin was from Sigma. Anti-GFP was a custom polyclonal antibody.

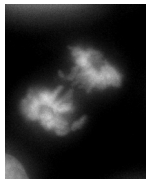

Identification of mitotic phosphorylation sites

Cells were blocked in mitosis by treatment with nocodazole for 18 hrs and harvested by mitotic shake-off. LAP-Mps1 was isolated by tandem affinity purification[185] and phosphorylated residues were identified using mass spectrometry as described[167].

In vitro recombinant kinase assay

Wild-type GST-Mps1 was expressed and purified from High-Five insect cells using the Life Technologies Bac-to-Bac system. Recombinant active Mps1 was incubated in kinase buffer (50 mM Tris pH 7.4, 10 mM $MgCl_2$, 0.5 mM DTT, 40 μM ATP) at 30°C for 30 minutes. (Auto-) phosphorylated residues were identified using mass-spectrometry as described[211].

IP kinase assay

U2OS cells transfected with the various LAP-Mps1 alleles were released from a 24 hours thymidine block into nocodazole for 18 hours, harvested and lysed in 150 mM NaCl, 50 mM Hepes pH7.5, 5 mM EDTA and 0.1% NP40. LAP-Mps1 was removed from the lysates with S-protein agarose (Novagen) and tested for kinase activity towards recombinant kinase-dead His-

Mps1 (D664A) in kinase buffer (50 mM Tris pH 7.5, 10 mM $MgCl_2$, 0.5 mM DTT, 40 μM ATP) using [γ–^{32}P]-ATP.

Flow cytometry and colony outgrowth
U2OS cells were released from a 24 hours thymidine block into nocodazole for 18 hours, harvested and fixed in 70% ice-cold ethanol for 24 hours. Fixed cells were immunostained with anti-Mpm2 (Upstate Biotechnology) to determine the fraction of mitotic cells. Flow cytometric analysis of transfected cells was done based on Spectrin-GFP co-transfection. Colony outgrowth assays were done essentially as described[203].

Immunofluorescence
Immunostaining experiments were done as described[211]. For alignment analysis, U2OS cells plated on 15 mm coverslips were treated and fixed with 4% Shandar Zinc Formal-Fixx™ (Thermo electron corporation) for 20 minutes. Fixed cells were stained with DAPI and the percentage of cells with all chromosomes aligned to the metaphase plate was determined using fluorescence microscopy[211].

Timelapse video microscopy
Mps1 was depleted from U2OS cells using shRNA and replaced with RNAi-insensitive LAP-Mps1-WT or -T676A, and mitotic progression was followed with live cell imaging as described[211]. DNA was visualized by co-transfecting H2B-EYFP.

Acknowledgments

The authors thank Iain Cheeseman for help with LAP-tag purifications, Niels van den Broek for help with identification of *in vitro* phosphorylation sites and the Kops and Medema labs for insights and discussions.

Supporting Information

Supplementary Figure

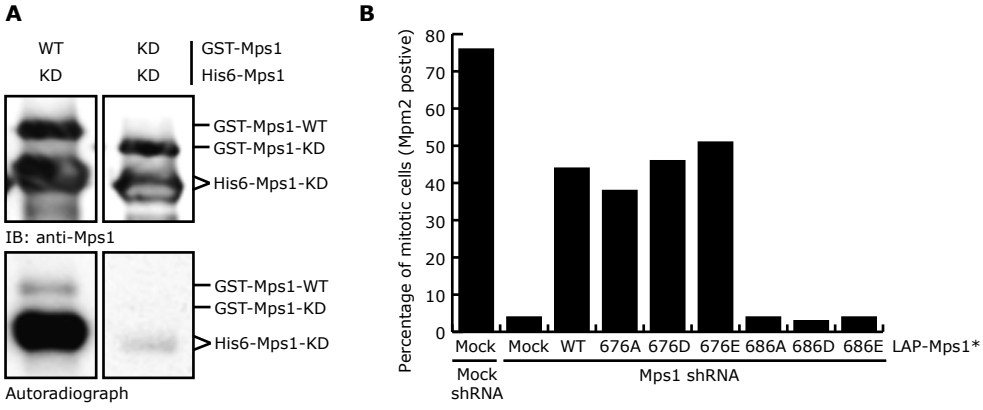

Figure S1
(A) Wild-type GST-Mps1 (WT) cross-phosphorylates kinase-dead His-Mps1 (KD) *in vitro* as measured by 32P incorporation from [γ-^{32}P]-ATP. (B) U2OS cells were transfected with the indicated constructs (asterisk (*) indicates mutations that confer resistance to Mps1 shRNA). Cells were treated as in (2B) and the percentage of mitotic cells was determined as in (2B).

Supplementary Movies

Movie S1
Mps1 was depleted from U2OS cells using shRNA and replaced with RNAi-insensitive LAP-Mps1-T676A, and mitotic progression was followed with live cell imaging as described[211]. DNA was visualized by co-transfecting H2BEYFP. Movie can be found at: doi:10.1371/journal.pone.0002415.s002[210].

Movie S2
Mps1 was depleted from U2OS cells using shRNA and replaced with RNAi-insensitive LAP-Mps1-T676A, and mitotic progression was followed with live cell imaging as described[211]. DNA was visualized by co-transfecting H2BEYFP. Movie can be found at: doi:10.1371/journal.pone.0002415.s003[210].

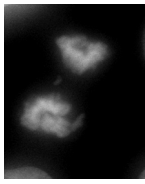

Chapter 6

Release of Mps1 from kinetochores by auto-regulation is crucial for timely anaphase onset

Nannette Jelluma[1], Tobias B. Dansen[1], Tale Sliedrecht[1], Nicholas P. Kwiatkowski[2], and Geert J.P.L. Kops[1]

[1]Department of Physiological Chemistry and Cancer Genomics Centre UMC, Utrecht, Universiteitsweg 100, 3584 CG, Utrecht, The Netherlands; [2]Department of Cancer Biology, Dana Farber Cancer Institute, Department of Biological Chemistry and Molecular Pharmacology, Harvard Medical School, 250 Longwood Avenue, Boston, Massachusetts 02115

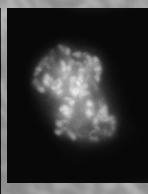

Submitted for publication

Abstract

Mps1 kinase activity is required for proper chromosome segregation during mitosis through its involvements in the microtubule-chromosome attachment error-correction process and the mitotic checkpoint. Mps1 auto-activates by phosphorylation of its activation loop and dynamically exchanges on unattached kinetochores during mitosis. Here we show that Mps1 activity promotes its own dissociation from kinetochores. When Mps1 was inhibited, its turnover rate at unattached kinetochores was reduced and elevated Mps1 protein levels could be detected at these sites. Strikingly, preventing the dissociation of active Mps1 from kinetochores delayed anaphase onset despite normal chromosome attachment and biorientation. This delay was due to continued recruitment of Mad2 to bioriented chromosomes, indicating chronic engagement of the mitotic checkpoint. We propose that Mps1 activity continuously directs its own release from kinetochores to allow satisfaction of the mitotic checkpoint and a fast metaphase-to-anaphase transition.

Introduction

To prevent chromosome missegregations, the onset of anaphase is inhibited by coordinated actions of the error-correction and mitotic checkpoint machineries until all chromosomes have stably bioriented. The mitotic checkpoint directs formation of the mitotic checkpoint complex (MCC), which is catalyzed on unattached kinetochores and inhibits the Anaphase Promoting Complex/Cyclosome (APC/C) (reviewed in [205]). As soon as all kinetochores have attached to microtubules in a stable fashion, the mitotic checkpoint is satisfied and inhibition of APC/C is released, ultimately causing anaphase initiation and mitotic exit (reviewed in [205]).

The Mps1 kinase is an important player in prevention of chromosomal instability[208,211 (Chapter 2 of this thesis)], as its activity is crucial both for achieving biorientation and for mitotic checkpoint function. In human cells, Mps1 stimulates Aurora B activity by phosphorylating the Chromosomal Passenger Complex (CPC) member Borealin. Mps1-dependent regulation of Aurora B activity is required for error-correction and subsequent biorientation of chromosomes [211,271 (Chapter 2 of this thesis)]. In addition, loss of Mps1 activity abrogates the mitotic checkpoint in many model systems[106,124-126,130-132,211,272 (Chapter 2 of this thesis)], resulting in gross missegregations and eventually cell death[210 (Chapter 5 of this thesis)]. Although the direct targets of Mps1 in the mitotic checkpoint are yet to be discovered, Mps1 depletion has been shown to prevent the recruitment of Mad1 and Mad2 heterodimers to unattached kinetochores, thereby disabling mitotic checkpoint signaling[106,107,211 (Chapter 2 of this thesis)].

Whereas it is clear that Mps1 kinase activity is important for chromosome biorientation and checkpoint function, it is unclear how Mps1 itself is regulated. Activity levels rise during mitosis and Mps1 can auto-activate by cross-phosphorylation of its activation loop. This auto-activation could be induced in interphase by artificial dimerization of Mps1 or by overexpression of wild-type Mps1[210,222,264 (Chapter 5 of this thesis)], prompting the hypothesis that concentration of Mps1 on kinetochores is sufficient to drive auto-activation. What the precise underlying mechanism is, however, remains elusive. Although not investigated for error-correction, Mps1 needs to be at kinetochores to perform its functions in the mitotic checkpoint. Truncation of the first 300 amino acids causes Mps1 mislocalization and mitotic checkpoint defects[106]. GFP-Mps1 only transiently associates with kinetochores in PtK2 cells, with a half-life of 9 seconds[85]. It is, however, unknown why Mps1 presence at the site of attachment is so dynamic. Here, we sought to investigate the regulation of Mps1 activity in space and time. We found that Mps1 is recruited to unattached and tension-less kinetochores in prometaphase and continuously directs its release by its own activity. This dynamic behavior was found to be crucial for inhibiting the checkpoint signal from kinetochores and a fast metaphase-to-anaphase transition upon satisfaction of the mitotic checkpoint.

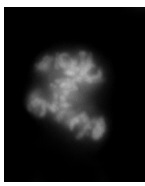

Results & Discussion

Mps1 dynamically exchanges on kinetochores during mitosis in PtK2 cells showing monophasic recovery of 99% with a half-life of 9 seconds[85]. Using LAP-tagged wild-type Mps1, we were unable to detect GFP signal on kinetochores of mitotic human cells with live cell imaging. However, the kinetochore-localized GFP signal of a kinase-dead (KD) mutant of LAP-Mps1 was readily detected, and this signal diminished upon anaphase initiation (Figure 1A).

To further investigate the role of Mps1 kinase activity in recruitment and release of Mps1 at kinetochores, Mps1 kinetochore levels were examined by immunofluorescence after chemical inhibition of Mps1 in HeLa cells with the specific inhibitor Mps1-IN-1[239 (Chapter 3 of this thesis)]. In the absence of Mps1-IN-1, endogenous Mps1 was hardly detectable at kinetochores, but when inhibited, a clear signal was seen on kinetochores, representing a 4-fold increase. Mad2 levels were markedly reduced on kinetochores upon Mps1-IN-1 treatment, indicating that Mps1 inhibition was efficient[239 (Chapter 3 of this thesis)] (Figure 1B).

When endogenous Mps1 was replaced by LAP-tagged versions of Mps1, the level of LAP-Mps1-KD on unattached kinetochores was higher than that of LAP-Mps1-wild-type (WT) (Figure 1C). Western blot analysis of total lysate showed that the elevated kinetochores signal intensity of LAP-Mps1-KD was not simply due to higher expression levels (Figure 1C).

To exclude the possibility that differences in epitope recognition by Mps1 antibody could underlie the differences in kinetochore signal intensities between kinase-active versus kinase-inactive Mps1, localization of LAP-tagged Mps1 in a stable cell line in which endogenous Mps1 was replaced by LAP-Mps1-WT (UTRM10-WT[210 (Chapter 5 of this thesis)]) was examined using an antibody directed to the epitope tag. In agreement with our previous experiments, LAP-Mps1 levels were higher on prometaphase kinetochores when cells were treated with Mps1-IN-I (Figure 1D). Together, these results show that the levels of Mps1 at kinetochores in prometaphase increase when Mps1 kinase activity is impaired.

Since short-term inhibition of Mps1 had no overt effects on its total cellular protein levels (Figure 1D), higher concentration on kinetochores of inactivated Mps1 can be explained by 1) lower exchange rate or loss of exchange of inactivated Mps1 on kinetochores, and/or 2) presence of more available binding sites for Mps1 when it is inactivated. Therefore, the exchange rates of Mps1 before and after inhibition were studied using FRAP (Fluorescence Recovery After Photobleaching). For this, a stable U2OS cell line was used in which endogenous Mps1 is replaced with a LAP-tagged gatekeeper mutant[182] that can specifically be inhibited with the bulky PP1 analog 23-dMB-PP1 (UTRM-LAP-Mps1^{M602G}), leading to abrogation of mitotic checkpoint function (Supplementary Figure S1A). This cell line expresses higher levels of Mps1 than our wild-type LAP-Mps1-expressing cell line, which made it possible to detect kinetochore signals of the uninhibited protein during live-imaging (Figures 2A, S1B). Inhibition of Mps1 by addition of 23-dMB-PP1 to these cells resulted in higher Mps1 levels on kinetochores during live imaging (Figure 2A) and in fixed cells (Supplementary Figure S1B). After photobleaching, Mps1 in untreated cells recovered to 99% with a half-life of less than 1 second. This high speed of recovery prevented us from obtaining a more precise estimate of Mps1 half-life at kinetochores in these cells. Both exchange and recovery of Mps1 were reduced after addition of 23dMB-PP1 (Figure 2A). This suggested a slower exchange rate and possibly an increase in a stable, non-exchanging pool on kinetochores when Mps1 is inhibited, which could explain the higher protein levels detected by immunofluorescence. However, differences in recovery were small and it cannot be excluded that additional factors contributed to the detection of higher levels of

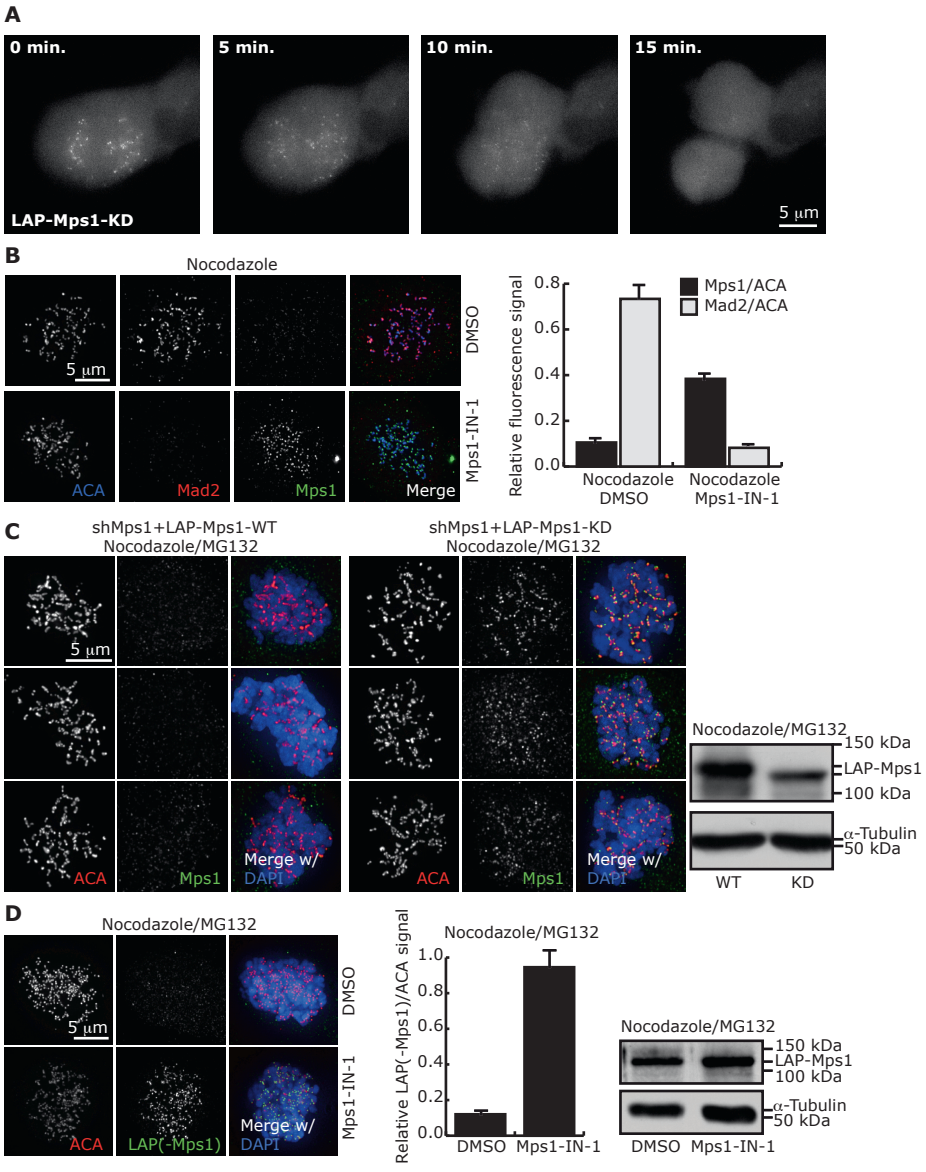

Figure 1. Mps1 accumulates on kinetochores when inhibited.
(A) Stills of timelapse movie showing a U2OS cell transfected with LAP-Mps1-KD. (B) Immuno fluorescence showing endogenous Mps1 and Mad2 localization at kinetochores in HeLa cells treated as indicated. Graph represents quantitation of fluorescence intensities; error bars represent standard error of the mean (per condition n=5 cells, fluorescence intensities of 22 separate kinetochores per cell were determined). (C) Mps1 localization at kinetochores of U2OS cell co-transfected with LAP-Mps1-WT or LAP-Mps1-KD treated with nocodazole and MG132. Western blot shows total expression levels of LAP-Mps1-WT and -KD in U2OS cells. (D) LAP-Mps1-WT localization at kinetochores of UTRM10-WT cells treated as indicated, detected by immunofluorescence using anti-GFP antibody to detect the LAP-tag. Graph represents quantitation of fluorescence intensities; error bars represent standard error of the mean (per condition n=5 cells, fluorescence intensities of 22 separate kinetochores per cell were determined). Western blot shows total expression levels of uninhibited and inhibited LAP-Mps1-WT. Note that UTRM10-WT cells express near-endogenous levels of LAP-Mps1-WT[210] (Chapter 5 of this thesis), and levels are not changed upon inhibition, as judged by the levels of the loading control α-Tubulin.

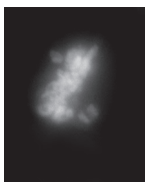

kinetochore-associated Mps1 upon its inhibition.

Because Mps1 can modify itself in *trans* and in *cis* by auto-phosphorylation[210,222,264] (Chapter 5 of this thesis) and likely phosphorylates other kinetochore-localized proteins, we next addressed which of these caused Mps1 auto-release from kinetochores. Strikingly, compared to control RNAi, LAP-Mps1-KD levels at kinetochores were increased 2-fold upon depletion of endogenous Mps1 by RNAi (Figure 2B). This increase could be reduced by co-expression of LAP-Mps1-WT, while subsequent addition of the Mps1 inhibitor Mps1-IN-1 prevented this reduction (Figure 2C). These results indicate that LAP-Mps1-KD can be displaced from kinetochores by the action of endogenous or exogenous active Mps1. Hence, either modification of other mitotic proteins by Mps1 or Mps1 in *trans* auto-phosphorylation, but not in *cis* auto-phosphorylation, caused release of Mps1 from kinetochores.

One of the few known substrates of Mps1 in human cells is Borealin, a member of the CPC that directs Aurora B localization and activity. Since Mps1 promotes Aurora B activation by phosphorylation of Borealin[211,271] (Chapter 2 of this thesis), we asked whether reduction of Aurora B activity by Mps1 inhibition underlies accumulation of Mps1 on kinetochores. Analysis of Mps1 localization in cells treated with the Aurora B inhibitor ZM447439[168] showed that while full inhibition of Aurora B was achieved (Supplementary Figure S1C), Mps1 concentration on kinetochores was not increased (Figure 2D). Therefore, the effect of Mps1 activity on its own turnover at kinetochores is unlikely to be mediated via phosphorylation of Borealin.

Interestingly, a similar influence of Mps1 activity on its localization was observed when Mps1 was artificially targeted to peroxisomes by mutation of the last three C-terminal amino acids to the peroxisomal targeting sequence SKL (PTS1[273]). Mps1-PTS1 was only localized to peroxisomes in interphase cells when inhibited or expressed in kinase-dead form (Supplementary Figure S1D). When Mps1-KD was co-expressed with Mps1-WT, however, no Mps1 was found located in peroxisomes (Supplementary Figure S1D). Thus, when artificially targeted to a different location in a different phase of the cell cycle, Mps1 activity can also regulate its own localization. Although the mechanism of auto-regulation might be different from what happens on kinetochores, given that the kinetochore targeting sequence and the artificial PTS1 reside in opposite protein termini, these data suggest that direct *in-trans* auto-phosphorylation can cause decreased localization of Mps1 in peroxisomes. Structural rearrangement of Mps1 by in *trans* auto-phosphorylation could therefore potentially also account for delocalization from kinetochores.

Our data seemingly contradict a previous study showing that in *trans* phosphorylation of two sites in the N-terminus of Mps1 (T12 and S15) are needed for localization of Mps1 to kinetochores[214]. Although we currently have no explanation for this, it is possible that T12 and S15 are phosphorylated by other kinases or that mutation of these sites disturbs protein function independent of phosphorylation.

The data thus far support the hypothesis that Mps1 is efficiently recruited to kinetochores and rapidly released by its own activity through a mechanism that involves phosphorylation of (an) unknown target sites(s). Although recruitment of Mps1 to kinetochores has been shown to be essential for the mitotic checkpoint[106], it is unclear if release of Mps1 is functionally relevant. To address this, LAP-Mps1 was prevented from leaving the kinetochore by fusion to the Mis12 protein. Mis12 is a constitutive kinetochore protein[22,274] and fusion to INCENP was previously shown to efficiently recruit INCENP/Aurora B to metaphase kinetochores[59]. LAP-tagged Mis12-Mps1 (LAP-Mis12-Mps1-WT) was readily visible on kinetochores in prophase, prometaphase and metaphase (Figure 3A). Mis12-Mps1 fully supported mitotic checkpoint activity in Mps1-depleted, nocodazole-treated cells, showing the fusion did not prevent Mps1 functioning (Figure

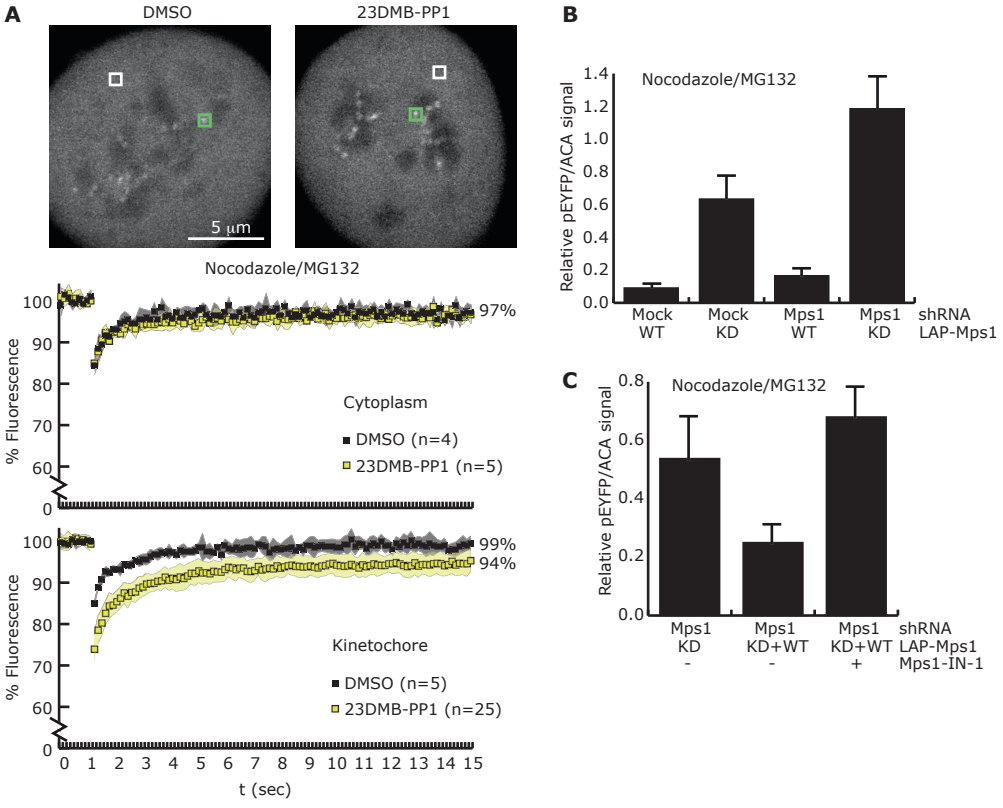

Figure 2. Mps1 activity increases its turnover at kinetochores by in trans phosphorylation.
(A) UTRM-LAP-Mps1^{M602G} cells were treated as indicated, and 0.81 μm^2 square areas around single kinetochores (green squares in upper panel) or in the cytoplasm (white squares in upper panel) were bleached at t=1. Images were acquired subsequently every 125 milliseconds to follow fluorescence recovery. Graphs show average fluorescence intensities, shaded areas indicate standard deviations, and percentages indicate average recovery between 10 and 12 seconds. (B) Quantitation of fluorescence intensities at kinetochores of U2OS cells transfected and treated as indicated; error bars represent standard error of the mean (per condition n=8 cells, fluorescence intensities of 22 separate kinetochores per cell were determined). (C) Quantitation of fluorescence intensities at kinetochores of U2OS cells transfected and treated as indicated; error bars represent standard error of the mean (per condition n=8 cells, fluorescence intensities of 22 separate kinetochores per cell were determined). (D) LAP-Mps1-WT localization at kinetochores of UTRM10-WT cells treated as indicated.

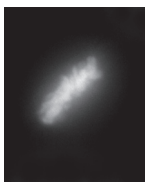

3B). As expected, a kinase-dead mutant of the Mis12-Mps1 fusion (LAP-Mis12-Mps1-KD) did not rescue checkpoint function (Figure 3B). Strikingly, overexpression of LAP-Mis12-Mps1-WT but not LAP-Mis12-Mps1-KD or LAP-Mps1-WT in U2OS cells caused pronounced extension of metaphase in more than 50% of cells, even up to 10 hours in some cases (Figures 3C, D and 4A). These prolonged metaphases were prevented when LAP-Mis12-Mps1-WT-expressing cells were treated with Mps1-IN-1 (Figure 4A). Therefore, the metaphase extensions were due to sustained Mps1 activity on kinetochores.

The mitotic checkpoint inhibits APC/C activity through formation of the mitotic checkpoint complex (MCC). This is dependent on the recruitment of the checkpoint protein Mad2 to kinetochores, which is controlled by Mps1 activity[208,211,239 (Chapter 2 and 3 of this thesis)]. To investigate whether LAP-Mis12-Mps1-WT-induced metaphase arrest depended on persistent Mad2 recruitment, LAP-Mis12-Mps1-WT was co-transfected with Mad2 shRNA to deplete Mad2. Removal of Mad2 effectively prevented metaphase delays in cells expressing Mis12-Mps1 (Figure 4A). Indeed, Mad2 was localized to kinetochores of bioriented chromosomes in metaphase cells expressing LAP-Mis12-Mps1-WT, but not LAP-Mps1-WT (Figure 4B). This localization was effectively lost when Mps1 activity was inhibited for a short time with Mps1-IN-1 (Supplementary Figure S1E). These results support the hypothesis that sustained activity of Mps1 on kinetochores prevents satisfaction of the mitotic checkpoint and argues that Mps1 removal is a prerequisite for mitotic checkpoint silencing.

Since Mps1 activates Aurora B through Borealin phosphorylation[211,271 (Chapter 2 of this thesis)], continued mitotic checkpoint signaling could have been due to unstable attachments created by sustained Aurora B activity. If so, stabilization of these attachments by inhibition of Aurora B activity is predicted to revert this. Importantly, however, treatment of Mis12-Mps1-expressing cells with the Aurora B inhibitor ZM447439 did not prevent the mitotic delay (Figure 4A). In agreement with this, no errors in chromosome alignment or segregation were observed in the cells expressing the Mis12-Mps1 fusion protein (Figure 4A). These data also show that proper biorientation and k-fiber stabilization did not require removal of Mps1 from kinetochores. The results strongly suggest that preventing Mps1 from leaving kinetochores causes mitotic delays by persistent engagement of the mitotic checkpoint directly, independent of the attachment status of kinetochores.

Our results indicate that under normal circumstances Mps1 needs to be removed from metaphase kinetochores when the cell is ready to undergo anaphase. Treatment of asynchronous cells with Mps1-IN-1 allowed visualization of Mps1 on kinetochores and simultaneously created cells with both misaligned and aligned chromosomes that are nevertheless attached[211 (Chapter 2 of this thesis)]. Under this condition, Mps1 was clearly visible on misaligned kinetochores, but not on kinetochores that were bioriented (Figure 4C). Since Mps1, even when inhibited, could not be detected on these kinetochores, it is likely that recruitment of Mps1 to kinetochores is strongly reduced as soon as chromosomes have bioriented. We therefore propose that in prometaphase, Mps1 is only recruited to unattached and/or tension-less kinetochores where it promotes error-correction by Aurora B activation and mitotic checkpoint activation by Mad1/Mad2 recruitment. Almost simultaneously, Mps1 is released from kinetochores by its own activity, but is recruited again and again as long as biorientation is not achieved. In this way, Mps1 activity is very efficiently lost from bioriented kinetochores, allowing local checkpoint silencing and a fast metaphase-to-anaphase transition.

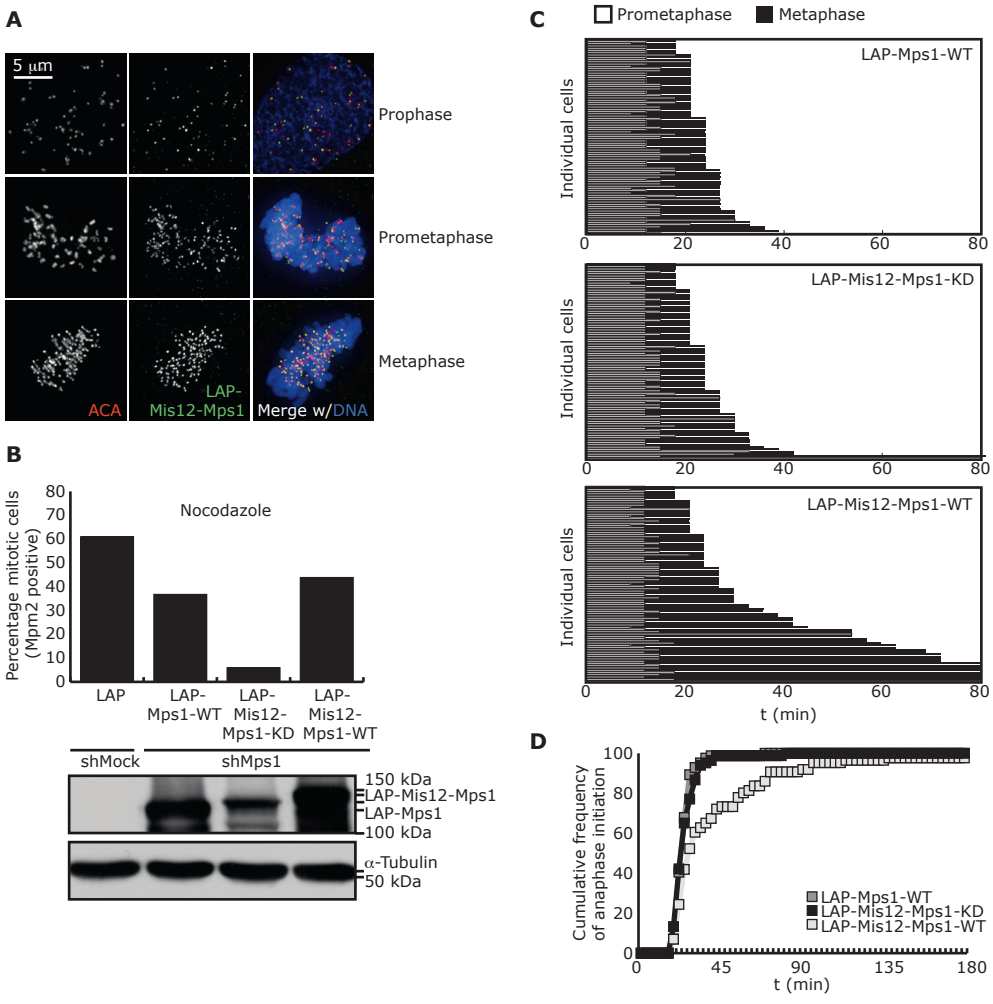

Figure 3. Sustained Mps1 activity on kinetochores after biorientation extends metaphase.
(A) Localization of transiently transfected LAP-Mis12-Mps1(-WT) in U2OS during indicated phases of cell cycle. (B) Graph shows percentage of mitotic (Mpm2 positive) U2OS cells that were transfected and treated as indicated, as determined by flow cytometry. Western blot shows relative expression levels in total lysate of cells treated as in (A). (C) Bar graphs showing time spent in prophase and metaphase of transiently transfected U2OS cells with indicated plasmids. Each horizontal bar represents a single cell. (D) Graphs represent cumulative frequency of anaphase initiation versus time of cells shown in (C). Nuclear envelope breakdown is set to t=0.

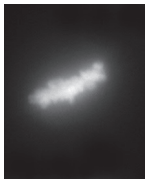

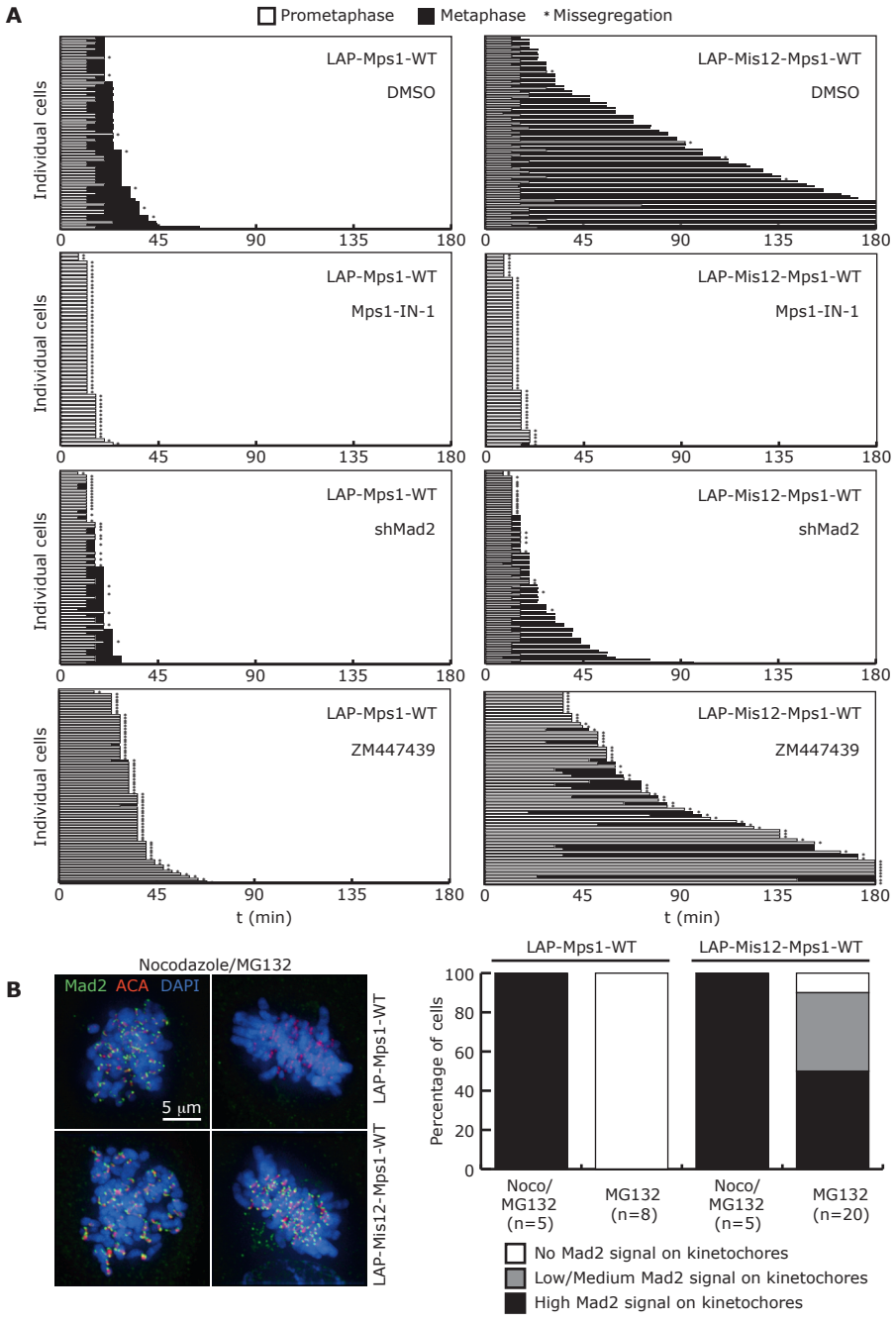
A
Prometaphase
Metaphase
* Missegregation
Individual cells
LAP-Mps1-WT
DMSO
LAP-Mis12-Mps1-WT
DMSO
Mps1-IN-1
shMad2
ZM447439
0
45
90
135
180
t (min)
B
Nocodazole/MG132
Mad2 ACA DAPI
5 μm
LAP-Mps1-WT
LAP-Mis12-Mps1-WT
Percentage of cells
100
80
60
40
20
0
Noco/ MG132 (n=5)
MG132 (n=8)
Noco/ MG132 (n=5)
MG132 (n=20)
No Mad2 signal on kinetochores
Low/Medium Mad2 signal on kinetochores
High Mad2 signal on kinetochores
C
5 μm
ACA
Mps1
Merge
Mps1-IN-1/MG132

Materials & Methods

Cell culture, plasmids and transfections

U2OS and HeLa cells were grown in DMEM with 8% FBS, supplemented with pen/strep. UTRM10-WT cells[210] and UTRM-LAP-Mps1^{M602G} cells created as described in [210] were grown in DMEM with 8% FBS, supplemented with pen/strep, and 1 $\mu g \cdot ml^{-1}$ doxycycline (Sigma) for continuous knockdown of the endogenous protein[210].

pSuper-Mock, pSuper-Mps1, pcDNA-LAP-Mps1 and pSuper-Mad2 have been described[95,211]. pcDNA-LAP-Mps1-M602G was created by site-directed mutagenesis of pcDNA-LAP-Mps1. Endogenous Mps1 replacement assays were done as in [211]. To add a PTS1 signal to Mps1, point mutations in pCDNA3-LAP-Mps1 construct were introduced by site-directed mutagenesis to alter the last three C-terminal amino-acids to Serine-Lysine-Leucine or to Alanine-Lysine-Leucine[273]. pcDNA-LAP-Mis12-Mps1 constructs were created by inserting the full Mis12 sequence in pcDNA-LAP-Mps1. All sequences were verified by automated sequencing. Plasmid transfections in U2OS cells were done with Calcium Phosphate.

Timelapse live cell imaging

U2OS cells were grown in 8-well chambered glass-bottom slides (LabTek), and co-transfected with the indicated plasmids and H2B-pEYFP for visualization of DNA. Cells were blocked in S-phase with thymidine (2.5 mM, Sigma) 24 hours after transfection for 24 hours. After release from thymidine, mitotic progression was followed with live cell imaging for Figure 1A as described[211] and for Figures 3C, 3D, 4A on an Olympus IX-81 microscope, controlled by Cell-M software (Olympus), in a heated chamber (37°C and 5% CO2) using a 20X/0.5NA UPLFLN objective. Every 3 minutes yellow fluorescent images were acquired (15 msec exposure) with a Hamamatsu ORCA-ER camera. Images were processed for analysis to maximum intensity projections of all Z-planes and using Cell-M software.

Immunoblotting and immunofluorescence

Immunoblotting was performed according to standard procedures, antibodies used were anti-Mps1-NT (Upstate Biotechnology) and anti-α-Tubulin (Sigma).

For immunofluorescence analysis, cells were treated 45 minutes before fixation with the indicated compounds (Nocodazole (200 $ng \cdot ml^{-1}$, Sigma), MG132 (10 μM, Sigma), ZM447439 (2 μM, Tocris Bioscience), 23dMB-PP1 (1 μM, gift from K. Shokat), Mps1-IN-1 (10 μM, gift from N. Gray). Fixation and immunostaining were done as described in [211]. Antibodies used were anti-Mps1-NT (Upstate Biotechnology), anti-GFP (custom rabbit serum), anti-phospho-(T232)-Aurora B (Rockland), anti-Mad2 (custom rabbit serum). Images were acquired on a DeltaVision RT system (Applied Precision) with a100X/1.40NA UPlanSApo objective (Olympus) using SoftWorx software. Images are maximum projections of a deconvolved stack and adjusted (identically within experiments) with SoftWorx and Adobe Photoshop CS3. Quantitations were done as described[211].

Figure 4. Chronic engagement of the mitotic checkpoint by persistent presence of Mps1 on bioriented chromosomes.
(A) Bar graphs showing time spent in prophase and metaphase of transiently transfected U2OS cells with indicated plasmids and treated as indicated. Each horizontal bar represents a single cell. (B) Mad2 localization at kinetochores of U2OS cells transiently transfected with LAP-Mps1-WT or LAP-Mis12-Mps1-WT, treated as indicated. Graph shows distribution of cells with high, low/medium or no Mad2 signal on kinetochores. (C) Mps1 localization on bioriented and mono-oriented kinetochores in a HeLa cell treated as indicated.

Fluorescence Recovery After Photobleaching (FRAP)
UTRM-LAP-Mps1^{M602G} cells were grown in glass bottom dishes (Willco-wells), released from a 24 hours thymidine block in nocodazole for 16 hours. The media was replaced with Leibovitz L-15 media (Gibco) supplemented with 10% FCS, 2 mM Glutamine and 100 U·ml^{-1} Pen/strep and cells were transferred to an incubator with atmospheric CO_2 at 37°C. Cells were treated with MG132 (10 μM, Sigma) +/- 1 μM 23dMB-PP1 30 minutes prior to imaging. Samples were imaged on a Zeiss LSM 510 META equipped with a heated chamber and lens warmer (both set at 37°C), using Zeiss LSM software. The EYFP based LAP-tag of LAP-MPS1 was both excited and bleached using the 514 nm laser line of an Argon laser (max 30 mW) set to 60% (Tube current 5.5 A). Excitation was done using 6% laserpower and emission was detected on the META detector set from 529 to 614 nm. Areas of 25x25 pixels (0.81 μm^2) were bleached at 100% laser power for 10 iterations once the fluorescence signal of LAP-Mps1 had become stable for a few seconds (after ~6 seconds). Fluorescence intensity in the bleached square was acquired every 125 ms before and after bleaching. For each measurement, the average fluorescence intensity in the 25x25 pixel square during the last second before bleaching was set to 100% and the measured signal after bleaching was normalized to this value. Since kinetochores are highly mobile, only those measurements were taken into account in which the kinetochore remained visible within the 25x25 pixel square during the entire measurement.

Flow cytometry analysis:
Cells were released from a 24 hr thymidine-induced block into nocodazole for 16 hours and analyzed by flow cytometry as described[167]. Flow cytometric analysis of transfected cells was based on Spectrin-GFP expression.

Acknowledgments

We would like to thank Jagesh Shah and Yinghua Guan for efforts on Mps1 FRAP, Chao Zhang and Kevan Shokat for providing 23dMB-PP1, Nathanael Gray for providing Mps1-IN-1, Susanne Lens for providing Mis12-INCENP plasmid, the Kops, Medema and Lens labs for discussions and insights, and Adrian Saurin and René Medema for critically reading the manuscript. This work was supported by a grant to GJPLK from the Netherlands Organization for Scientific Research (NWO-VIDI 91776336).

Figure S1
(A) Graph shows percentage of mitotic (Mpm2 positive) UTRM-LAP-Mps1^{M602G} cells treated as indicated, as determined by flow cytometry. Error bars indicate standard deviation (n=3 (602G) and n=2 (WT) individual experiments). (B) Mps1 localization in UTRM-LAP-Mps1^{M602G} cells treated as indicated. Graph shows quantitation of fluorescence intensities at kinetochores; error bars represent standard error of the mean (per condition n=8 cells, fluorescence intensities of 22 separate kinetochores per cell were determined). (C) Phospho-Aurora B intensity levels in UTRM10-WT cells treated as indicated. (D) Live fluorescence images of U2OS cells transfected with the indicated constructs and treated as indicated. Peroxisomal localization is identifiable by the punctate pattern of fluorescence in the cytosol[273] (E) Mad2 localization at kinetochores of U2OS cells transiently transfected with LAP-Mps1-WT or LAP-Mis12-Mps1-WT, treated as indicated. Graph shows distribution of cells with high, low/medium or no Mad2 signal on kinetochores.

Supplementary Material

Supplementary Figure

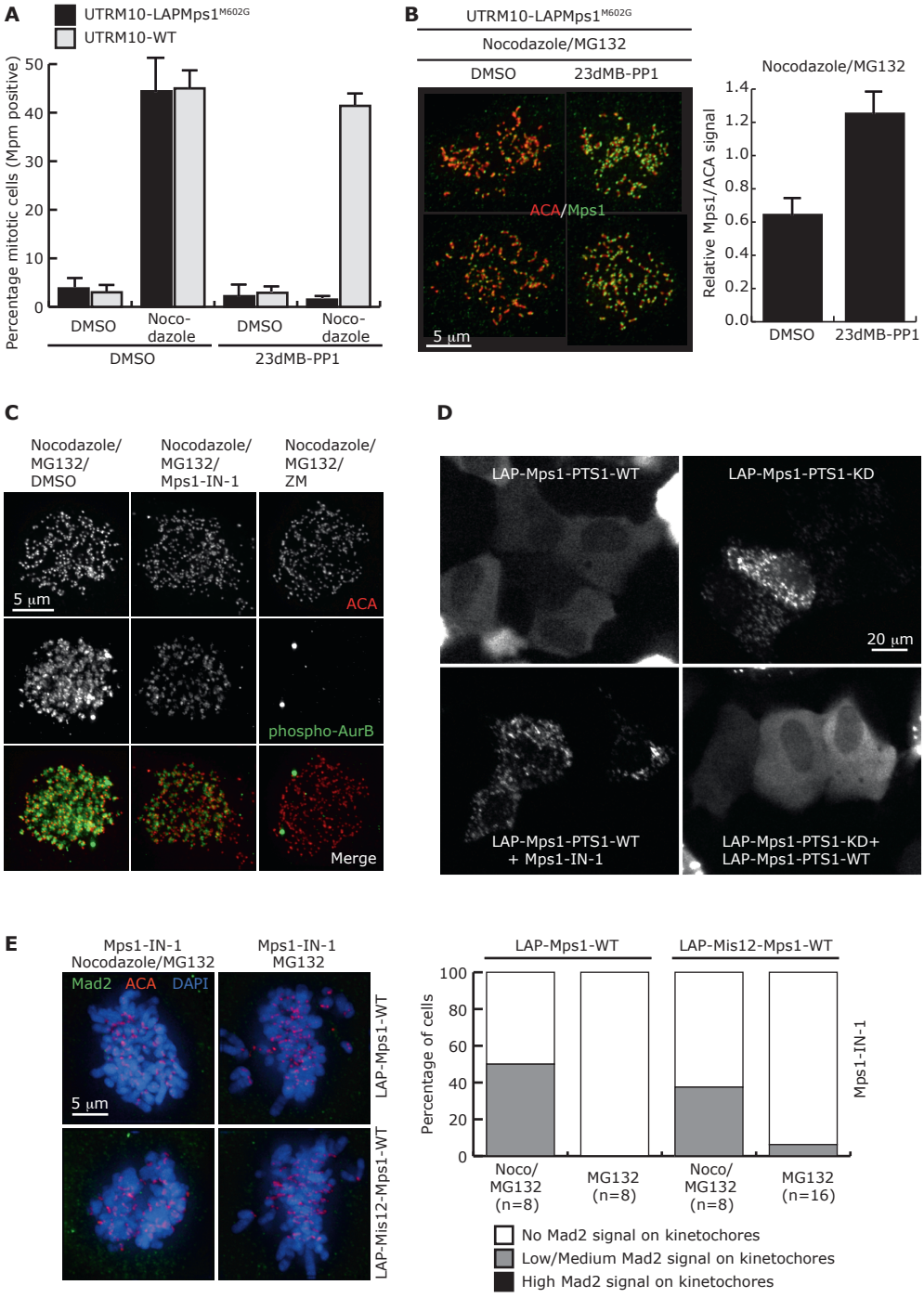

Chapter 7

Summary & Discussion

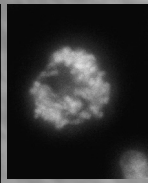

Summary

Mps1 was known to be a critical component of mitotic checkpoint signaling, but at the onset of the studies described in this thesis, not much was known about the upstream regulation and the downstream signaling of this protein kinase. We found that Mps1 activity not only is indispensable for checkpoint signaling, but also coordinates attachment-error-correction by enhancing Aurora B activity through Borealin phosphorylation (Chapter 2). Development and characterization of a specific Mps1 inhibitor (Mps1-IN-1) provided new opportunities to study the effects of (short-term) Mps1 inhibition (Chapter 3). When studying Mps1 function in the mitotic checkpoint in particular, we found that Mps1 prevents APC/C mediated disassembly of MCC to maintain a mitotic arrest (Chapter 4). Regarding the regulation of Mps1 activity during mitosis, we identified an auto-phosphorylation event on Mps1 that is required for full kinase activity, checkpoint function and prevention of chromosomal instability (Chapter 5). In addition, we show that Mps1 continuously directs its own release from kinetochores, allowing satisfaction of the mitotic checkpoint and a fast metaphase-to-anaphase transition (Chapter 6).

Discussion

How can phosphorylation of Borealin by Mps1 contribute to Aurora B activity?
Although it is evident from our results that Mps1 enhances Aurora B activity through phosphorylation of Borealin (Chapter 2), the mechanism by which Borealin phosphorylation contributes to Aurora B activity is unknown. Within the CPC, Aurora B associates with INCENP, Survivin and Borealin, and complex formation is essential for protein stability[42]. Survivin and Borealin mediate centromere localization of the complex[43-45], and Aurora B is activated through INCENP phosphorylation and auto-phosphorylation in the activation loop of the kinase domain[49]. Mitotic Borealin phosphorylation was previously observed but, although Aurora B was excluded, the sites and an upstream kinase were not identified[275].

Recently, a dimerization motif in Borealin was found by E. Bourhis *et al*., and dimerization of Borealin was modulated when Threonine 230 (T230) was mutated[271]. T230 is one of the four residues that we identified as Mps1 phosphorylation sites that mediate Aurora B activation (Chapter 2). E. Bourhis *et al*. extend our findings and show that phosphorylation on T230 is essential for maximal Aurora B activity in cells and for chromosome alignment[271]. Based on these data, the authors suggest that phosphorylation of Borealin by Mps1 *in vivo* might keep more Aurora B in close proximity to its substrates when there is low tension on the kinetochores[271]. Alternatively, given the observation that local clustering of CPC enhances Aurora B activity[47], Borealin phosphorylation by Mps1 might promote this. However, it is unclear whether Borealin dimerization is regulated in cells and how T230 phosphorylation affects this, as both non-phosphorylatable and phosphomimetic mutations of T230 had the same effect of disturbing the dimer *in vitro*. Since Borealin fragments carrying T230D did not increase Aurora B activity *in vitro*, more studies on the effect of Borealin phosphorylation by Mps1 on *in vitro* CPC structure as a whole and during the biorientation process in the cell are needed to get a better understanding hereof.

Mps1 and Aurora B: Linear pathway or positive feedback loop?
We showed that Aurora B activation depends on Mps activity, and Mps1 localization does not depend on Aurora B activity (Chapter 2). This suggests that a linear pathway exists in which Mps1 functions upstream of Aurora B. However, in *Xenopus* extracts Aurora B activity was proposed to control Mps1 localization[193]. Our results and those of others[135] cannot, however, exclude the possibility of a positive feedback mechanism between Mps1 and Aurora B. Subtle changes in Mps1 localization and/or activity by Aurora B may exist but may not have been detected by our methods used. Interestingly, Aurora B was suggested to have a separate function in the checkpoint (besides the indirect effect of creating unattached kinetochores)[181], but that mechanism remains to be elucidated. A positive feedback through modulating Mps1 function could, in theory, partly explain this. Careful analyses using specific inhibitors to Aurora B and Mps1 need to be done to get more clarity on this issue. The new Mps1 inhibitor Mps1-IN-1 presented in Chapter 3 opens new opportunities to perform such analyses.

Coordination between chromosome biorientation and mitotic checkpoint
With the finding that Mps1 activity is not only needed for checkpoint function but also for achieving biorientation (Chapter 2), Mps1 could be added to a small list of kinases that play a role in both processes. For example, the checkpoint kinases Bub1 and BubR1 also have a clear additional function in chromosome alignment, and have been, together with Mps1, proposed to constitute a functional subfamily, referred to as Bi-MC (Biorientation and Mitotic Checkpoint) kinases (reviewed in [276]).

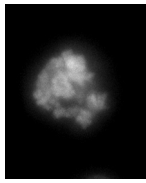

Although generally required for chromosome biorientation, the way these kinases contribute to this differs. BubR1 is required for the establishment of stable attachments of chromosomes to spindle microtubules[30,168] and Bub1 is required for the formation of proper end-on attachments[172]. Mps1 on the other hand is required for correction of erroneous attachments[211] (Chapter 2 of this thesis), but all have the dual function to coordinate chromosome biorientation with mitotic checkpoint signalling. Although it seems logical that these processes which inevitably happen at the same time are controlled by the same proteins, an obvious downside of this is that misregulation of any of such multifunctional mitotic kinases is expected to cause massive chromosome missegregations: The improper attachments would not inhibit anaphase onset as they would go unnoticed due to absence of a checkpoint, when in fact defects in attachment processes may be expected to demand a robust checkpoint response in order to maintain chromosomal stability. On the other hand, massive missegregations due to mitotic checkpoint inhibition cause lethality very efficiently by activating apoptotic pathways[95]. When faced with diminished activity of a Bi-MC kinase, cells may therefore allow severe missegregations in order to induce apoptosis, and thus prevent chromosomal instability. This could then make the dual function of these kinases an extra protection against tumorigenesis in an organism.

Mps1 substrates in mitotic checkpoint signaling

We showed in Chapter 4 that Mps1 prevents APC/C mediated disassembly of MCC to maintain a mitotic arrest. It is unknown which Mps1 substrates mediate this function, but we showed that both the E2 enzyme UbcH10 and the deubiquitinating enzyme USP44 are phosphorylated by Mps1 *in vitro*. Since both these proteins have been reported to impact MCC stability, more studies have to be done to find out whether they may constitute functional targets of Mps1 in the mitotic checkpoint *in vivo*. Interestingly, an *in vivo* mouse model was reported recently in which mice overexpressing UbcH10 show premature Cyclin B degradation and an increase of chromosome missegregations. In addition, the mice developed spontaneous tumors in a variety of tissues, and carcinogen-induced tumor formation was enhanced[277]. If Mps1 phosphorylates UbcH10 *in vivo* to inhibit its function, overexpression of UbcH10 might be able to overcome this inhibition.

Several other potential substrates of Mps1 have been suggested. First, Ndc80 can be phosphorylated by Mps1 *in vitro* and Ndc80 phospho-site mutant strains were checkpoint defective. However, although able to sustain mitotic checkpoint signaling in wild-type yeast cells, an Ndc80 mutant carrying phospho-mimetic mutations in 14 putative Mps1 target sites was unable to restore a mitotic checkpoint response in the absence of Mps1 activity[137]. It is therefore likely that Ndc80 is not the only Mps1 substrate in the yeast checkpoint. Moreover, as it was not investigated whether Ndc80 is phosphorylated on the proposed Mps1 sites in mitotic yeast cells, it remains to be investigated whether Ndc80 plays a role downstream of Mps1 in mitotic checkpoint activity. Second, Mad1 is a substrate for Mps1 in yeast[125], but no specific sites or a role of phosphorylated Mad1 in the yeast mitotic checkpoint were examined. Mad1 localization to unattached kinetochores in vertebrates is dependent on Mps1, and it would be interesting to find out whether 1) this depends on direct phosphorylation of Mad1 by Mps1, and 2) constitutive localization of Mad1 to unattached kinetochores (for instance by fusion to Mis12) can rescue MCC catalysis, and thereby the timing and/or checkpoint defect seen upon Mps1 inhibition. Third, Mps1 directly phosphorylates BLM on multiple residues and cells expressing BLM phospho-mutants displayed compromised ability to arrest in response to spindle poisons[141]. Fourth, CENP-E is directly phosphorylated by Mps1 in a *Xenopus in vitro* system, which relieves auto-inhibition of CENP-E[142]. These last two substrates are however unlikely

candidates to play a direct role in the mitotic checkpoint in human cells. BLM is a helicase[139,140] and the effects observed with mutants of this protein on checkpoint activity are therefore likely to be indirect. CENP-E was only shown to be a mitotic checkpoint protein in *Xenopus* egg extract[114], but does not appear to have a role in the checkpoint in mammalian cells[278].

A candidate mechanism under control of Mps1 is acetylation on BubR1. This modification was found to protect BubR1 from APC/C mediated degradation[121], and given that Mps1 activity protects MCC from APC/C mediated disassembly, it would be interesting to find out whether acetylation of BubR1 depends on Mps1 activity. In addition, the high phosphorylation states of Cdc20 and several subunits of APC/C[279-281] make these proteins potential targets of Mps1 activity, which should be investigated. Also p31^{comet} is an attractive candidate for inhibition by direct Mps1 phosphorylation, since it collaborates with UbcH10 in mediating Cdc20 multi-ubiquitination[119] and is needed for mitotic checkpoint silencing.

Perhaps similar to our proposed feedback mechanisms of APC/C activity towards MCC in Chapter 4, a feedback mechanism of APC/C activity towards Securin in budding yeast was proposed[282]. Phosphorylation of Securin by Cdk1 was shown to protect it from ubiquitination by APC/C and subsequent destruction. Dephosphorylation was mediated by the phosphatase Cdc14, of which the activity was enhanced by Separase. Since Separase is activated upon Securin degradation, this mechanism of positive feedback can explain the fast metaphase-to-anaphase switch[282]. Although this feedback has not yet been validated in mammalian cells, Mps1 could block, for example, the action of the phosphatase; thereby blocking activation of APC/C and APC/C mediated MCC disassembly.

It is clear that there are a lot of potential substrates and mechanisms by which Mps1 activity could mediate mitotic checkpoint signaling. A significant effort is thus needed to clarify the role of Mps1 downstream signaling in the mitotic checkpoint.

Regulation of Mps1

By identifying the auto-phosphorylation site T676 in the activation loop in the kinase domain in Mps1 (Chapter 5), we have gained more insight into the regulation of Mps1 itself. We and others proposed that Mps1 can auto-activate in a concentration dependent manner. Together with the findings from Chapter 6, the data of Chapter 5 suggest the following model for regulation of Mps1 activity: Mps1 is targeted in an inactive state to non-bioriented kinetochores, auto-activates by auto-phosphorylation due to high local protein concentration, and is subsequently released from the kinetochore. Question remains what the mechanism of release is. Although we cannot exclude that phosphorylation of other kinetochore proteins underlies release, we have shown that it is likely that Mps1 *in trans* auto-phosphorylation results in a conformational change, which might shield the targeting domain (see peroxisome targeting experiments, Chapter 6). However, we have not been able to pinpoint any of the described *in trans* phosphorylation sites to be responsible for such a mechanism. Further attempts at finding a relevant trans-phosphorylation site that promotes Mps1 kinetochore dissociation are ongoing. Additionally, it was shown that Mps1 dimerization *in vitro* causes Mps1 auto-activation[264], making *in trans* auto-phosphorylation-mediated dimerization (or release hereof) a very interesting potential mechanism to mediate release from kinetochores.

Another open question is how Mps1 is specifically targeted to unattached or low-tension kinetochores. It is not known what recruits Mps1 to kinetochores, and finding a binding partner of Mps1 on the kinetochore could help to answer this question. This will potentially also clarify the mechanism of fast turnover of Mps1 on kinetochores.

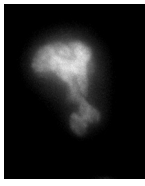

The mitotic checkpoint and cancer: a new mouse model

Several *in vivo* (mouse) models exist to study the effect of interfering in the function of the mitotic checkpoint on tumorigenesis. Although complete loss of the checkpoint results in embryonic lethality, reduction of checkpoint function by loss of one allele of a checkpoint gene induces aneuploidy and can result in spontaneous tumor formation. This tumor formation is however not observed for all checkpoint genes. Nevertheless, in many models reduction of checkpoint function enhances tumor formation induced by carcinogens or loss of tumor suppressor alleles. Differences between all reported models include the affected tissue types and severity of tumor formation. A general effect of aneuploidy cannot therefore be derived from these models (for more details, see the general introduction of this thesis, and [165]). Also, human tumors usually arise at later age, after development, but the effects of the heterozygous deletions in these models are not inducible in an adult mouse. Instead they are present from early development, and hence possible early effects cannot be excluded to play a role in later tumor formation. Inducible reduction of Mps1 activity in an adult mouse is therefore an attractive model to study the effects of chromosomal instability in the occurrence of sporadic tumors.

In collaboration with Drs. Aniek Janssen and Prof.dr. René Medema, we are in the process of developing two conditional mouse models with partial or complete reductions in Mps1 activity in a tissue-specific manner. To do this we make use of a technique by which a kinase-dead mutant Mps1 allele (mouse Mps1^{D637A}, analogous to human Mps1^{D664A}, see Chapter 2) is incorporated in the genome by homologous recombination in embryonic stem cells. This allele is designed in such a way that it can be conditionally induced to replace expression of endogenous wild-type Mps1 with mutant Mps1. Induction of mutant expression is mediated by inducible Cre activity (Cre-lox system) (Figure 1 and [283]. Crossing this mouse (CiMKi^{D637A}: Cre-inducible Mps1 Knock-in^{D637A}) with a conditionally active tissue-specific Cre-expressing mouse will therefore make conditional mutant Mps1 expression in a tissue-specific manner possible. Expression of the mutant protein will be driven from the endogenous promoter, and is expected to be at physiological levels. Therefore, total kinase activity in Cre-targeted cells will theoretically be reduced to 50% after induction in a heterozygous mouse, and to 0% in a homozygous mouse. A second model is designed in the same way, but using a Threonine-to-Alanine mutation of T649 (CiMKi^{T649A}). This site is analogous to the human T676 in humans, which we and others have identified as an auto-phosphorylation site needed for full activity of Mps1[210,221,222,264 (Chapter 5 of this thesis)]. We determined that a threonine-to-alanine mutant of this site reduced kinase activity to about 20% in human tumor cells, resulting in increased chromosomal instability[210 (Chapter 5 of this thesis)]. By using and crossing both models, we can theoretically achieve a range of reduced Mps1 activities in an inducible manner. For example, a mouse with one allele of each mutation can be generated by crossing CiMKi^{D637A} with CiMKi^{T649A} to reduce Mps1 activity to 10% after Cre induction.

The advantage of such a system is that it can provide information about two important issues. First, Mps1 activity is expected to be inhibited completely in a homozygous CiMKi^{D637A} mouse after Cre-induction. This can be used to examine whether loss of Mps1 activity (and thereby mitotic checkpoint function) can lead to regression of otherwise induced tumors. Although it has been shown in human tumor cells in culture that full inhibition of the checkpoint leads to cell death[95,166], it has never been shown *in vivo*. Our model could thus provide that information, which would greatly support the clinical relevance of targeting the mitotic checkpoint and in particular Mps1 for cancer treatment. In addition, the mice with graded reductions in Mps1 activity will likely teach us what level of Mps1 inhibition is needed for efficient tumor cell killing. Second, reducing the kinase activity of Mps1 in the mouse most probably will lead to reduced checkpoint

activity and increased levels of aneuploidy. With this model, in contrast to the existing models, we can induce this in an adult mouse, without interfering with (early) development, and we can do so in a tissue-specific manner. Therefore it might provide more clarity on the question whether aneuploidy can induce tumor formation by itself or enhance or reduce severity of otherwise induced tumors. This information would also be of clinical importance in cancer treatment. If reduction of Mps1 activity can sensitize healthy tissue to tumor formation for instance, the potential benefits of treatment with an Mps1 inhibitor should be weighed carefully against the significant drawbacks of such treatment. In addition, it was found recently that partial depletion of Mps1 sensitizes a variety of tumor cell lines to cell death when treated with clinically relevant doses of the anti-tumor drug paclitaxel[166]. The CiMKi mouse model offers the opportunity to validate this finding *in vivo* to support the clinical relevance of such a combination treatment.

Summarized, the CiMKi mouse model can be of great support to gather important information about the role of aneuploidy in tumor formation and about the relevance of targeting Mps1 for cancer treatment.

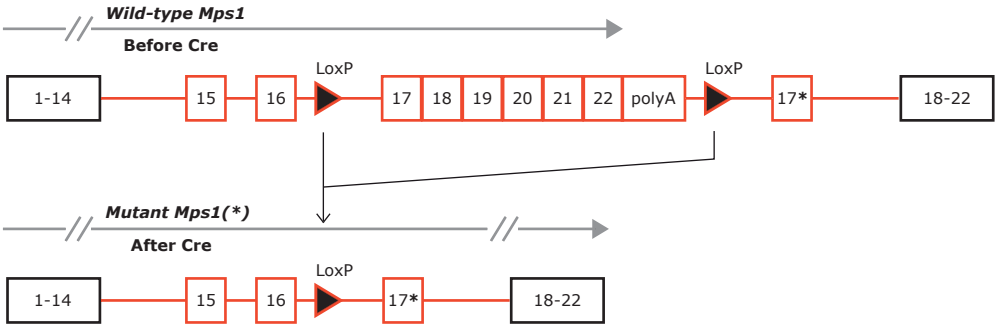

Figure 1
Schematic overview of the Mps1 mutant allele designed to generate the CiMKi mouse model. Black boxes show genomic DNA sequence surrounding the targeted allele (red boxes (exons) and red lines (introns)). Asterisks indicate a mutation in exon 17 (D637A or T649A).

Concluding Remarks

Overall, the work presented in this thesis provides new mechanistic insights on Mps1 signaling in the mitotic checkpoint and reveals a function of Mps1 in coordinating chromosome biorientation and the mitotic checkpoint. Many aspects of mitotic checkpoint signaling and the precise role of Mps1 herein however remain to be uncovered. Our findings contribute to the basis for future fundamental research in the field of mitosis and mitotic checkpoint signaling, and to further possibilities to explore the mitotic checkpoint as a possible target for cancer treatment.

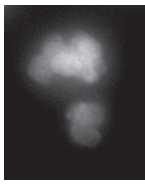

References

1. Errico, A., Deshmukh, K., Tanaka, Y., Pozniakovsky, A. & Hunt, T. Identification of Substrates for Cyclin Dependent Kinases. Advances in enzyme regulation (2009).
2. Cohen, M. M. Syndromology: an updated conceptual overview. V. Aspects of aneuploidy. Int J Oral Maxillofac Surg 18, 333-8 (1989).
3. Epstein, C. J. Developmental genetics. Experientia 42, 1117-28 (1986).
4. Kops, G., Weaver, B. & Cleveland, D. On the road to cancer: aneuploidy and the mitotic checkpoint. Nat Rev Cancer 5, 773-85 (2005).
5. Pines, J. & Rieder, C. L. Re-staging mitosis: a contemporary view of mitotic progression. Nat Cell Biol 3, E3-6 (2001).
6. Swedlow, J. R. & Hirano, T. The making of the mitotic chromosome: modern insights into classical questions. Mol Cell 11, 557-69 (2003).
7. Nasmyth, K. & Haering, C. H. Cohesin: its roles and mechanisms. Annu Rev Genet 43, 525-58 (2009).
8. Uhlmann, F. & Nasmyth, K. Cohesion between sister chromatids must be established during DNA replication. Curr Biol 8, 1095-101 (1998).
9. Nasmyth, K. Segregating sister genomes: the molecular biology of chromosome separation. Science 297, 559-65 (2002).
10. Allshire, R. C. & Karpen, G. H. Epigenetic regulation of centromeric chromatin: old dogs, new tricks? Nat Rev Genet 9, 923-37 (2008).
11. Cleveland, D. W., Mao, Y. & Sullivan, K. F. Centromeres and kinetochores: from epigenetics to mitotic checkpoint signaling. Cell 112, 407-21 (2003).
12. Santaguida, S. & Musacchio, A. The life and miracles of kinetochores. Embo J 28, 2511-31 (2009).
13. Raff, J. W. Centrosomes and microtubules: wedded with a ring. Trends Cell Biol 6, 248-51 (1996).
14. O'Connell, C. B. & Khodjakov, A. L. Cooperative mechanisms of mitotic spindle formation. J Cell Sci 120, 1717-22 (2007).
15. Tanaka, T. U. Bi-orienting chromosomes: acrobatics on the mitotic spindle. Chromosoma 117, 521-33 (2008).
16. Walczak, C. E., Cai, S. & Khodjakov, A. Mechanisms of chromosome behaviour during mitosis. Nat Rev Mol Cell Biol 11, 91-102 (2010).
17. de Gramont, A. & Cohen-Fix, O. The many phases of anaphase. Trends Biochem Sci 30, 559-68 (2005).
18. Barr, F. A. & Gruneberg, U. Cytokinesis: placing and making the final cut. Cell 131, 847-60 (2007).
19. Cheeseman, I. M. & Desai, A. Molecular architecture of the kinetochore-microtubule interface. Nat Rev Mol Cell Biol 9, 33-46 (2008).
20. Kline-Smith, S. L., Sandall, S. & Desai, A. Kinetochore-spindle microtubule interactions during mitosis. Curr Opin Cell Biol 17, 35-46 (2005).
21. Cheeseman, I. M., Chappie, J. S., Wilson-Kubalek, E. M. & Desai, A. The conserved KMN network constitutes the core microtubule-binding site of the kinetochore. Cell 127, 983-97 (2006).
22. Cheeseman, I. M. *et al*. A conserved protein network controls assembly of the outer kinetochore and its ability to sustain tension. Genes Dev 18, 2255-68 (2004).
23. Deluca, J. G. *et al*. Hec1 and nuf2 are core components of the kinetochore outer plate essential for organizing microtubule attachment sites. Mol Biol Cell 16, 519-31 (2005).
24. Kline, S. L., Cheeseman, I. M., Hori, T., Fukagawa, T. & Desai, A. The human Mis12 complex is required for kinetochore assembly and proper chromosome segregation. J Cell Biol 173, 9-17 (2006).
25. Hanisch, A., Silljé, H. H. W. & Nigg, E. A. Timely anaphase onset requires a novel spindle and kinetochore complex comprising Ska1 and Ska2. Embo J 25, 5504-15 (2006).
26. Gaitanos, T. N. *et al*. Stable kinetochore-microtubule interactions depend on the Ska complex and its new component Ska3/C13Orf3. Embo J 28, 1442-52 (2009).
27. Welburn, J. P. I. *et al*. The human kinetochore Ska1 complex facilitates microtubule depolymerization-coupled motility. Dev Cell 16, 374-85 (2009).
28. Raaijmakers, J. A., Tanenbaum, M. E., Maia, A. F. & Medema, R. H. RAMA1 is a novel kinetochore protein involved in kinetochore-microtubule attachment. J Cell Sci 122, 2436-45 (2009).
29. Putkey, F. *et al*. Unstable kinetochore-microtubule capture and chromosomal instability following deletion of CENP-E. Dev Cell 3, 351-65 (2002).
30. Lampson, M. & Kapoor, T. The human mitotic checkpoint protein BubR1 regulates chromosome-spindle attachments. Nat Cell Biol 7, 93-8 (2005).

31. Elowe, S., Hummer, S., Uldschmid, A., Li, X. & Nigg, E. A. Tension-sensitive Plk1 phosphorylation on BubR1 regulates the stability of kinetochore microtubule interactions. Genes Dev 21, 2205-19 (2007).
32. Matsumura, S., Toyoshima, F. & Nishida, E. Polo-like kinase 1 facilitates chromosome alignment during prometaphase through BubR1. J Biol Chem 282, 15217-27 (2007).
33. Salmon, E. D. Microtubules: a ring for the depolymerization motor. Curr Biol 15, R299-302 (2005).
34. Indjeian, V. B. & Murray, A. W. Budding yeast mitotic chromosomes have an intrinsic bias to biorient on the spindle. Curr Biol 17, 1837-46 (2007).
35. Kapoor, T. *et al*. Chromosomes can congress to the metaphase plate before biorientation. Science 311, 388-91 (2006).
36. Cimini, D. Detection and correction of merotelic kinetochore orientation by Aurora B and its partners. Cell Cycle 6, 1558-64 (2007).
37. Pinsky, B. & Biggins, S. The spindle checkpoint: tension versus attachment. Trends Cell Biol 15, 486-93 (2005).
38. Lampson, M., Renduchitala, K., Khodjakov, A. & Kapoor, T. Correcting improper chromosome-spindle attachments during cell division. Nat Cell Biol 6, 232-7 (2004).
39. Tanaka, T. U. *et al*. Evidence that the Ipl1-Sli15 (Aurora kinase-INCENP) complex promotes chromosome bi-orientation by altering kinetochore-spindle pole connections. Cell 108, 317-29 (2002).
40. Ruchaud, S., Carmena, M. & Earnshaw, W. C. Chromosomal passengers: conducting cell division. Nat Rev Mol Cell Biol 8, 798-812 (2007).
41. Vader, G., Medema, R. H. & Lens, S. M. A. The chromosomal passenger complex: guiding Aurora-B through mitosis. J Cell Biol 173, 833-7 (2006).
42. Honda, R., Körner, R. & Nigg, E. A. Exploring the functional interactions between Aurora B, INCENP, and survivin in mitosis. Mol Biol Cell 14, 3325-41 (2003).
43. Vader, G., Kauw, J. J. W., Medema, R. H. & Lens, S. M. A. Survivin mediates targeting of the chromosomal passenger complex to the centromere and midbody. EMBO Rep 7, 85-92 (2006).
44. Klein, U. R., Nigg, E. A. & Gruneberg, U. Centromere targeting of the chromosomal passenger complex requires a ternary subcomplex of Borealin, Survivin, and the N-terminal domain of INCENP. Mol Biol Cell 17, 2547-58 (2006).
45. Jeyaprakash, A. A. *et al*. Structure of a Survivin-Borealin-INCENP core complex reveals how chromosomal passengers travel together. Cell 131, 271-85 (2007).
46. Wheatley, S. P., Henzing, A. J., Dodson, H., Khaled, W. & Earnshaw, W. C. Aurora-B phosphorylation in vitro identifies a residue of survivin that is essential for its localization and binding to inner centromere protein (INCENP) in vivo. J Biol Chem 279, 5655-60 (2004).
47. Sampath, S. C. *et al*. The chromosomal passenger complex is required for chromatin-induced microtubule stabilization and spindle assembly. Cell 118, 187-202 (2004).
48. Bishop, J. D. & Schumacher, J. M. Phosphorylation of the carboxyl terminus of inner centromere protein (INCENP) by the Aurora B Kinase stimulates Aurora B kinase activity. J Biol Chem 277, 27577-80 (2002).
49. Sessa, F. *et al*. Mechanism of Aurora B activation by INCENP and inhibition by hesperadin. Mol Cell 18, 379-91 (2005).
50. Gassmann, R. *et al*. Borealin: a novel chromosomal passenger required for stability of the bipolar mitotic spindle. J Cell Biol 166, 179-91 (2004).
51. Ciferri, C. *et al*. Implications for kinetochore-microtubule attachment from the structure of an engineered Ndc80 complex. Cell 133, 427-39 (2008).
52. Guimaraes, G. J., Dong, Y., McEwen, B. F. & Deluca, J. G. Kinetochore-microtubule attachment relies on the disordered N-terminal tail domain of Hec1. Curr Biol 18, 1778-84 (2008).
53. Lan, W. *et al*. Aurora B phosphorylates centromeric MCAK and regulates its localization and microtubule depolymerization activity. Curr Biol 14, 273-86 (2004).
54. Zhang, X., Lan, W., Ems-McClung, S. C., Stukenberg, P. T. & Walczak, C. E. Aurora B phosphorylates multiple sites on mitotic centromere-associated kinesin to spatially and temporally regulate its function. Mol Biol Cell 18, 3264-76 (2007).
55. Andrews, P. D. *et al*. Aurora B regulates MCAK at the mitotic centromere. Dev Cell 6, 253-68 (2004).
56. Knowlton, A. L., Lan, W. & Stukenberg, P. T. Aurora B is enriched at merotelic attachment sites, where it regulates MCAK. Curr Biol 16, 1705-10 (2006).
57. Cheeseman, I. M. *et al*. Phospho-regulation of kinetochore-microtubule attachments by the Aurora kinase Ipl1p. Cell 111, 163-72 (2002).
58. Keating, P., Rachidi, N., Tanaka, T. U. & Stark, M. J. R. Ipl1-dependent phosphorylation of Dam1 is reduced by tension applied on kinetochores. Journal of Cell Science 122, 4375-4382 (2009).
59. Liu, D., Vader, G., Vromans, M. J. M., Lampson, M. A. & Lens, S. M. A. Sensing chromosome bi-orientation by spatial separation of aurora B kinase from kinetochore substrates. Science 323, 1350-3 (2009).

60. Liu, D. & Lampson, M. A. Regulation of kinetochore-microtubule attachments by Aurora B kinase. Biochem Soc Trans 37, 976-80 (2009).
61. Nasmyth, K. How do so few control so many? Cell 120, 739-46 (2005).
62. Nigg, E. Mitotic kinases as regulators of cell division and its checkpoints. Nat Rev Mol Cell Biol 2, 21-32 (2001).
63. Yu, H., King, R. W., Peters, J. M. & Kirschner, M. W. Identification of a novel ubiquitin-conjugating enzyme involved in mitotic cyclin degradation. Curr Biol 6, 455-66 (1996).
64. Townsley, F. M., Aristarkhov, A., Beck, S., Hershko, A. & Ruderman, J. V. Dominant-negative cyclin-selective ubiquitin carrier protein E2-C/UbcH10 blocks cells in metaphase. Proc Natl Acad Sci USA 94, 2362-7 (1997).
65. Williamson, A. *et al*. Identification of a physiological E2 module for the human anaphase-promoting complex. Proc Natl Acad Sci USA 106, 18213-8 (2009).
66. Wu, T. *et al*. UBE2S drives elongation of K11-linked ubiquitin chains by the anaphase-promoting complex. Proc Natl Acad Sci USA 107, 1355-60 (2010).
67. Garnett, M. J. *et al*. UBE2S elongates ubiquitin chains on APC/C substrates to promote mitotic exit. Nat Cell Biol 11, 1363-9 (2009).
68. Visintin, R., Prinz, S. & Amon, A. CDC20 and CDH1: a family of substrate-specific activators of APC-dependent proteolysis. Science 278, 460-3 (1997).
69. Pfleger, C. M. & Kirschner, M. W. The KEN box: an APC recognition signal distinct from the D box targeted by Cdh1. Genes Dev 14, 655-65 (2000).
70. Geley, S. *et al*. Anaphase-promoting complex/cyclosome-dependent proteolysis of human cyclin A starts at the beginning of mitosis and is not subject to the spindle assembly checkpoint. J Cell Biol 153, 137-48 (2001).
71. den Elzen, N. & Pines, J. Cyclin A is destroyed in prometaphase and can delay chromosome alignment and anaphase. J Cell Biol 153, 121-36 (2001).
72. Lindqvist, A., Rodríguez-Bravo, V. & Medema, R. H. The decision to enter mitosis: feedback and redundancy in the mitotic entry network. J Cell Biol 185, 193-202 (2009).
73. Hames, R. S., Wattam, S. L., Yamano, H., Bacchieri, R. & Fry, A. M. APC/C-mediated destruction of the centrosomal kinase Nek2A occurs in early mitosis and depends upon a cyclin A-type D-box. Embo J 20, 7117-27 (2001).
74. Kashevsky, H. *et al*. The anaphase promoting complex/cyclosome is required during development for modified cell cycles. Proc Natl Acad Sci USA 99, 11217-22 (2002).
75. Golden, A. *et al*. Metaphase to anaphase (mat) transition-defective mutants in Caenorhabditis elegans. J Cell Biol 151, 1469-82 (2000).
76. Wehman, A. M., Staub, W. & Baier, H. The anaphase-promoting complex is required in both dividing and quiescent cells during zebrafish development. Dev Biol 303, 144-56 (2007).
77. Wirth, K. G. *et al*. Loss of the anaphase-promoting complex in quiescent cells causes unscheduled hepatocyte proliferation. Genes Dev 18, 88-98 (2004).
78. Li, M., York, J. P. & Zhang, P. Loss of Cdc20 causes a securin-dependent metaphase arrest in two-cell mouse embryos. Mol Cell Biol 27, 3481-8 (2007).
79. Rieder, C. L., Schultz, A., Cole, R. & Sluder, G. Anaphase onset in vertebrate somatic cells is controlled by a checkpoint that monitors sister kinetochore attachment to the spindle. J Cell Biol 127, 1301-10 (1994).
80. Kops, G. J. P. L. The kinetochore and spindle checkpoint in mammals. Front Biosci 13, 3606-20 (2008).
81. Sudakin, V., Chan, G. K. & Yen, T. J. Checkpoint inhibition of the APC/C in HeLa cells is mediated by a complex of BUBR1, BUB3, CDC20, and MAD2. J Cell Biol 154, 925-36 (2001).
82. Herzog, F. *et al*. Structure of the Anaphase-Promoting Complex/Cyclosome Interacting with a Mitotic Checkpoint Complex. Science 323, 1477-1481 (2009).
83. Hardwick, K. G., Johnston, R. C., Smith, D. L. & Murray, A. W. MAD3 encodes a novel component of the spindle checkpoint which interacts with Bub3p, Cdc20p, and Mad2p. J Cell Biol 148, 871-82 (2000).
84. Poddar, A., Stukenberg, P. T. & Burke, D. J. Two complexes of spindle checkpoint proteins containing Cdc20 and Mad2 assemble during mitosis independently of the kinetochore in Saccharomyces cerevisiae. Eukaryotic Cell 4, 867-78 (2005).
85. Howell, B. *et al*. Spindle checkpoint protein dynamics at kinetochores in living cells. Curr Biol 14, 953-64 (2004).
86. Shah, J. V. & Cleveland, D. W. Waiting for anaphase: Mad2 and the spindle assembly checkpoint. Cell 103, 997-1000 (2000).
87. Fang, G. Checkpoint protein BubR1 acts synergistically with Mad2 to inhibit anaphase-promoting complex. Mol Biol Cell 13, 755-66 (2002).
88. Wu, H. *et al*. p55CDC/hCDC20 is associated with BUBR1 and may be a downstream target of the spindle checkpoint kinase. Oncogene 19, 4557-62 (2000).

89. Tang, Z., Bharadwaj, R., Li, B. & Yu, H. Mad2-Independent inhibition of APCCdc20 by the mitotic checkpoint protein BubR1. Dev Cell 1, 227-37 (2001).
90. Chan, G. K., Jablonski, S. A., Sudakin, V., Hittle, J. C. & Yen, T. J. Human BUBR1 is a mitotic checkpoint kinase that monitors CENP-E functions at kinetochores and binds the cyclosome/APC. J Cell Biol 146, 941-54 (1999).
91. Sczaniecka, M. *et al*. The spindle checkpoint functions of Mad3 and Mad2 depend on a Mad3 KEN box-mediated interaction with Cdc20-anaphase-promoting complex (APC/C). J Biol Chem 283, 23039-47 (2008).
92. Malureanu, L. A. *et al*. BubR1 N terminus acts as a soluble inhibitor of cyclin B degradation by APC/C(Cdc20) in interphase. Dev Cell 16, 118-31 (2009).
93. Burton, J. L. & Solomon, M. J. Mad3p, a pseudosubstrate inhibitor of APCCdc20 in the spindle assembly checkpoint. Genes Dev 21, 655-67 (2007).
94. King, E. M. J., van der Sar, S. J. A. & Hardwick, K. G. Mad3 KEN boxes mediate both Cdc20 and Mad3 turnover, and are critical for the spindle checkpoint. PLoS ONE 2, e342 (2007).
95. Kops, G., Foltz, D. & Cleveland, D. Lethality to human cancer cells through massive chromosome loss by inhibition of the mitotic checkpoint. Proc Natl Acad Sci U S A 101, 8699-704 (2004).
96. Mapelli, M., Massimiliano, L., Santaguida, S. & Musacchio, A. The Mad2 conformational dimer: structure and implications for the spindle assembly checkpoint. Cell 131, 730-43 (2007).
97. Luo, X. *et al*. The Mad2 spindle checkpoint protein has two distinct natively folded states. Nat Struct Mol Biol 11, 338-45 (2004).
98. De Antoni, A. *et al*. The Mad1/Mad2 complex as a template for Mad2 activation in the spindle assembly checkpoint. Curr Biol 15, 214-25 (2005).
99. Luo, X., Tang, Z., Rizo, J. & Yu, H. The Mad2 spindle checkpoint protein undergoes similar major conformational changes upon binding to either Mad1 or Cdc20. Mol Cell 9, 59-71 (2002).
100. Luo, X. *et al*. Structure of the Mad2 spindle assembly checkpoint protein and its interaction with Cdc20. Nat Struct Biol 7, 224-9 (2000).
101. Sironi, L. *et al*. Crystal structure of the tetrameric Mad1-Mad2 core complex: implications of a 'safety belt' binding mechanism for the spindle checkpoint. Embo J 21, 2496-506 (2002).
102. Yu, H. Structural activation of Mad2 in the mitotic spindle checkpoint: the two-state Mad2 model versus the Mad2 template model. J Cell Biol 173, 153-7 (2006).
103. Nilsson, J., Yekezare, M., Minshull, J. & Pines, J. The APC/C maintains the spindle assembly checkpoint by targeting Cdc20 for destruction. Nat Cell Biol 10, 1411-20 (2008).
104. Kulukian, A., Han, J. S. & Cleveland, D. W. Unattached kinetochores catalyze production of an anaphase inhibitor that requires a Mad2 template to prime Cdc20 for BubR1 binding. Dev Cell 16, 105-17 (2009).
105. Tang, Z., Shu, H., Oncel, D., Chen, S. & Yu, H. Phosphorylation of Cdc20 by Bub1 provides a catalytic mechanism for APC/C inhibition by the spindle checkpoint. Mol Cell 16, 387-97 (2004).
106. Liu, S. *et al*. Human MPS1 kinase is required for mitotic arrest induced by the loss of CENP-E from kinetochores. Mol Biol Cell 14, 1638-51 (2003).
107. Martin-Lluesma, S., Stucke, V. & Nigg, E. Role of Hec1 in spindle checkpoint signaling and kinetochore recruitment of Mad1/Mad2. Science 297, 2267-70 (2002).
108. Pinsky, B., Kung, C., Shokat, K. & Biggins, S. The Ipl1-Aurora protein kinase activates the spindle checkpoint by creating unattached kinetochores. Nat Cell Biol 8, 78-83 (2006).
109. Cimini, D., Wan, X., Hirel, C. B. & Salmon, E. D. Aurora kinase promotes turnover of kinetochore microtubules to reduce chromosome segregation errors. Curr Biol 16, 1711-8 (2006).
110. Hoffman, D. B., Pearson, C. G., Yen, T. J., Howell, B. J. & Salmon, E. D. Microtubule-dependent changes in assembly of microtubule motor proteins and mitotic spindle checkpoint proteins at PtK1 kinetochores. Mol Biol Cell 12, 1995-2009 (2001).
111. Howell, B. J. *et al*. Cytoplasmic dynein/dynactin drives kinetochore protein transport to the spindle poles and has a role in mitotic spindle checkpoint inactivation. J Cell Biol 155, 1159-72 (2001).
112. Mao, Y., Abrieu, A. & Cleveland, D. W. Activating and silencing the mitotic checkpoint through CENP-E-dependent activation/inactivation of BubR1. Cell 114, 87-98 (2003).
113. Mao, Y., Desai, A. & Cleveland, D. W. Microtubule capture by CENP-E silences BubR1-dependent mitotic checkpoint signaling. J Cell Biol 170, 873-80 (2005).
114. Abrieu, A., Kahana, J. A., Wood, K. W. & Cleveland, D. W. CENP-E as an essential component of the mitotic checkpoint in vitro. Cell 102, 817-26 (2000).
115. Xia, G. *et al*. Conformation-specific binding of p31(comet) antagonizes the function of Mad2 in the spindle checkpoint. Embo J 23, 3133-43 (2004).
116. Yang, M. *et al*. p31comet blocks Mad2 activation through structural mimicry. Cell 131, 744-55 (2007).
117. Habu, T., Kim, S. H., Weinstein, J. & Matsumoto, T. Identification of a MAD2-binding protein, CMT2, and its role in mitosis. Embo J 21, 6419-28 (2002).

118. Wassmann, K., Liberal, V. & Benezra, R. Mad2 phosphorylation regulates its association with Mad1 and the APC/C. Embo J 22, 797-806 (2003).
119. Reddy, S. K., Rape, M., Margansky, W. A. & Kirschner, M. W. Ubiquitination by the anaphase-promoting complex drives spindle checkpoint inactivation. Nature 446, 921-5 (2007).
120. Stegmeier, F. *et al*. Anaphase initiation is regulated by antagonistic ubiquitination and deubiquitination activities. Nature 446, 876-81 (2007).
121. Choi, E. *et al*. BubR1 acetylation at prometaphase is required for modulating APC/C activity and timing of mitosis. Embo J 28, 2077-89 (2009).
122. Winey, M., Goetsch, L., Baum, P. & Byers, B. MPS1 and MPS2: novel yeast genes defining distinct steps of spindle pole body duplication. J Cell Biol 114, 745-54 (1991).
123. Lauze, E. *et al*. Yeast spindle pole body duplication gene MPS1 encodes an essential dual specificity protein kinase. Embo J 14, 1655-63 (1995).
124. Weiss, E. & Winey, M. The Saccharomyces cerevisiae spindle pole body duplication gene MPS1 is part of a mitotic checkpoint. J Cell Biol 132, 111-23 (1996).
125. Hardwick, K., Weiss, E., Luca, F., Winey, M. & Murray, A. Activation of the budding yeast spindle assembly checkpoint without mitotic spindle disruption. Science 273, 953-6 (1996).
126. He, X., Jones, M., Winey, M. & Sazer, S. Mph1, a member of the Mps1-like family of dual specificity protein kinases, is required for the spindle checkpoint in S. pombe. J Cell Sci 111 (Pt 12), 1635-47 (1998).
127. Mills, G. B. *et al*. Expression of TTK, a novel human protein kinase, is associated with cell proliferation. J Biol Chem 267, 16000-6 (1992).
128. Hogg, D. *et al*. Cell cycle dependent regulation of the protein kinase TTK. Oncogene 9, 89-96 (1994).
129. Douville, E. M. *et al*. Multiple cDNAs encoding the esk kinase predict transmembrane and intracellular enzyme isoforms. Mol Cell Biol 12, 2681-9 (1992).
130. Stucke, V., Sillje, H., Arnaud, L. & Nigg, E. Human Mps1 kinase is required for the spindle assembly checkpoint but not for centrosome duplication. Embo J 21, 1723-32 (2002).
131. Abrieu, A. *et al*. Mps1 is a kinetochore-associated kinase essential for the vertebrate mitotic checkpoint. Cell 106, 83-93 (2001).
132. Fisk, H. & Winey, M. The mouse Mps1p-like kinase regulates centrosome duplication. Cell 106, 95-104 (2001).
133. Fisk, H., Mattison, C. & Winey, M. Human Mps1 protein kinase is required for centrosome duplication and normal mitotic progression. Proc Natl Acad Sci U S A 100, 14875-80 (2003).
134. Kanai, M. *et al*. Physical and functional interaction between mortalin and Mps1 kinase. Genes Cells 12, 797-810 (2007).
135. Stucke, V., Baumann, C. & Nigg, E. Kinetochore localization and microtubule interaction of the human spindle checkpoint kinase Mps1. Chromosoma 113, 1-15 (2004).
136. Montembault, E., Dutertre, S., Prigent, C. & Giet, R. PRP4 is a spindle assembly checkpoint protein required for MPS1, MAD1, and MAD2 localization to the kinetochores. J Cell Biol 179, 601-9 (2007).
137. Kemmler, S. *et al*. Mimicking Ndc80 phosphorylation triggers spindle assembly checkpoint signalling. Embo J 28, 1099-110 (2009).
138. Huang, H. *et al*. Phosphorylation sites in BubR1 that regulate kinetochore attachment, tension, and mitotic exit. J Cell Biol 183, 667-80 (2008).
139. Ellis, N. A. *et al*. The Bloom's syndrome gene product is homologous to RecQ helicases. Cell 83, 655-66 (1995).
140. Neff, N. F. *et al*. The DNA helicase activity of BLM is necessary for the correction of the genomic instability of bloom syndrome cells. Mol Biol Cell 10, 665-76 (1999).
141. Leng, M. *et al*. MPS1-dependent mitotic BLM phosphorylation is important for chromosome stability. Proc Natl Acad Sci U S A 103, 11485-90 (2006).
142. Espeut, J. *et al*. Phosphorylation relieves autoinhibition of the kinetochore motor Cenp-E. Mol Cell 29, 637-43 (2008).
143. Shimogawa, M. *et al*. Mps1 phosphorylation of Dam1 couples kinetochores to microtubule plus ends at metaphase. Curr Biol 16, 1489-501 (2006).
144. Wei, J. *et al*. TTK/hMps1 participates in the regulation of DNA damage checkpoint response by phosphorylating CHK2 on threonine 68. J Biol Chem 280, 7748-57 (2005).
145. Bhonde, M. *et al*. DNA damage-induced expression of p53 suppresses mitotic checkpoint kinase hMps1: the lack of this suppression in p53MUT cells contributes to apoptosis. J Biol Chem 281, 8675-85 (2006).
146. Michel, L. *et al*. Complete loss of the tumor suppressor MAD2 causes premature cyclin B degradation and mitotic failure in human somatic cells. Proc Natl Acad Sci USA 101, 4459-64 (2004).
147. Teixeira, M. R. *et al*. Clonal heterogeneity in breast cancer: karyotypic comparisons of multiple intra- and extra-tumorous samples from 3 patients. Int J Cancer 63, 63-8 (1995).
148. Hartwell, L. H. & Kastan, M. B. Cell cycle control and cancer. Science 266, 1821-8 (1994).

149. Lengauer, C., Kinzler, K. W. & Vogelstein, B. Genetic instabilities in human cancers. Nature 396, 643-9 (1998).
150. Jallepalli, P. V. & Lengauer, C. Chromosome segregation and cancer: cutting through the mystery. Nat Rev Cancer 1, 109-17 (2001).
151. Dobles, M., Liberal, V., Scott, M. L., Benezra, R. & Sorger, P. K. Chromosome missegregation and apoptosis in mice lacking the mitotic checkpoint protein Mad2. Cell 101, 635-45 (2000).
152. Iwanaga, Y. *et al*. Heterozygous deletion of mitotic arrest-deficient protein 1 (MAD1) increases the incidence of tumors in mice. Cancer Res 67, 160-6 (2007).
153. Michel, L. S. *et al*. MAD2 haplo-insufficiency causes premature anaphase and chromosome instability in mammalian cells. Nature 409, 355-9 (2001).
154. Alizadeh, A. A. *et al*. Distinct types of diffuse large B-cell lymphoma identified by gene expression profiling. Nature 403, 503-11 (2000).
155. Chen, X. *et al*. Gene expression patterns in human liver cancers. Mol Biol Cell 13, 1929-39 (2002).
156. Garber, M. E. *et al*. Diversity of gene expression in adenocarcinoma of the lung. Proc Natl Acad Sci U S A 98, 13784-9 (2001).
157. Sotillo, R. *et al*. Mad2 overexpression promotes aneuploidy and tumorigenesis in mice. Cancer Cell 11, 9-23 (2007).
158. Baker, D. J. *et al*. BubR1 insufficiency causes early onset of aging-associated phenotypes and infertility in mice. Nat Genet 36, 744-9 (2004).
159. Jeganathan, K., Malureanu, L., Baker, D. J., Abraham, S. C. & van Deursen, J. M. Bub1 mediates cell death in response to chromosome missegregation and acts to suppress spontaneous tumorigenesis. J Cell Biol 179, 255-67 (2007).
160. Dai, W. *et al*. Slippage of mitotic arrest and enhanced tumor development in mice with BubR1 haploinsufficiency. Cancer Res 64, 440-5 (2004).
161. Babu, J. R. *et al*. Rae1 is an essential mitotic checkpoint regulator that cooperates with Bub3 to prevent chromosome missegregation. J Cell Biol 160, 341-53 (2003).
162. Baker, D. J., Jin, F., Jeganathan, K. B. & van Deursen, J. M. Whole chromosome instability caused by Bub1 insufficiency drives tumorigenesis through tumor suppressor gene loss of heterozygosity. Cancer Cell 16, 475-86 (2009).
163. Rao, C. V. *et al*. Colonic tumorigenesis in BubR1+/-ApcMin/+ compound mutant mice is linked to premature separation of sister chromatids and enhanced genomic instability. Proc Natl Acad Sci USA 102, 4365-70 (2005).
164. Weaver, B. A., Silk, A. D., Montagna, C., Verdier-Pinard, P. & Cleveland, D. W. Aneuploidy acts both oncogenically and as a tumor suppressor. Cancer Cell 11, 25-36 (2007).
165. Suijkerbuijk, S. J. E. & Kops, G. J. P. L. Preventing aneuploidy: the contribution of mitotic checkpoint proteins. Biochim Biophys Acta 1786, 24-31 (2008).
166. Janssen, A., Kops, G. J. P. L. & Medema, R. H. Elevating the frequency of chromosome mis-segregation as a strategy to kill tumor cells. Proc Natl Acad Sci USA 106, 19108-13 (2009).
167. Kops, G. *et al*. ZW10 links mitotic checkpoint signaling to the structural kinetochore. J Cell Biol 169, 49-60 (2005).
168. Ditchfield, C. *et al*. Aurora B couples chromosome alignment with anaphase by targeting BubR1, Mad2, and Cenp-E to kinetochores. J Cell Biol 161, 267-80 (2003).
169. Kitajima, T. S., Hauf, S., Ohsugi, M., Yamamoto, T. & Watanabe, Y. Human Bub1 defines the persistent cohesion site along the mitotic chromosome by affecting Shugoshin localization. Curr Biol 15, 353-9 (2005).
170. Tang, Z., Sun, Y., Harley, S. E., Zou, H. & Yu, H. Human Bub1 protects centromeric sister-chromatid cohesion through Shugoshin during mitosis. Proc Natl Acad Sci U S A 101, 18012-7 (2004).
171. Johnson, V., Scott, M., Holt, S., Hussein, D. & Taylor, S. Bub1 is required for kinetochore localization of BubR1, Cenp-E, Cenp-F and Mad2, and chromosome congression. J Cell Sci 117, 1577-89 (2004).
172. Meraldi, P. & Sorger, P. A dual role for Bub1 in the spindle checkpoint and chromosome congression. Embo J 24, 1621-33 (2005).
173. Draviam, V. M. *et al*. A functional genomic screen identifies a role for TAO1 kinase in spindle-checkpoint signalling. Nat Cell Biol 9, 556-64 (2007).
174. Hauf, S. *et al*. The small molecule Hesperadin reveals a role for Aurora B in correcting kinetochore-microtubule attachment and in maintaining the spindle assembly checkpoint. J Cell Biol 161, 281-94 (2003).
175. DeLuca, J. G. *et al*. Kinetochore microtubule dynamics and attachment stability are regulated by Hec1. Cell 127, 969-82 (2006).
176. Kallio, M. J., McCleland, M. L., Stukenberg, P. T. & Gorbsky, G. J. Inhibition of aurora B kinase blocks chromosome segregation, overrides the spindle checkpoint, and perturbs microtubule dynamics in mitosis. Curr Biol 12, 900-5 (2002).
177. Morrow, C. J. *et al*. Bub1 and aurora B cooperate to maintain BubR1-mediated inhibition of APC/CCdc20. J Cell Sci 118, 3639-52 (2005).

178. Adams, R. R. *et al*. INCENP binds the Aurora-related kinase AIRK2 and is required to target it to chromosomes, the central spindle and cleavage furrow. Curr Biol 10, 1075-8 (2000).
179. Bolton, M. A. *et al*. Aurora B kinase exists in a complex with survivin and INCENP and its kinase activity is stimulated by survivin binding and phosphorylation. Mol Biol Cell 13, 3064-77 (2002).
180. Kaitna, S., Mendoza, M., Jantsch-Plunger, V. & Glotzer, M. Incenp and an aurora-like kinase form a complex essential for chromosome segregation and efficient completion of cytokinesis. Curr Biol 10, 1172-81 (2000).
181. Vader, G., Maia, A. F. & Lens, S. M. The chromosomal passenger complex and the spindle assembly checkpoint: kinetochore-microtubule error correction and beyond. Cell division 3, 10 (2008).
182. Jones, M. *et al*. Chemical genetics reveals a role for Mps1 kinase in kinetochore attachment during mitosis. Curr Biol 15, 160-5 (2005).
183. Dorer, R. *et al*. A small-molecule inhibitor of Mps1 blocks the spindle-checkpoint response to a lack of tension on mitotic chromosomes. Curr Biol 15, 1070-6 (2005).
184. Schutz, A. & Winey, M. New alleles of the yeast MPS1 gene reveal multiple requirements in spindle pole body duplication. Mol Biol Cell 9, 759-74 (1998).
185. Cheeseman, I. & Desai, A. A combined approach for the localization and tandem affinity purification of protein complexes from metazoans. Sci STKE 2005, pl1 (2005).
186. Schmidt, M., Budirahardja, Y., Klompmaker, R. & Medema, R. Ablation of the spindle assembly checkpoint by a compound targeting Mps1. EMBO Rep 6, 866-72 (2005).
187. Dujardin, D. *et al*. Evidence for a role of CLIP-170 in the establishment of metaphase chromosome alignment. J Cell Biol 141, 849-62 (1998).
188. Tanenbaum, M. E., Galjart, N., van Vugt, M. A. T. M. & Medema, R. H. CLIP-170 facilitates the formation of kinetochore-microtubule attachments. Embo J 25, 45-57 (2006).
189. Skoufias, D. A. *et al*. S-trityl-L-cysteine is a reversible, tight binding inhibitor of the human kinesin Eg5 that specifically blocks mitotic progression. J Biol Chem 281, 17559-69 (2006).
190. Kapoor, T., Mayer, T., Coughlin, M. & Mitchison, T. Probing spindle assembly mechanisms with monastrol, a small molecule inhibitor of the mitotic kinesin, Eg5. J Cell Biol 150, 975-88 (2000).
191. Khodjakov, A., Copenagle, L., Gordon, M. B., Compton, D. A. & Kapoor, T. M. Minus-end capture of preformed kinetochore fibers contributes to spindle morphogenesis. J Cell Biol 160, 671-83 (2003).
192. Zeitlin, S., Shelby, R. & Sullivan, K. CENP-A is phosphorylated by Aurora B kinase and plays an unexpected role in completion of cytokinesis. J Cell Biol 155, 1147-57 (2001).
193. Vigneron, S. *et al*. Kinetochore localization of spindle checkpoint proteins: who controls whom? Mol Biol Cell 15, 4584-96 (2004).
194. Sumara, I. *et al*. Roles of polo-like kinase 1 in the assembly of functional mitotic spindles. Curr Biol 14, 1712-22 (2004).
195. van Vugt, M. A. *et al*. Polo-like kinase-1 is required for bipolar spindle formation but is dispensable for anaphase promoting complex/Cdc20 activation and initiation of cytokinesis. J Biol Chem 279, 36841-54 (2004).
196. Biggins, S. *et al*. The conserved protein kinase Ipl1 regulates microtubule binding to kinetochores in budding yeast. Genes Dev 13, 532-44 (1999).
197. Biggins, S. & Murray, A. The budding yeast protein kinase Ipl1/Aurora allows the absence of tension to activate the spindle checkpoint. Genes Dev 15, 3118-29 (2001).
198. Zachos, G. *et al*. Chk1 is required for spindle checkpoint function. Dev Cell 12, 247-60 (2007).
199. Kelly, A. E. *et al*. Chromosomal enrichment and activation of the aurora B pathway are coupled to spatially regulate spindle assembly. Dev Cell 12, 31-43 (2007).
200. Yasui, Y. *et al*. Autophosphorylation of a newly identified site of Aurora-B is indispensable for cytokinesis. J Biol Chem 279, 12997-3003 (2004).
201. Zhao, Y. & Chen, R. Mps1 phosphorylation by MAP kinase is required for kinetochore localization of spindle-checkpoint proteins. Curr Biol 16, 1764-9 (2006).
202. Liu, S., Rattner, J., Jablonski, S. & Yen, T. Mapping the assembly pathways that specify formation of the trilaminar kinetochore plates in human cells. J Cell Biol 175, 41-53 (2006).
203. Kops, G. J., Foltz, D. R. & Cleveland, D. W. Lethality to human cancer cells through massive chromosome loss by inhibition of the mitotic checkpoint. Proc Natl Acad Sci U S A 101, 8699-704 (2004).
204. Lebbink, R. J. *et al*. Collagens are functional, high affinity ligands for the inhibitory immune receptor LAIR-1. J Exp Med 203, 1419-25 (2006).
205. Musacchio, A. & Salmon, E. D. The spindle-assembly checkpoint in space and time. Nat Rev Mol Cell Biol 8, 379-93 (2007).
206. Kasbek, C. *et al*. Preventing the degradation of mps1 at centrosomes is sufficient to cause centrosome reduplication in human cells. Mol Biol Cell 18, 4457-69 (2007).
207. Schmidt, M. & Bastians, H. Mitotic drug targets and the development of novel anti-mitotic anticancer drugs. Drug Resist Updat 10, 162-81 (2007).

208. Tighe, A., Staples, O. & Taylor, S. Mps1 kinase activity restrains anaphase during an unperturbed mitosis and targets Mad2 to kinetochores. J Cell Biol 181, 893-901 (2008).
209. McDermott, U. *et al*. Identification of genotype-correlated sensitivity to selective kinase inhibitors by using high-throughput tumor cell line profiling. Proc Natl Acad Sci U S A 104, 19936-41 (2007).
210. Jelluma, N. *et al*. Chromosomal instability by inefficient Mps1 auto-activation due to a weakened mitotic checkpoint and lagging chromosomes. PLoS ONE 3, e2415 (2008).
211. Jelluma, N. *et al*. Mps1 phosphorylates Borealin to control Aurora B activity and chromosome alignment. Cell 132, 233-46 (2008).
212. Burds, A. A., Lutum, A. S. & Sorger, P. K. Generating chromosome instability through the simultaneous deletion of Mad2 and p53. Proc Natl Acad Sci USA 102, 11296-301 (2005).
213. Holland, A. J. & Cleveland, D. W. Boveri revisited: chromosomal instability, aneuploidy and tumorigenesis. Nat Rev Mol Cell Biol 10, 478-87 (2009).
214. Xu, Q. *et al*. Regulation of kinetochore recruitment of two essential mitotic spindle checkpoint proteins by Mps1 phosphorylation. Mol Biol Cell 20, 10-20 (2009).
215. Karaman, M. W. *et al*. A quantitative analysis of kinase inhibitor selectivity. Nat Biotechnol 26, 127-32 (2008).
216. Chu, M. L. H., Chavas, L. M. G., Douglas, K. T., Eyers, P. A. & Tabernero, L. Crystal structure of the catalytic domain of the mitotic checkpoint kinase Mps1 in complex with SP600125. J Biol Chem 283, 21495-500 (2008).
217. Fabian, M. A. *et al*. A small molecule-kinase interaction map for clinical kinase inhibitors. Nat Biotechnol 23, 329-36 (2005).
218. Galkin, A. V. *et al*. Identification of NVP-TAE684, a potent, selective, and efficacious inhibitor of NPM-ALK. Proc Natl Acad Sci U S A 104, 270-5 (2007).
219. Iwahara, T. *et al*. Molecular characterization of ALK, a receptor tyrosine kinase expressed specifically in the nervous system. Oncogene 14, 439-49 (1997).
220. Steegmaier, M. *et al*. BI 2536, a potent and selective inhibitor of polo-like kinase 1, inhibits tumor growth in vivo. Curr Biol 17, 316-22 (2007).
221. Wang, W. *et al*. Structural and Mechanistic Insights into Mps1 Kinase Activation. J Cell Mol Med (2008).
222. Mattison, C. P. *et al*. Mps1 activation loop autophosphorylation enhances kinase activity. J Biol Chem 282, 30553-61 (2007).
223. Harrington, E. A. *et al*. VX-680, a potent and selective small-molecule inhibitor of the Aurora kinases, suppresses tumor growth in vivo. Nat Med 10, 262-7 (2004).
224. Basto, R. *et al*. Centrosome amplification can initiate tumorigenesis in flies. Cell 133, 1032-42 (2008).
225. Yang, Z., Loncarek, J., Khodjakov, A. & Rieder, C. L. Extra centrosomes and/or chromosomes prolong mitosis in human cells. Nat Cell Biol 10, 748-51 (2008).
226. Kwon, M. *et al*. Mechanisms to suppress multipolar divisions in cancer cells with extra centrosomes. Genes Dev 22, 2189-203 (2008).
227. Kleylein-Sohn, J. *et al*. Plk4-induced centriole biogenesis in human cells. Dev Cell 13, 190-202 (2007).
228. Cahill, D. P. *et al*. Mutations of mitotic checkpoint genes in human cancers. Nature 392, 300-3 (1998).
229. Bodnar, A. G. *et al*. Extension of life-span by introduction of telomerase into normal human cells. Science 279, 349-52 (1998).
230. Soule, H. D. *et al*. Isolation and characterization of a spontaneously immortalized human breast epithelial cell line, MCF-10. Cancer Res 50, 6075-86 (1990).
231. Shah, J. V. *et al*. Dynamics of centromere and kinetochore proteins; implications for checkpoint signaling and silencing. Curr Biol 14, 942-52 (2004).
232. Leslie, A. G. W. & Powell, H. MOSFLM. 7.01 edn. MCR Laboratory of Molecular Biology, Cambridge (2007).
233. Evans, P. SCALA-scale together multiple observations of reflections. 3.3.0 edn. MRC Laboratory of Molecular Biology, Cambridge (2007).
234. McCoy, A. J., Grosse-Kunstleve, R. W., Storoni, L. C. & Read, R. J. Likelihood-enhanced fast translation functions. Acta Crystallogr D Biol Crystallogr 61, 458-64 (2005).
235. Emsley, P. & Cowtan, K. Coot: model-building tools for molecular graphics. Acta Crystallogr D Biol Crystallogr 60, 2126-32 (2004).
236. Murshudov, G. N., Vagin, A. A. & Dodson, E. J. Refinement of macromolecular structures by the maximum-likelihood method. Acta Crystallogr D Biol Crystallogr 53, 240-55 (1997).
237. Perrakis, A., Morris, R. & Lamzin, V. S. Automated protein model building combined with iterative structure refinement. Nat Struct Biol 6, 458-63 (1999).
238. Painter, J. & Merritt, E. A. Optimal description of a protein structure in terms of multiple groups undergoing TLS motion. Acta Crystallogr D Biol Crystallogr 62, 439-50 (2006).
239. Kwiatkowski, N. *et al*. Small Molecule Kinase Inhibitors Provide Insight ino Mps1 Cell Cycle Function. Nat Chem Biol 6(5):359-68 (2010).

240. Peters, J.-M. The anaphase promoting complex/cyclosome: a machine designed to destroy. Nat Rev Mol Cell Biol 7, 644-56 (2006).
241. Pesin, J. A. & Orr-Weaver, T. L. Regulation of APC/C activators in mitosis and meiosis. Annu Rev Cell Dev Biol 24, 475-99 (2008).
242. van Leuken, R., Clijsters, L. & Wolthuis, R. To cell cycle, swing the APC/C. Biochim Biophys Acta 1786, 49-59 (2008).
243. Di Fiore, B. & Pines, J. Defining the role of Emi1 in the DNA replication-segregation cycle. Chromosoma 117, 333-8 (2008).
244. Baker, D. J., Dawlaty, M. M., Galardy, P. & van Deursen, J. M. Mitotic regulation of the anaphase-promoting complex. Cell Mol Life Sci 64, 589-600 (2007).
245. Di Fiore, B. & Pines, J. Emi1 is needed to couple DNA replication with mitosis but does not regulate activation of the mitotic APC/C. J Cell Biol 177, 425-37 (2007).
246. Wassmann, K. & Benezra, R. Mad2 transiently associates with an APC/p55Cdc complex during mitosis. Proc Natl Acad Sci USA 95, 11193-8 (1998).
247. Fang, G., Yu, H. & Kirschner, M. W. The checkpoint protein MAD2 and the mitotic regulator CDC20 form a ternary complex with the anaphase-promoting complex to control anaphase initiation. Genes Dev 12, 1871-83 (1998).
248. Kallio, M., Weinstein, J., Daum, J. R., Burke, D. J. & Gorbsky, G. J. Mammalian p55CDC mediates association of the spindle checkpoint protein Mad2 with the cyclosome/anaphase-promoting complex, and is involved in regulating anaphase onset and late mitotic events. J Cell Biol 141, 1393-406 (1998).
249. Pan, J. & Chen, R.-H. Spindle checkpoint regulates Cdc20p stability in Saccharomyces cerevisiae. Genes Dev 18, 1439-51 (2004).
250. Meraldi, P., Draviam, V. & Sorger, P. Timing and checkpoints in the regulation of mitotic progression. Dev Cell 7, 45-60 (2004).
251. Kops, G. J. P. L. *et al*. APC16 is a novel, conserved subunit of the Anaphase Promoting Complex/Cyclosome. J Cell Sci. [Epub ahead of print, Apr 14] (2010).
252. Yu, H. *et al*. Identification of a cullin homology region in a subunit of the anaphase-promoting complex. Science 279, 1219-22 (1998).
253. Aristarkhov, A. *et al*. E2-C, a cyclin-selective ubiquitin carrier protein required for the destruction of mitotic cyclins. Proc Natl Acad Sci USA 93, 4294-9 (1996).
254. Skoufias, D. A., Andreassen, P. R., Lacroix, F. B., Wilson, L. & Margolis, R. L. Mammalian mad2 and bub1/bubR1 recognize distinct spindle-attachment and kinetochore-tension checkpoints. Proc Natl Acad Sci USA 98, 4492-7 (2001).
255. Taylor, S. S., Hussein, D., Wang, Y., Elderkin, S. & Morrow, C. J. Kinetochore localisation and phosphorylation of the mitotic checkpoint components Bub1 and BubR1 are differentially regulated by spindle events in human cells. J Cell Sci 114, 4385-95 (2001).
256. Simonetta, M. *et al*. The influence of catalysis on mad2 activation dynamics. PLoS Biol 7, e10 (2009).
257. Heim, S. & Mitelman, F. Cancer Cytogenics. New York: Wiley Liss, Inc (1995).
258. Cimini, D. *et al*. Merotelic kinetochore orientation is a major mechanism of aneuploidy in mitotic mammalian tissue cells. J Cell Biol 153, 517-27 (2001).
259. Ganem, N. J., Storchova, Z. & Pellman, D. Tetraploidy, aneuploidy and cancer. Curr Opin Genet Dev 17, 157-62 (2007).
260. Weaver, B. A. & Cleveland, D. W. Does aneuploidy cause cancer? Curr Opin Cell Biol 18, 658-67 (2006).
261. Doak, S. H. *et al*. Differential expression of the MAD2, BUB1 and HSP27 genes in Barrett's oesophagus-their association with aneuploidy and neoplastic progression. Mutat Res 547, 133-44 (2004).
262. Weitzel, D. H. & Vandre, D. D. Differential spindle assembly checkpoint response in human lung adenocarcinoma cells. Cell Tissue Res 300, 57-65 (2000).
263. Thompson, S. L. & Compton, D. A. Examining the link between chromosomal instability and aneuploidy in human cells. J Cell Biol 180, 665-72 (2008).
264. Kang, J., Chen, Y., Zhao, Y. & Yu, H. Autophosphorylation-dependent activation of human Mps1 is required for the spindle checkpoint. Proc Natl Acad Sci USA 104, 20232-7 (2007).
265. Nolen, B., Taylor, S. & Ghosh, G. Regulation of protein kinases; controlling activity through activation segment conformation. Mol Cell 15, 661-75 (2004).
266. Yang, J., Ten Eyck, L. F., Xuong, N. H. & Taylor, S. S. Crystal structure of a cAMP-dependent protein kinase mutant at 1.26A: new insights into the catalytic mechanism. J Mol Biol 336, 473-87 (2004).
267. Luciano, B. S., Hsu, S., Channavajhala, P. L., Lin, L. L. & Cuozzo, J. W. Phosphorylation of threonine 290 in the activation loop of Tpl2/Cot is necessary but not sufficient for kinase activity. J Biol Chem 279, 52117-23 (2004).

268. Weaver, B. *et al*. Centromere-associated protein-E is essential for the mammalian mitotic checkpoint to prevent aneuploidy due to single chromosome loss. J Cell Biol 162, 551-63 (2003).
269. Guardavaccaro, D. *et al*. Control of chromosome stability by the beta-TrCP-REST-Mad2 axis. Nature 452, 365-9 (2008).
270. Hernando, E. *et al*. Rb inactivation promotes genomic instability by uncoupling cell cycle progression from mitotic control. Nature 430, 797-802 (2004).
271. Bourhis, E., Lingel, A., Phung, Q., Fairbrother, W. J. & Cochran, A. G. Phosphorylation of a borealin dimerization domain is required for proper chromosome segregation. Biochemistry 48, 6783-93 (2009).
272. Fischer, M., Heeger, S., Hacker, U. & Lehner, C. The mitotic arrest in response to hypoxia and of polar bodies during early embryogenesis requires Drosophila Mps1. Curr Biol 14, 2019-24 (2004).
273. Gould, S. J., Keller, G. A., Hosken, N., Wilkinson, J. & Subramani, S. A conserved tripeptide sorts proteins to peroxisomes. J Cell Biol 108, 1657-64 (1989).
274. Obuse, C. *et al*. A conserved Mis12 centromere complex is linked to heterochromatic HP1 and outer kinetochore protein Zwint-1. Nat Cell Biol 6, 1135-41 (2004).
275. Kaur, H., Stiff, A. C., Date, D. A. & Taylor, W. R. Analysis of mitotic phosphorylation of borealin. BMC Cell Biol 8, 5 (2007).
276. Kops, G. J. P. L. Dividing the goods: co-ordination of chromosome biorientation and mitotic checkpoint signalling by mitotic kinases. Biochem Soc Trans 37, 971-5 (2009).
277. van Ree, J. H., Jeganathan, K. B., Malureanu, L. & van Deursen, J. M. Overexpression of the E2 ubiquitin-conjugating enzyme UbcH10 causes chromosome missegregation and tumor formation. J Cell Biol 188, 83-100 (2010).
278. Tanudji, M. *et al*. Gene silencing of CENP-E by small interfering RNA in HeLa cells leads to missegregation of chromosomes after a mitotic delay. Mol Biol Cell 15, 3771-81 (2004).
279. Chung, E. & Chen, R.-H. Phosphorylation of Cdc20 is required for its inhibition by the spindle checkpoint. Nat Cell Biol 5, 748-53 (2003).
280. Rudner, A. D. & Murray, A. W. Phosphorylation by Cdc28 activates the Cdc20-dependent activity of the anaphase-promoting complex. J Cell Biol 149, 1377-90 (2000).
281. Kraft, C. *et al*. Mitotic regulation of the human anaphase-promoting complex by phosphorylation. Embo J 22, 6598-609 (2003).
282. Holt, L. J., Krutchinsky, A. N. & Morgan, D. O. Positive feedback sharpens the anaphase switch. Nature 454, 353-7 (2008).
283. Dankort, D. *et al*. A new mouse model to explore the initiation, progression, and therapy of BRAFV600E-induced lung tumors. Genes Dev 21, 379-84 (2007).

Samenvatting in het Nederlands

Celdeling (Mitose)

Mensen, dieren en planten moeten groeien om zich uiteindelijk voort te kunnen planten om het voortbestaan van de soort te kunnen waarborgen. Hiervoor delen cellen zich vanaf de bevruchting tot het organisme volgroeid is. Als cellen beschadigd raken en niet meer kunnen functioneren, kan dit hersteld worden door deling van andere cellen daaromheen. Celdeling is dus nodig voor groei en herstel van een organisme. Elke cel bevat het erfelijk materiaal van het organisme, dat bij mensen bestaat uit 46 chromosomen. Deze chromosomen worden voorafgaand aan de deling gekopieerd in de cel. Vervolgens kan de cel zich delen in twee dochtercellen, die beiden weer een set van 46 chromosomen bevatten.

Het is belangrijk dat elke dochtercel na een deling een originele set chromosomen heeft, omdat dit genetisch materiaal de basis is voor het juist functioneren van de cel. Teveel of te weinig chromosomen (aneuploidy) in een cel bij de mens net na bevruchting kan leiden tot embryosterfte of grote problemen in de ontwikkeling. Het syndroom van Down wordt bijvoorbeeld veroorzaakt door de aanwezigheid van een extra chromosoom 21. Bovendien komt aneuploidy vaak voor in cellen van tumoren, en men denkt dat het optreden van aneuploidy na een celdeling de oorzaak zou kunnen zijn voor het vormen van de tumor, en/of bijdraagt aan de groeisnelheid of agressiviteit van de tumor.

Het Mitotische Checkpoint

Om te kunnen garanderen dat de chromosomen tijdens een celdeling eerlijk verdeeld worden over de twee dochtercellen hebben cellen een controle mechanisme. Dit mechanisme (het mitotische checkpoint) houdt de laatste stap van de celdeling tegen totdat zeker is dat de chromosomen op correcte wijze gescheiden en eerlijk verdeeld zullen worden. De laatste stappen van mitose waarin de chroosoomverdeling plaatsvindt en de rol van het mitotische checkpoint hierin worden hieronder beschreven en zijn schematisch weergegeven in het figuur op de volgende pagina.

Elk chromosoompaar dat ontstaat na het kopiëren wordt bij elkaar gehouden door een soort lijm (Cohesin). Het scheiden van zo'n paar gebeurt doordat de chromosomen vastgemaakt worden aan kabels in de cel (microtubuli) die elk chromosoom of naar de ene kant of naar de andere kant van de cel zullen trekken. Als de twee chromosomen van zo'n paar op de juiste wijze verbonden zijn aan microtubuli (één kopie met de ene kant van de cel en de andere met de andere kant van de cel), ontstaat er een spanning (trekkracht) tussen de twee kopieën, omdat de microtubuli al een beetje beginnen te trekken naar de tegengestelde richtingen van de cel. Pas als alle chromosoomparen op deze wijze vastgemaakt zijn en spanning hebben, wordt Cohesin afgebroken en trekken de microtubuli de chromosomen naar de tegenoverliggende kanten van de cel. Zo worden alle chromosoomparen eerlijk verdeeld over twee kanten van de cel, die dan door het midden in tweeën deelt.

Deze scheiding van de chromosoomparen wordt door het mitotische checkpoint tegengehouden zolang niet alle chromosomen op de juiste manier vastgemaakt zijn aan de microtubuli. Het mooie aan dit mechanisme is dat het checkpoint geactiveerd wordt via de nog niet vastgemaakte chromosomen. De plek waar de microtubuli kunnen binden aan het chromosoom bestaat

namelijk uit een groot complex van eiwitten, waarvan een aantal een stopsignaal geneert (het mitotische checkpoint), maar alleen als er geen microtubuli gebonden zijn. In het geval dat een chromosoompaar wel is vastgemaakt, maar er geen spanning is (bijvoorbeeld als beide kopieën aan een kant van de cel zijn vastgemaakt), is er een enzym (Aurora B) dat zorgt dat deze foute verbindingen verbroken worden. Op deze manier blijft het checkpoint actief, net zolang totdat alle chromosoomparen goed vastgemaakt zijn en overal spanning op staat. Als dit mechanisme op de juiste manier functioneert zal elke cel na deling precies de juiste chromosomen bevatten, maar als er ergens iets fout gaat kan er zogenoemde chromosoom instabiliteit en aneuploidy ontstaan.

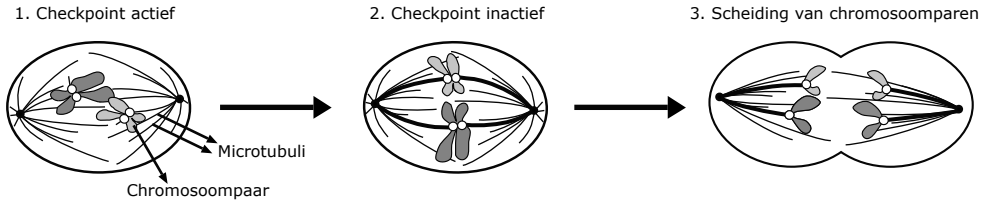

Schematische voorstelling van de laatste stappen van mitose.
1. De chromosoomparen zijn nog niet op de juiste wijze vastgemaakt aan microtubuli. Het checkpoint is daarom actief en houdt de laatste stap, de scheiding van de chromosoomparen (3), tegen. 2. De chromosoomparen zijn op de juiste manier vastgemaakt aan microtubuli, er staat spanning op en het checkpoint wordt geïnactiveerd. 3. De chromosoomparen worden gescheiden en op de juiste manier verdeeld naar twee kanten van de cel, die hierna in tweeën kan splitsen.

Teruggaande naar het feit dat aneuploidy vaak voorkomt in tumorcellen, en de gedachte dat aneuploidy misschien de oorzaak zou kunnen zijn van het ontstaan en/of bevorderen van tumorgroei, is het checkpoint dus een zeer interessant aspect van de celdeling om te onderzoeken. Bovendien is het bekend dat als het checkpoint zodanig slecht functioneert dat de chromosoomverdeling heel erg fout gaat, de cellen na deling doodgaan. Van tumorcellen wordt gedacht dat ze hier gevoeliger voor zijn dan gezonde cellen, wat van het checkpoint een aantrekkelijk doelwit maakt voor kankertherapie bij patiënten. Om dit in de praktijk te kunnen gaan realiseren, is het wel belangrijk dat we eerst op fundamenteel niveau weten hoe het checkpoint precies werkt.

Het onderzoek beschreven in dit proefschrift

Het onderzoek dat beschreven wordt in dit proefschrift brengt een aantal aspecten aan het licht over het functioneren van het checkpoint. Hierbij is de nadruk gelegd op de functie van het eiwit Mps1. Mps1 is een van de eiwitten op het grote complex waar de microtubuli aan binden, en zonder Mps1 kan het checkpoint niet functioneren. Mps1 is een kinase, die andere eiwitten kan modificeren (fosforyleren) en ze daarmee kan activeren of deactiveren. Er was echter maar weinig bekend over hoe Mps1 precies functioneert in het checkpoint op het moment dat dit onderzoek begon. In hoofdstuk 1 wordt in een uitgebreide inleiding samengevat wat in de literatuur bekend is over mitose, het mitotische checkpoint en Mps1.

In hoofdstuk 2 laten we zien dat Mps1 nodig is voor het functioneren van het checkpoint, en dat dit specifiek afhankelijk is van de kinase activiteit van Mps1. Verder laten we zien dat Mps1 buiten het checkpoint nog een functie heeft, namelijk er zorg voor dragen dat alle chromosomen op de juiste manier verbonden kunnen worden aan de microtubuli. Mps1 doet dit door Aurora

B, het enzym dat er voor zorgt dat foute verbindingen verbroken worden, te activeren. Ook deze functie hangt af van de kinase activiteit van Mps1. Mps1 fosforyleert namelijk Borealin, dat in complex zit met Aurora B. Deze fosforylering is nodig voor maximale activering van Aurora B en als dit niet gebeurt is de cel niet in staat om alle chromosomen op de juiste manier te verbinden met microtubuli, met als gevolg een foute scheiding van de chromosomen.

In hoofdstuk 3 wordt een nieuwe Mps1-remmer (Mps1-IN-1) beschreven, waarbij wordt ingegaan op de werking en specificiteit hiervan. Er wordt uitgebreid beschreven wat de gevolgen zijn van het toedienen van Mps1-IN-1 aan tumorcellen en aan niet-tumorcellen. Deze remmer is zeer specifiek gebleken voor de remming van Mps1, en is een heel handig hulpmiddel om de functie van Mps1 tijdens mitose te onderzoeken. Bij het onderzoek dat beschreven is in de hierop volgende hoofdstukken is Mps1-IN-1 veelvuldig gebruikt.

In hoofdstuk 4 beschrijven we een feedback loop interactie tussen Mps1, APC/C (een eiwitcomplex dat ervoor zorgt dat cellen de laatste fase van mitose ingaan en echt delen) en MCC (een eiwitcomplex dat het ingaan van de laatste fase van mitose voorkomt zolang dit nodig is; de uitvoerder van het checkpoint). Zolang nog niet alle chromosomen op de juiste wijze verbonden zijn met microtubuli, remt het MCC het APC/C, maar zodra alles goed verbonden is valt het MCC uit elkaar en kan het APC/C de deling gaan inzetten. Wij beschrijven in dit hoofdstuk dat Mps1 een functie heeft in het beschermen en in stand houden van het MCC.

In hoofdstuk 5 beschrijven we onze bevinding dat auto-fosforylering van Mps1 nodig is voor het bereiken van maximale activiteit van Mps1. Met andere woorden, Mps1 fosforyleert zichzelf om zichzelf verder te activeren. Ervoor zorgen dat deze fosforylering niet kan plaatsvinden heeft tot gevolg dat cellen een verzwakt checkpoint hebben en daardoor chromosomaal instabiel worden. Per deling krijgen de dochtercellen af en toe een chromosoom teveel of te weinig, maar ze overleven wel. Deze bevinding geeft aan dat cellen volledige Mps1 activiteit nodig hebben om de juiste hoeveelheid chromosomen door te geven na een deling, maar dat de gevolgen niet zo erg zijn dat de cel eraan doodgaat. Het zou wel zo kunnen zijn dat cellen dan gevoeliger kunnen worden om een tumorcel te worden, en/of als tumorcel makkelijker overleven. Dit zal met toekomstig onderzoek uitgezocht moeten worden.

Hoofdstuk 6 beschrijft hoe Mps1 beweegt van en naar de plek waar microtubuli binden aan de chromosomen. We laten zien dat Mps1 naar deze plek toe gaat, maar door zijn eigen activiteit er ook weer weggaat. Als actief Mps1 vastgehouden wordt op deze plek, gaan de cellen de laatste fase van mitose niet in. Dit ondanks dat alle chromosomen op de juiste manier verbonden zijn en de cel er dus wel klaar voor is. We laten zien dat in deze situatie het checkpoint niet uitgezet wordt. De regulatie van Mps1 activiteit en lokalisatie is dus ook bepalend voor het kunnen uitzetten van het checkpoint en het starten van de uiteindelijke celdeling.

In hoofdstuk 7 worden alle hoofdstukken samengevat en bediscussieerd in het kader van recente literatuur. Het onderzoek beschreven in dit proefschrift geeft nieuwe inzichten in de functie van Mps1 binnen het functioneren van het mitotische checkpoint. Verder beschrijft het een nog niet eerder geobserveerde functie van Mps1, namelijk in het reguleren van het tot stand komen van de juiste verbindingen van chromosomen aan de microtubuli. Deze bevindingen dragen bij aan de basis voor toekomstig fundamenteel onderzoek naar mitose en het mitotische checkpoint, en voor verder onderzoek naar het checkpoint als mogelijk doelwit voor nieuwe kankertherapieën in de toekomst. Suggesties hiervoor worden gegeven in hoofdstuk 7.

Curriculum Vitae

Nannette Jelluma werd geboren op 30 maart 1978 te Woerden. In 1990 behaalde zij het VWO-diploma aan het Minkema College te Woerden, waarna zij in hetzelfde jaar begon met de studie Scheikunde aan de Universiteit Utrecht. Tijdens deze studie doorliep zij een onderzoeksstage van zes maanden bij de vakgroep Biochemie van Membranen onder begeleiding van Dr. Koert Burger en Prof.dr. Ben de Kruijff, en een afsluitende onderzoeksstage van negen maanden bij de vakgroep Biochemie van Lipiden onder begeleiding van Dr. Tobias Dansen en Prof.dr. Karel Wirtz. In augustus 2001 behaalde zij het doctoraal diploma Scheikunde, waarna zij van januari 2002 tot maart 2005 als Junior Specialist werkzaam was aan de University of California San Francisco in de Verenigde Staten van Amerika, eerst in het lab van Dr. Jeff Arbeit en vervolgens in het lab van Dr. Daphne Haas-Kogan. Van mei 2005 tot mei 2010 werkte zij aan haar promotieonderzoek, beschreven in dit proefschrift, bij de afdelingen Experimentele Oncologie en Fysiologische Chemie van het Universtitair Medisch Centrum Utrecht onder begeleiding van Dr. Geert Kops en Prof.dr. René Medema.

Publications

N. Kwiatkowski, **N. Jelluma**, P. Filippakopoulos, M. Soundararajan, M.S. Manak, M. Kwon, H.G. Choi, T. Sim, Q.L. Deveraux, S. Rottmann, D. Pellman, J.V. Shah, G.J.P.L. Kops, S. Knapp, N.S. Gray.
Small-molecule kinase inhibitors provide insight into Mps1 cell cycle function.
Nat Chem Biol. 6: 359–368 (2010).

R.P. Ermoian, T. Kaprealian, K.R. Lamborn, X. Yang, **N. Jelluma**, N.D. Arvold, R. Zeidman, M.S. Berger, D. Stokoe, D.A. Haas-Kogan.
Signal transduction molecules in gliomas of all grades.
J Neurooncol. 91(1):19-26 (2009).

N. Jelluma, A.B. Brenkman, I. McLeod, J.R. Yates 3rd, D.W. Cleveland, R.H. Medema, G.J.P.L. Kops.
Chromosomal instability by inefficient Mps1 auto-activation due to a weakened mitotic checkpoint and lagging chromosomes.
PLoS One. 3(6):e2415 (2008).

N. Jelluma, A.B. Brenkman, N.J. van den Broek, C.W.A. Cruijsen, M.H.J. van Osch, S.M.A. Lens, R.H. Medema, G.J.P.L. Kops.
Mps1 phosphorylates Borealin to control Aurora B activity and chromosome alignment.
Cell. 132(2):233-46 (2008).

J.K. Wiencke, S. Zheng, **N. Jelluma**, T. Tihan, S. Vandenberg, T. Tamgüney, R. Baumber, R. Parsons, K.R. Lamborn, M.S. Berger, M.R. Wrensch, D.A. Haas-Kogan, D. Stokoe.
Methylation of the PTEN promoter defines low-grade gliomas and secondary glioblastoma.
Neuro Oncol. 9(3):271-9 (2007)

N. Jelluma, X. Yang, D. Stokoe, G.I. Evan, T.B. Dansen, D.A. Haas-Kogan.
Glucose withdrawal induces oxidative stress followed by apoptosis in glioblastoma cells but not in normal human astrocytes.
Mol Cancer Res. (5):319-30 (2006).

G. Afshar*, **N. Jelluma***, X. Yang, D. Basila, N.D. Arvold, A. Karlsson, G.L. Yount, T.B. Dansen, E. Koller, D.A. Haas-Kogan. (*Equal author contribution)
Radiation-induced caspase-8 mediates p53-independent apoptosis in glioma cells.
Cancer Res. 66(8):4223-32 (2006).

D.A. Haas-Kogan, M.D. Prados, T. Tihan, D.A. Eberhard, **N. Jelluma**, N.D. Arvold, R. Baumber, K.R. Lamborn, A. Kapadia, M. Malec, M.S. Berger, D. Stokoe.
Epidermal growth factor receptor, protein kinase B/Akt, and glioma response to erlotinib.
J Natl Cancer Inst. 97(12):880-7 (2005)

T.B. Dansen, G.J.P.L. Kops, S. Denis, **N. Jelluma,** R.J.A. Wanders, J.L. Bos, B.M.T. Burgering, K.W.A. Wirtz.
Regulation of sterol carrier protein gene expression by the forkhead transcription factor FOXO3a.
J Lipid Res. 45(1):81-8 (2004).

Dankwoord

Graag wil ik de mensen bedanken die op een of andere manier hebben bijgedragen aan het tot stand komen van dit proefschrift.

Allereerst Dr. Geert Kops, G, co-promotor, voor de kans om in zijn lab onder zijn begeleiding mijn promotieonderzoek in de wereld van mitose te hebben kunnen aanvangen en afmaken. Ik denk niet dat ik het beter had kunnen treffen, en het is ook niet voor niks dat ik voorlopig nog niet weg wil!

Prof.dr. René Medema, promotor, voor de begeleiding, kritiek, en blijk van vertrouwen gedurende de afgelopen vijf jaar.

Dank aan alle mensen die een directe bijdrage hebben geleverd aan de totstandkoming van de verschillende hoofdstukken in dit proefschrift. Speciale dank aan Arjan Brenkman voor de goede samenwerking met als resultaat twee publicaties. Special thanks to Nick Kwiatkowski, for the fruitful collaboration.

Voor de ondersteuning op het gebied van de duistere wereld van computerzaken, waar je tijdens je hele promotieonderzoek echt niet buiten kunt, bedank ik het Genomics Systems team, en in het bijzonder Wim van Driel, die altijd bereid is om buiten in zijn koffiepauze nog wat ingewikkelde zaken uit te leggen.

De mensen in de beoordelingscommissie: Prof.dr. Paul Coffer, Prof.dr. Hans Bos, Prof.dr. Jeroen den Hertog, Prof.dr. Sander van den Heuvel en Dr. Rob Wolthuis bedank ik voor het lezen en beoordelen van dit proefschrift.

Verder bedank ik al mijn labgenoten, oud-labgenoten en (oud)-stagiaires voor de vele wetenschappelijke en niet-wetenschappelijk discussies, het samen biertjes drinken en daarbij de discussies over niks. Naar een paar mensen gaat bijzondere dank uit: Renske en Carin, die bewijzen dat collega-af zijn niet betekent dat je samen geen sushi meer kunt maken. Emma, waarvan ik veel heb geleerd toen ik haar mocht begeleiden tijdens haar afstudeerstage. Livio, zonder wie elke microscoop na twee keer gebruiken bij het grof vuil zou staan. Aniek, met haar is het altijd lachen op het lab (zelfs als er niks te lachen valt) en zonodig ook bij een hoorzitting in Den Haag, een betere bondgenoot kun je niet hebben, CiMKi rules! En natuurlijk Saskia, twee handen op één buik in het lab en daarbuiten, en dat is ook wel nodig om de wereld een beetje in het gareel te houden! Het is dan ook niet voor niks dat zij me bijstaat als paranymf bij de promotie.
Voor deze mensen geldt ook dat ze voorlopig nog niet van me af zijn, en andersom dus ook niet, waar ik blij om ben.

Ook wil ik de mensen bedanken die niet direct betrokken zijn geweest bij de totstandkoming van dit proefschrift, maar desalniettemin een belangrijke rol hebben gespeeld. Mijn ouders, grote broers, schoonzusjes, schoonouders en vrienden bedank ik omdat ik altijd bij ze terecht heb gekund en zal kunnen, dat weet ik zeker.

Martha, mede-scheikel, samen met haar heb ik mogen ontdekken hoe leuk scheikunde is, en dat alles altijd wel weer goed komt als je het maar vaak genoeg zegt, en als je er maar voor zorgt dat je altijd de boel onder controle houdt. Ik ben blij dat zij mijn paranymf wilt zijn.

Tenslotte bedank ik Tobias, zonder wie ik nooit hieraan begonnen zou zijn, en met wie ik alles wil beginnen. Hij weet wel waarom.

Counting flowers on the wall that don't bother me at all

Playing solitaire till dawn with a deck of fifty-one

Smoking cigarettes and watching Captain Kangaroo

Now don't tell me I've nothing to do

-The Statler Brothers-